超越标准模型讲座

暗物质

宋宁强

中国科学院理论物理研究所

2026年4月24日

Outline

- ❖ Introduction
- ❖ Direct detection of dark matter
- ❖ Astrophysical probes of dark matter

Evidence of Dark Matter

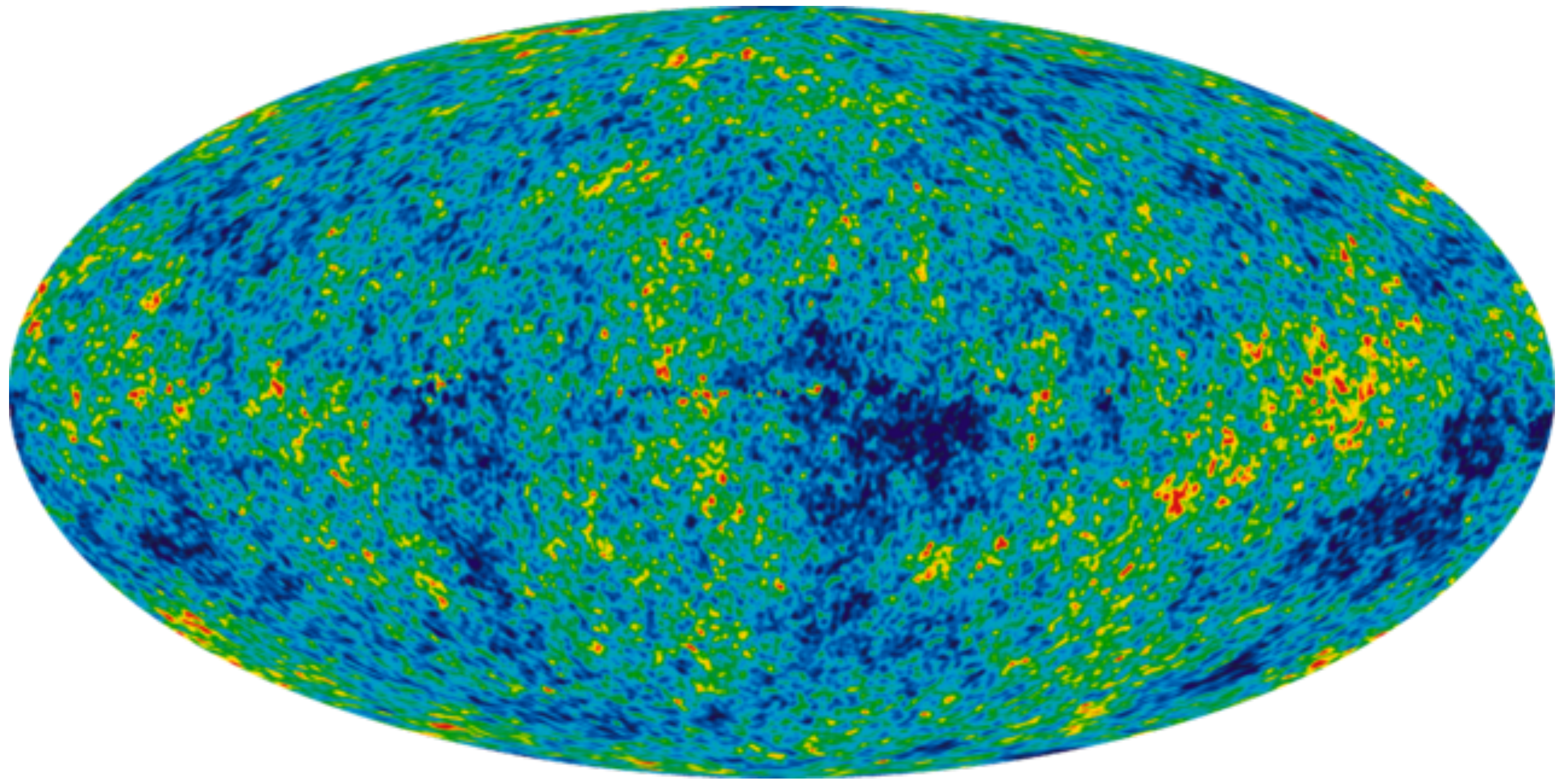

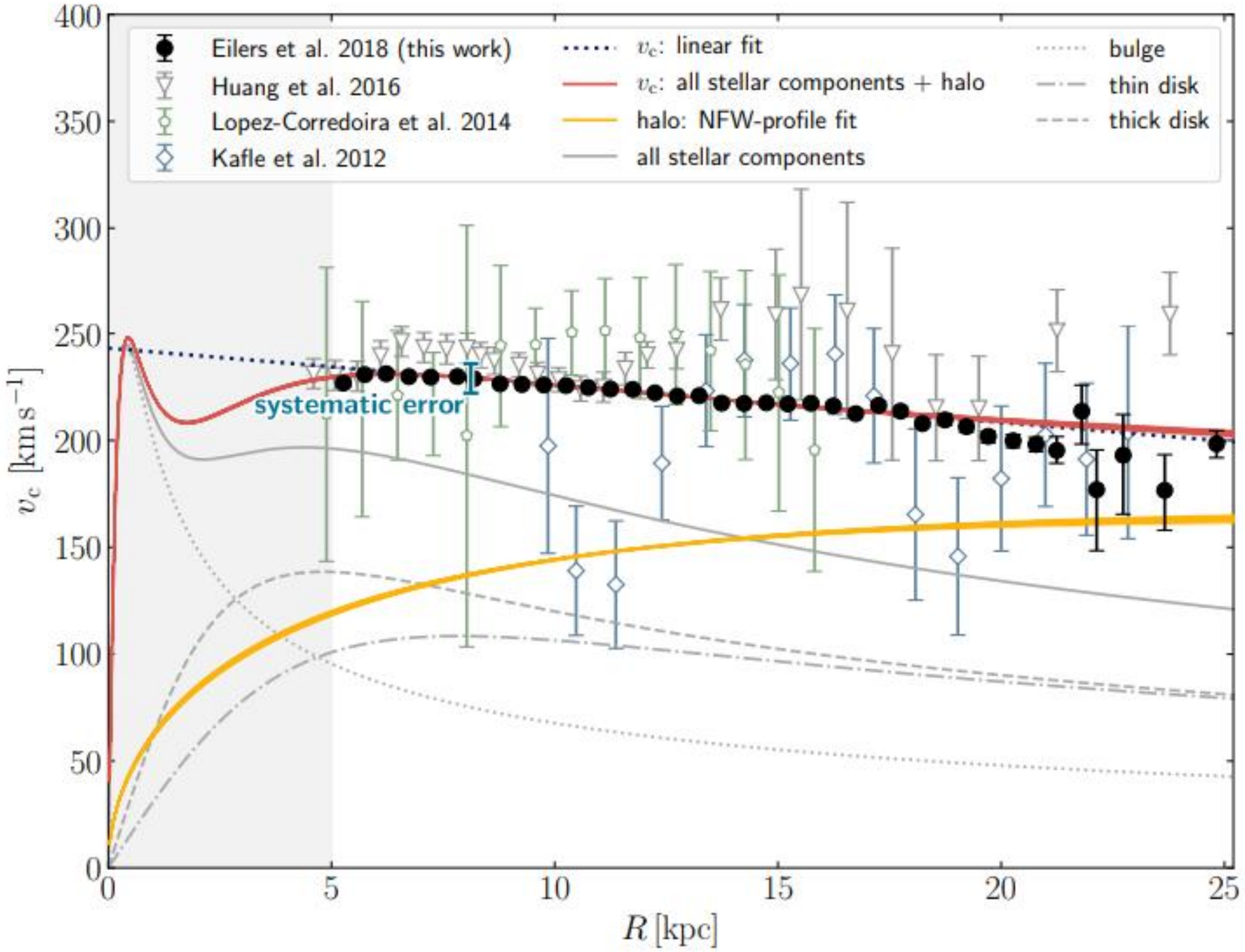

Eilers *et al.*, arXiv:1810.09466

Gravitational Lensing

The image of distant galaxy is distorted by gravity of dark matter

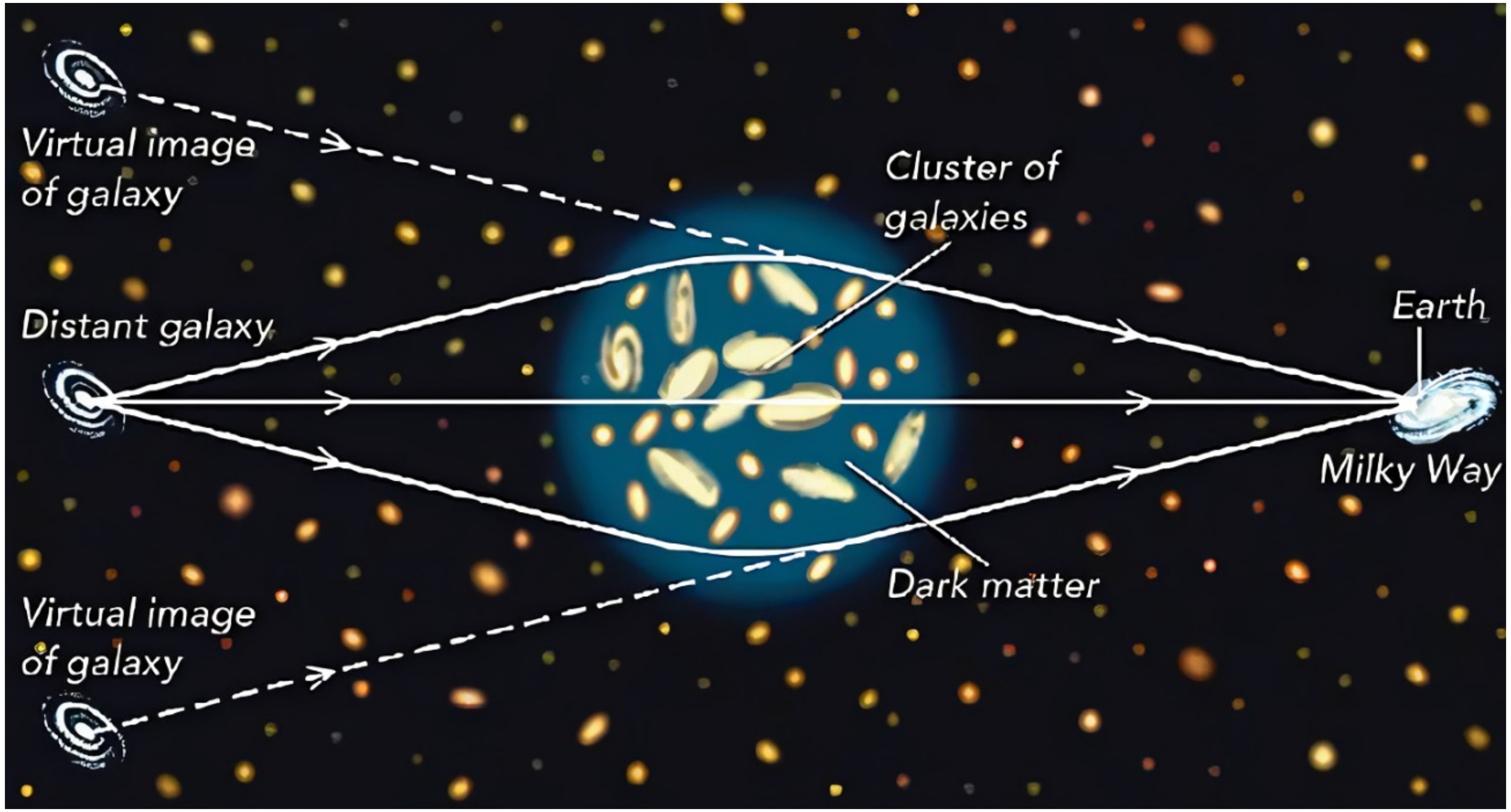

The Bullet Cluster

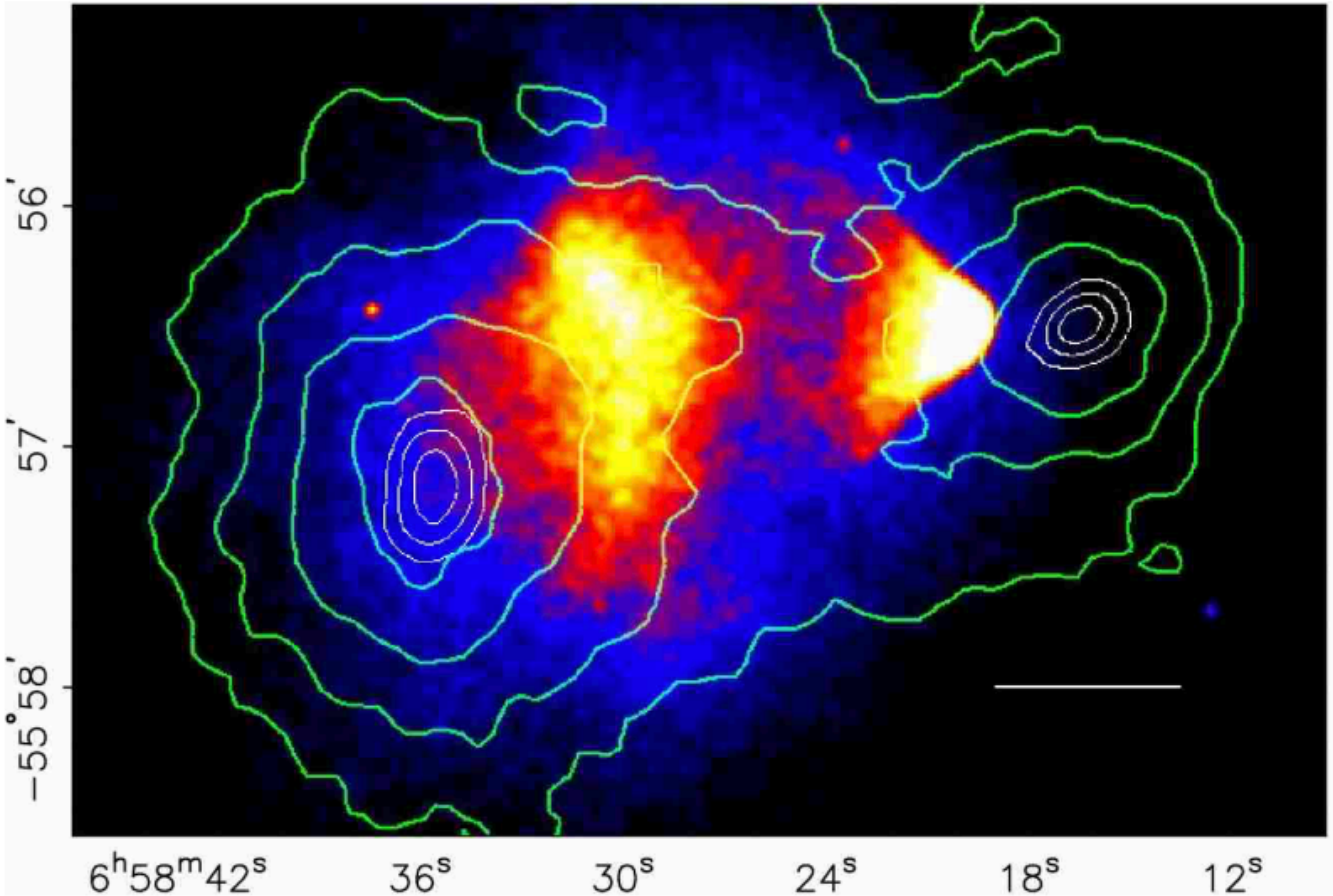

Clowe *et al.*, arXiv:1612.03906

Cosmic Microwave Background

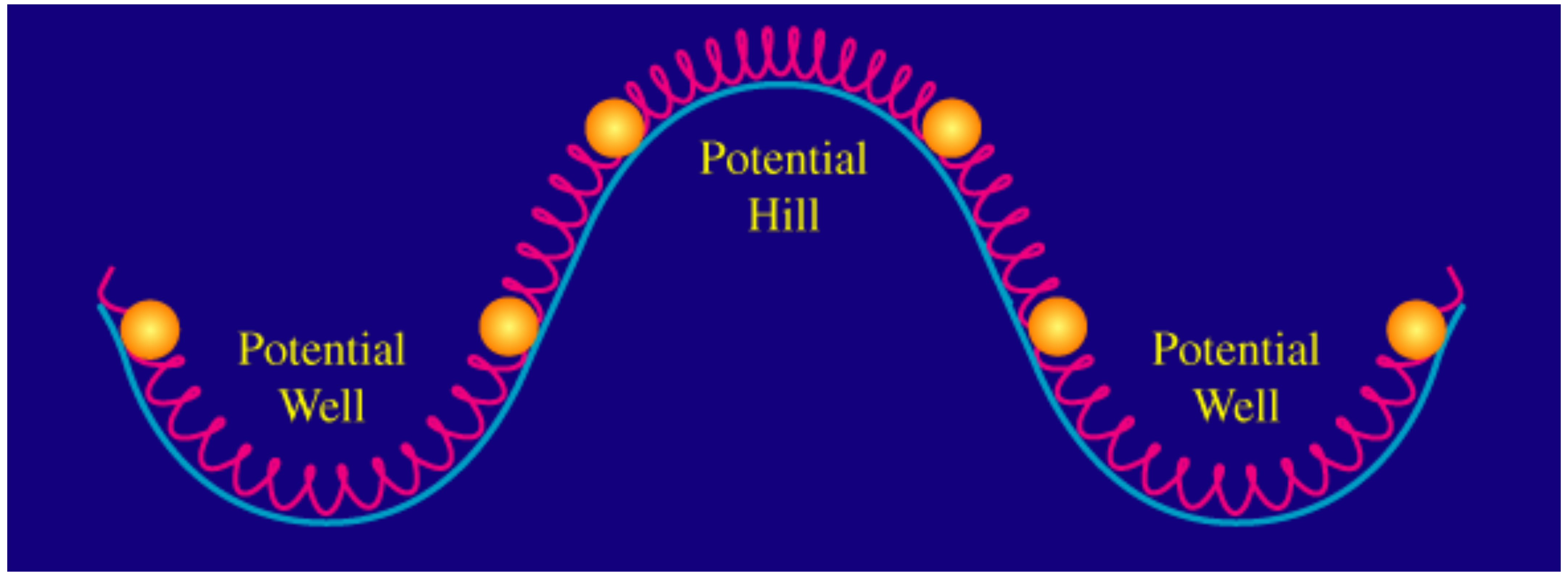

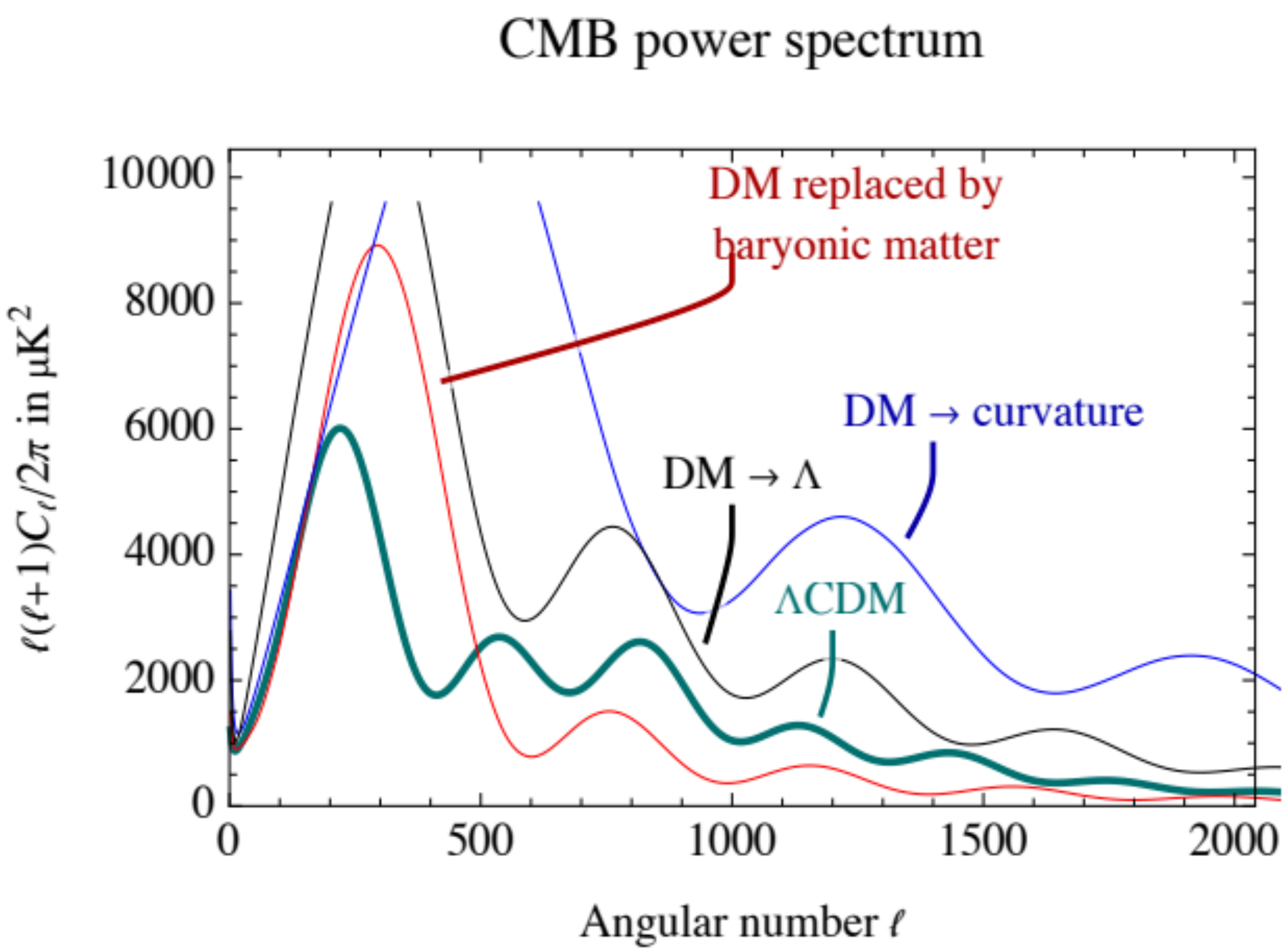

Cirelli *et al.*, arXiv:2406.01705

暗物质是什么

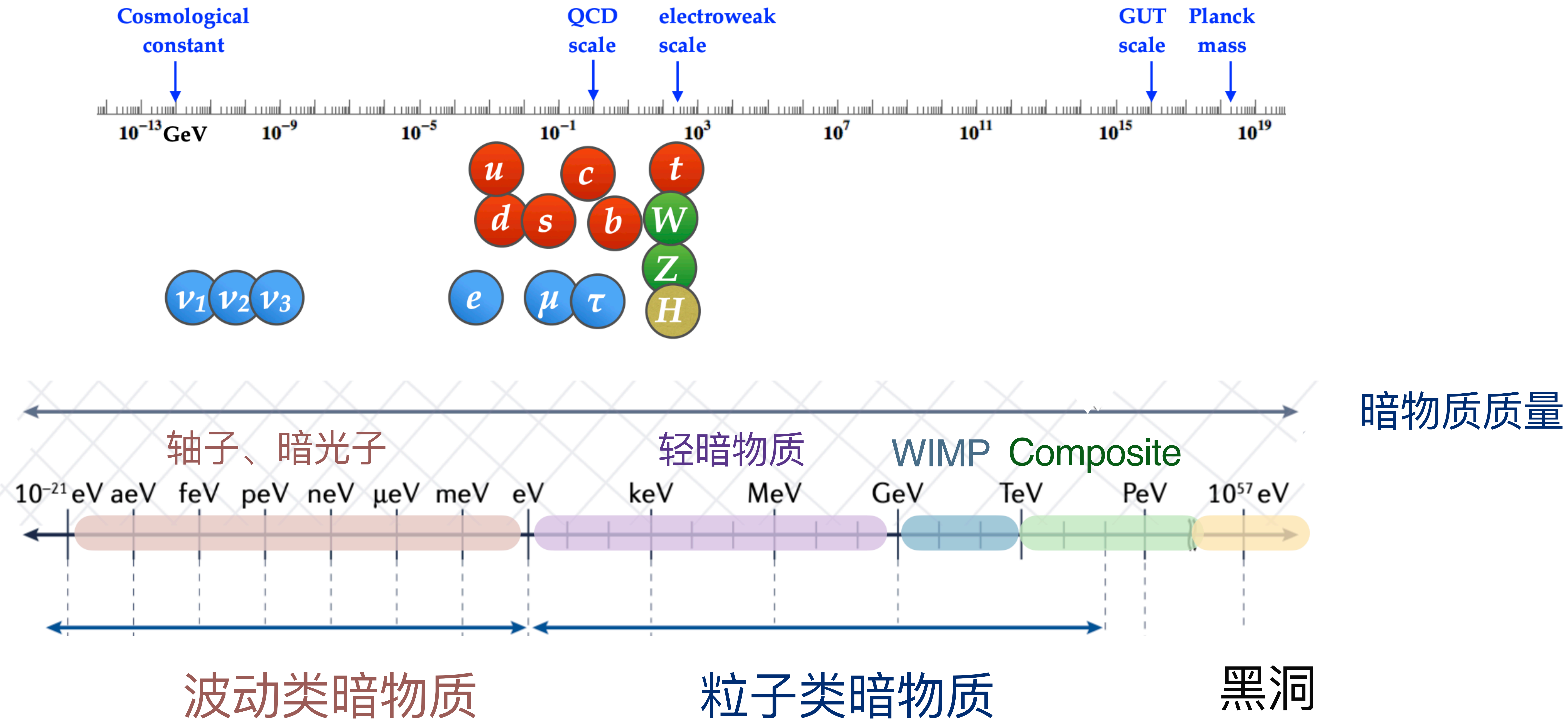

Cosmological constant
QCD scale
electroweak scale
GUT scale
Planck mass
10^-13 GeV
10^-9
10^-5
10^-1
10^3
10^7
10^11
10^15
10^19
u c t
d s b W
Z
ν1 ν2 ν3
e μ τ H
暗物质质量
轴子、暗光子
轻暗物质
WIMP
Composite
10^-21 eV aeV feV peV neV μeV meV eV keV MeV GeV TeV PeV 10^57 eV
波动类暗物质
粒子类暗物质
黑洞

A “Standard” Cosmological History of Dark Matter

- Dark matter in thermal equilibrium with SM at high temperature
- As the Universe cools down, chemical equilibrium is no longer maintained when $T < M_\chi$, and the dark matter abundance drops exponentially
- The Universe expansion rate eventually exceeds the dark matter annihilation rate, and the comoving dark matter density “freezes”
- A cold dark matter relic is left over

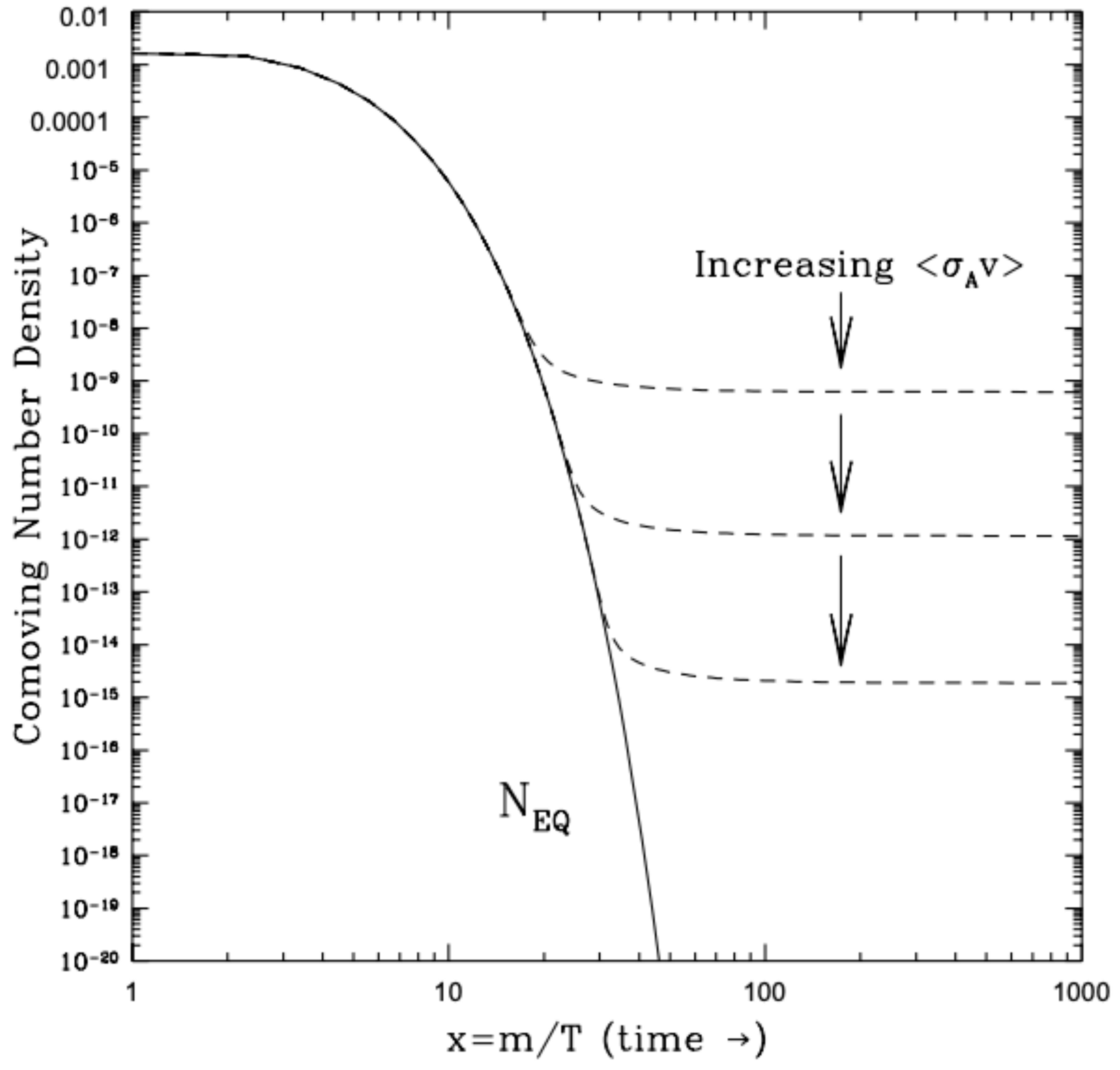

Hooper, arxiv: 0901.4090

$$\langle \sigma v \rangle \sim 3 \times 10^{-26} \mathrm{cm}^3/\mathrm{s}$$

Thermal Freeze-out

Boltzmann equation of dark matter

$$\boxed{\dot{n}(t) + 3H(t)n(t) = -\langle \sigma_{\chi\chi}\, v\rangle \; \left(n(t)^2 - n_{\text{eq}}(t)^2\right)}\;.$$

expansion of the universe — DM annihiliation — regeneration from the SM plasma

$$\frac{1}{a(t)^3}\,\frac{d}{dt}\left(n(t)a(t)^3\right) = -\langle \sigma_{\chi\chi}\, v\rangle \; \left(n(t)^2 - n_{\text{eq}}(t)^2\right)$$

$$\Leftrightarrow \quad T(t)^3\,\frac{d}{dt}\left(\frac{n(t)}{T(t)^3}\right) = -\langle \sigma_{\chi\chi}\, v\rangle \; \left(n(t)^2 - n_{\text{eq}}(t)^2\right)$$

$$\Leftrightarrow \quad \frac{dY(t)}{dt} = -\langle \sigma_{\chi\chi}\, v\rangle\, T(t)^3 \; \left(Y(t)^2 - Y_{\text{eq}}(t)^2\right) \qquad \text{with} \quad Y(t) := \frac{n(t)}{T^3}\;.$$

Thermal Freeze-out

$$\boxed{\dot{n}(t) + 3H(t)n(t) = -\langle\sigma_{\chi\chi}\, v\rangle \;\left(n(t)^2 - n_{\rm eq}(t)^2\right)} \,.$$

Radiation domination

$$\frac{1}{2t} \overset{\text{Eq.(1.31)}}{=} H \overset{\text{Eq.(1.47)}}{=} \frac{H(x=1)}{x^2} \quad\Leftrightarrow\quad x = \sqrt{2tH(x=1)}$$

$$\Leftrightarrow\quad \frac{dx}{dt} = \frac{2H(x=1)}{2\sqrt{2tH(x=1)}} = \frac{H(x=1)}{x}\,, \qquad x = m_\chi/T$$

$$\begin{aligned}
\frac{dY(x)}{dx} &= \frac{x}{H(x=1)}\,\frac{dY(t)}{dt} \\
&= -\langle\sigma_{\chi\chi}\, v\rangle\,\frac{x}{H(x=1)}\,\frac{m_\chi^3}{x^3}\,\left(Y(x)^2 - Y_{\rm eq}(x)^2\right) \\
&= -\frac{\lambda(x)}{x^2}\,\left(Y(x)^2 - Y_{\rm eq}(x)^2\right) \qquad \text{with} \quad \lambda(x) := \frac{m_\chi^3\,\langle\sigma_{\chi\chi}\, v\rangle}{H(x=1)} = \frac{\sqrt{90}\,M_{\rm Pl} m_\chi}{\pi\sqrt{g_{\rm eff}}}\,\langle\sigma_{\chi\chi}\, v\rangle(x)\,.
\end{aligned}$$

Thermal Freeze-out

$$\boxed{\dot{n}(t) + 3H(t)n(t) = -\langle\sigma_{\chi\chi}\, v\rangle\ \left(n(t)^2 - n_{\rm eq}(t)^2\right)}\,.$$

$$\frac{1}{Y(x'_{\rm dec})} - \frac{1}{Y(x_{\rm dec})} = \overline{Y}(x'_{\rm dec}) - \overline{Y}(x_{\rm dec}) = -\frac{\bar{\lambda}}{x'^{3/2}_{\rm dec}} + \frac{\bar{\lambda}}{x^{3/2}_{\rm dec}}\,. \qquad x = m_\chi/T$$

At late time $T' \ll T$, $x' \gg x$, $Y' \ll Y$

$$\frac{1}{Y(x'_{\rm dec})} = \frac{\bar{\lambda}}{x^{3/2}_{\rm dec}} \qquad \Leftrightarrow \qquad Y(x'_{\rm dec}) = \frac{m_\chi^3\,\langle\sigma_{\chi\chi}\, v\rangle}{H(x=1)} = \frac{x_{\rm dec}}{\lambda(x_{\rm dec})} \overset{\text{Eq.(3.24)}}{=} x_{\rm dec}\,\frac{\pi\sqrt{g_{\rm eff}}}{\sqrt{90}\,M_{\rm Pl} m_\chi}\,\frac{1}{\langle\sigma_{\chi\chi}\, v\rangle}\,.$$

$$\begin{aligned}\rho_\chi(T_0) &= m_\chi n_\chi(T_0)\\ &= m_\chi Y(x'_{\rm dec}) T'^3_{\rm dec}\left(\frac{a(T'_{\rm dec})}{a(T_0)}\right)^3 \overset{\text{Eq.(3.11)}}{=} m_\chi Y(x'_{\rm dec})\ T_0^3\,\frac{g_{\rm eff}(T_0)}{g_{\rm eff}(T'_{\rm dec})} = m_\chi\frac{Y(x'_{\rm dec})T_0^3}{28}\,.\end{aligned}$$

Thermal Freeze-out

$$\boxed{\dot{n}(t) + 3H(t)n(t) = -\langle \sigma_{\chi\chi} v \rangle \; \left(n(t)^2 - n_{\text{eq}}(t)^2 \right)} \,.$$

$$\begin{aligned}
\rho_\chi(T_0) &= m_\chi n_\chi(T_0) \\
&= m_\chi Y(x'_{\text{dec}}) T'^3_{\text{dec}} \left(\frac{a(T'_{\text{dec}})}{a(T_0)} \right)^3 \overset{\text{Eq.(3.11)}}{=} m_\chi Y(x'_{\text{dec}}) \, T_0^3 \, \frac{g_{\text{eff}}(T_0)}{g_{\text{eff}}(T'_{\text{dec}})} = m_\chi \frac{Y(x'_{\text{dec}}) T_0^3}{28} \,.
\end{aligned}$$

$$\begin{aligned}
\Omega_\chi h^2 &= m_\chi \, \frac{Y(x'_{\text{dec}}) T_0^3}{28} \, \frac{h^2}{3 M_{\text{Pl}}^2 H_0^2} \\
&= \frac{h^2 \pi \sqrt{g_{\text{eff}}}}{28 \sqrt{90} \, M_{\text{Pl}}} \, \frac{x_{\text{dec}}}{\langle \sigma_{\chi\chi} v \rangle} \, \frac{T_0^3}{3 M_{\text{Pl}}^2 H_0^2} \\
&= \frac{h^2 \pi \sqrt{g_{\text{eff}}}}{28 \sqrt{90} \, M_{\text{Pl}}} \, \frac{x_{\text{dec}}}{\langle \sigma_{\chi\chi} v \rangle} \, \frac{(2.4 \cdot 10^{-4})^3}{(2.5 \cdot 10^{-3})^4} \, \frac{1}{\text{eV}}
\end{aligned}$$

$$\Omega_\chi h^2 \approx 0.12 \, \frac{x_{\text{dec}}}{23} \, \frac{\sqrt{g_{\text{eff}}}}{10} \, \frac{1.7 \cdot 10^{-9} \, \text{GeV}^{-2}}{\langle \sigma_{\chi\chi} v \rangle} \approx 0.12 \, \frac{x_{\text{dec}}}{23} \, \frac{\sqrt{g_{\text{eff}}}}{10} \, \frac{2.04 \cdot 10^{-26} \text{cm}^3/\text{s}}{\langle \sigma_{\chi\chi} v \rangle} \,.$$

See, e.g. Bauer and Plehn, arxiv: 1705.01987

Thermal Freeze-out: WIMP Miracle

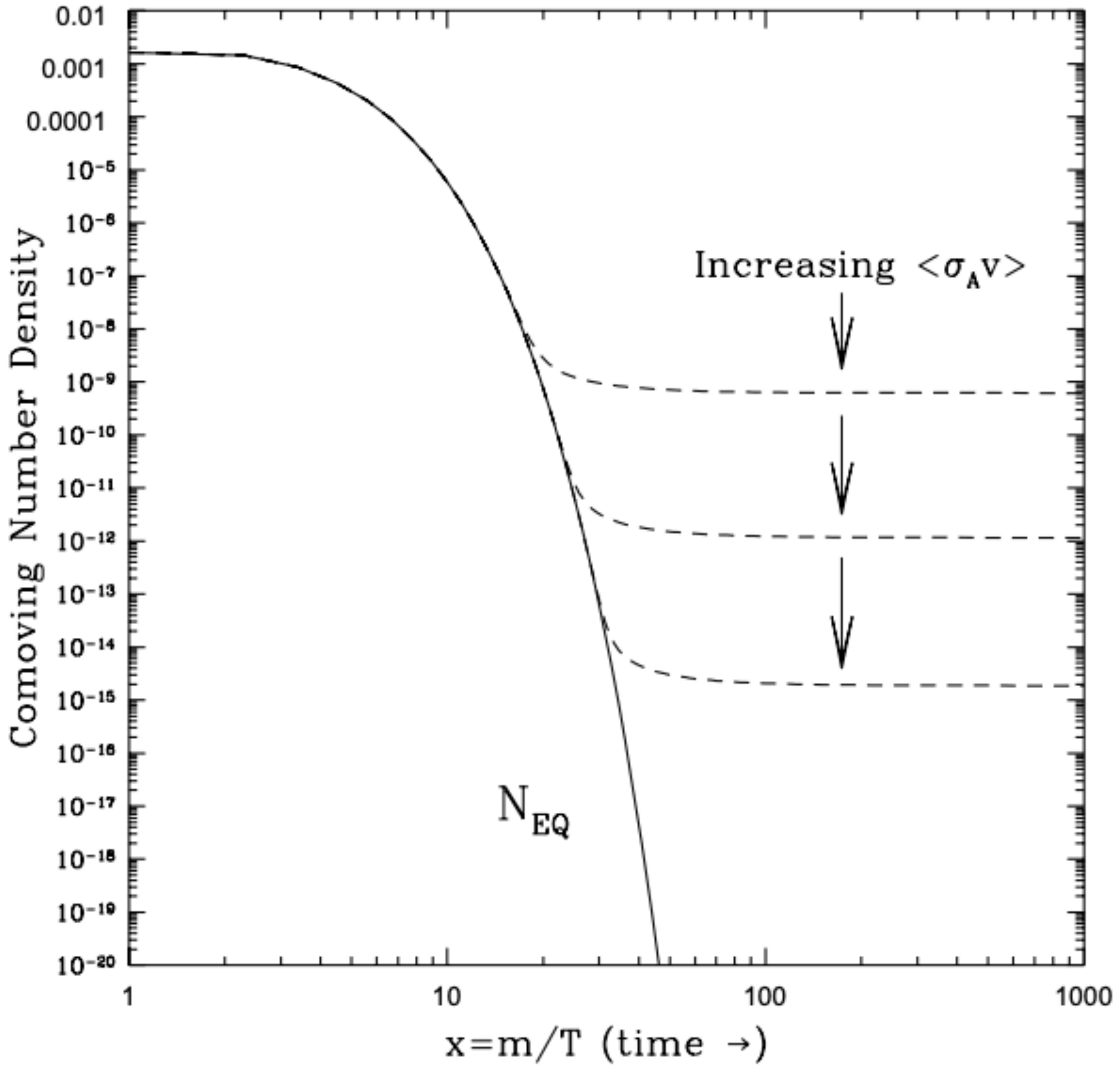

$$\Omega_\chi h^2 \approx 0.12\, \frac{x_{\rm dec}}{23}\, \frac{\sqrt{g_{\rm eff}}}{10}\, \frac{1.7\cdot 10^{-9}\,\mathbf{GeV}^{-2}}{\langle \sigma_{\chi\chi}\, v\rangle} \approx 0.12\, \frac{x_{\rm dec}}{23}\, \frac{\sqrt{g_{\rm eff}}}{10}\, \frac{2.04\cdot 10^{-26}\mathbf{cm}^3/\mathbf{s}}{\langle \sigma_{\chi\chi}\, v\rangle}\,.$$

Dark Matter Detection

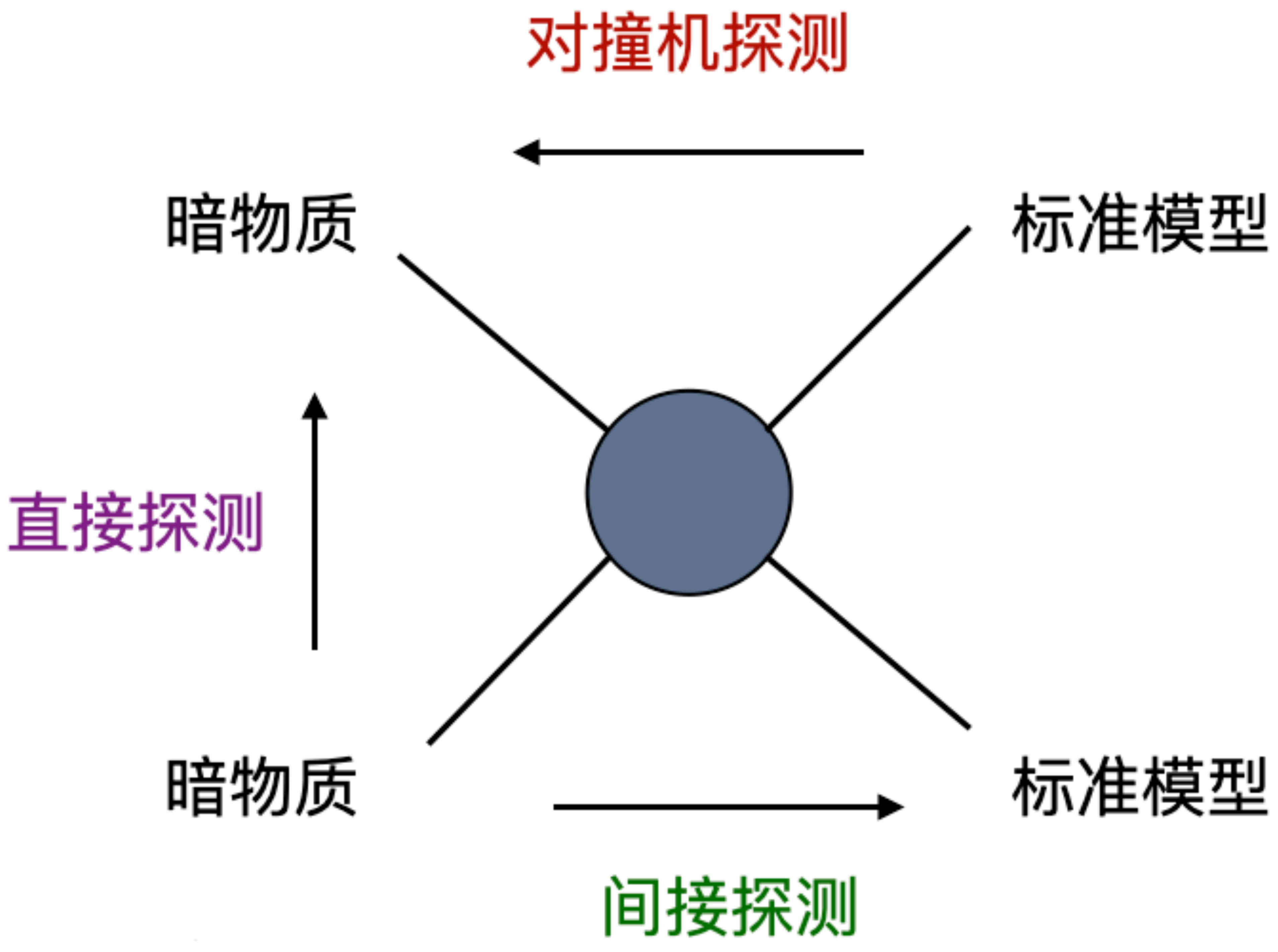

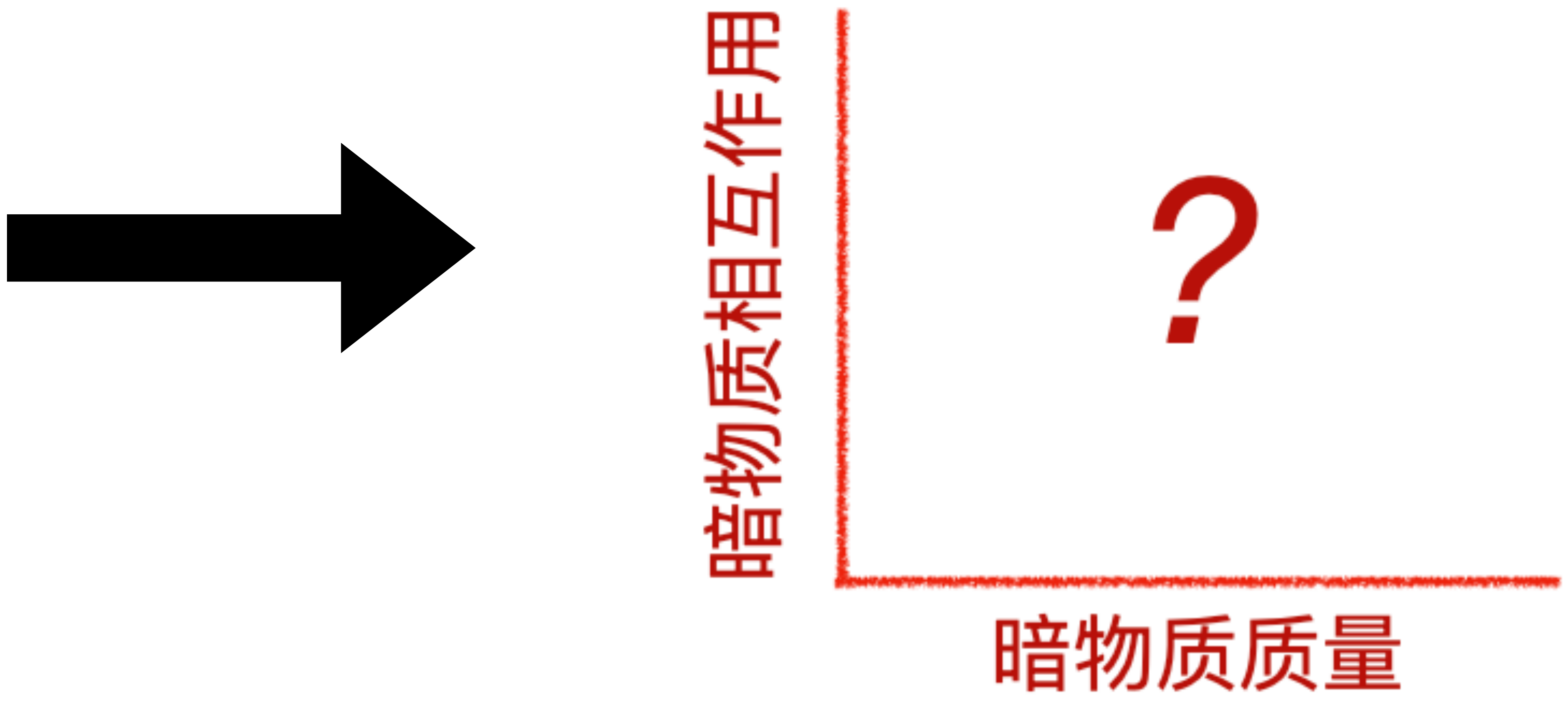

Dark Matter Detection

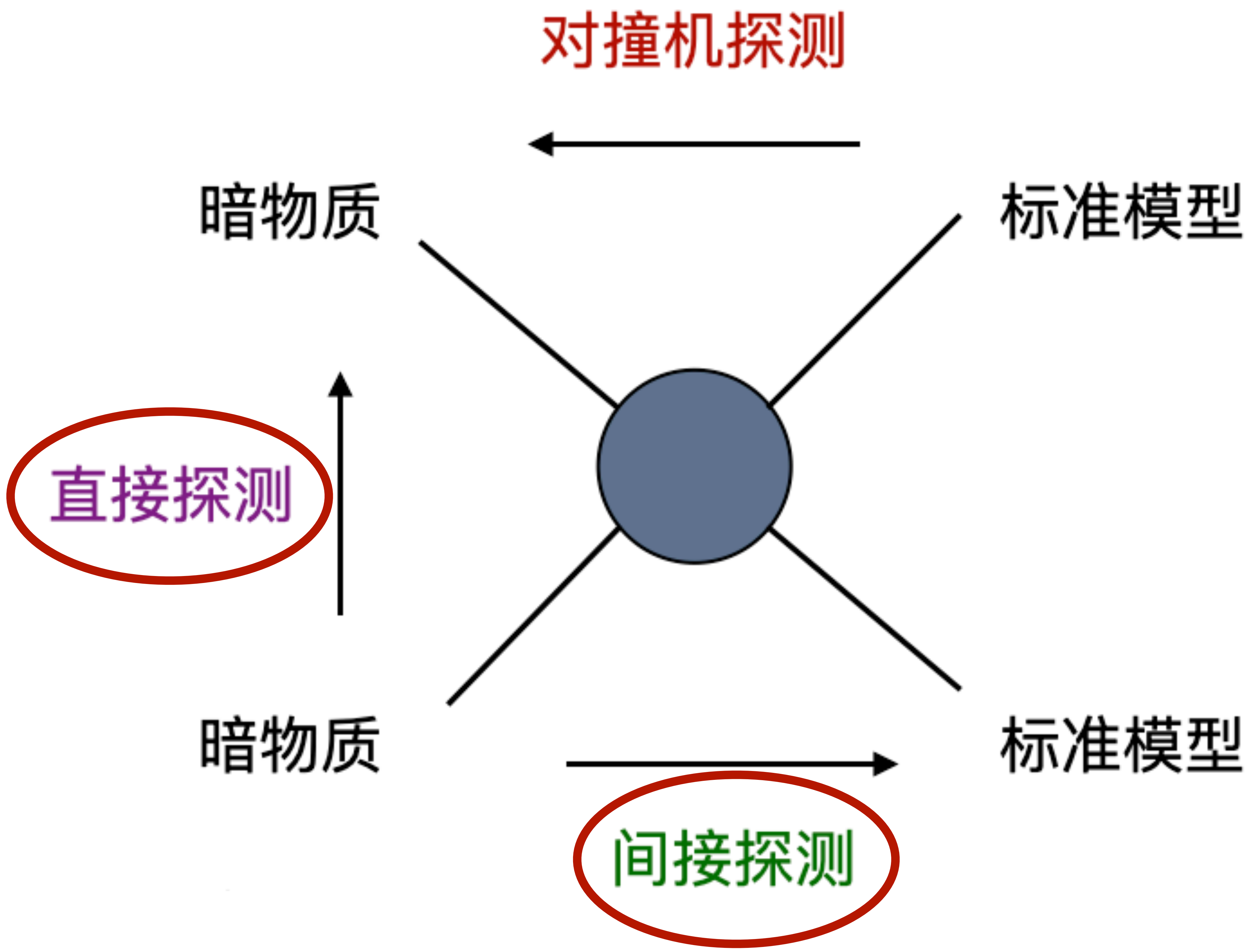

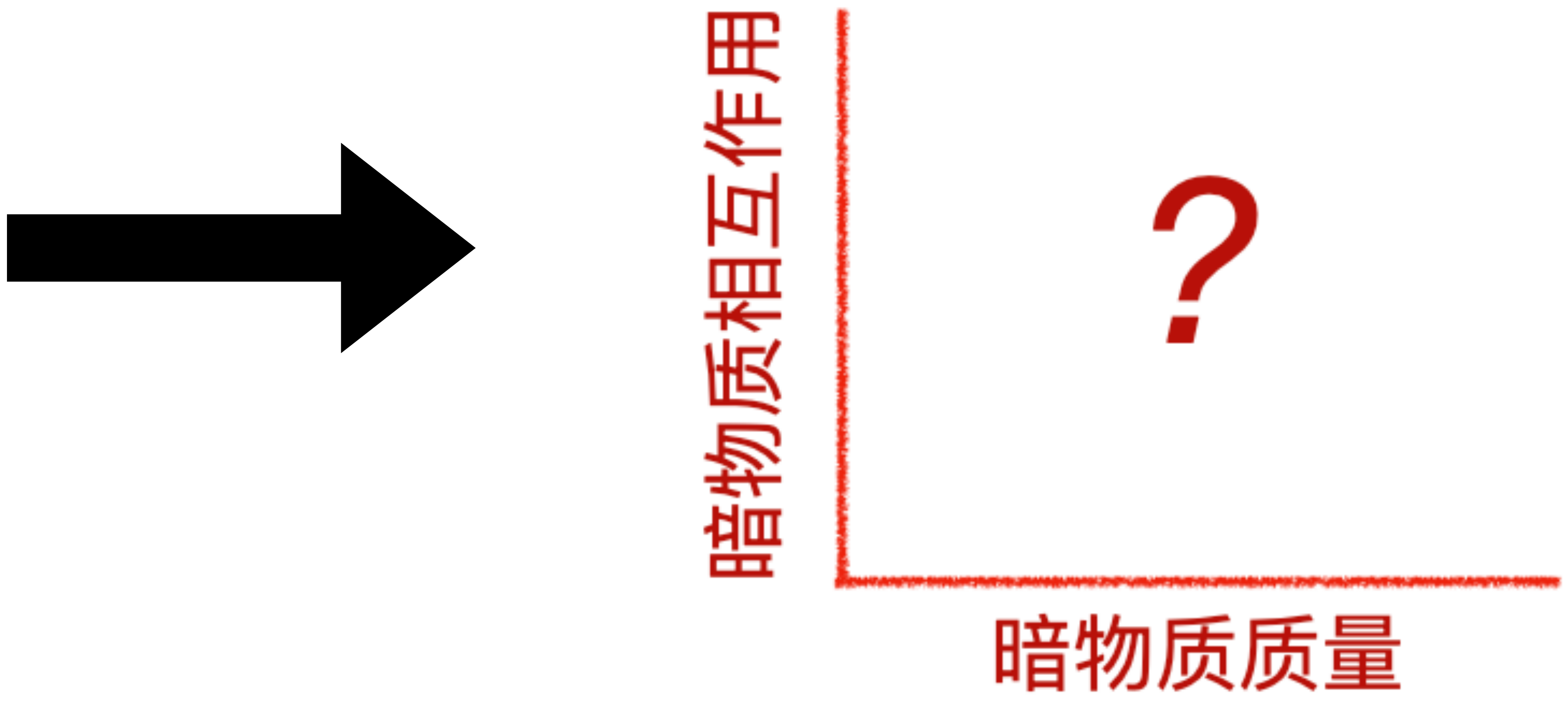

Dark Matter Direct Detection

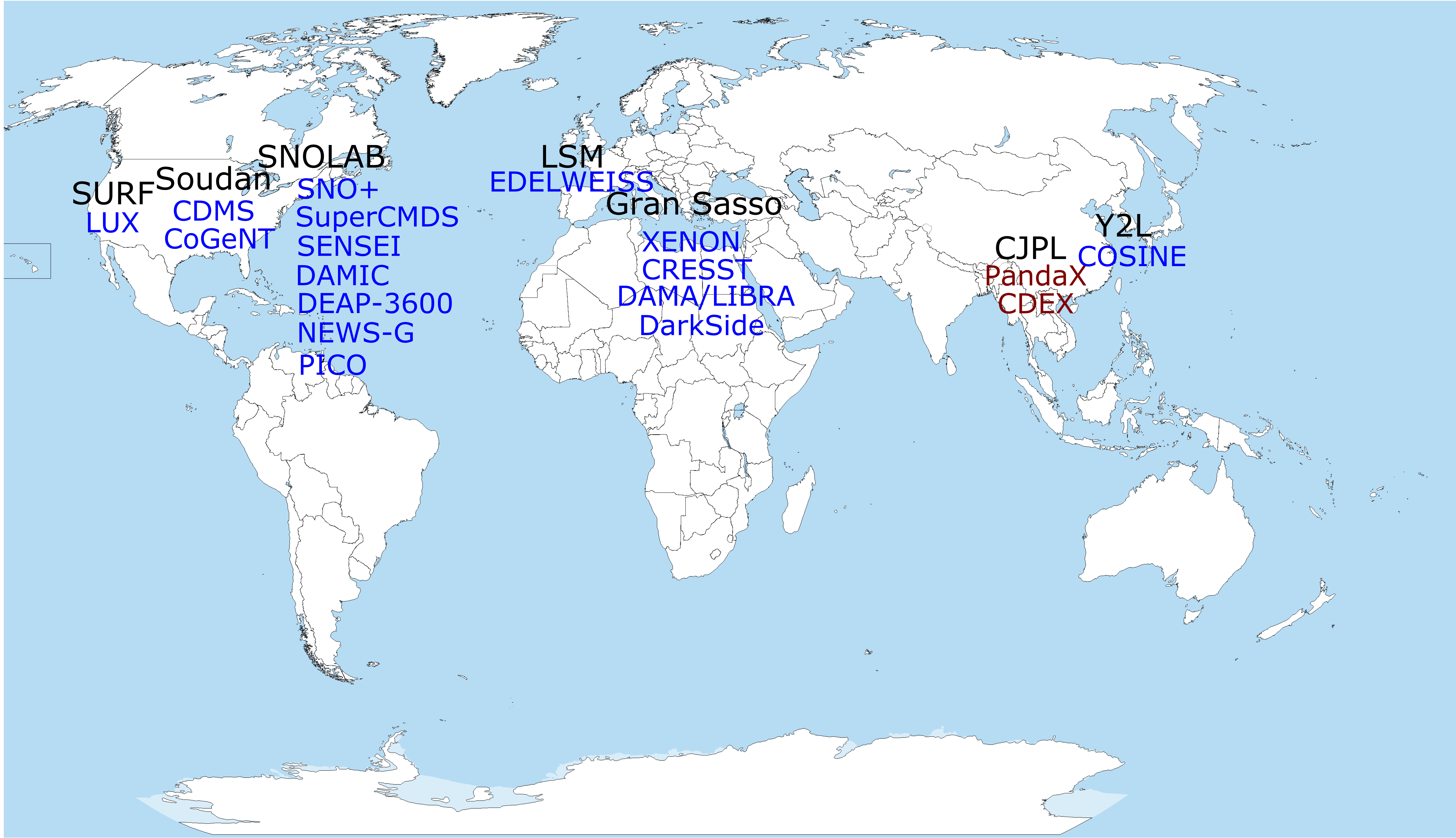
SURF
LUX
Soudan
CDMS
CoGeNT
SNOLAB
SNO+
SuperCMDS
SENSEI
DAMIC
DEAP-3600
NEWS-G
PICO
LSM
EDELWEISS
Gran Sasso
XENON
CRESST
DAMA/LIBRA
DarkSide
CJPL
PandaX
CDEX
Y2L
COSINE

Constraints on WIMP Dark Matter

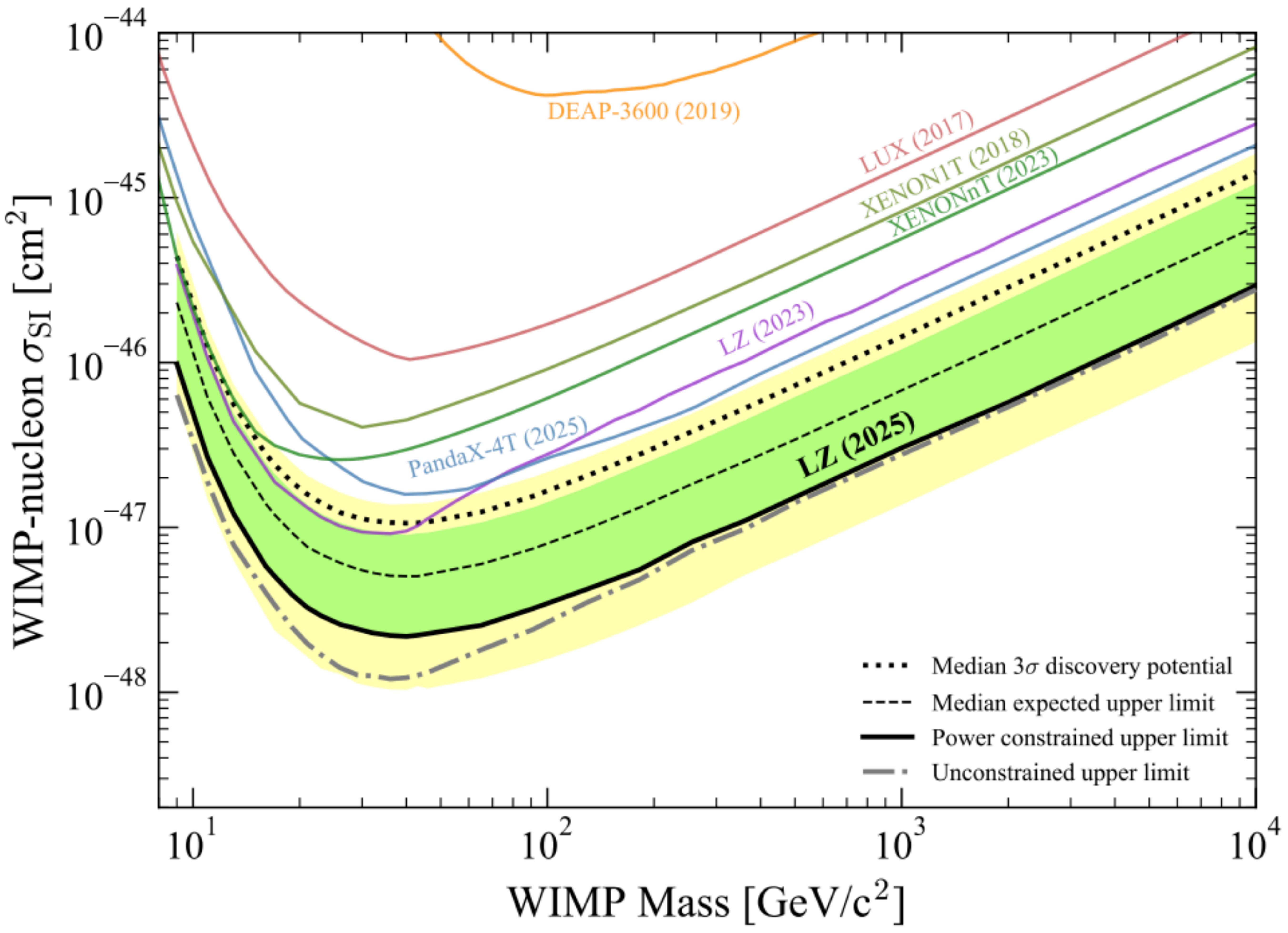

How???

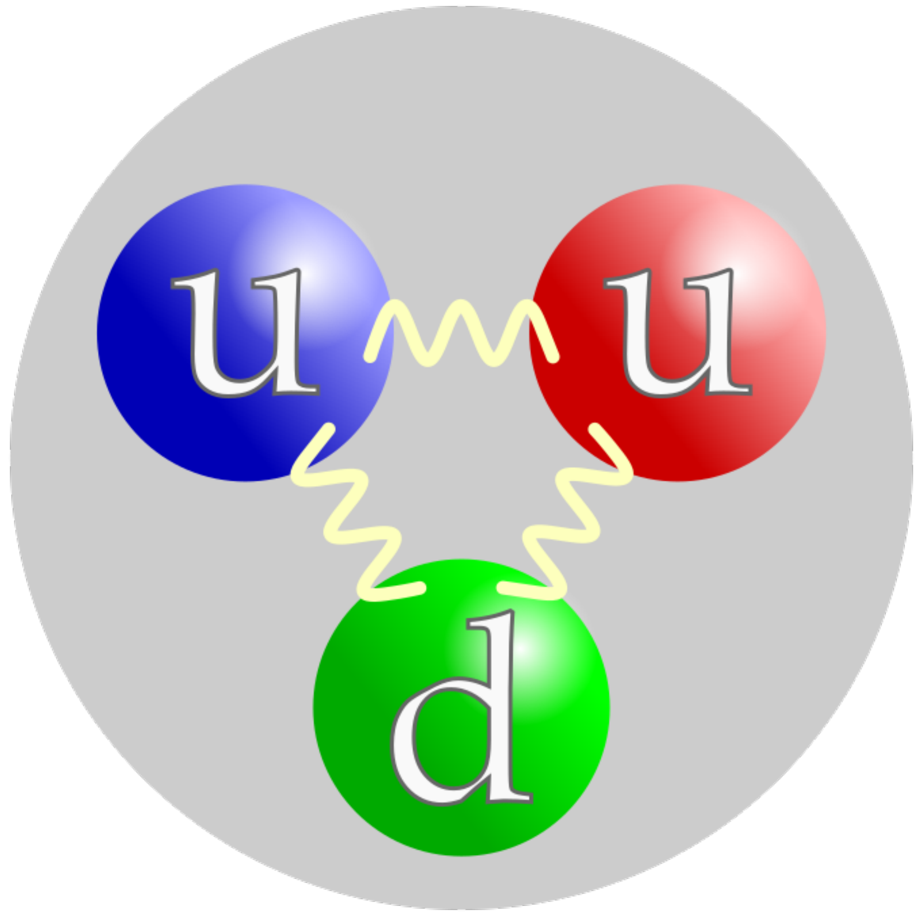

$$\sigma_p \sim 10^{-25}\ \mathrm{cm}^2$$

LZ 2207.03764

XENONnT 2303.14729
PandaX-4t 2408.00664
LZ 2410.17036

Dark Matter Distribution

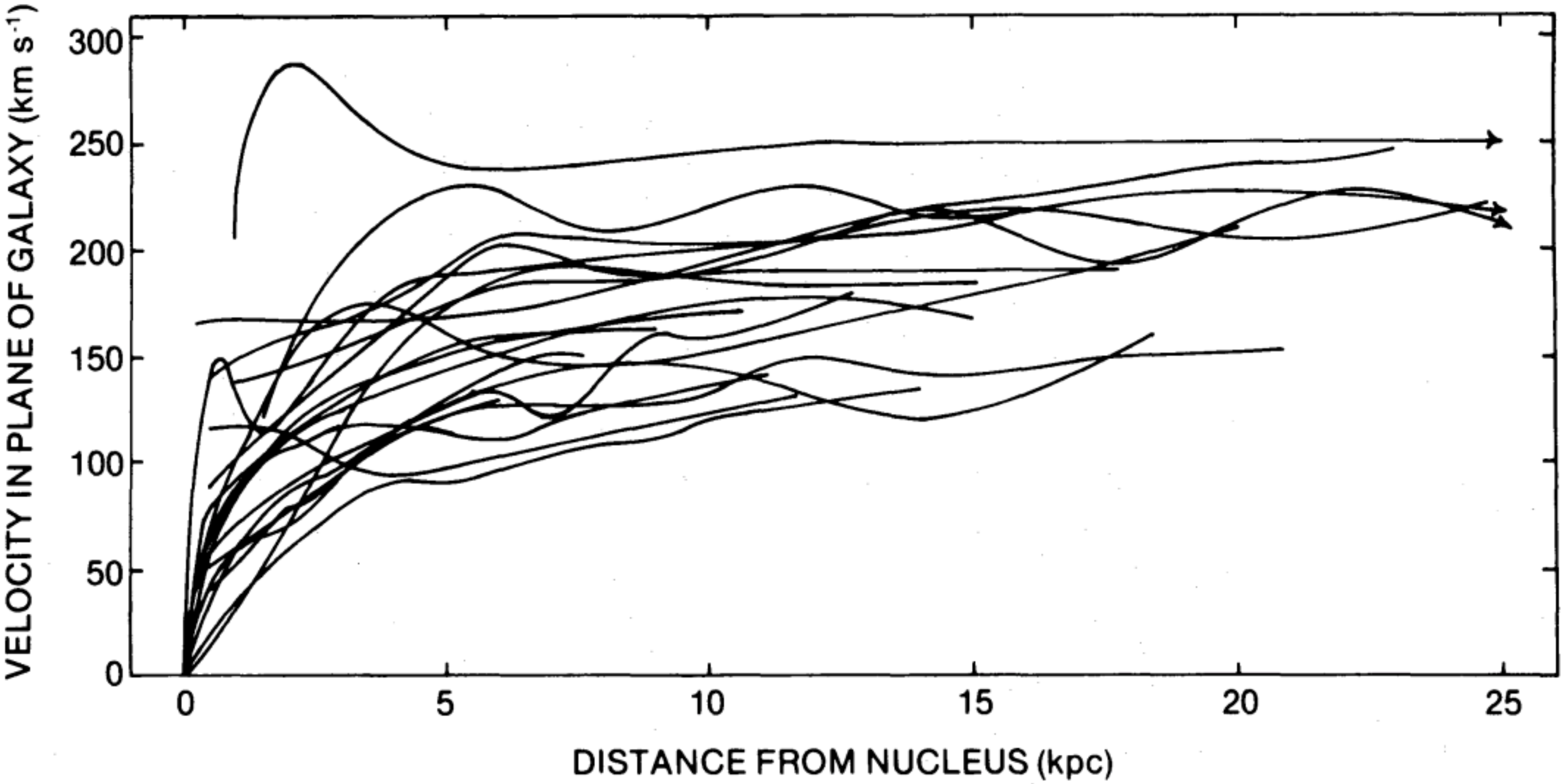

Rotation curves of spiral galaxies

Rubin et al, Atrophy’s. J. 1980

Dark Matter Distribution

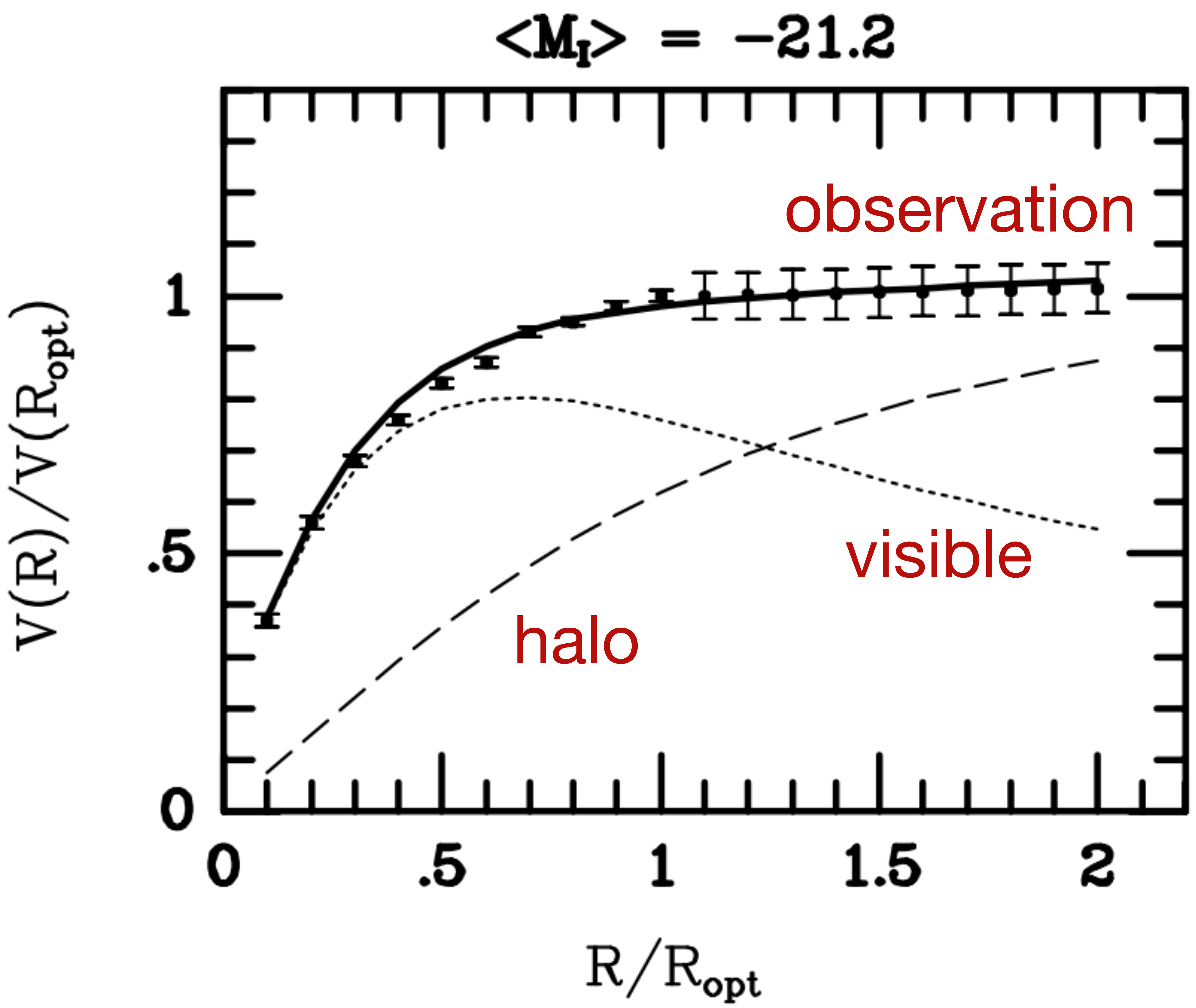

$$v_c(r) = \sqrt{\frac{GM}{r}}$$

Persic et al MNRAS 1996

Dark Matter Distribution

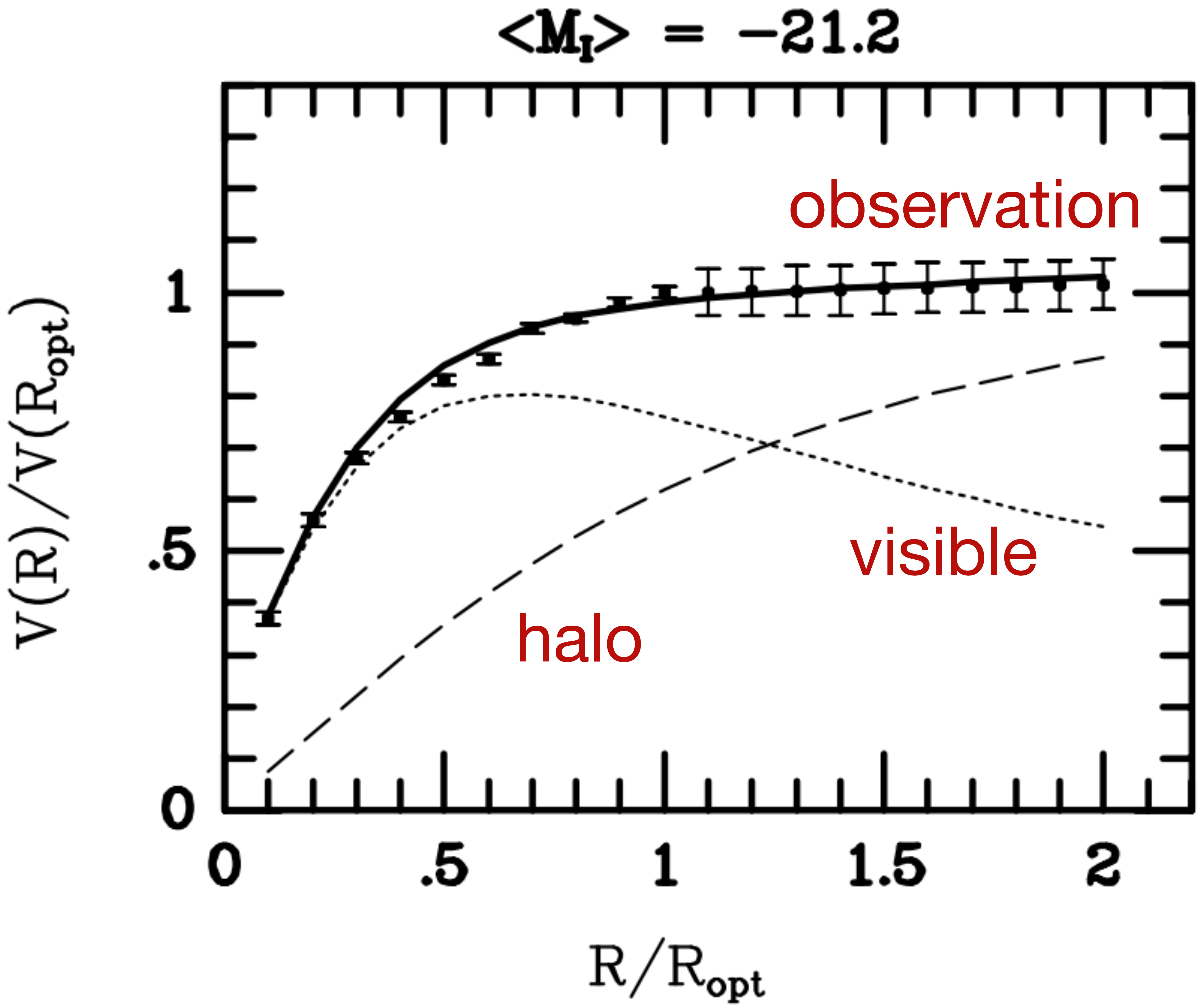

Persic et al MNRAS 1996

Milky Way

$$M_{\rm halo} \sim 10^{12}\ \mathrm{M}_\odot$$

$$\rho_0 \sim 0.3\ \mathrm{GeV/cm^3}$$

$$M_{\rm halo} \sim 4\pi \int_0^{R_{\rm halo}} dr\, r^2 \rho(r) \longrightarrow R_{\rm halo}\ ??$$

$$\langle v \rangle \sim \sqrt{\frac{G M_{\rm halo}}{R_{\rm halo}}} \quad ??$$

Dark Matter Distribution

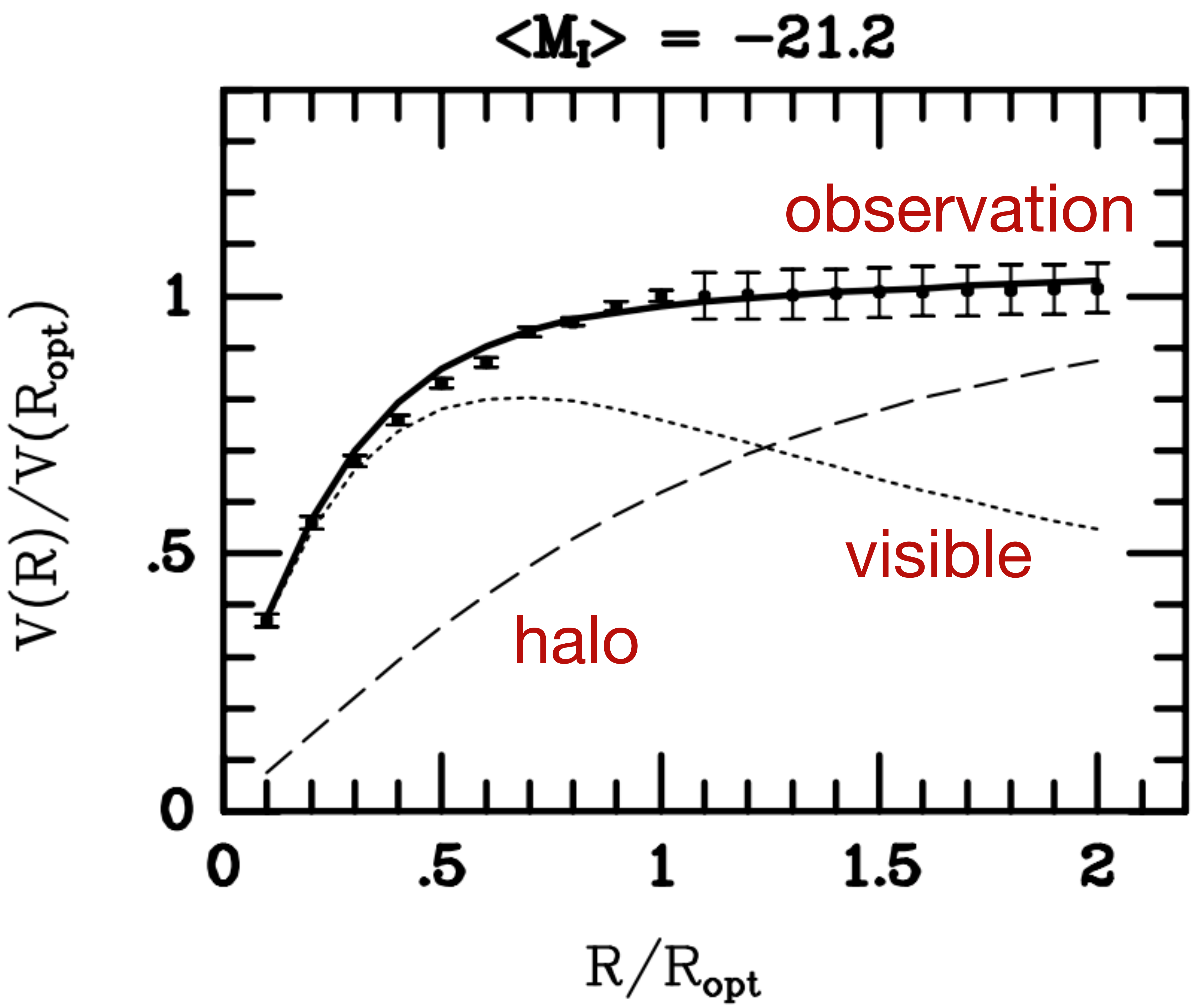

Persic et al MNRAS 1996

Milky Way

$$M_{\rm halo} \sim 10^{12}\ \mathrm{M}_\odot$$

$$\rho_0 \sim 0.3\ \mathrm{GeV/cm^3}$$

$$M_{\rm halo} \sim 4\pi \int_0^{R_{\rm halo}} dr\, r^2 \rho(r) \longrightarrow R_{\rm halo}$$

~100 kpc

$$\langle v \rangle \sim \sqrt{\frac{G M_{\rm halo}}{R_{\rm halo}}}$$

~200 km/s

Dark Matter Distribution

Boltzmann equation of the phase space

$$\mathbf{L}[f] = \mathbf{C}[f]$$

$$\frac{\partial f}{\partial t} + \dot{\mathbf{x}}\,\frac{\partial f}{\partial \mathbf{x}} + \dot{\mathbf{v}}\,\frac{\partial f}{\partial \mathbf{v}} = 0$$ ⟵ assuming DM is collisionless

Dark Matter Distribution

Boltzmann equation of the phase space

Binney, Galactic Dynamics

$$\mathbf{L}[f] = \mathbf{C}[f]$$

$$\frac{\partial f}{\partial t} + \dot{\mathbf{x}} \frac{\partial f}{\partial \mathbf{x}} + \dot{\mathbf{v}} \frac{\partial f}{\partial \mathbf{v}} = 0$$

Jeans theorem *Any steady-state solution of the collisionless Boltzmann equation depends on the phase-space coordinates only through integrals of motion in the given potential, and any function of the integrals yields a steady-state solution of the collisionless Boltzmann equation.*

$$f(\mathbf{x}, \mathbf{v}) = f(\mathcal{E})$$

$$\mathcal{E} = \Psi - \frac{1}{2} v^2$$

Let's guess!

$$f(\mathcal{E}) \propto e^{\mathcal{E}}$$

Dark Matter Distribution

Boltzmann equation of the phase space

$$\mathbf{L}[f] = \mathbf{C}[f]$$

$$f(\mathbf{x}, \mathbf{v}) = f(\mathcal{E}) \qquad \mathcal{E} = \Psi - \frac{1}{2}v^2$$

$$\frac{\partial f}{\partial t} + \dot{\mathbf{x}}\frac{\partial f}{\partial \mathbf{x}} + \dot{\mathbf{v}}\frac{\partial f}{\partial \mathbf{v}} = 0$$

$$f(\mathcal{E}) \propto e^{\mathcal{E}}$$

$$\rho \propto \int_0^\infty dv\, v^2\, f(v) = \int_0^\infty dv\, v^2\, \exp\left(\frac{\Psi - v^2/2}{\sigma^2}\right) \propto e^{\Psi/\sigma^2}$$

Dark Matter Distribution

Boltzmann equation of the phase space

$$\mathbf{L}[f] = \mathbf{C}[f]$$

$$f(\mathbf{x}, \mathbf{v}) = f(\mathcal{E}) \qquad \mathcal{E} = \Psi - \frac{1}{2}v^2$$

$$\frac{\partial f}{\partial t} + \dot{\mathbf{x}}\,\frac{\partial f}{\partial \mathbf{x}} + \dot{\mathbf{v}}\,\frac{\partial f}{\partial \mathbf{v}} = 0$$

$$f(\mathcal{E}) \propto e^{\mathcal{E}}$$

$$\rho \propto \int_0^\infty dv\, v^2\, f(v) = \int_0^\infty dv\, v^2\, \exp\left(\frac{\Psi - v^2/2}{\sigma^2}\right) \propto e^{\Psi/\sigma^2}$$

$$\nabla^2\Psi = -4\pi G\rho \longrightarrow \rho(r) = \frac{\sigma^2}{2\pi G r^2}$$

$$\rho(r) \propto 1/r^2$$

Dark Matter Distribution

$$\rho \propto \int_0^\infty dv\, v^2 f(v) = \int_0^\infty dv\, v^2 \exp\left(\frac{\Psi - v^2/2}{\sigma^2}\right) \propto e^{\Psi/\sigma^2}$$

$$\nabla^2\Psi = -4\pi G\rho \longrightarrow \rho(r) = \frac{\sigma^2}{2\pi G r^2}$$

$$\rho(r) \propto 1/r^2$$

$$M_{\rm halo} \sim 4\pi \int_0^{R_{\rm halo}} dr\, r^2 \rho(r) \longrightarrow R_{\rm halo}$$

$$\langle v \rangle \sim \sqrt{\frac{G M_{\rm halo}}{R_{\rm halo}}}$$

$$M(r) = \frac{2\sigma^2 r}{G}$$

$$v_0 = v_c = \sqrt{2}\sigma$$

Maxwell-Boltzmann distribution

$$f \sim \frac{1}{(\pi v_0)^{3/2}} e^{-v^2/v_0^2}$$

Dark Matter Distribution

Cohen et al, 1307. 4082

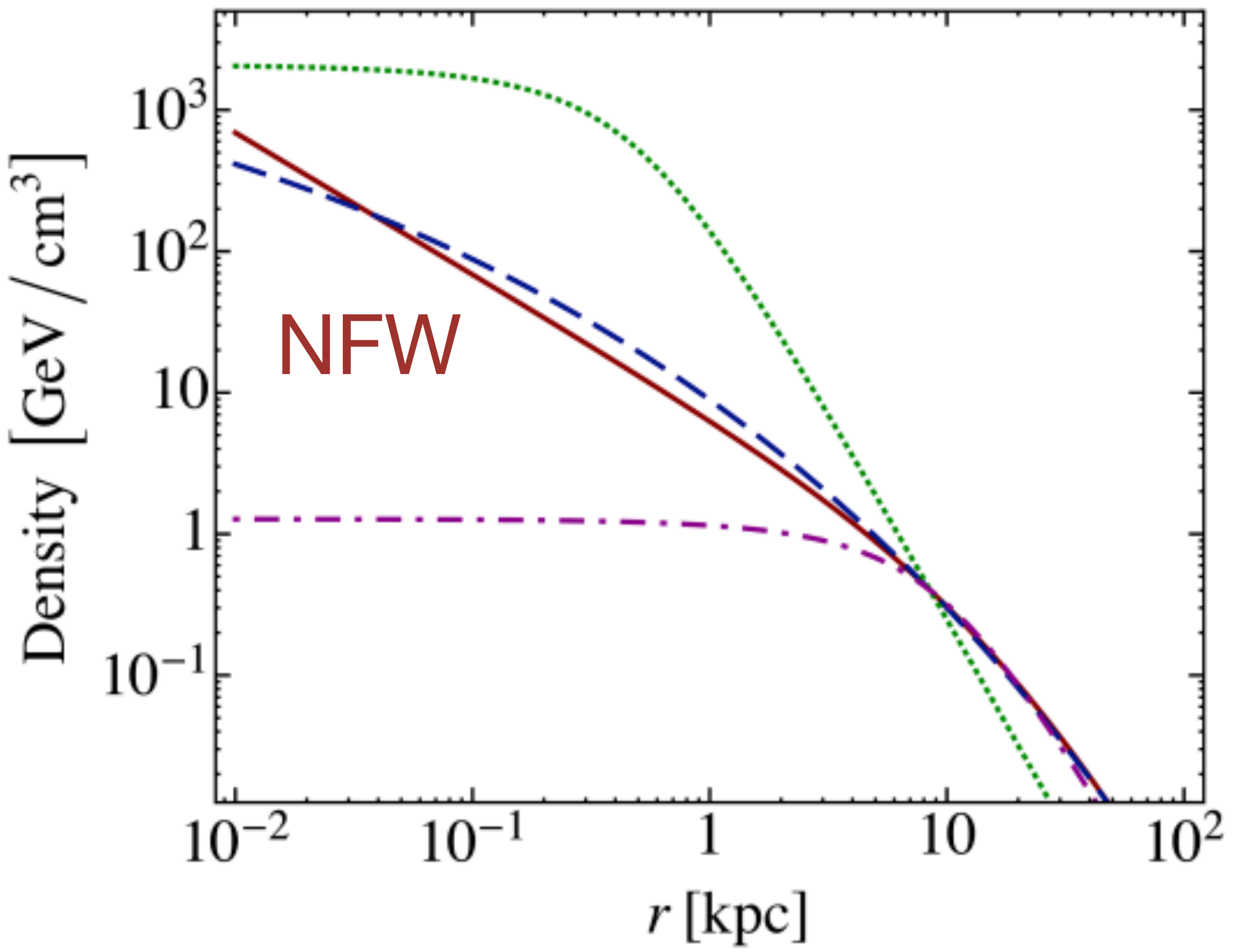

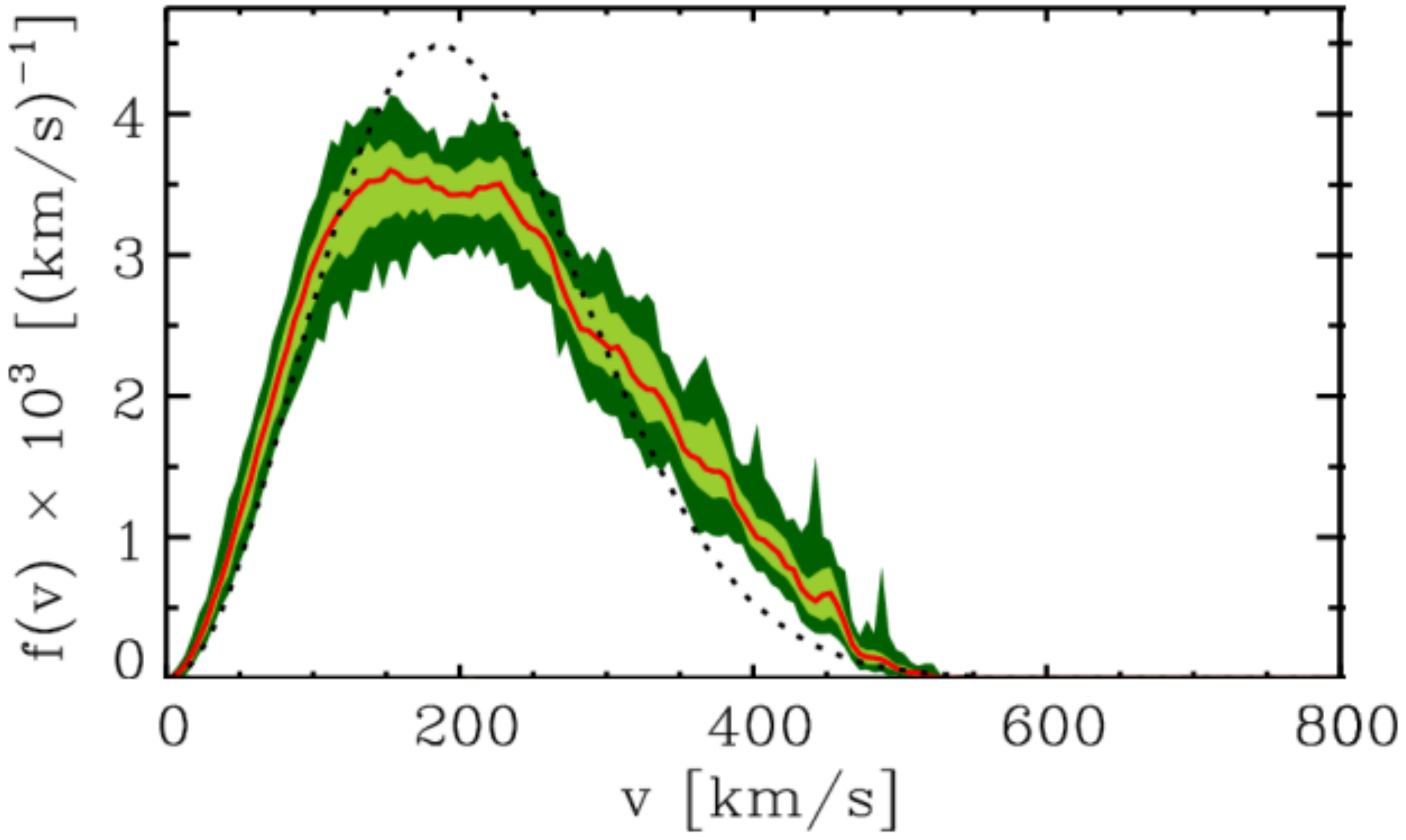

Navarro-Frenk-White (NFW)

$$\rho_{\rm NFW}(r) = \frac{\rho_0}{r/r_s(1 + r/r_s)^2}$$

Einasto

$$\rho_{\rm Ein}(r) = \rho_0 \exp\left[-\frac{2}{\gamma}\left(\left(\frac{r}{r_s}\right)^\gamma - 1\right)\right]$$

Burkert

$$\rho_{\rm Burk}(r) = \frac{\rho_0}{(1 + r/r_s)(1 + (r/r_s)^2)}$$

Exercise: Kinematics

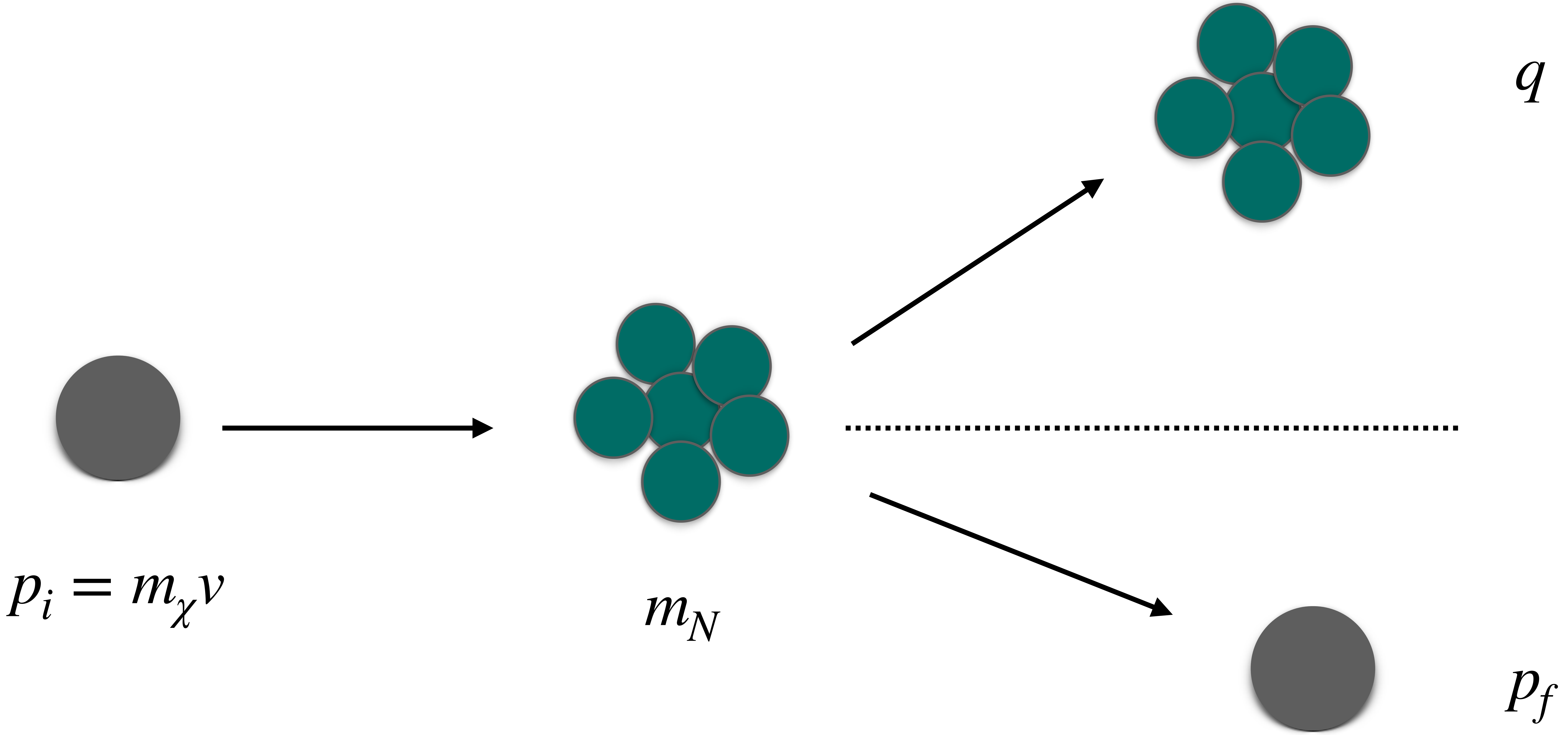

Recoil energy of the nucleus?

Kinematics

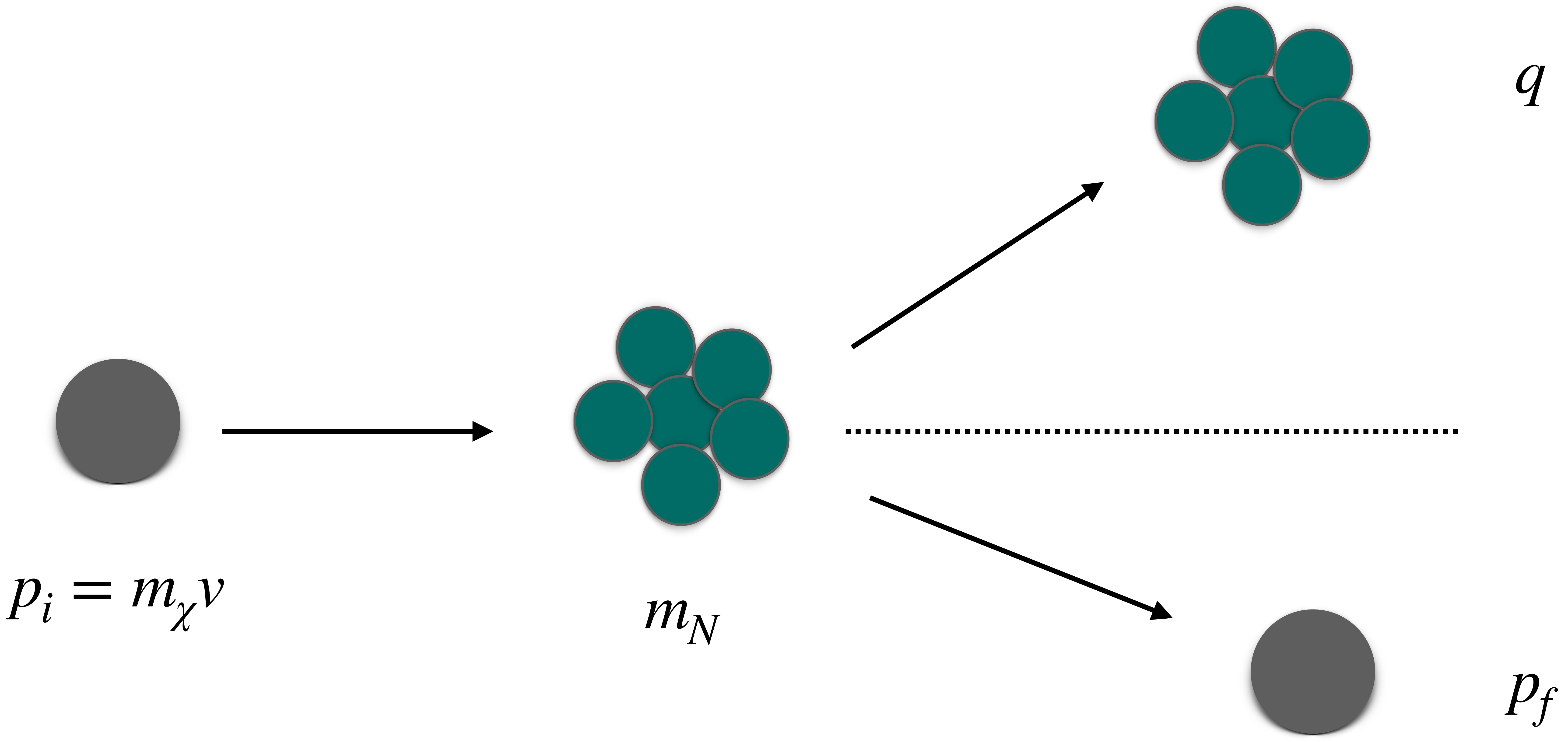

$$q = 2\mu_{\chi N} v \cos\theta \qquad \mu_{\chi N} = \frac{m_\chi m_N}{m_\chi + m_N} \sim m_N \quad \text{if } m_\chi \gg m_N$$

$$v \sim 300 \text{ km/s} \sim 10^{-3} c \qquad E_R \sim 50 \text{ keV} \quad \text{if } m_N \sim 50 \text{ GeV}$$

Dark Matter Scattering Cross Section

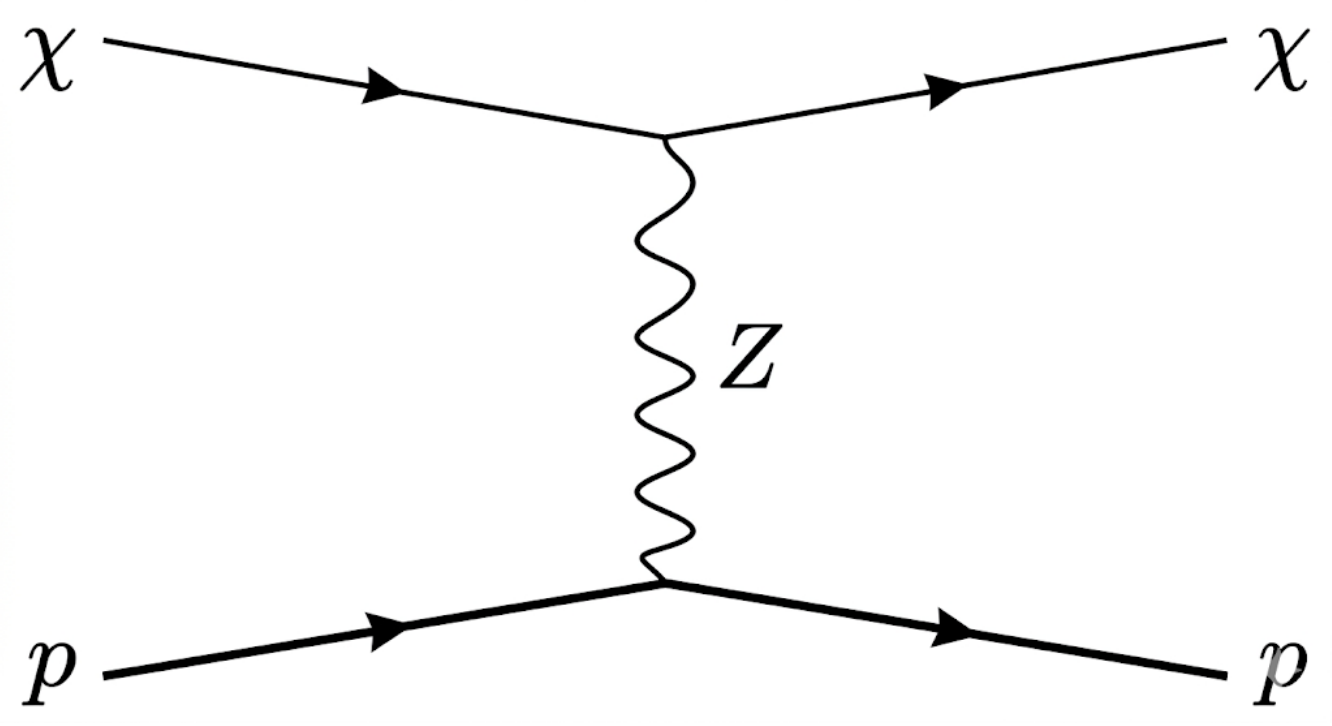

Dark matter scatters though the Z boson mediator

$$\sigma_{\chi N} = \frac{g^4 m_\chi^2 m_N^2}{4\pi(m_\chi + m_N)^2} \frac{(Zf_p + (A-Z)f_n)^2}{m_Z^4} F^2(E_R)$$

$$\sigma_{\chi p} = \frac{g^4 m_\chi^2 m_p^2}{4\pi(m_\chi + m_p)^2} \frac{1}{m_Z^4}$$

form factor

$$\sigma_{\chi N} = \sigma_{\chi p} \frac{\mu_{\chi N}^2}{\mu_{\chi p}^2} \frac{(Zf_p + (A-Z)f_n)^2}{f_p^2} F^2(E_R) \sim A^4 \sigma_{\chi p}$$

The Form Factors

$$\sigma_{\chi N} = \sigma_{\chi p} \frac{\mu_{\chi N}^2}{\mu_{\chi p}^2} \frac{(Zf_p + (A - Z)f_n)^2}{f_p^2} F^2(E_R)$$

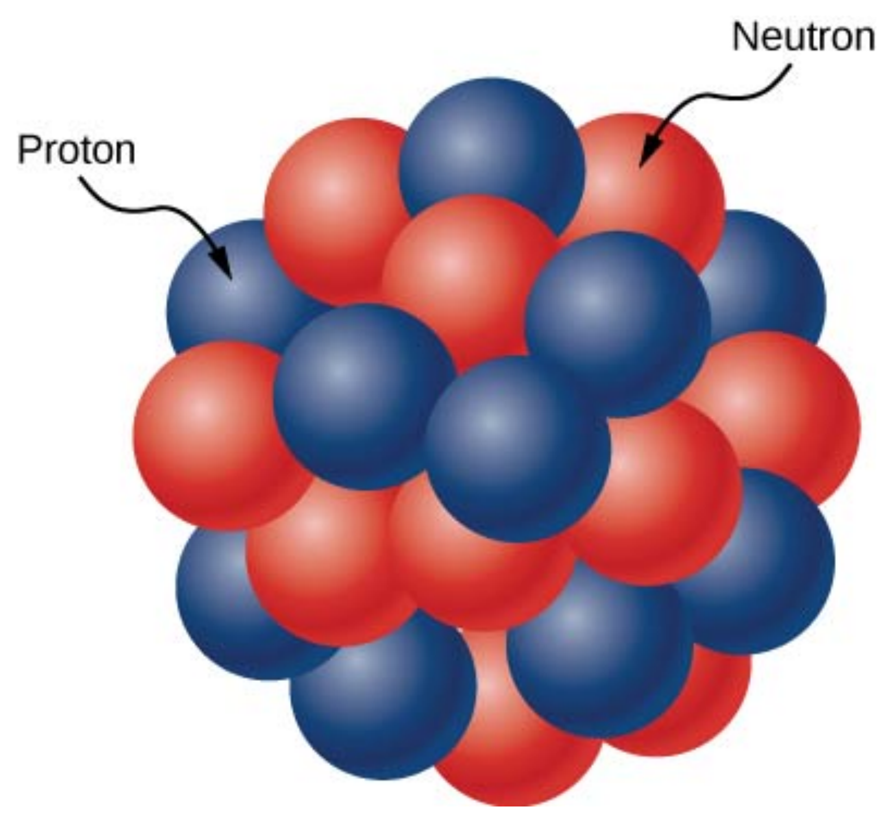

$$F(q) = \frac{1}{M} \int \rho_{\text{mass}}(r) e^{-i\mathbf{q}\cdot\mathbf{r}} d^3 r$$

$$\rho_U(r) = \begin{cases} \frac{3Ze}{4\pi R^3}, & r < R, \\ 0, & r > R, \end{cases}$$

assuming constant nucleon density distribution

$$F(q) = \frac{3j_1(qR)}{qR} e^{-(qs)^2/2}$$

$$j_1(x) = \frac{\sin x}{x^2} - \frac{\cos x}{x}$$

The Form Factors

$$F(q) = \frac{3j_1(qR)}{qR}e^{-(qs)^2/2}$$

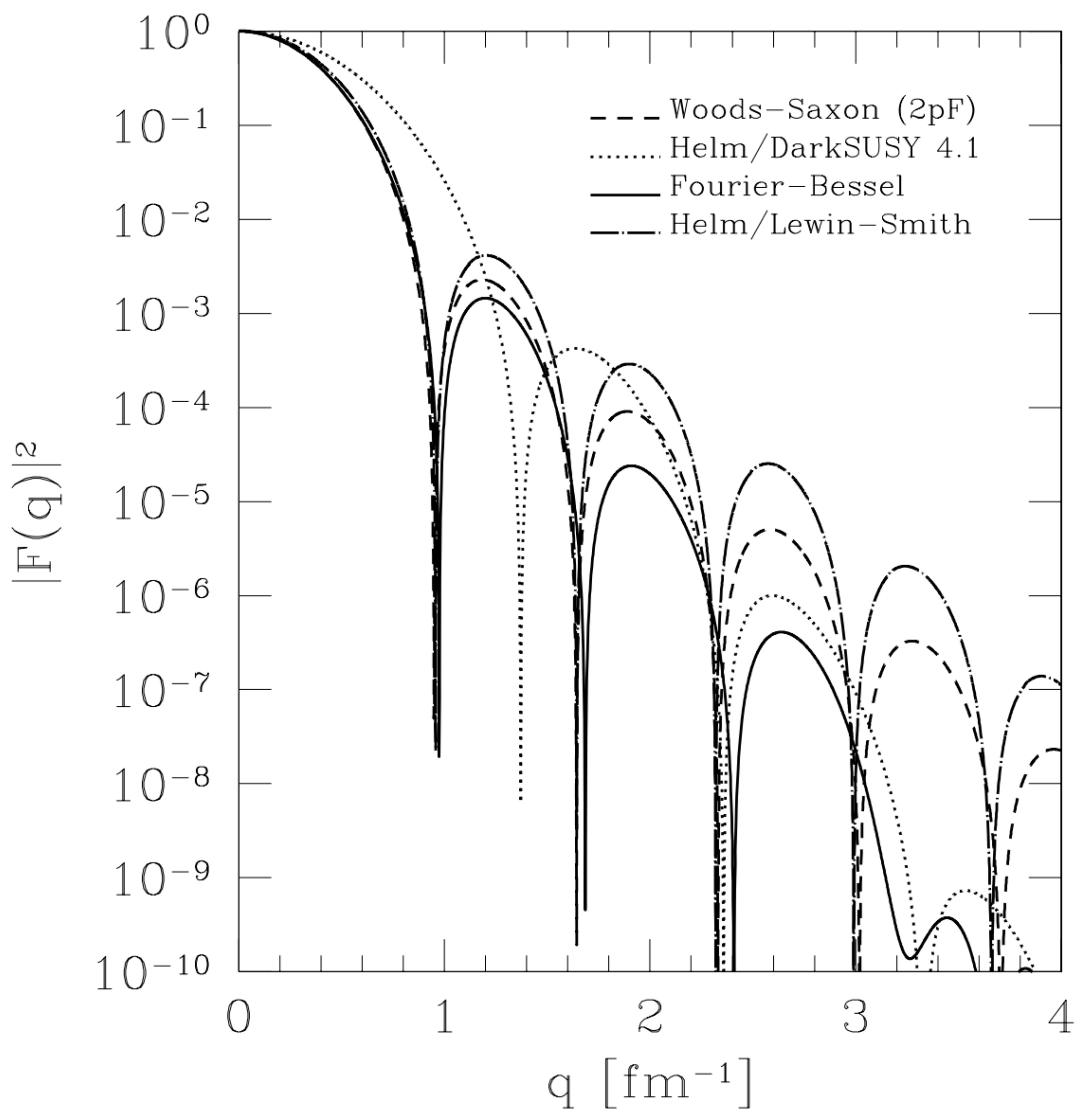

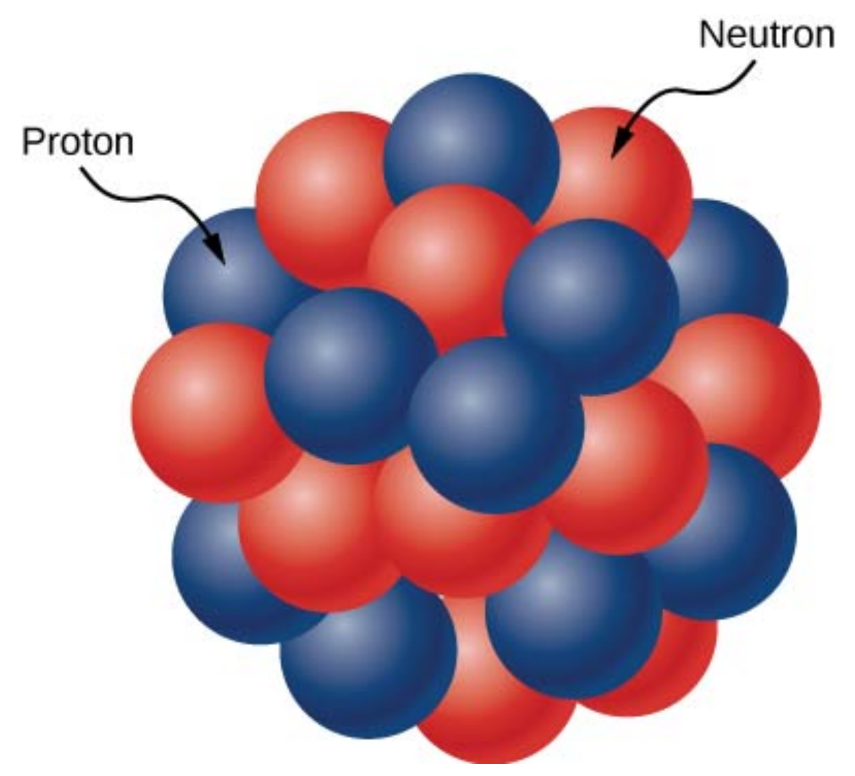

The form factor measures how coherent it is to scatter with the nucleons in the nucleus

Duda et al, hep-ph/0608035

Spin-dependent Form Factors

Spin-independent $\mathcal{O}_{SI} = (\bar{\chi}\gamma_\mu\chi)(\bar{q}\gamma^\mu q)$

Spin-dependent $\mathcal{O}_{SD} = (\bar{\chi}\gamma_\mu\gamma_5\chi)(\bar{q}\gamma^\mu\gamma_5 q)$

$$\sigma_{j,0}^{\mathrm{SD}} = \left(\frac{\mu_{A_j}}{\mu_N}\right)^2 S_{J_j}\left(a_p\langle S_p\rangle + a_n\langle S_n\rangle\right)^2 \sigma_{\chi N}^{\mathrm{SD}} \qquad N = n, p$$

$$S_A(q) = a_0^2 S_{00}(q) + a_0 a_1 S_{01}(q) + a_1^2 S_{11}(q).$$

$$S_A(0) = \frac{(2J+1)(J+1)}{4\pi J} \times |(a_0 + a_1')\langle \mathbf{S}_\mathrm{p}\rangle + (a_0 - a_1')\langle \mathbf{S}_\mathrm{n}\rangle|^2$$

$$\sigma_{\chi A}^{SD} \sim A^2 \sigma_{\chi p}^{SD}$$

Spin-dependent Form Factors

$$S_A(q) = a_0^2 S_{00}(q) + a_0 a_1 S_{01}(q) + a_1^2 S_{11}(q).$$

$$S_A(0) = \frac{(2J+1)(J+1)}{4\pi J} \times |(a_0 + a_1')\langle \mathbf{S}_\mathrm{p} \rangle + (a_0 - a_1')\langle \mathbf{S}_\mathrm{n} \rangle|^2$$

	^{129}Xe		^{131}Xe		^{127}I		^{73}Ge		^{29}Si		^{27}Al		^{23}Na		^{19}F	
	$\langle \mathbf{S}_n \rangle$	$\langle \mathbf{S}_p \rangle$	$\langle \mathbf{S}_n \rangle$	$\langle \mathbf{S}_p \rangle$	$\langle \mathbf{S}_n \rangle$	$\langle \mathbf{S}_p \rangle$	$\langle \mathbf{S}_n \rangle$	$\langle \mathbf{S}_p \rangle$	$\langle \mathbf{S}_n \rangle$	$\langle \mathbf{S}_p \rangle$	$\langle \mathbf{S}_n \rangle$	$\langle \mathbf{S}_p \rangle$	$\langle \mathbf{S}_n \rangle$	$\langle \mathbf{S}_p \rangle$	$\langle \mathbf{S}_n \rangle$	$\langle \mathbf{S}_p \rangle$
This work	0.329	0.010	−0.272	−0.009	0.031	0.342	0.439	0.031	0.156	0.016	0.038	0.326	0.024	0.224	−0.002	0.478
(Int. 1)							0.450	0.006								
[20] (Bonn A)	0.359	0.028	−0.227	−0.009	0.075	0.309							0.020	0.248		
[20] (Nijm. II)	0.300	0.013	−0.217	−0.012	0.064	0.354										
[18]											0.030	0.343				
[17]							0.468	0.011	0.13	−0.002						
[19]							0.378	0.030								
[23]	0.273	−0.002	−0.125	$-7{\cdot}10^{-4}$	0.030	0.418										
[22]					0.038	0.330	0.407	0.005					0.020	0.248		
[21]									0.133	−0.002			0.020	0.248	−0.009	0.475
[13]	0.248	0.007	−0.199	−0.005	0.066	0.264	0.475	0.008					0.020	0.248	−0.009	0.475

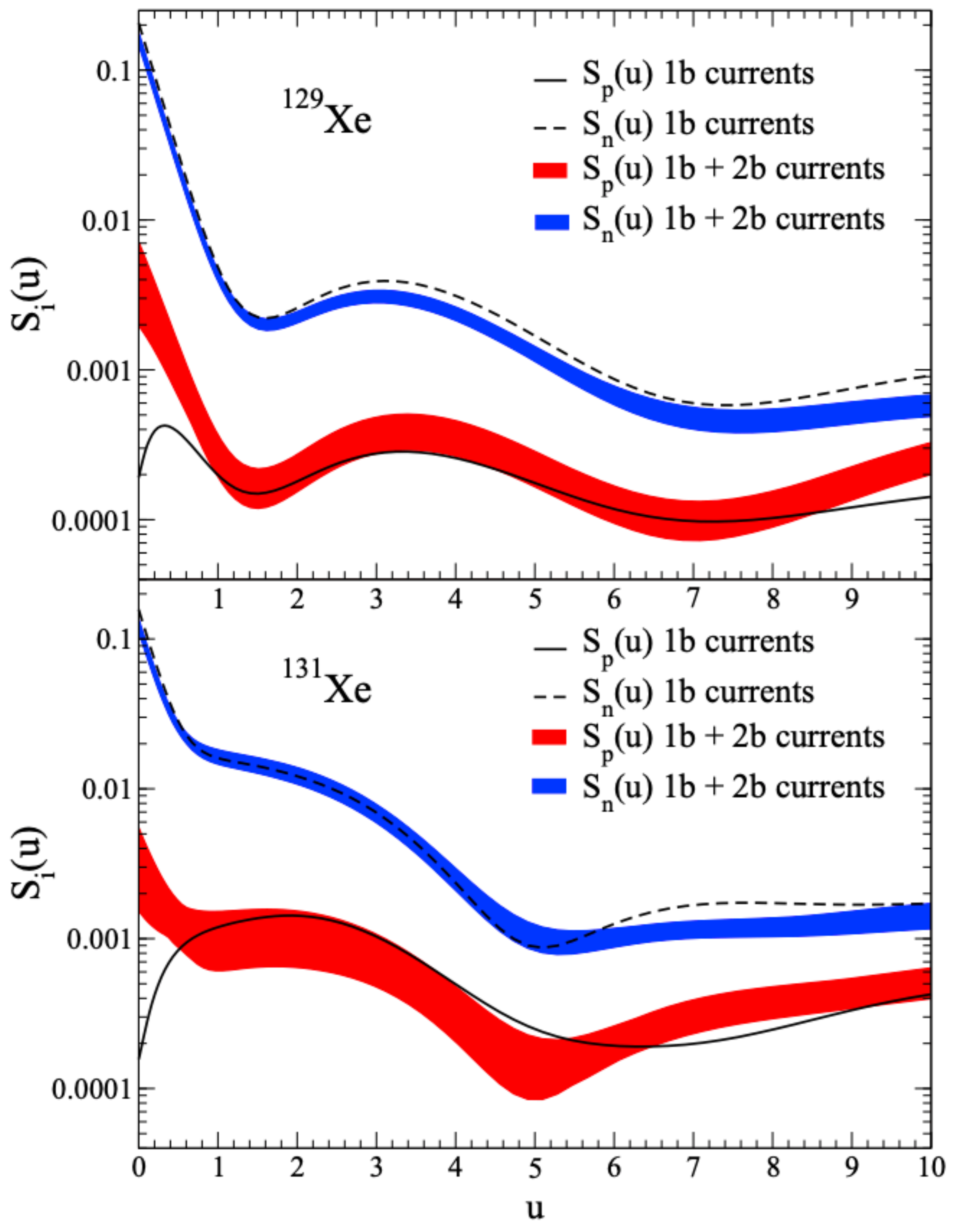

Klos et al, 1304.7684

Xenon Experiments

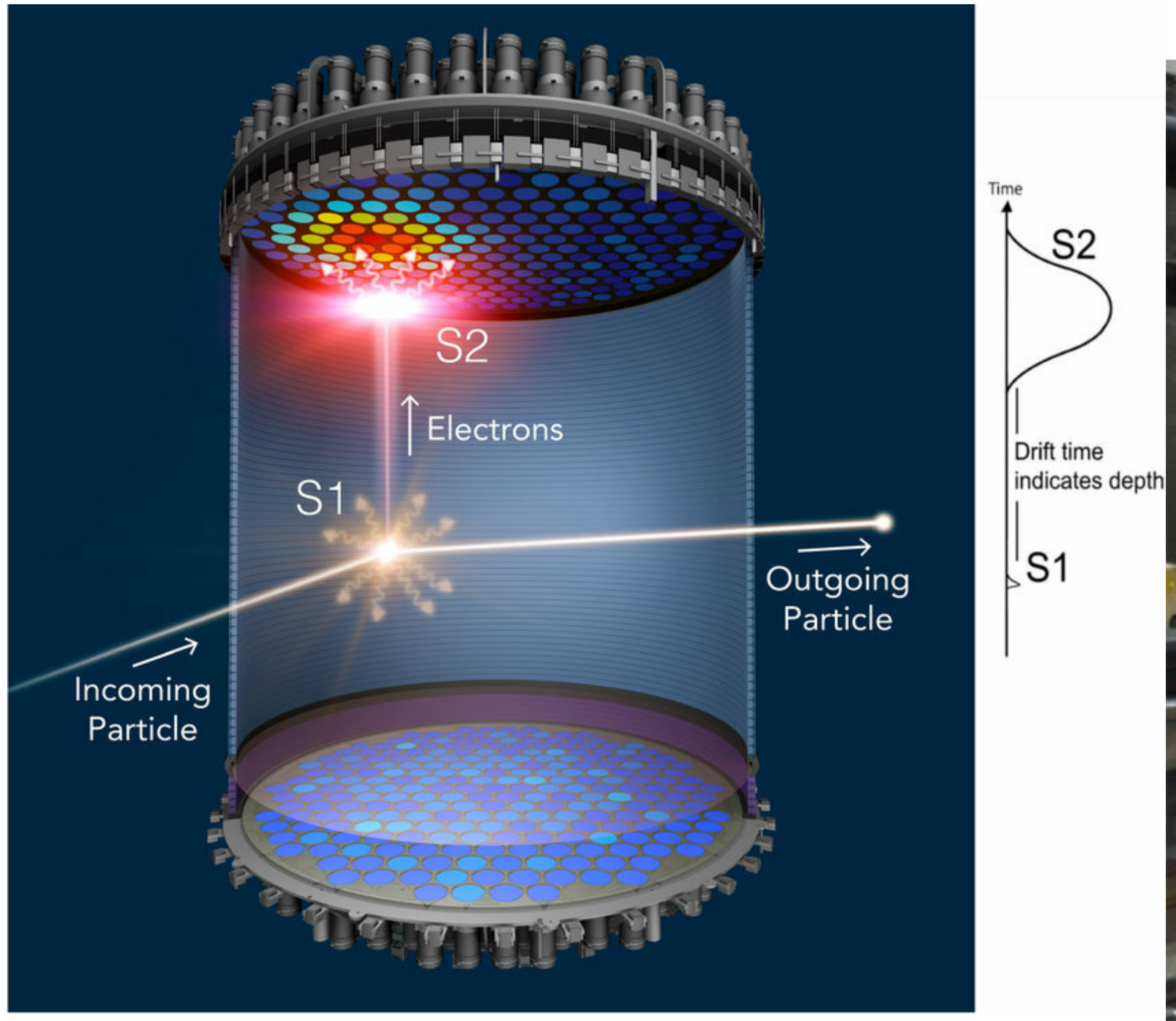

- Particle interacts and produces the prompt scintillation signal (S1), and the electrons drifted to the top generate the delayed scintillation signal (S2)
- The ratio of S1 and S2 can be used to distinguish different particles, or electron vs nuclear recoil

The Scattering Rate

$$\Gamma = n\sigma v$$

number of target nuclei

detection efficiency

$$N_{\exp} = \sum_i N_i T \frac{\rho_\chi}{m_\chi} \int u_f f(u_f) du_f \int \frac{d\sigma_i}{dE_R} \epsilon(E_R) dE_R$$

dark matter velocity distribution

Constraints on WIMP Dark Matter

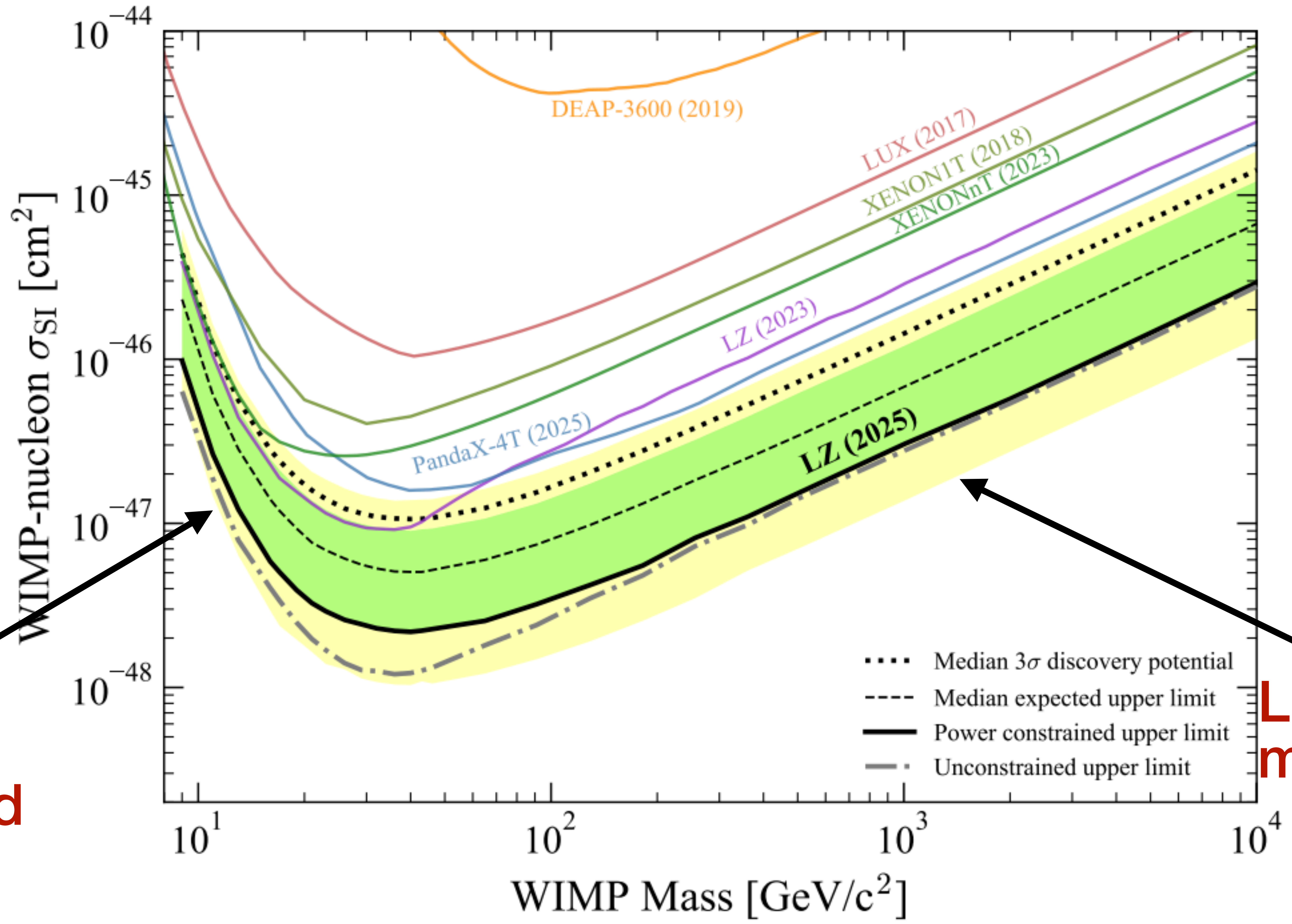

Limited by the detection threshold

Limited by the dark matter flux

How???

Strongly Interacting Dark Matter

Are the above all excluded???

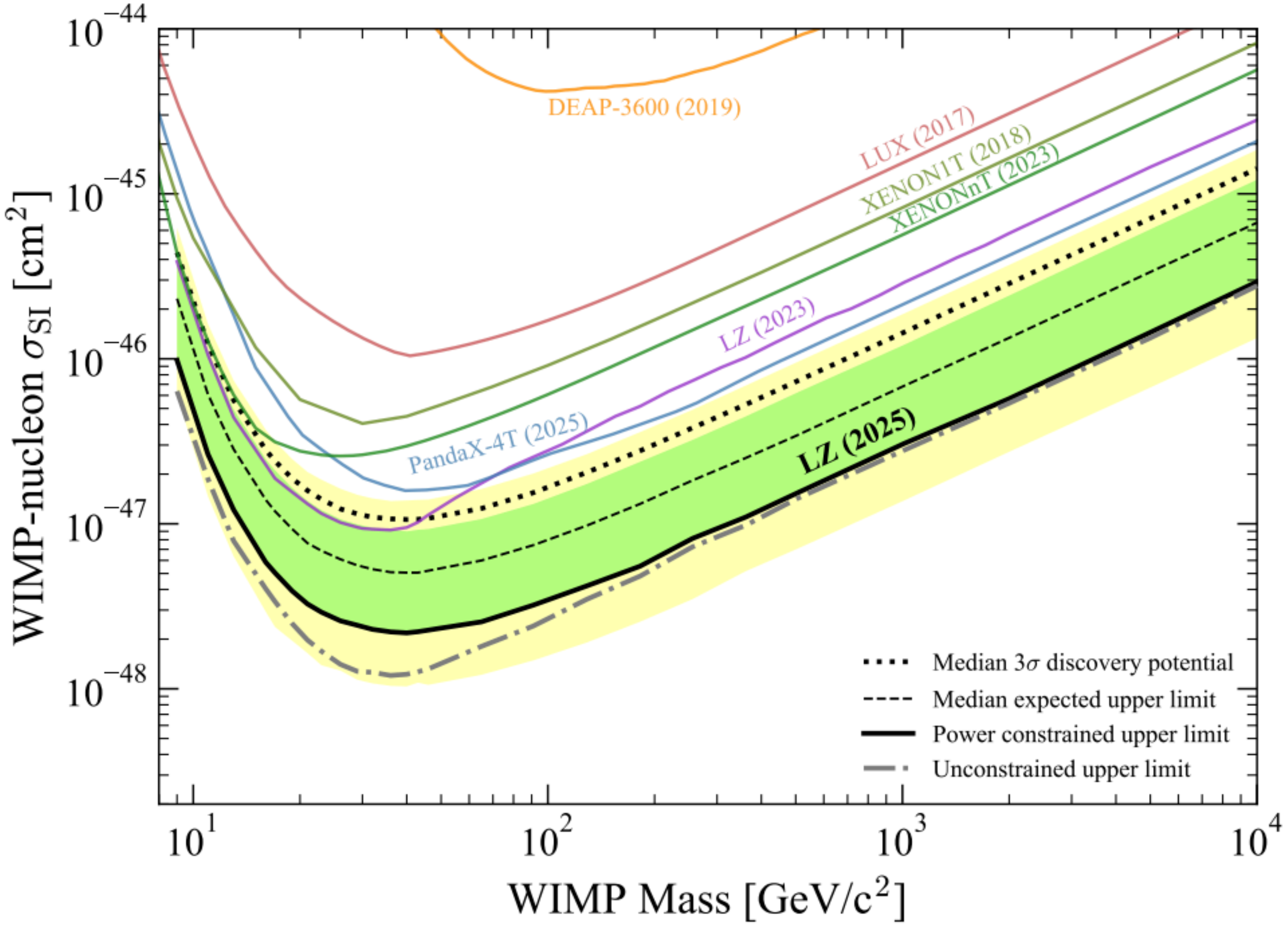

Overburden

$$N_{\rm exp} = \sum_i N_i T \frac{\rho_\chi}{m_\chi} \int u_f f(u_f) du_f \int \frac{d\sigma_i}{dE_R} \epsilon(E_R) dE_R$$

dark matter velocity distribution

Dark matter velocity distribution at the underground detector could be different from the halo

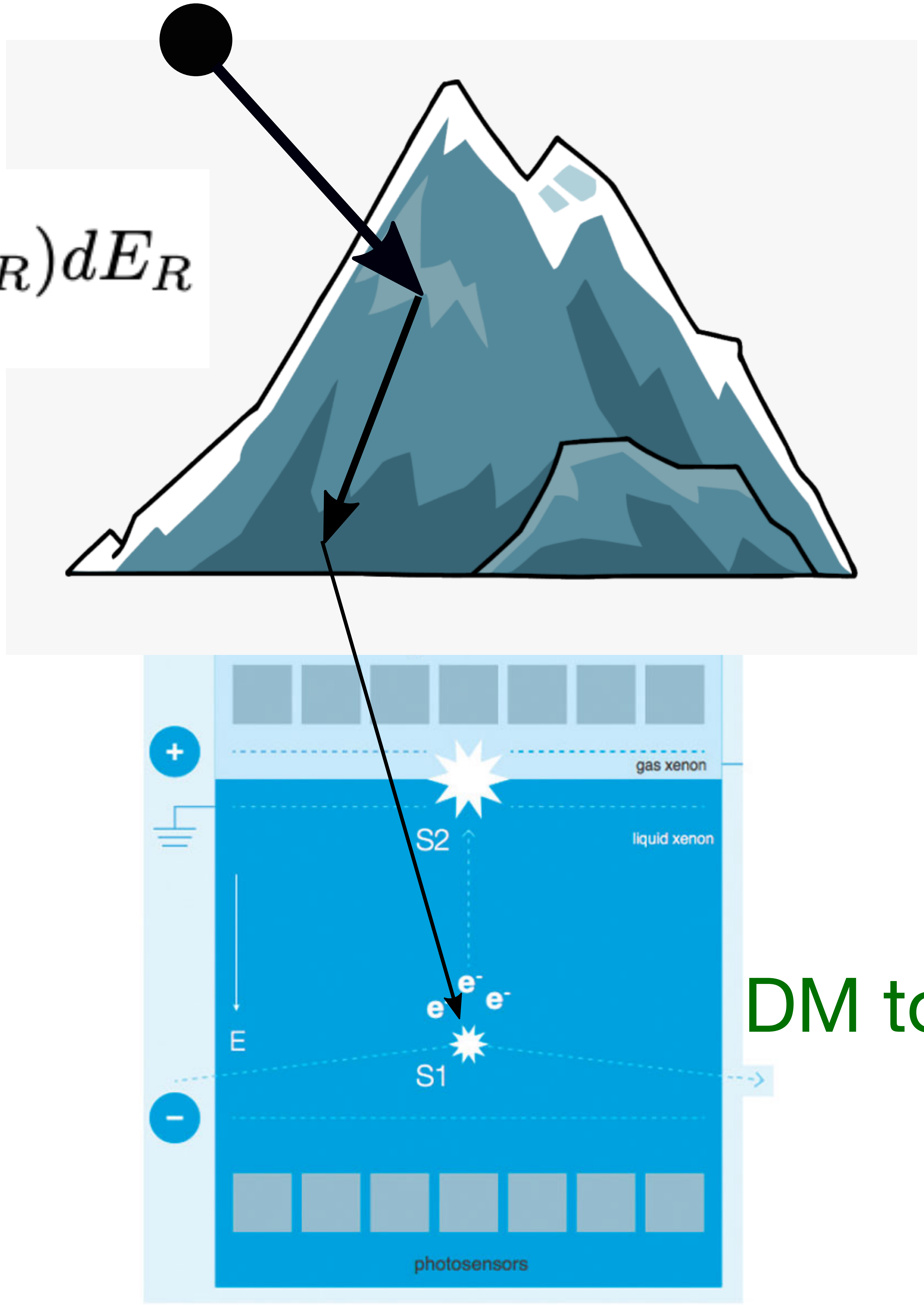

DM too slow?

Overburden

$$\tilde{f}(\mathbf{v}_f)\,\mathrm{d}^3\mathbf{v}_f = f(\mathbf{v}_i)\,\mathrm{d}^3\mathbf{v}_i$$

$$\Rightarrow \tilde{f}(\mathbf{v}_f)v_f^2\,\mathrm{d}v_f\,\mathrm{d}\hat{\mathbf{v}}_f^2 = f(\mathbf{v}_i)v_i^2\,\mathrm{d}v_i\,\mathrm{d}\hat{\mathbf{v}}_f^2$$

$$\Rightarrow \tilde{f}(\mathbf{v}_f) = f(\mathbf{v}_i)\left(\frac{v_i^2}{v_f^2}\right)\frac{\mathrm{d}v_i}{\mathrm{d}v_f}\,,$$

$$\frac{\mathrm{d}\langle E_\chi\rangle}{\mathrm{d}t} = -\sum_i n_i(\mathbf{r})\,\langle E_R\rangle_i\,\sigma_i(v)\,v\,, \qquad \langle E_R\rangle_i = \frac{1}{\sigma_i(v)}\int_0^{E_i^{\mathrm{max}}} E_R\frac{\mathrm{d}\sigma_i}{\mathrm{d}E_R}\,\mathrm{d}E_R\,.$$

$$N_{\mathrm{scat}} = \sum_i n_i\sigma_i L \approx 500\left(\frac{\sigma_p^{\mathrm{SI}}}{10^{-28}\,\mathrm{cm}^2}\right)\left(\frac{D}{\mathrm{m}}\right)$$

$$\frac{\mathrm{d}v}{\mathrm{d}D} = -\frac{v}{m_\chi\mu_{\chi p}^2}\sigma_p^{\mathrm{SI}}\sum_i^{\mathrm{species}} n_i(\mathbf{r})\frac{\mu_{\chi i}^4}{m_i}A_i^2C_i(m_\chi, v)$$

$$\approx -m_p v\left(\frac{\sigma_p^{\mathrm{SI}}}{m_\chi}\right)\sum_i^{\mathrm{species}} n_i(\mathbf{r})A_i^5C_i(m_\chi\to\infty, v)\,,$$

Overburden

$$\frac{\mathrm{d}v}{\mathrm{d}D} = -\frac{v}{m_\chi \mu_{\chi p}^2}\sigma_p^{\mathrm{SI}} \sum_i^{\mathrm{species}} n_i(\mathbf{r})\frac{\mu_{\chi i}^4}{m_i} A_i^2 C_i(m_\chi, v)$$

$$\approx -m_p v \left(\frac{\sigma_p^{\mathrm{SI}}}{m_\chi}\right) \sum_i^{\mathrm{species}} n_i(\mathbf{r}) A_i^5 C_i(m_\chi \to \infty, v)\,;$$

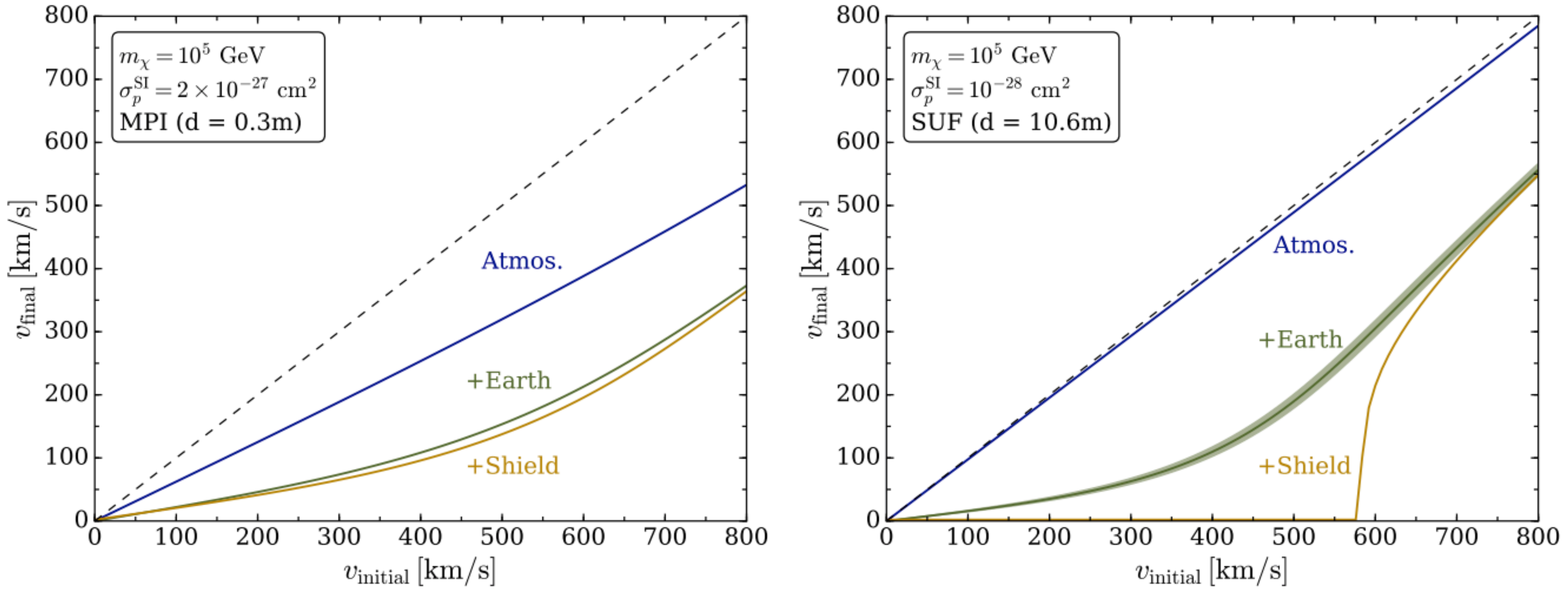

Kavanagh, arXiv:1712.04901

Overburden

$$\frac{\mathrm{d}v}{\mathrm{d}D} = -\frac{v}{m_\chi \mu_{\chi p}^2} \sigma_p^{\mathrm{SI}} \sum_i^{\mathrm{species}} n_i(\mathbf{r}) \frac{\mu_{\chi i}^4}{m_i} A_i^2 C_i(m_\chi, v)$$

$$\approx -m_p v \left(\frac{\sigma_p^{\mathrm{SI}}}{m_\chi}\right) \sum_i^{\mathrm{species}} n_i(\mathbf{r}) A_i^5 C_i(m_\chi \to \infty, v)\,,$$

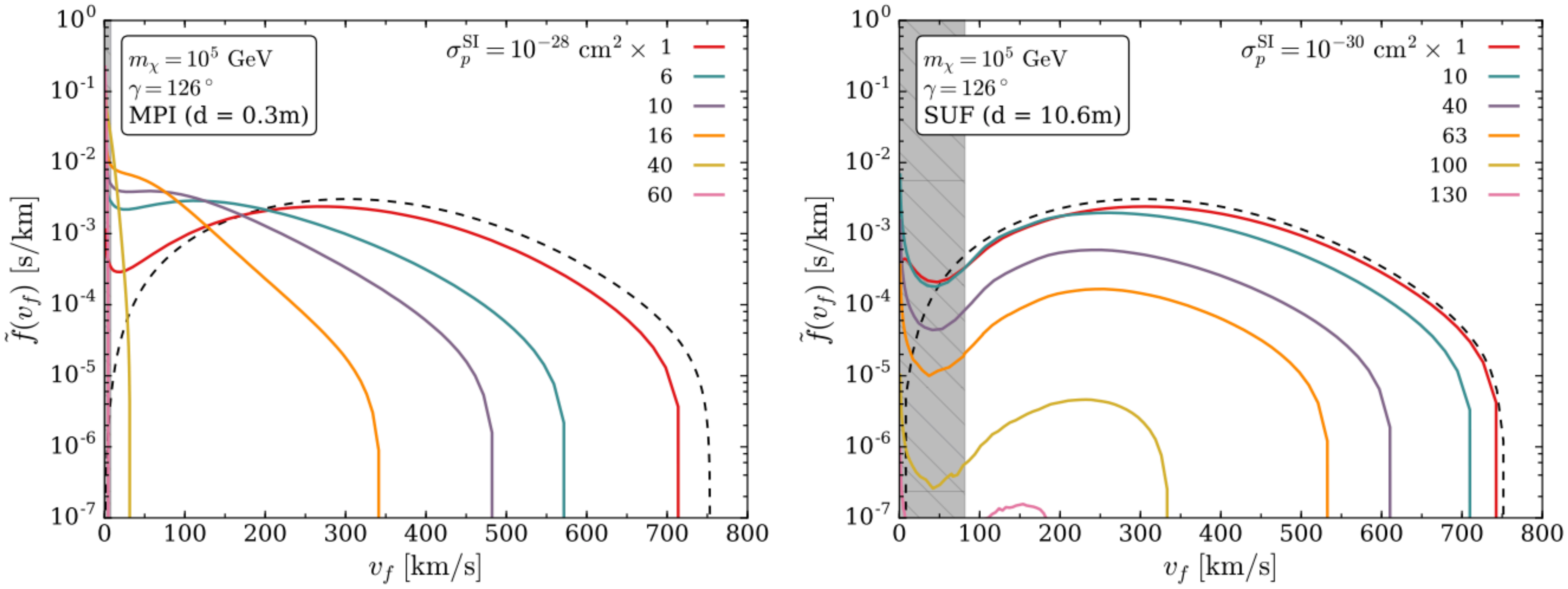

Kavanagh, arXiv:1712.04901

Overburden

$$N_{\mathrm{exp}} = \sum_i N_i T \frac{\rho_\chi}{m_\chi} \int u_f f(u_f) du_f \int \frac{d\sigma_i}{dE_R} \epsilon(E_R) dE_R$$

dark matter velocity distribution

minimum exclusion

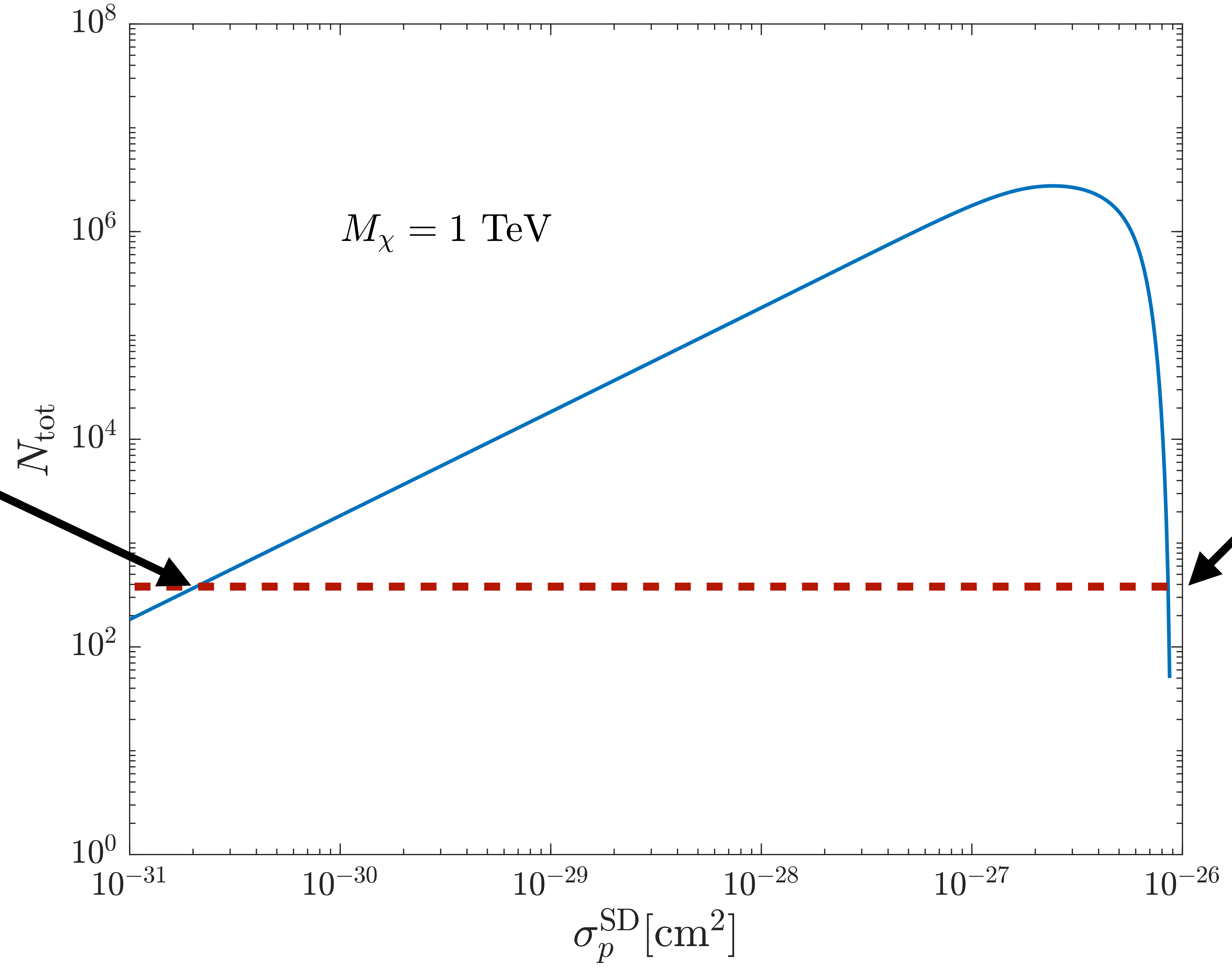

maximum exclusion

observation

Skylab and Ohyia

Etching holes

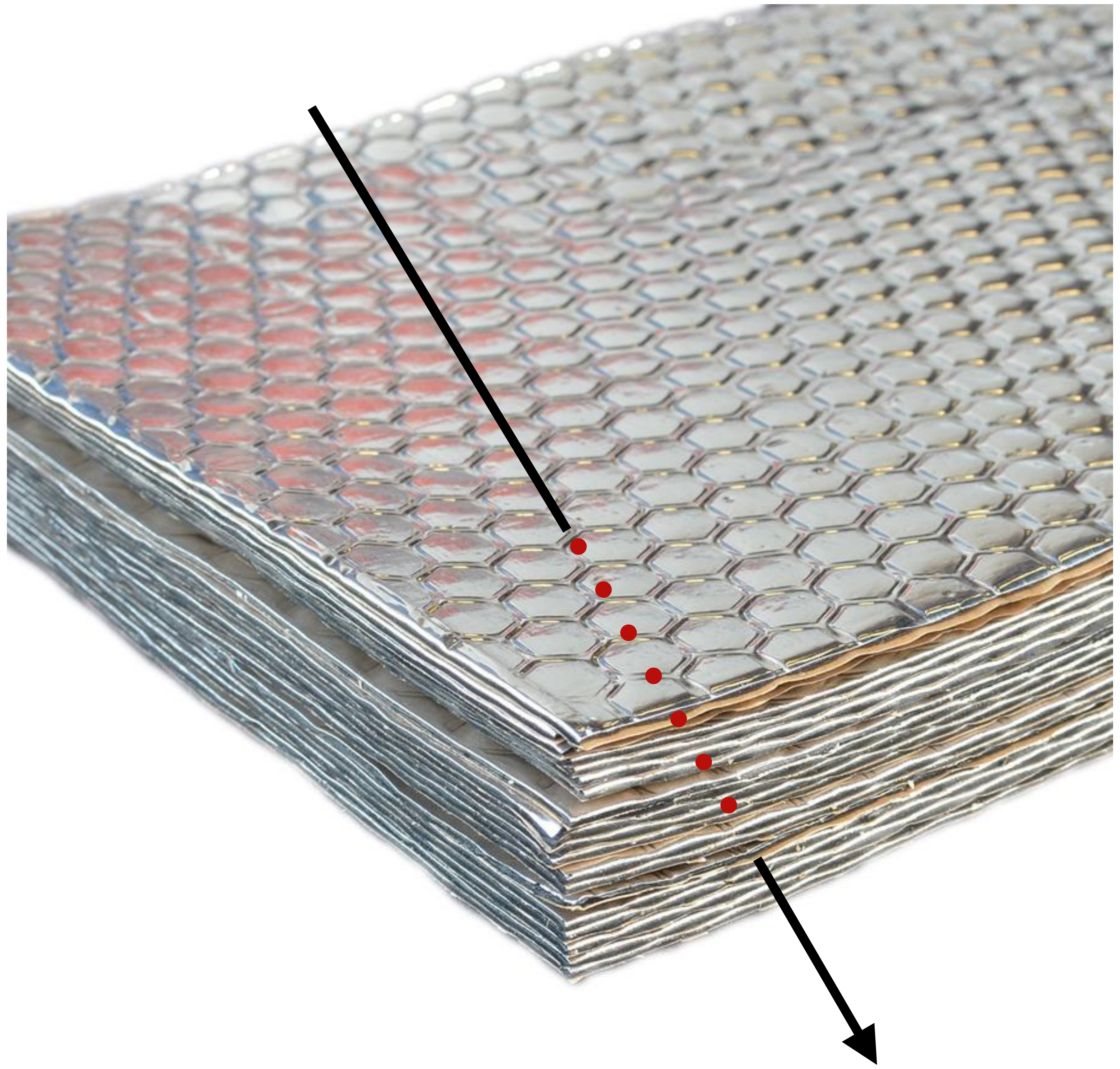

Constraints on Multiple Scattering Dark Matter

$$\left.\frac{dE}{dx}\right|_{th} = \frac{2E_i}{m_\chi}\left(\sum_{A\subset D}\frac{\mu_{\chi A}^2}{m_A}n_A\sigma_{\chi A}\right)\exp\left[\frac{-2}{m_\chi}\left(x_O\sum_{A\subset O}n_A\frac{\mu_{\chi A}^2}{m_A}\sigma_{\chi A}+x_D\sum_{A\subset D}n_A\frac{\mu_{\chi A}^2}{m_A}\sigma_{\chi A}\right)\right]$$

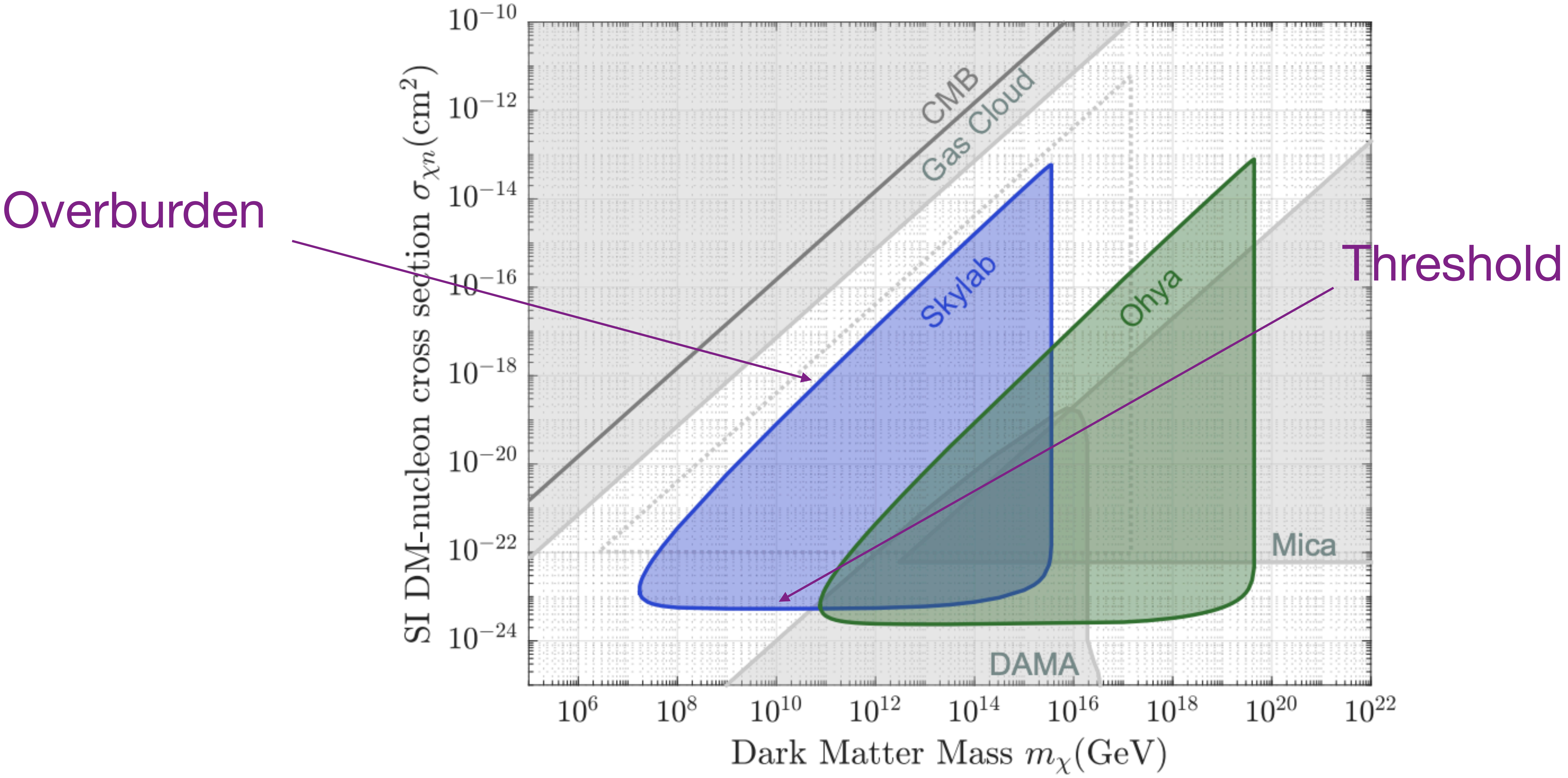

Bhoonah, Bramante, Courtman, **NS**, PRD/2012.13406

Daily Modulation

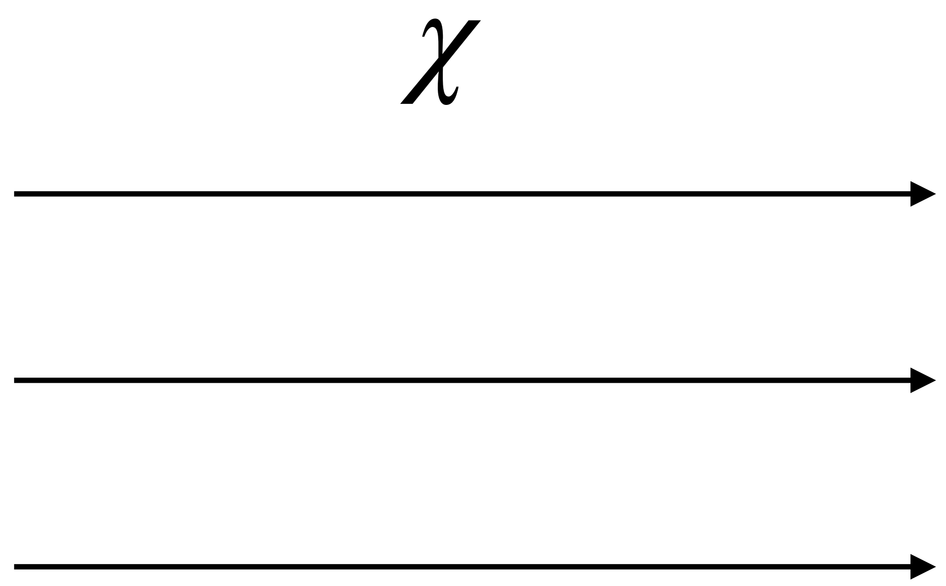

DM Wind

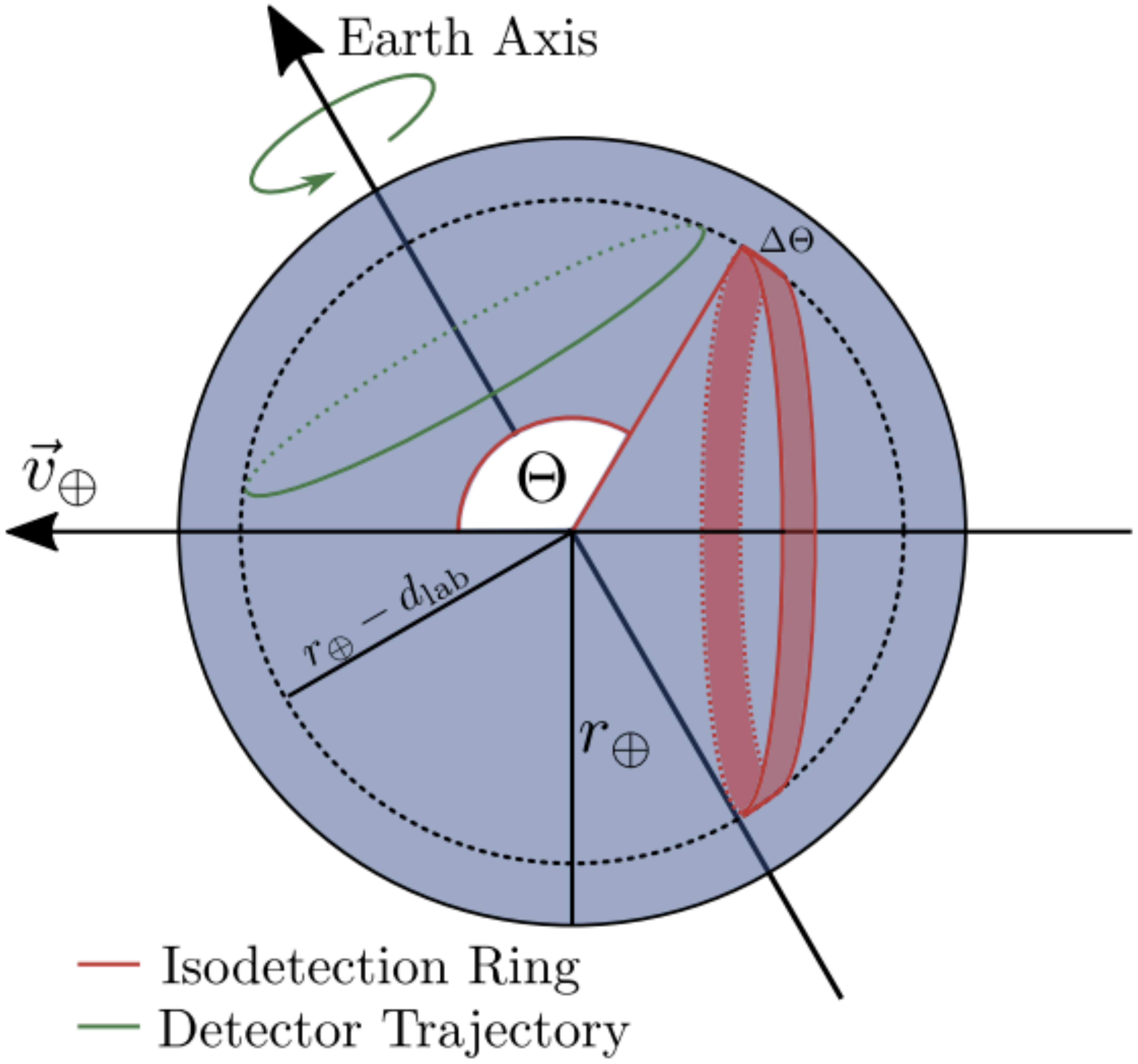

Emken, Kouvaris 1706.02249

Daily Modulation

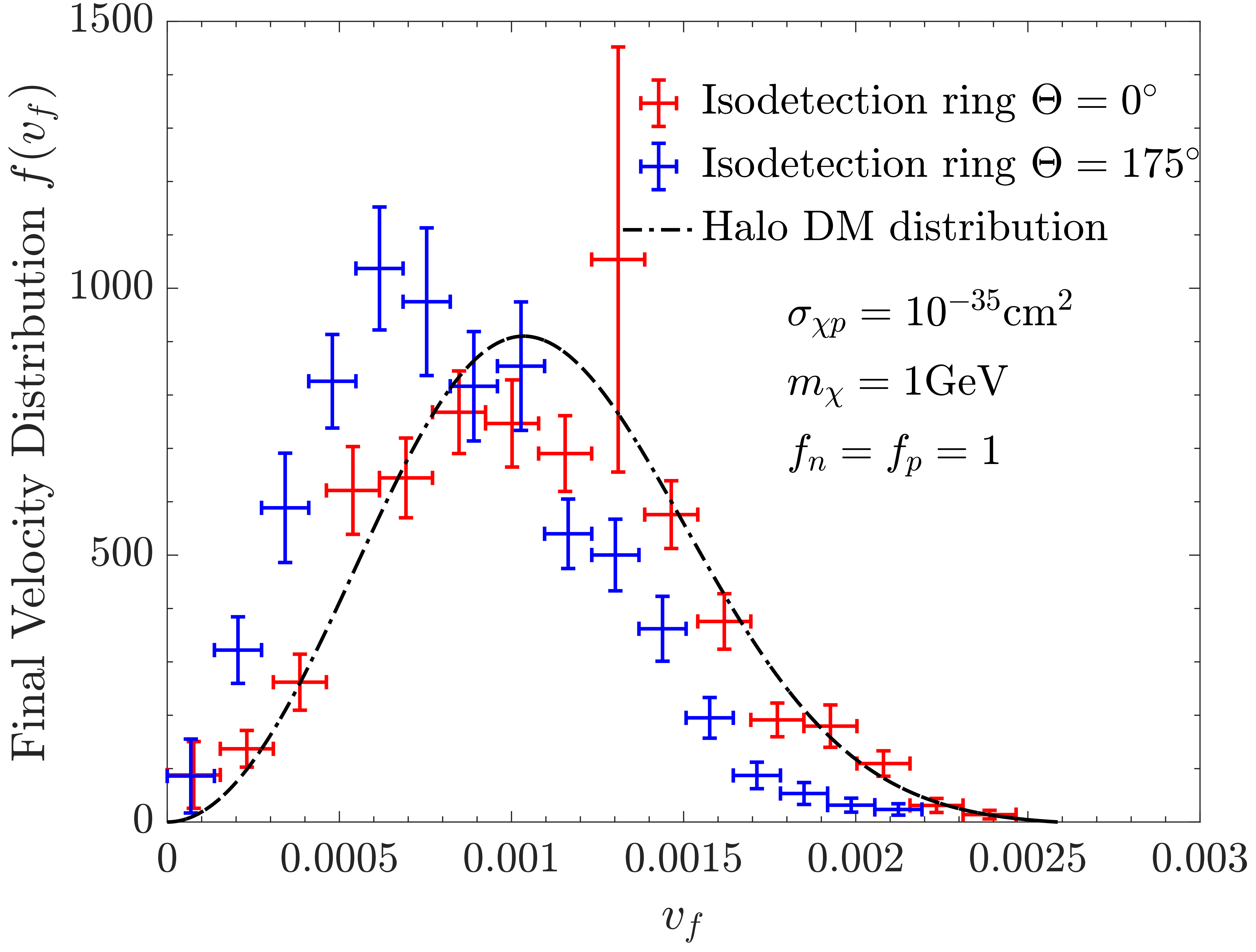

Daily Modulation

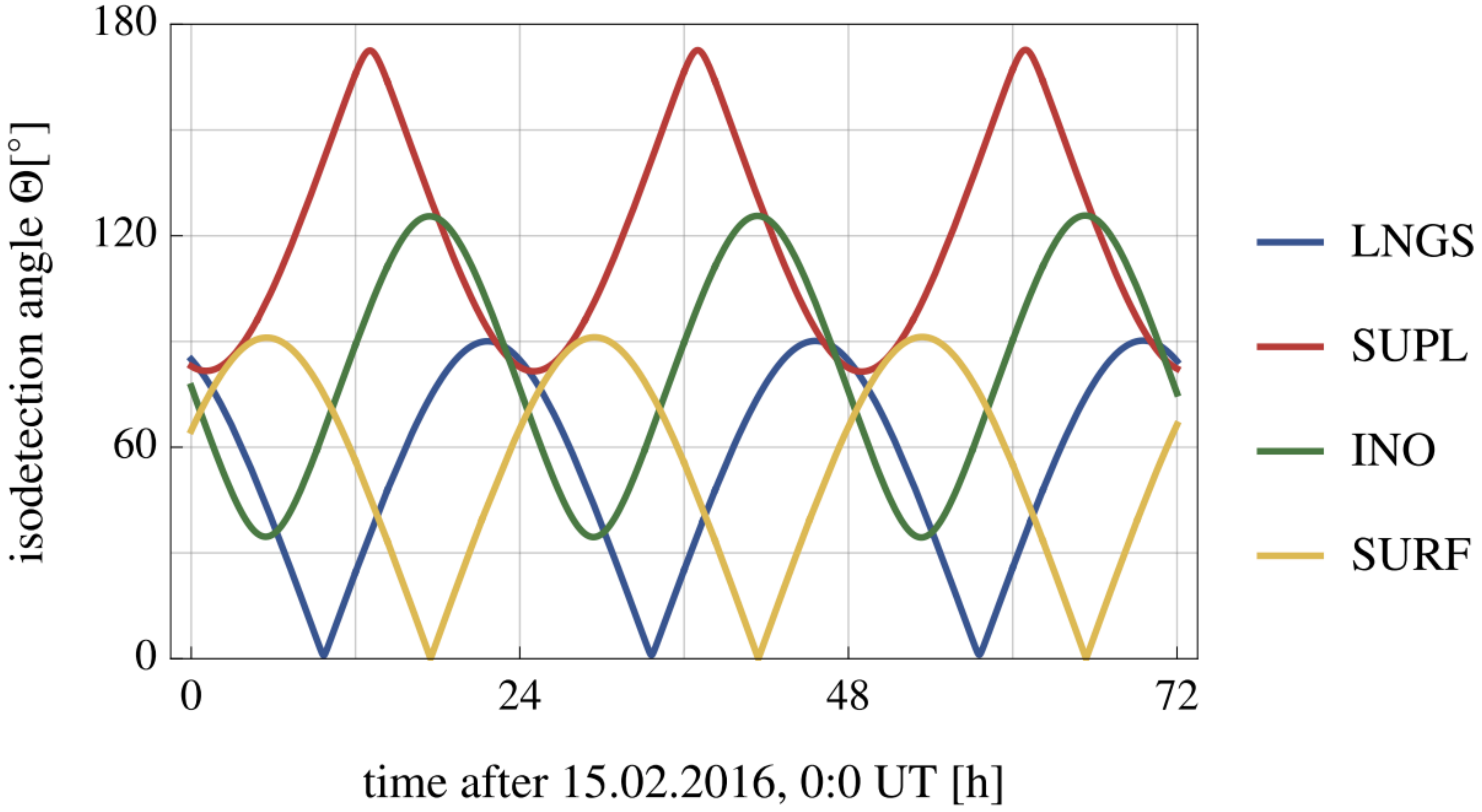

Emken, Kouvaris 1706.02249

Annual Modulation

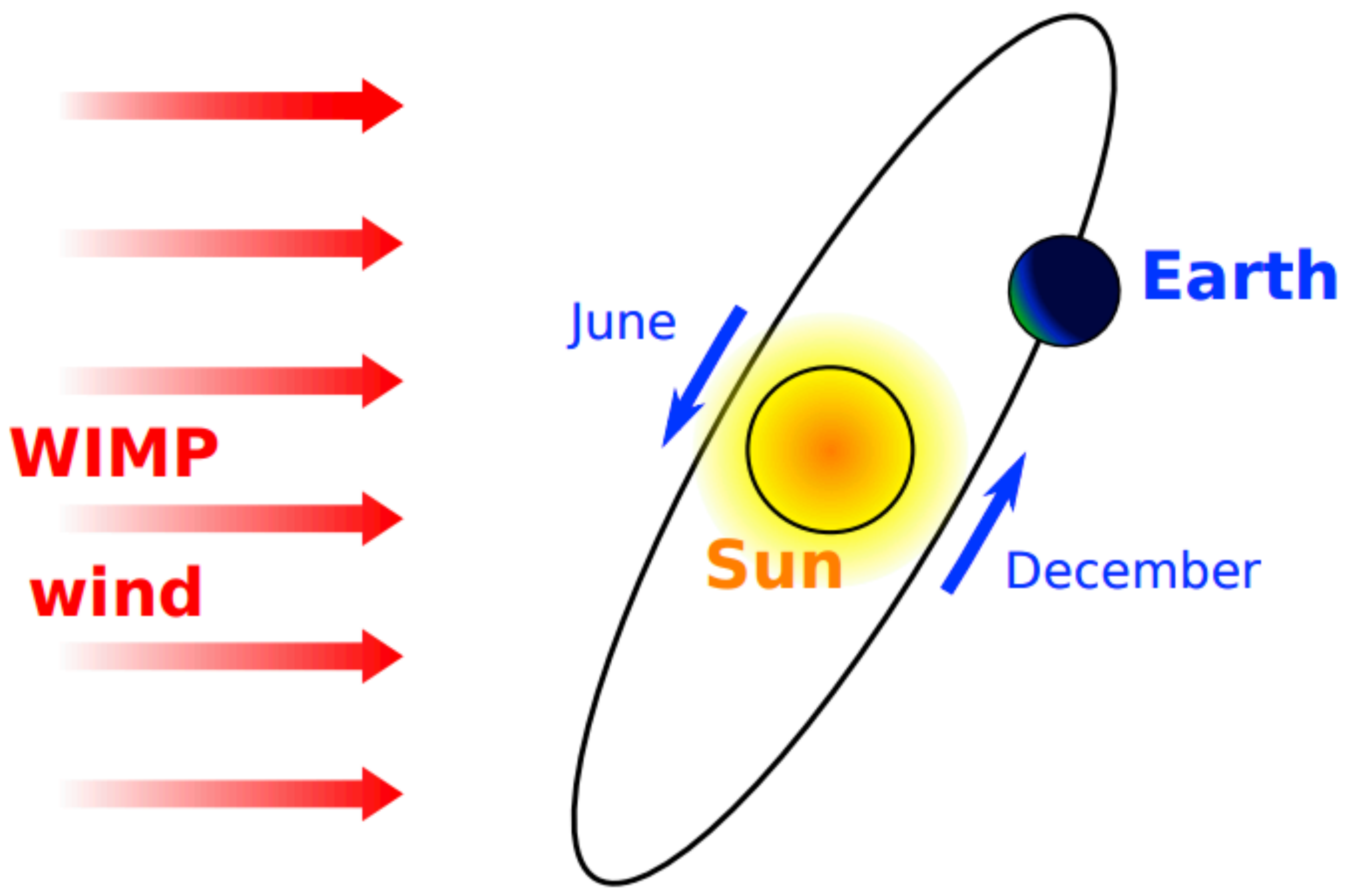

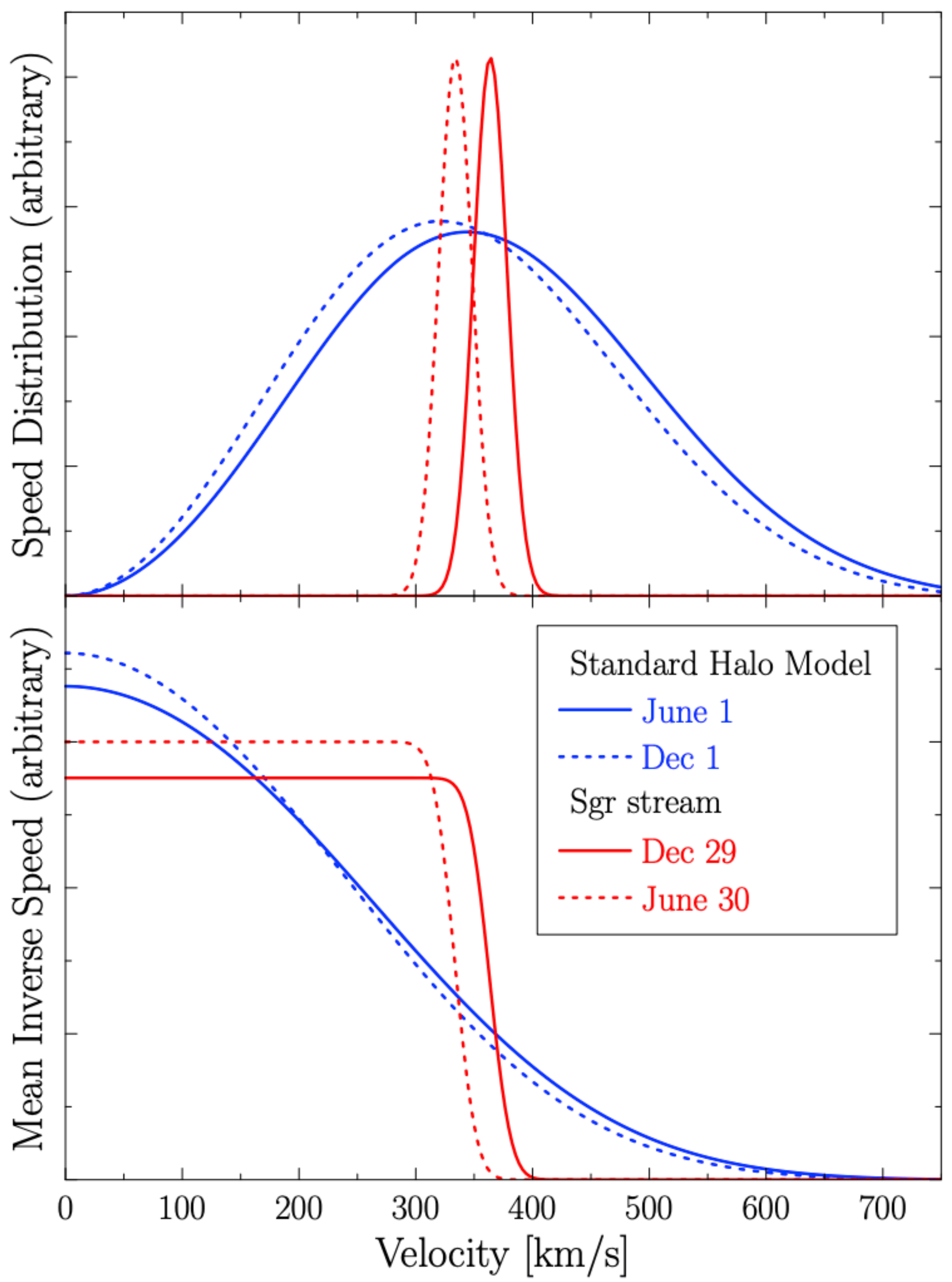

Freese *et al.*, arXiv:1209.3339

The DAMA Experiment

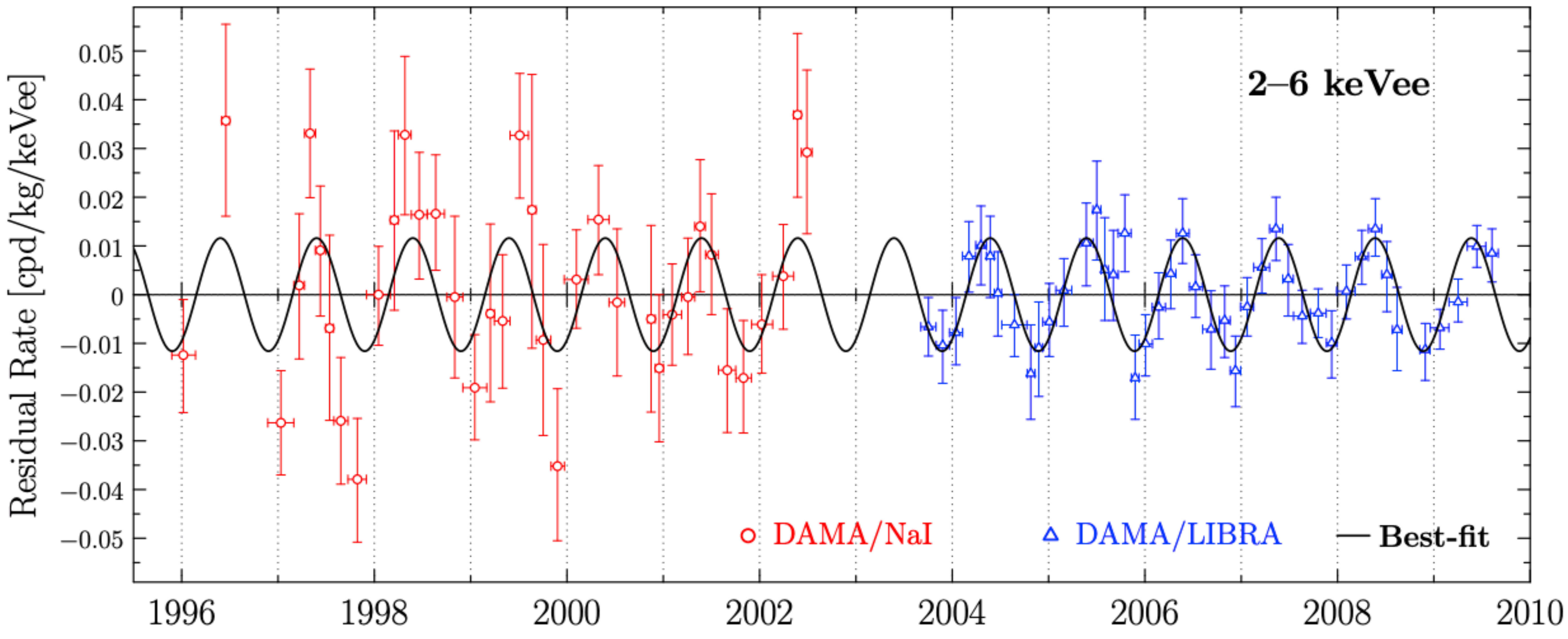

Freese *et al.*, arXiv:1209.3339

The COSINE-100 Experiment

COSINE-100 Full Dataset Challenges the Annual Modulation Signal of DAMA/LIBRA

For over 25 years, the DAMA/LIBRA collaboration has claimed to observe an annual modulation signal, suggesting the existence of dark matter interactions. However, no other experiments have replicated their result using different detector materials. To address this puzzle, the COSINE-100 collaboration conducted a model-independent test using 106 kg of sodium iodide as detectors, the same target material as DAMA/LIBRA. Analyzing data collected over 6.4 years, with improved energy calibration and time-dependent background description, we found no evidence of an annual modulation signal, challenging the DAMA/LIBRA result with a confidence level greater than 3σ. This finding represents a significant step toward resolving the long-standing debate surrounding DAMA/LIBRA's dark matter claim, indicating that the observed modulation is unlikely to be caused by dark matter interactions.

The COSINE-100 Experiment

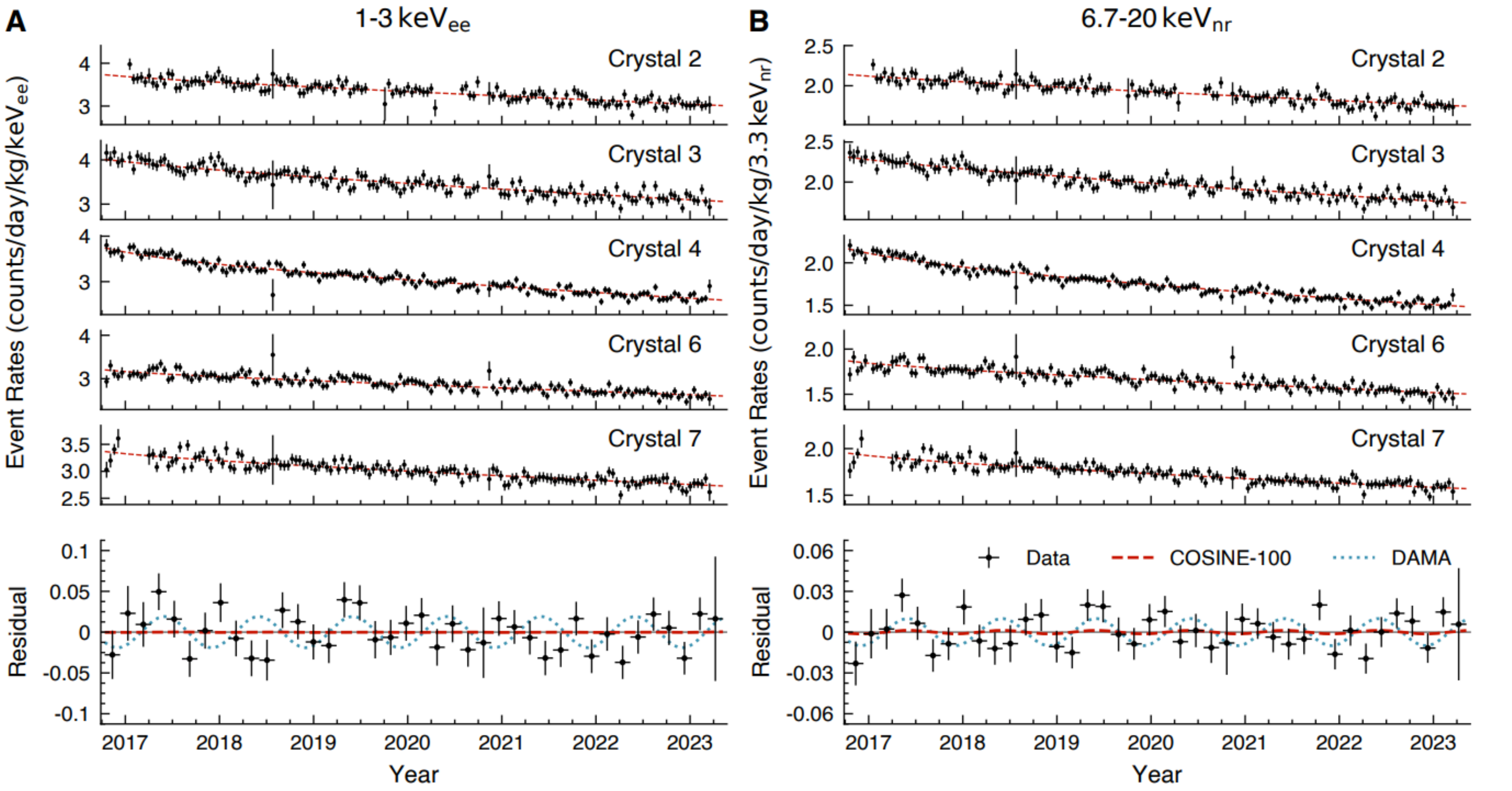

COSINE-100 collaboration, arXiv:2409.13226

Constraints on WIMP Dark Matter

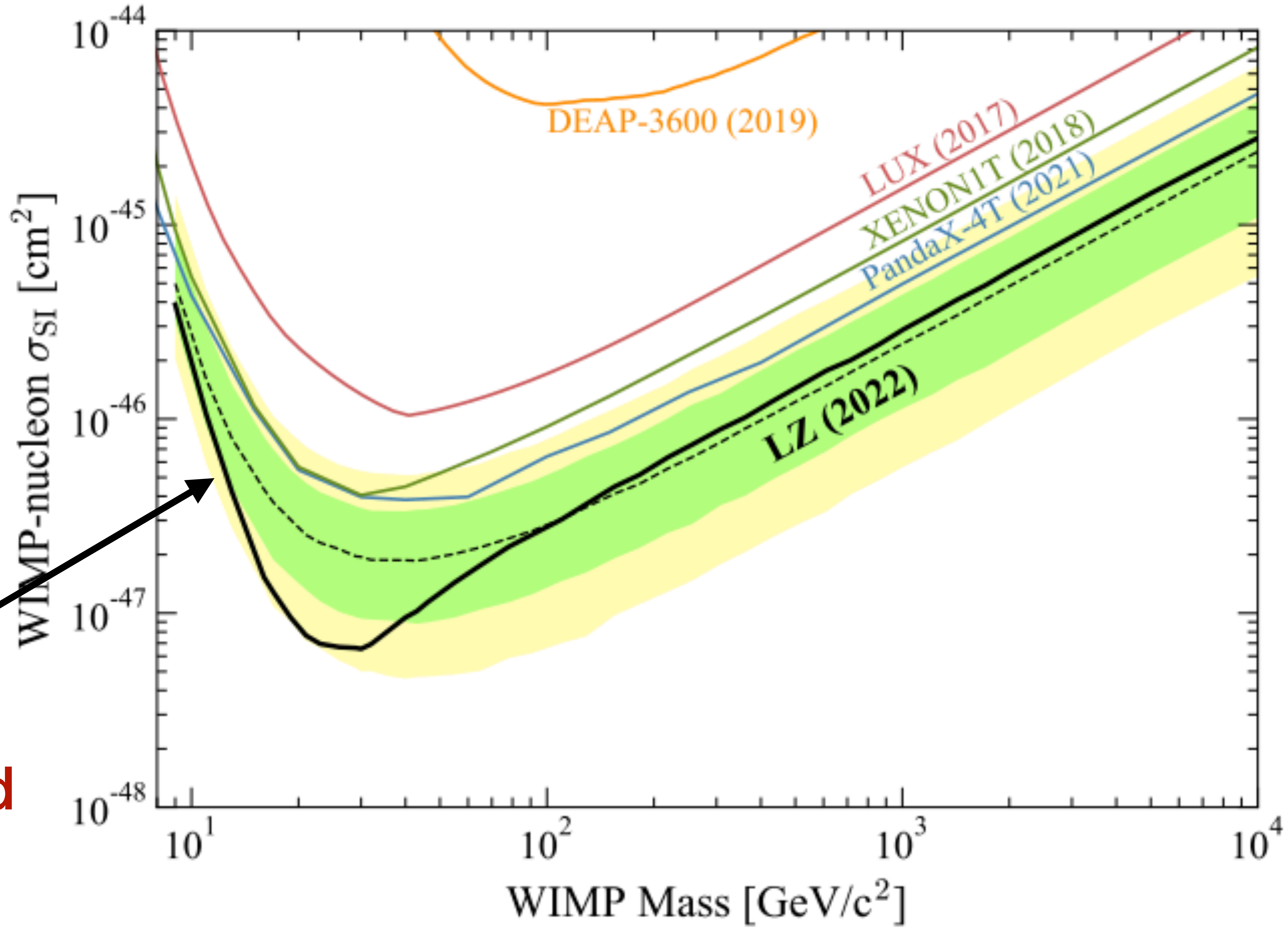

Limited by the detection threshold

How to overcome the detection threshold?

Boosted Dark Matter

Cosmic Rays

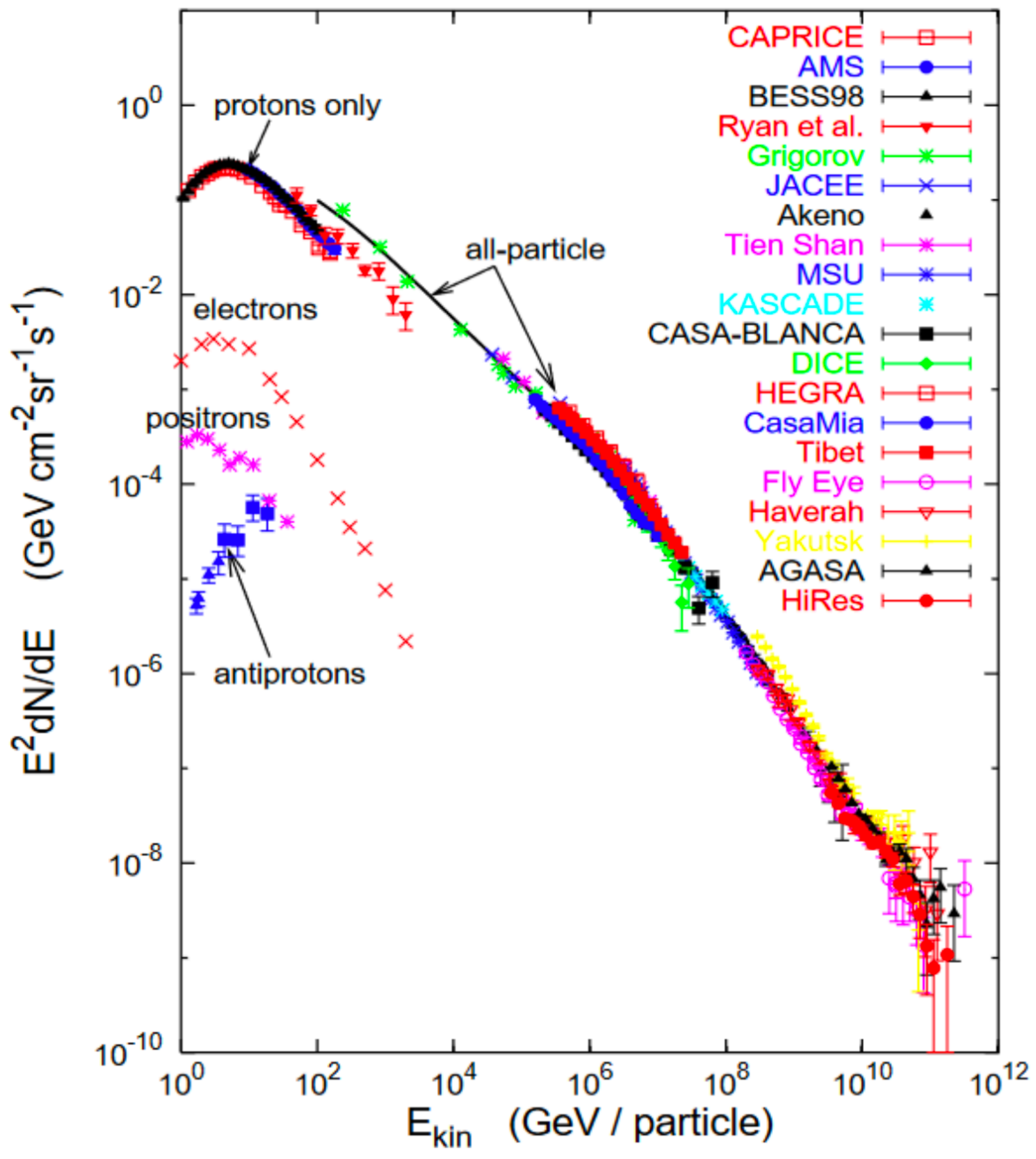

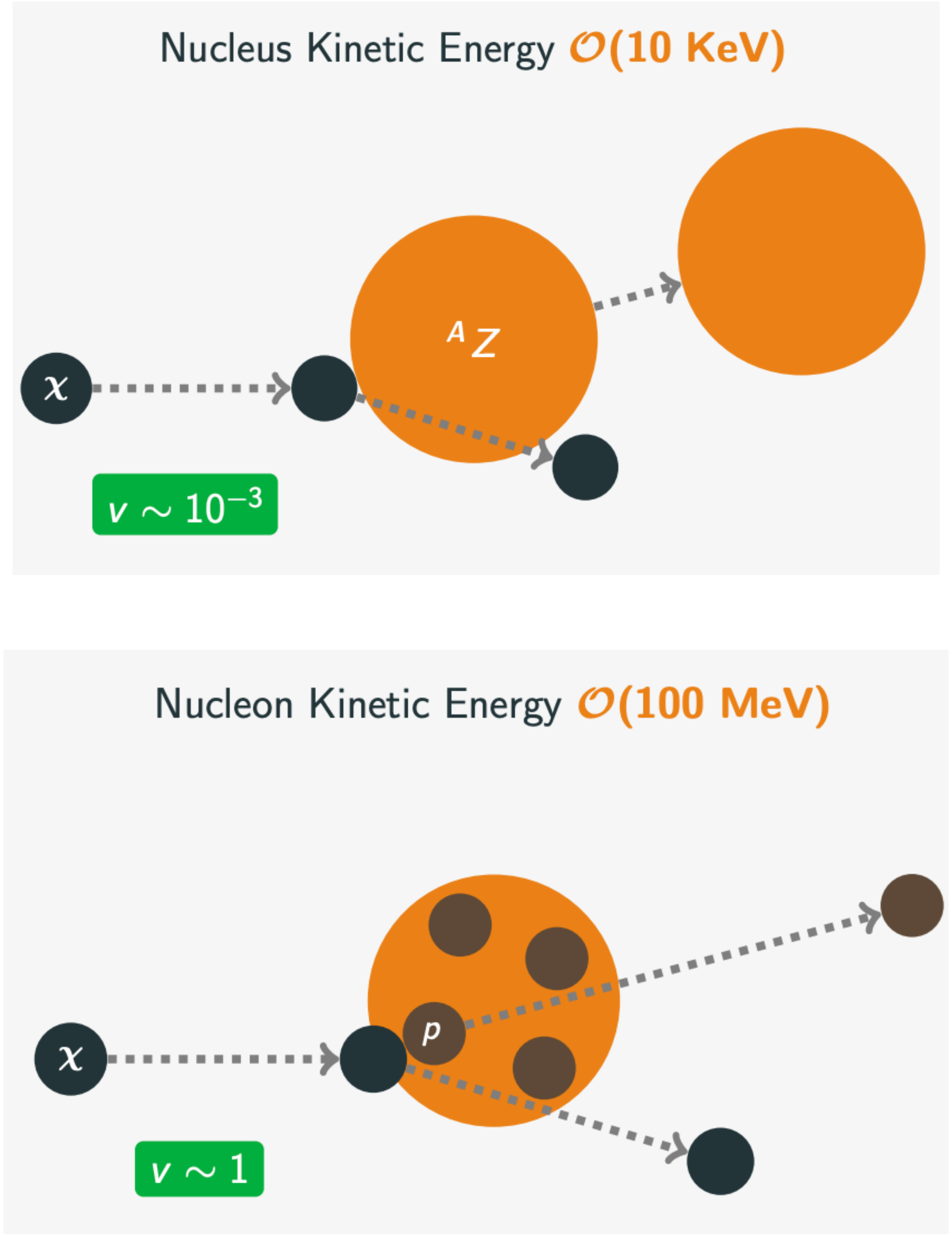

Credit: Joshua Berger

Cosmic Ray Boosted Dark Matter: Kinematics

Kinematics:

$$T_\chi = T_\chi^{\max}\frac{1-\cos\theta}{2}\,,\quad T_\chi^{\max} = \frac{T_i^2 + 2m_i T_i}{T_i + (m_i+m_\chi)^2/(2m_\chi)}$$

$$T_i^{\min} = \left(\frac{T_\chi}{2} - m_i\right)\left[1 \pm \sqrt{1 + \frac{2T_\chi}{m_\chi}\frac{(m_i+m_\chi)^2}{(2m_i - T_\chi)^2}}\right],$$

Cosmic Ray Boosted Dark Matter: Boost

Kinematics:

$$T_\chi = T_\chi^{\max}\frac{1-\cos\theta}{2}\,,\quad T_\chi^{\max} = \frac{T_i^2+2m_iT_i}{T_i+(m_i+m_\chi)^2/(2m_\chi)}$$

$$T_i^{\min} = \left(\frac{T_\chi}{2}-m_i\right)\left[1\pm\sqrt{1+\frac{2T_\chi}{m_\chi}\frac{(m_i+m_\chi)^2}{(2m_i-T_\chi)^2}}\right],$$

$$d\Gamma_{\mathrm{CR}_i\to\chi} = \sigma_{\chi i}\times\frac{\rho_\chi}{m_\chi}\frac{d\Phi_i^{LIS}}{dT_i}dT_i dV$$

$$\frac{d\Phi_\chi}{dT_i} = \int\frac{d\Omega}{4\pi}\int_{l.o.s.}d\ell\,\sigma_{\chi i}\frac{\rho_\chi}{m_\chi}\frac{d\Phi_i}{dT_i}\equiv\sigma_{\chi i}\frac{\rho_\chi^{\mathrm{local}}}{m_\chi}\frac{d\Phi_i^{LIS}}{dT_i}D_{\mathrm{eff}}$$

$$\frac{d\Phi_\chi}{dT_\chi} = \int_0^\infty dT_i\frac{d\Phi_\chi}{dT_i}\frac{1}{T_\chi^{\max}(T_i)}\Theta\left[T_\chi^{\max}(T_i)-T_\chi\right]$$

Cosmic Ray Boosted Dark Matter: Boost

Kinematics:

$$T_\chi = T_\chi^{\max}\frac{1-\cos\theta}{2}\,,\quad T_\chi^{\max} = \frac{T_i^2+2m_iT_i}{T_i+(m_i+m_\chi)^2/(2m_\chi)}$$

$$T_i^{\min} = \left(\frac{T_\chi}{2}-m_i\right)\left[1\pm\sqrt{1+\frac{2T_\chi}{m_\chi}\frac{(m_i+m_\chi)^2}{(2m_i-T_\chi)^2}}\right],$$

$$d\Gamma_{\mathrm{CR}_i\to\chi} = \sigma_{\chi i}\times\frac{\rho_\chi}{m_\chi}\frac{d\Phi_i^{LIS}}{dT_i}dT_i dV$$

$$\frac{d\Phi_\chi}{dT_i} = \int\frac{d\Omega}{4\pi}\int_{l.o.s.}d\ell\,\sigma_{\chi i}\frac{\rho_\chi}{m_\chi}\frac{d\Phi_i}{dT_i} \equiv \sigma_{\chi i}\frac{\rho_\chi^{\mathrm{local}}}{m_\chi}\frac{d\Phi_i^{LIS}}{dT_i}D_{\mathrm{eff}}$$

$$\frac{d\Phi_\chi}{dT_\chi} = \int_0^\infty dT_i\frac{d\Phi_\chi}{dT_i}\frac{1}{T_\chi^{\max}(T_i)}\Theta\left[T_\chi^{\max}(T_i)-T_\chi\right]$$

Hadronic elastic scattering form factor

$$G_i(Q^2) = 1/(1+Q^2/\Lambda_i^2)^2\,,\qquad \frac{d\sigma_{\chi i}}{d\Omega} = \left.\frac{d\sigma_{\chi i}}{d\Omega}\right|_{Q^2=0}G_i^2(2m_\chi T_\chi)$$

Cosmic Ray Boosted Dark Matter: Spectrum

$$\frac{d\Phi_\chi}{dT_\chi} = D_{\rm eff} \frac{\rho_\chi^{\rm local}}{m_\chi} \times \times \sum_i \sigma^0_{\chi i} G_i^2(2m_\chi T_\chi) \int_{T_i^{\rm min}}^{\infty} dT_i \frac{d\Phi_i^{LIS}/dT_i}{T_\chi^{\rm max}(T_i)}$$

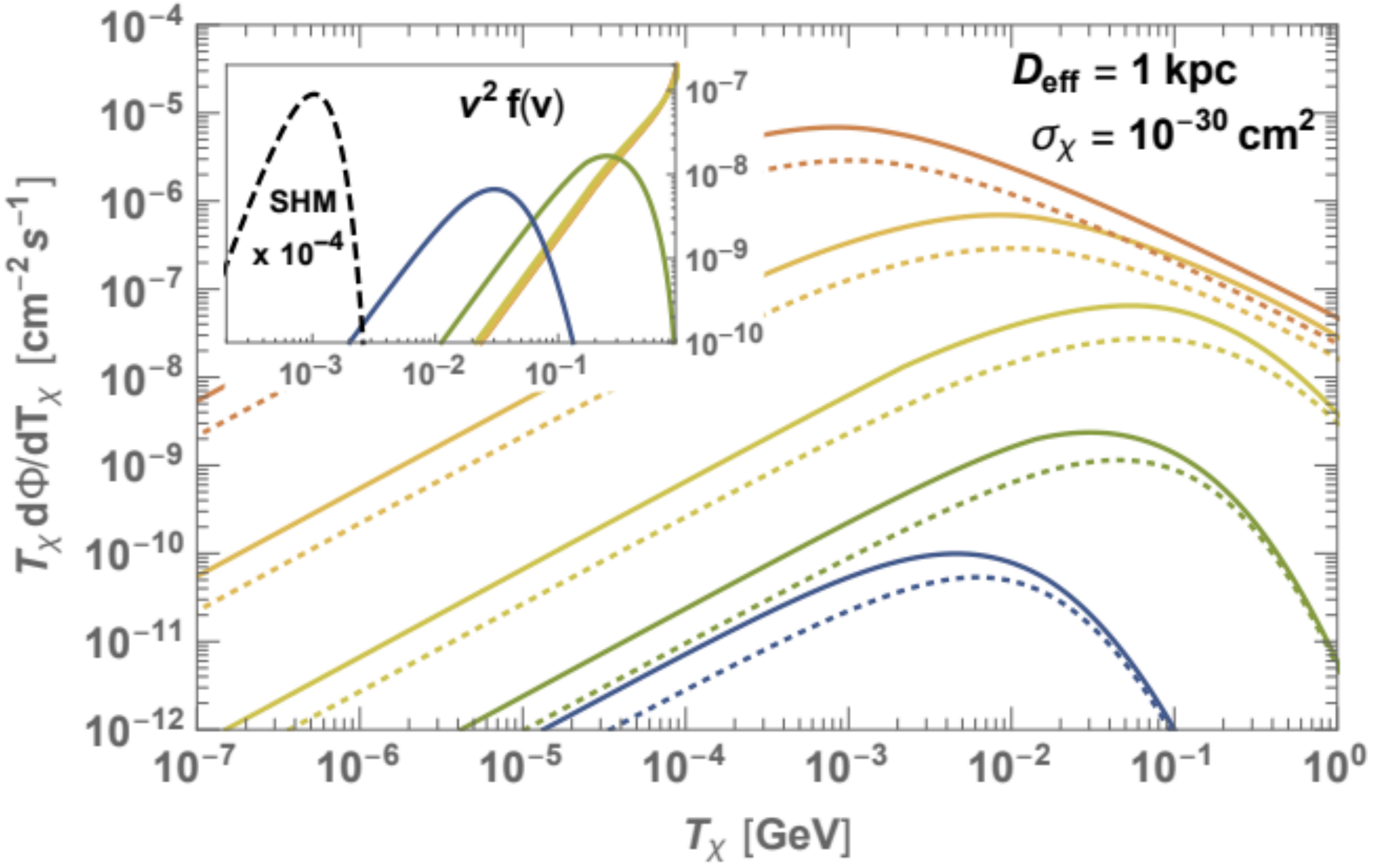

Bringmann et al, arXiv:1810.10543

Cosmic Ray Boosted Dark Matter: Detection

Attenuation

$$\frac{dT_{DM}}{dx} = -\sum_N n_N \int_0^{T_r^{\max}} \frac{d\sigma_{\chi N}}{dT_r} T_r dT_r$$

Detection

$$\frac{d\Gamma_N}{dT_N} = \sigma^0_{\chi N} G_N^2 (2m_N T_N) \int_{T_\chi(T_\chi^{z,\min})}^{\infty} \frac{dT_\chi}{T_{r,N}^{\max}(T_\chi^z)} \frac{d\Phi_\chi}{dT_\chi}$$

Bringmann et al, arXiv:1810.10543

Cosmic Ray Boosted Dark Matter: Constraints

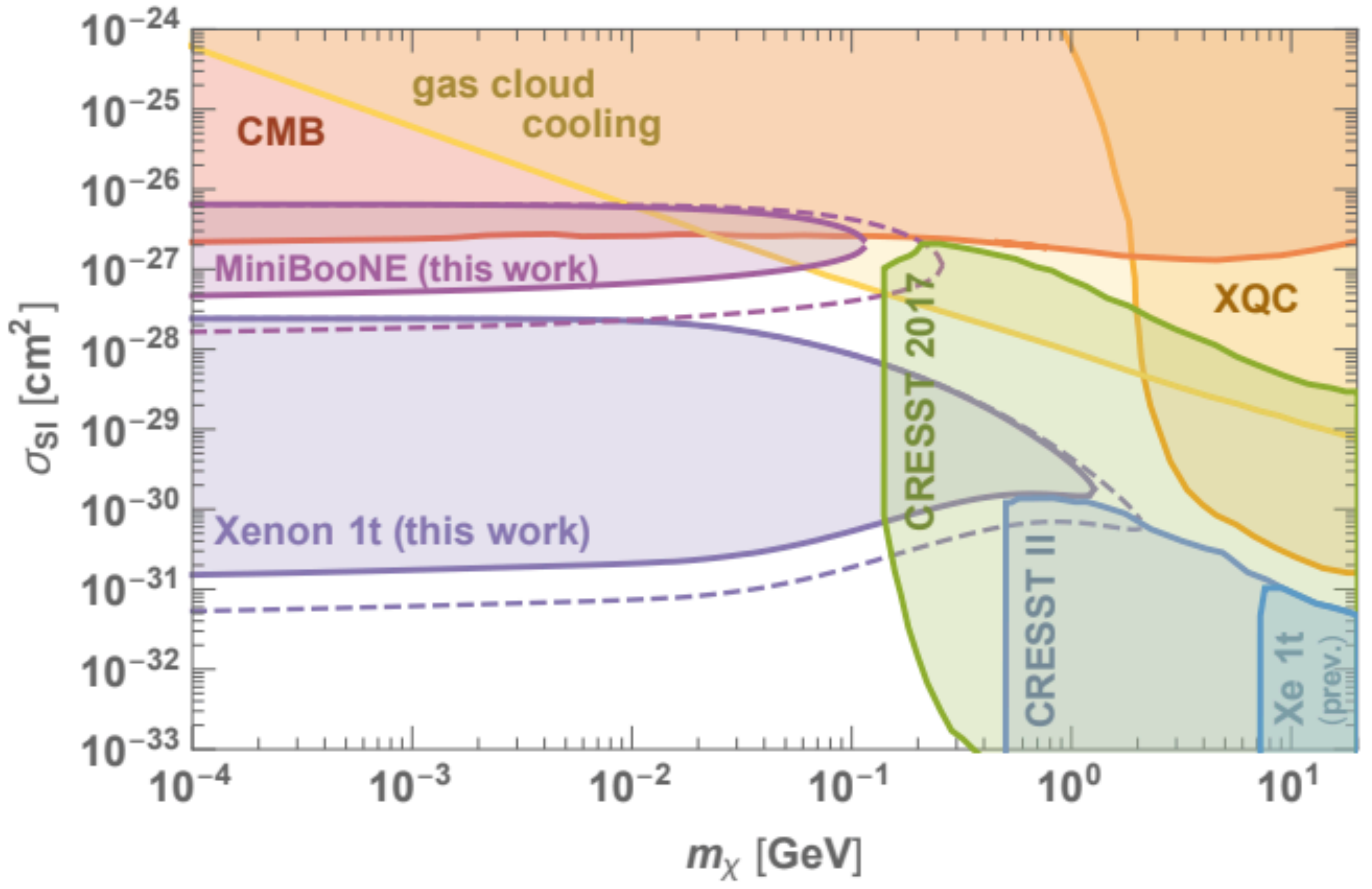

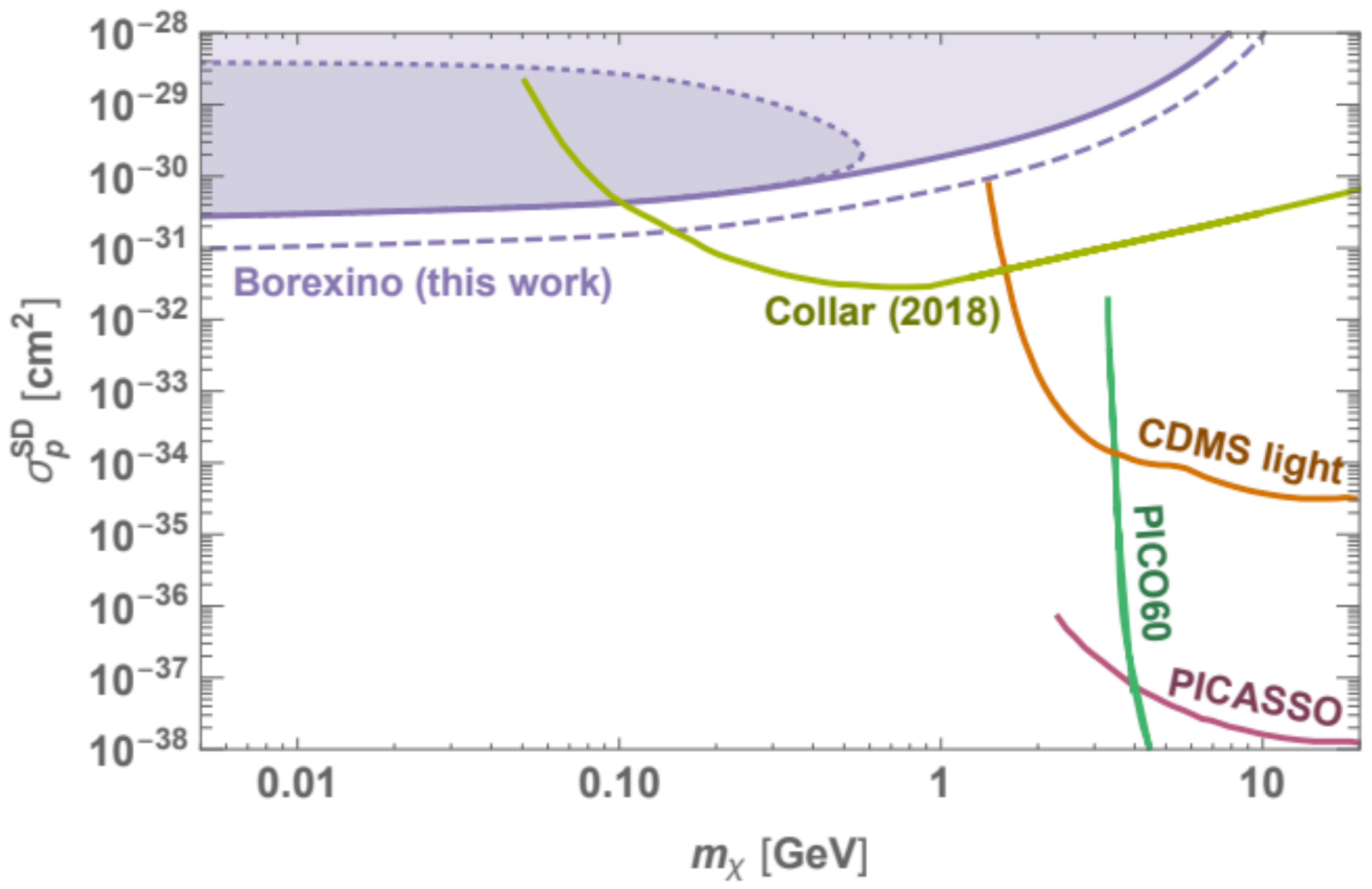

Bringmann et al, arXiv:1810.10543

Blazar Boosted Dark Matter

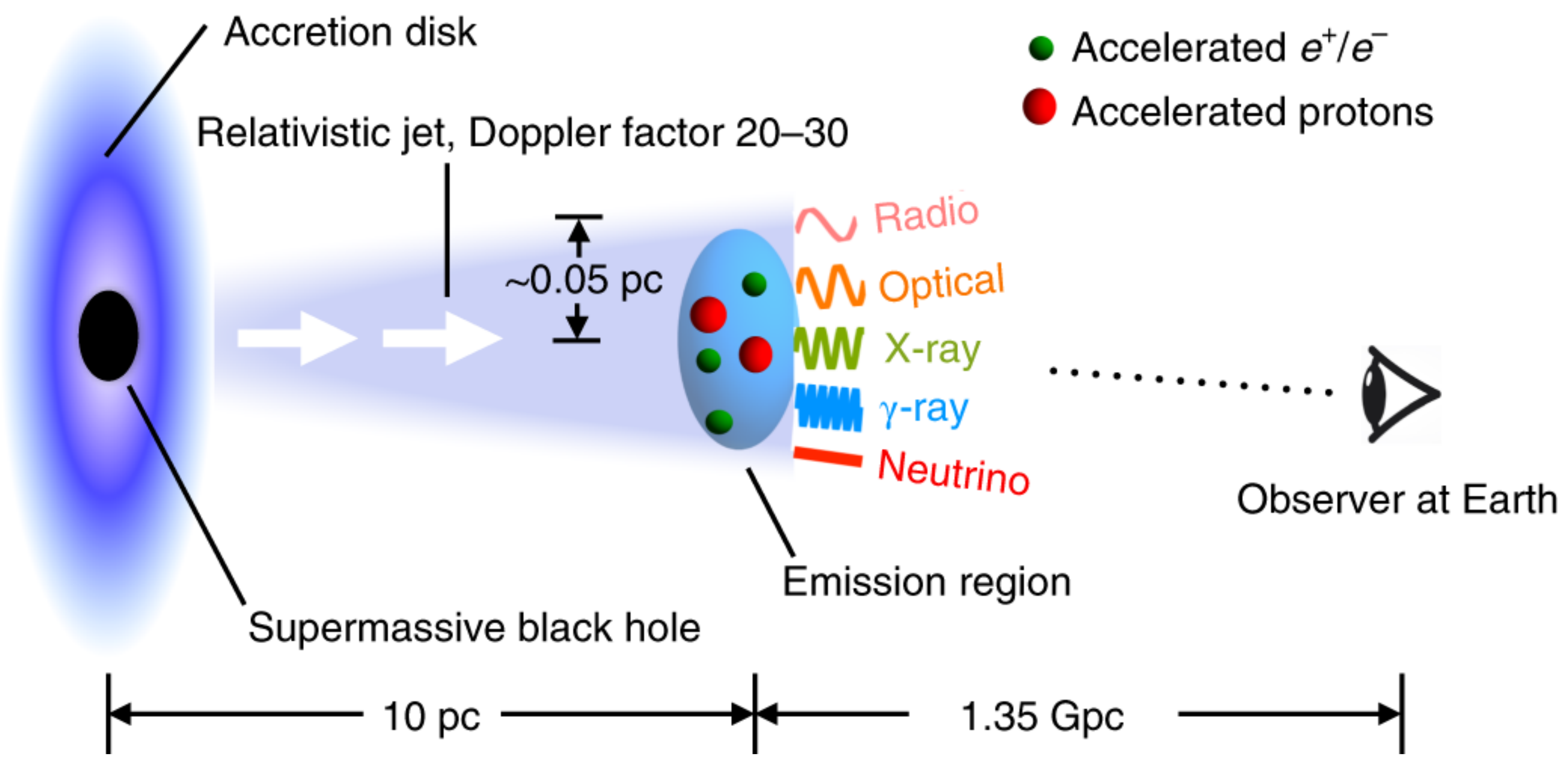

$$p + \gamma \rightarrow \Delta^+ \rightarrow \pi^+ + n$$

$$p + p \rightarrow n_\pi \, [\pi^0 + \pi^+ + \pi^-]$$

Gao et al, Nature Astronomy, 2019

A Dark Matter Spike?

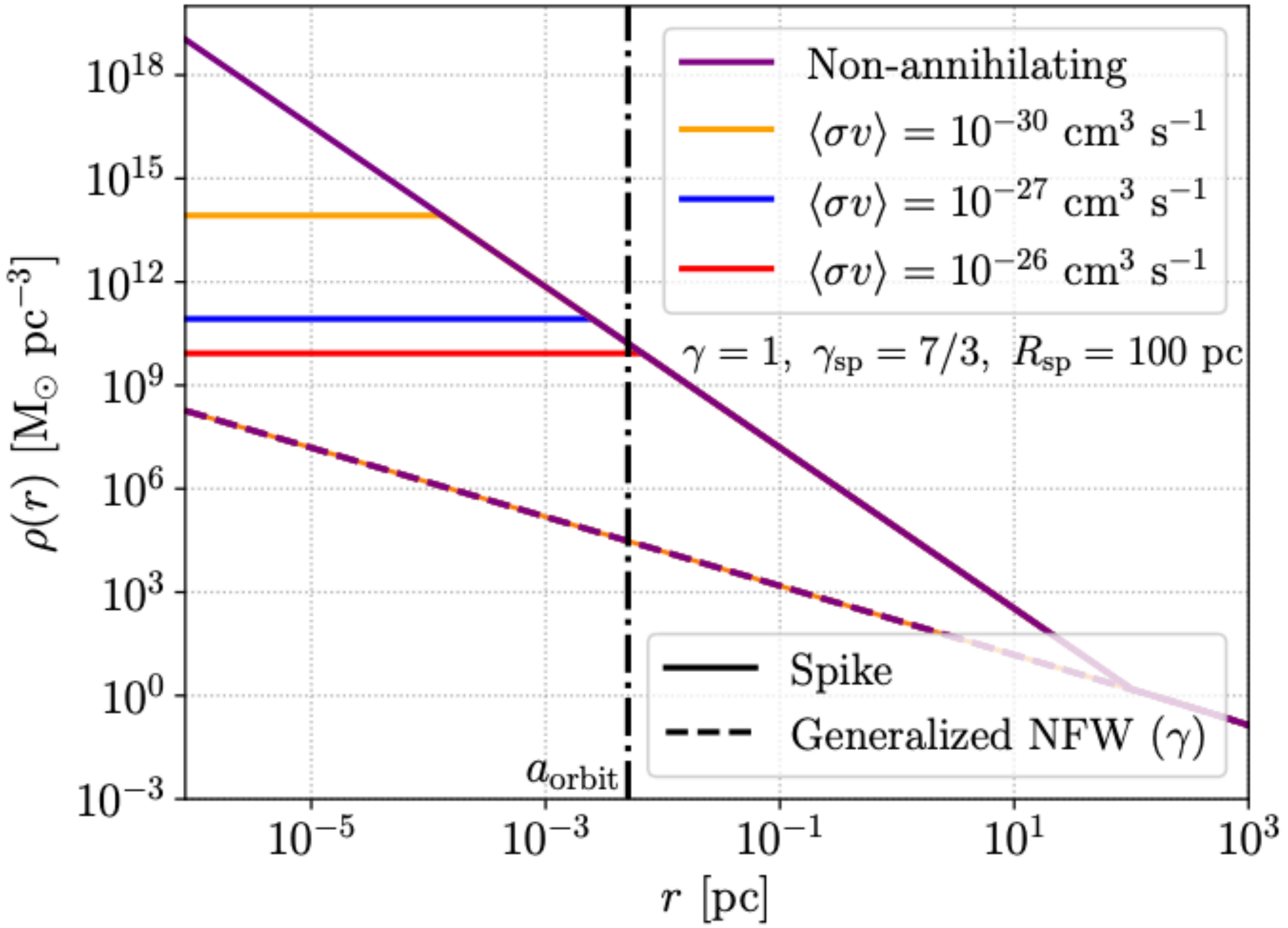

Lacroix, arXiv: 1801.01308

$$\rho(r) = \begin{cases} 0 & r < 2R_S \\ \rho_{halo}(R_{sp})\left(\frac{r}{R_{sp}}\right)^{-\gamma_{sp}} & 2R_S \leqslant r < R_{sp} \\ \rho_{halo}(r) & r \geqslant R_{sp}, \end{cases}$$

$$\rho_{halo}(r) = \rho_s \left(\frac{r}{r_s}\right)^{-\gamma}\left(1 + \frac{r}{r_s}\right)^{\gamma-3},$$

Spike inside, NFW outside

Blazar Boosted Dark Matter

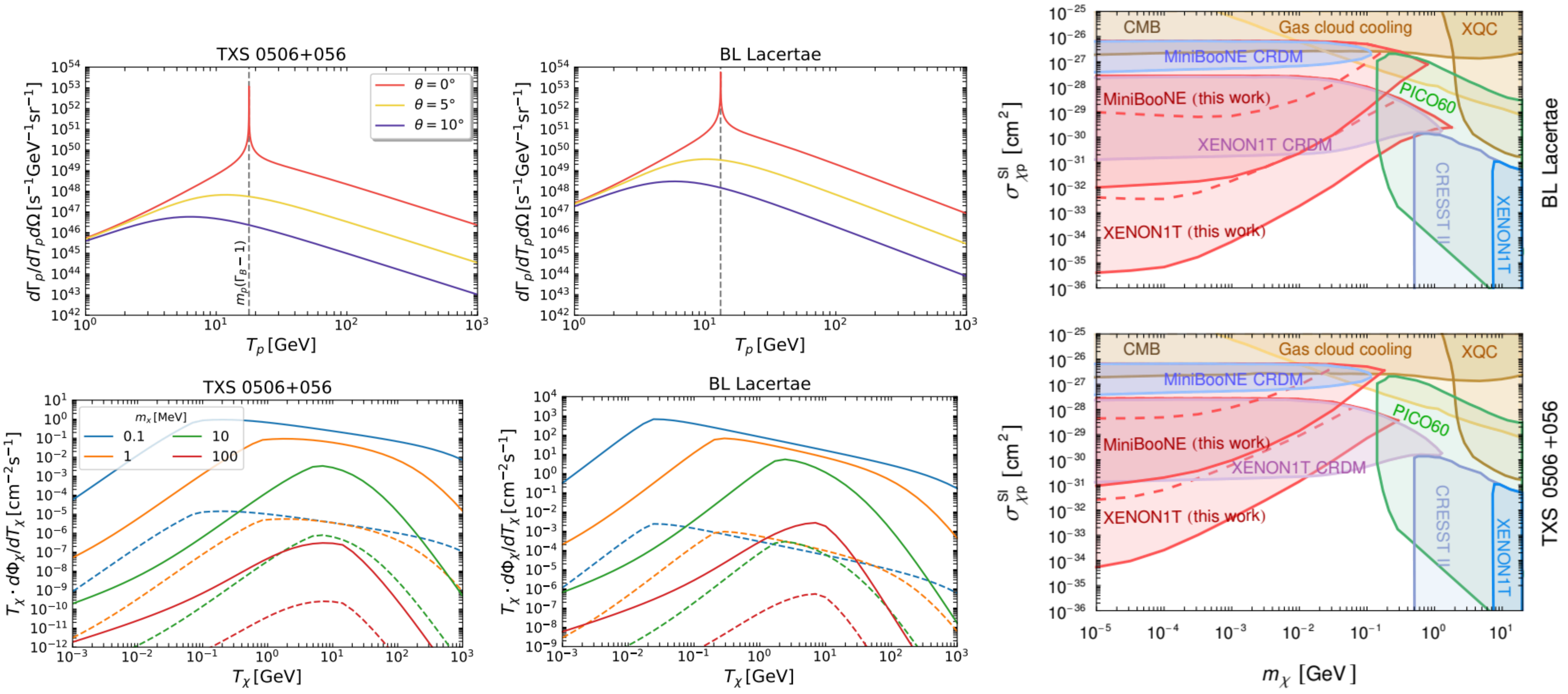

Wang et al, arXiv: 2111.13644

Solar Reflected Dark Matter

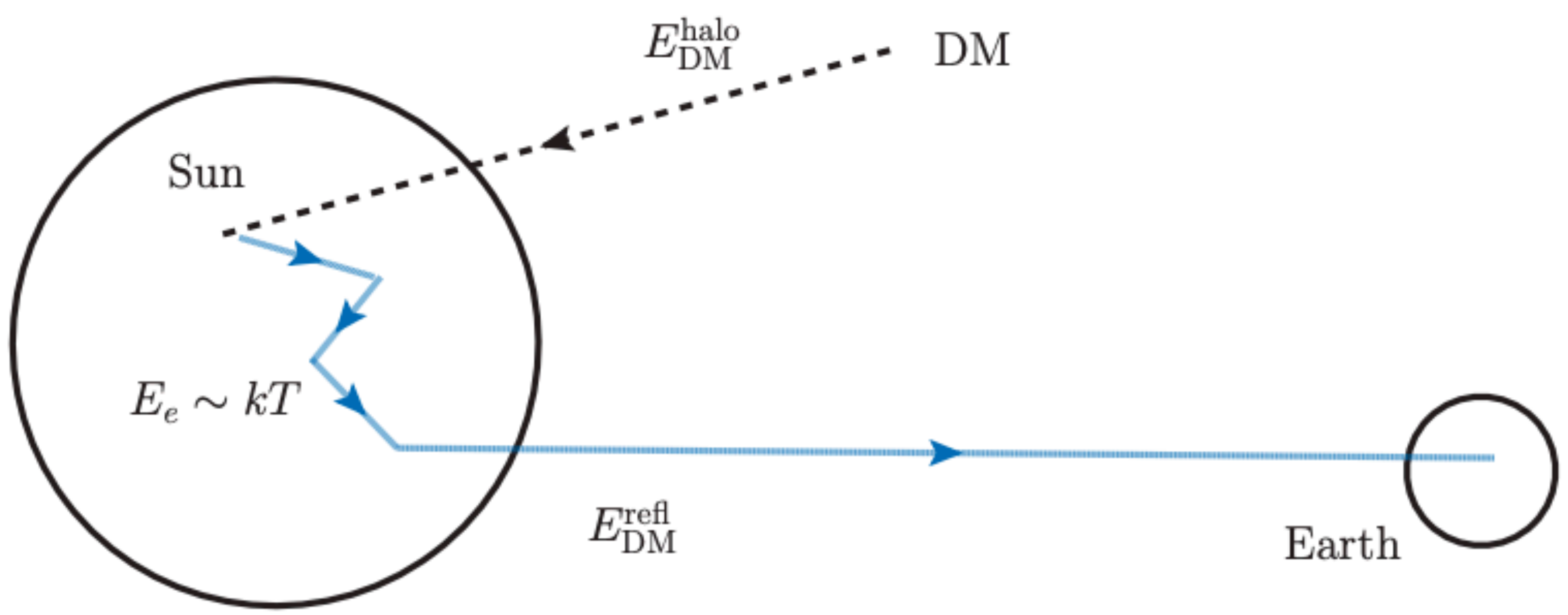

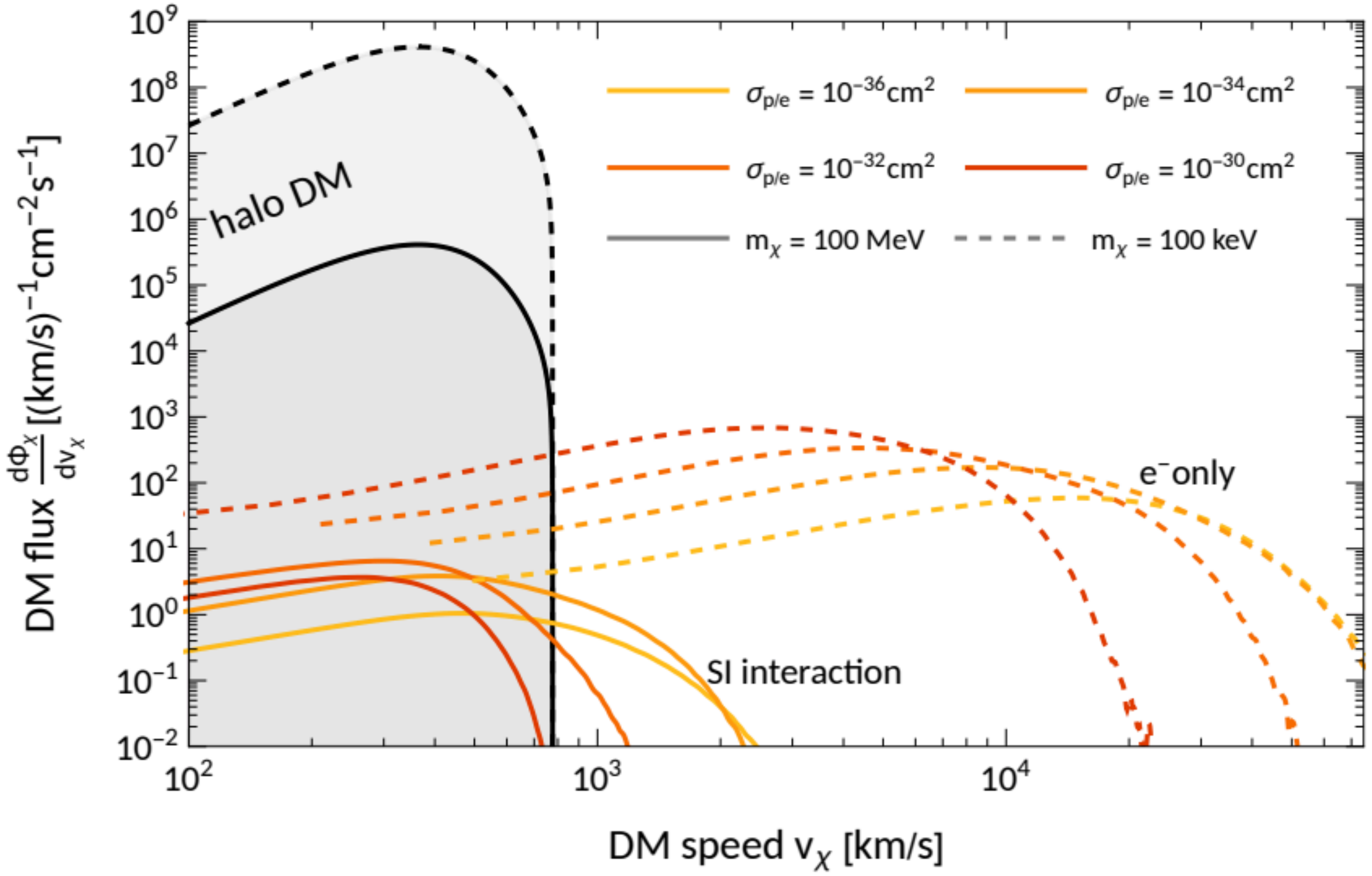

Need dedicated simulations!

Emken, arXiv: 2102.12483

Solar Reflected Dark Matter

Heavy mediator

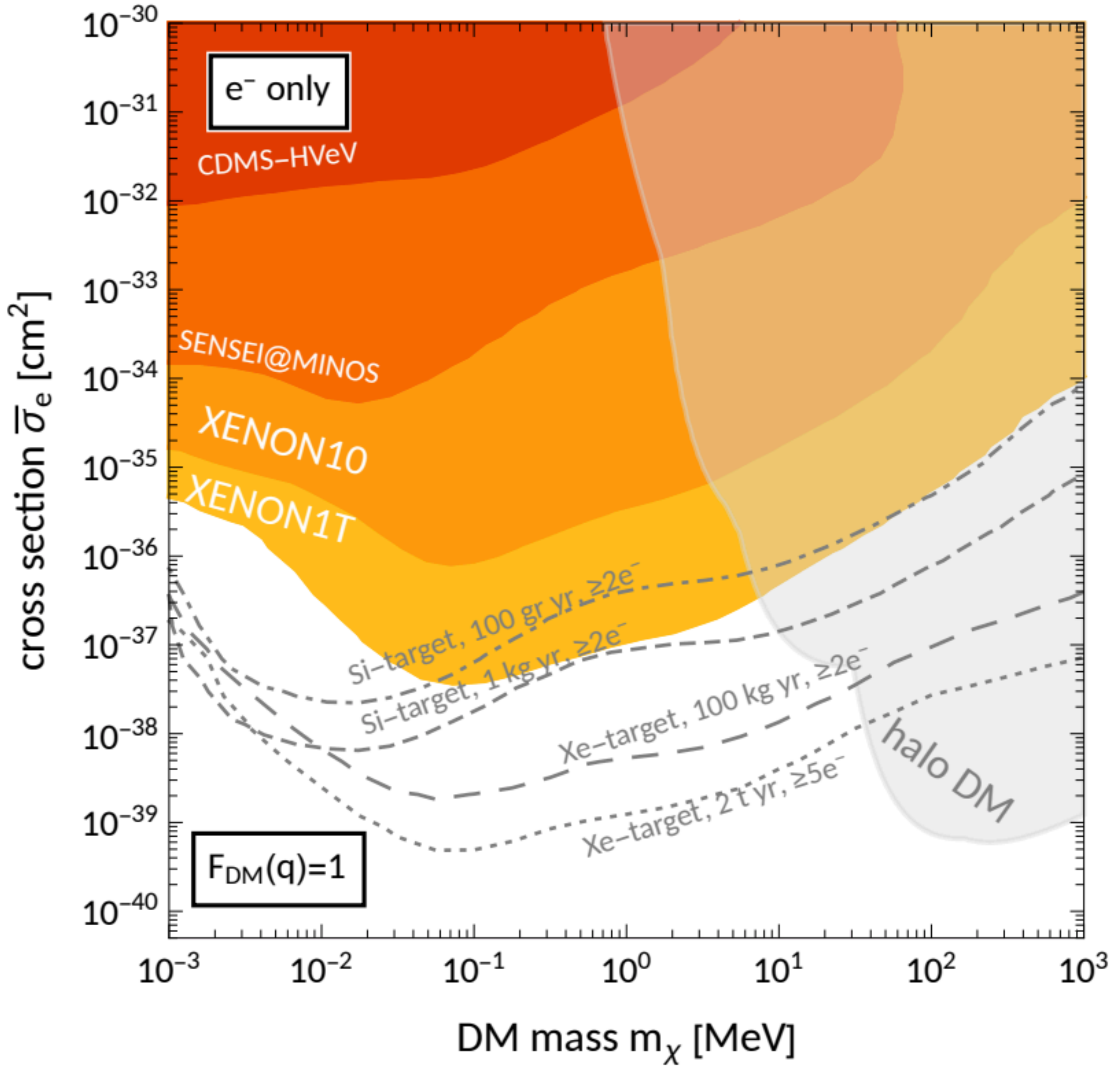

Emken, arXiv: 2102.12483

Light mediator

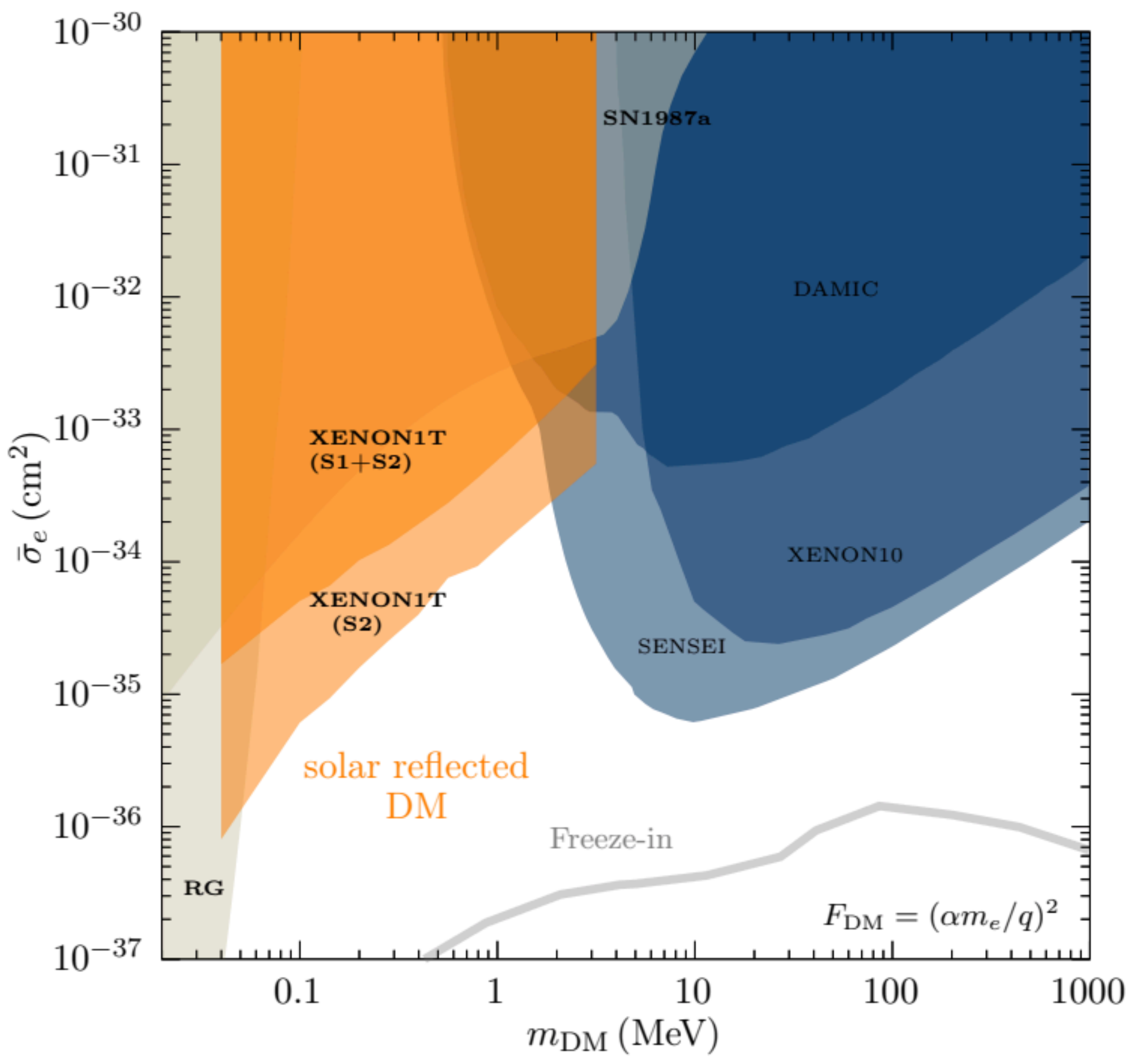

An et al, arXiv: 2108.10332

Supernova Neutrino Boosted Dark Matter

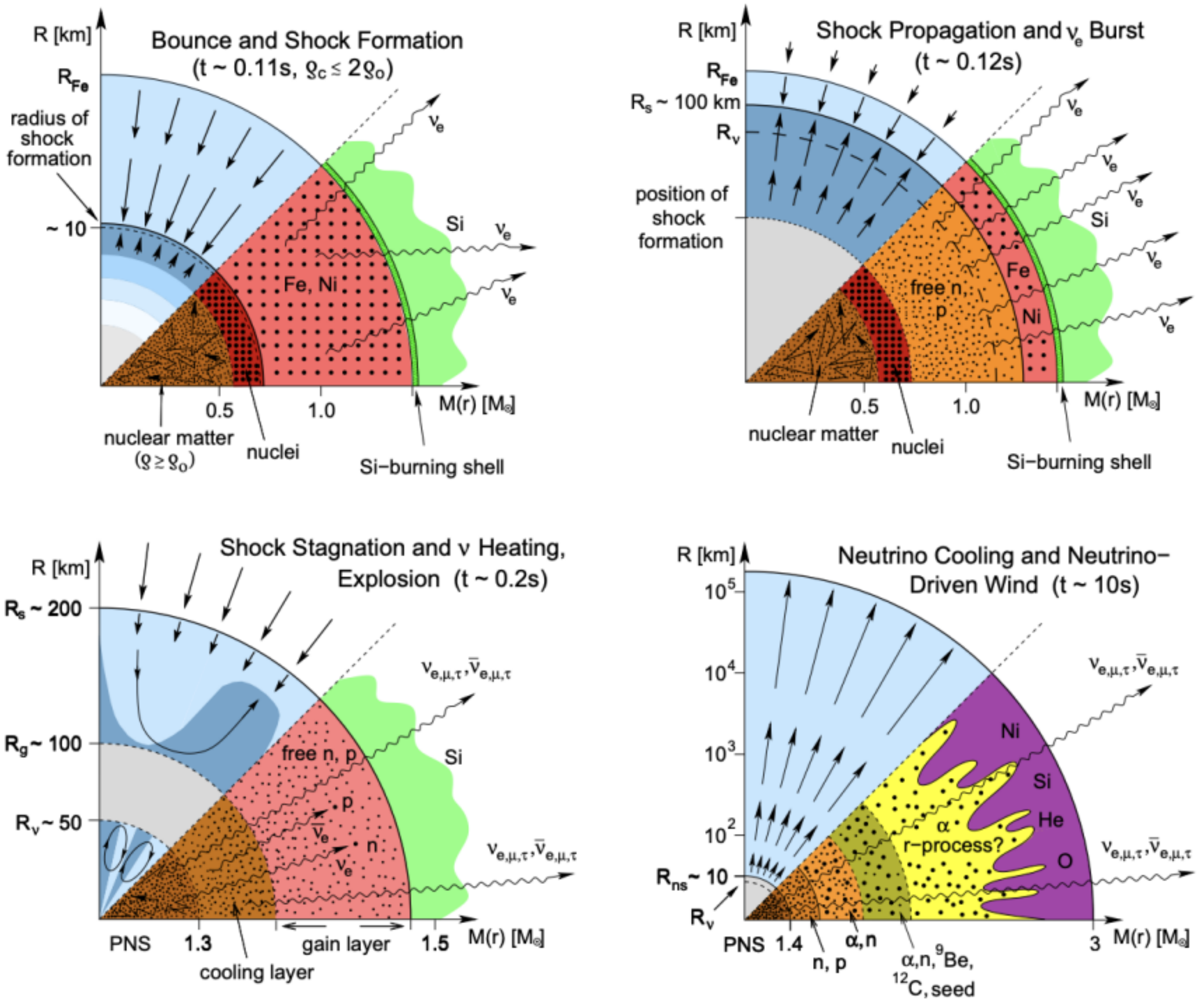

Janka et al, arXiv: astro-ph/0612072

Supernova Neutrino Boosted Dark Matter

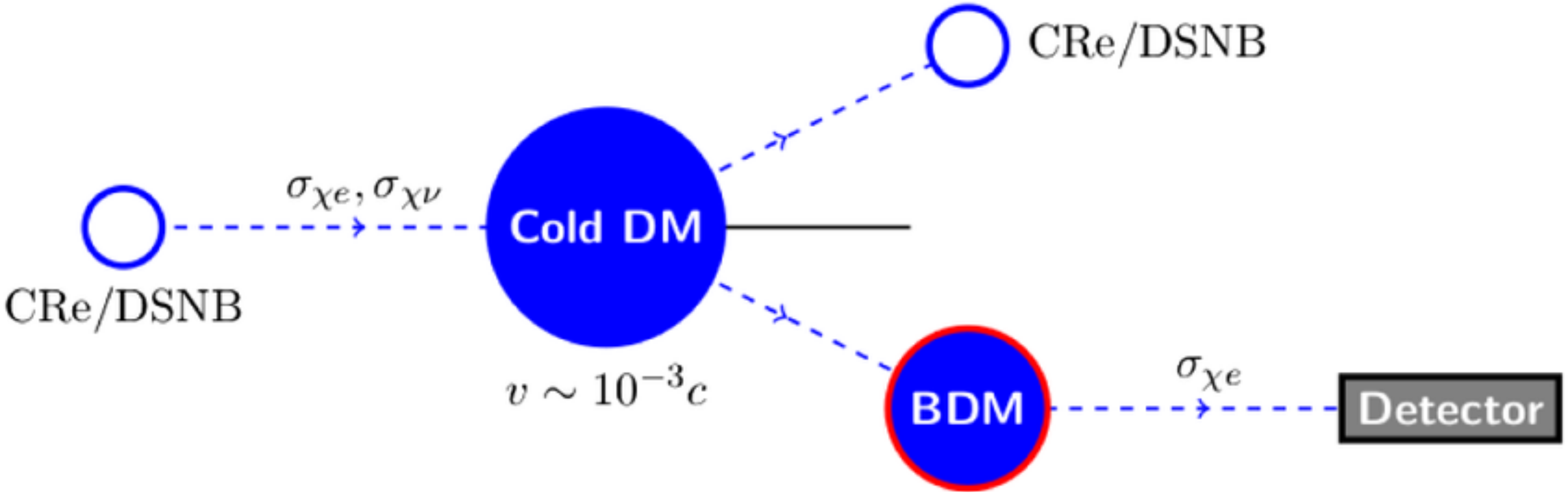

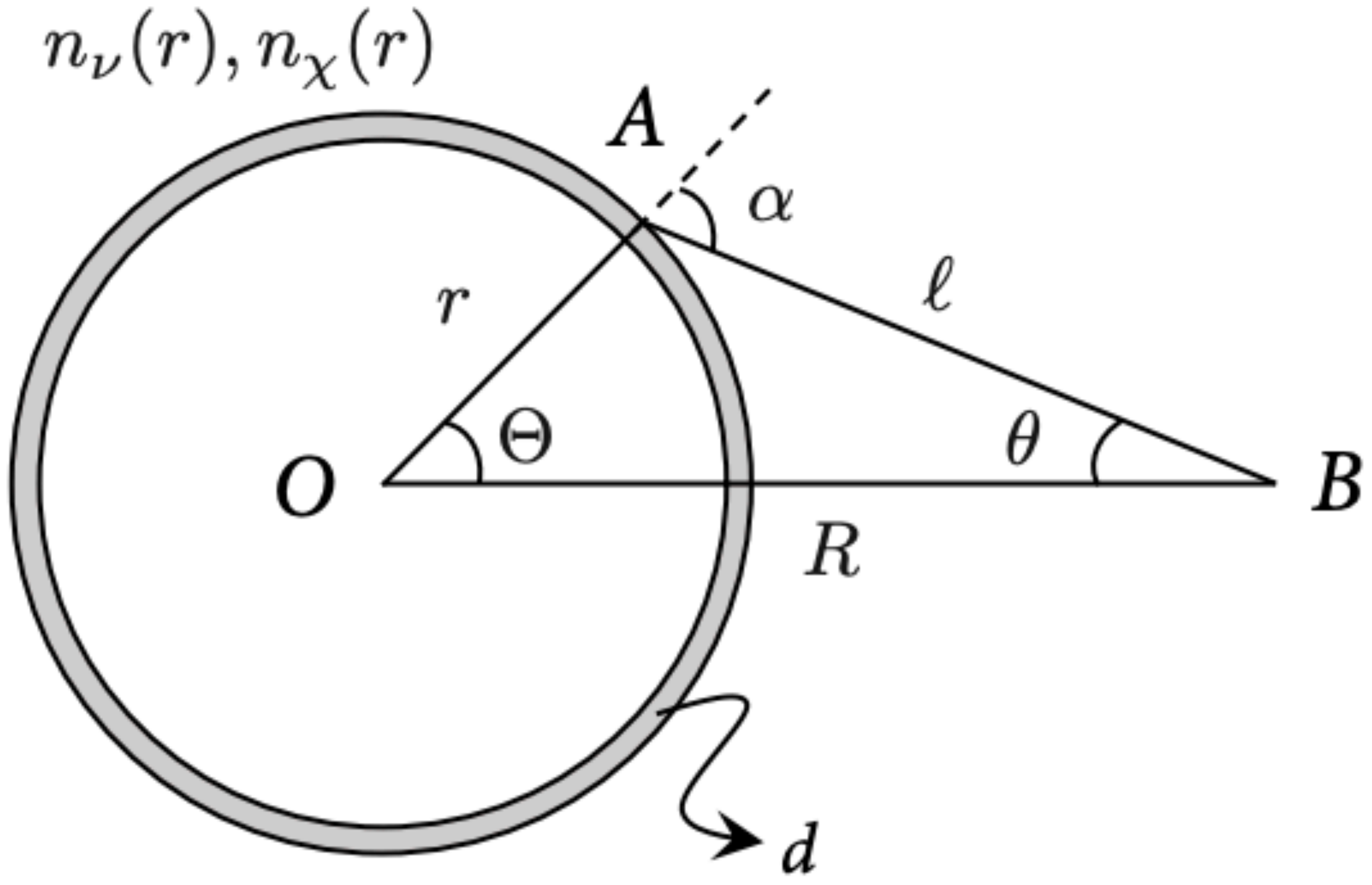

Supernova Neutrino Boosted Dark Matter

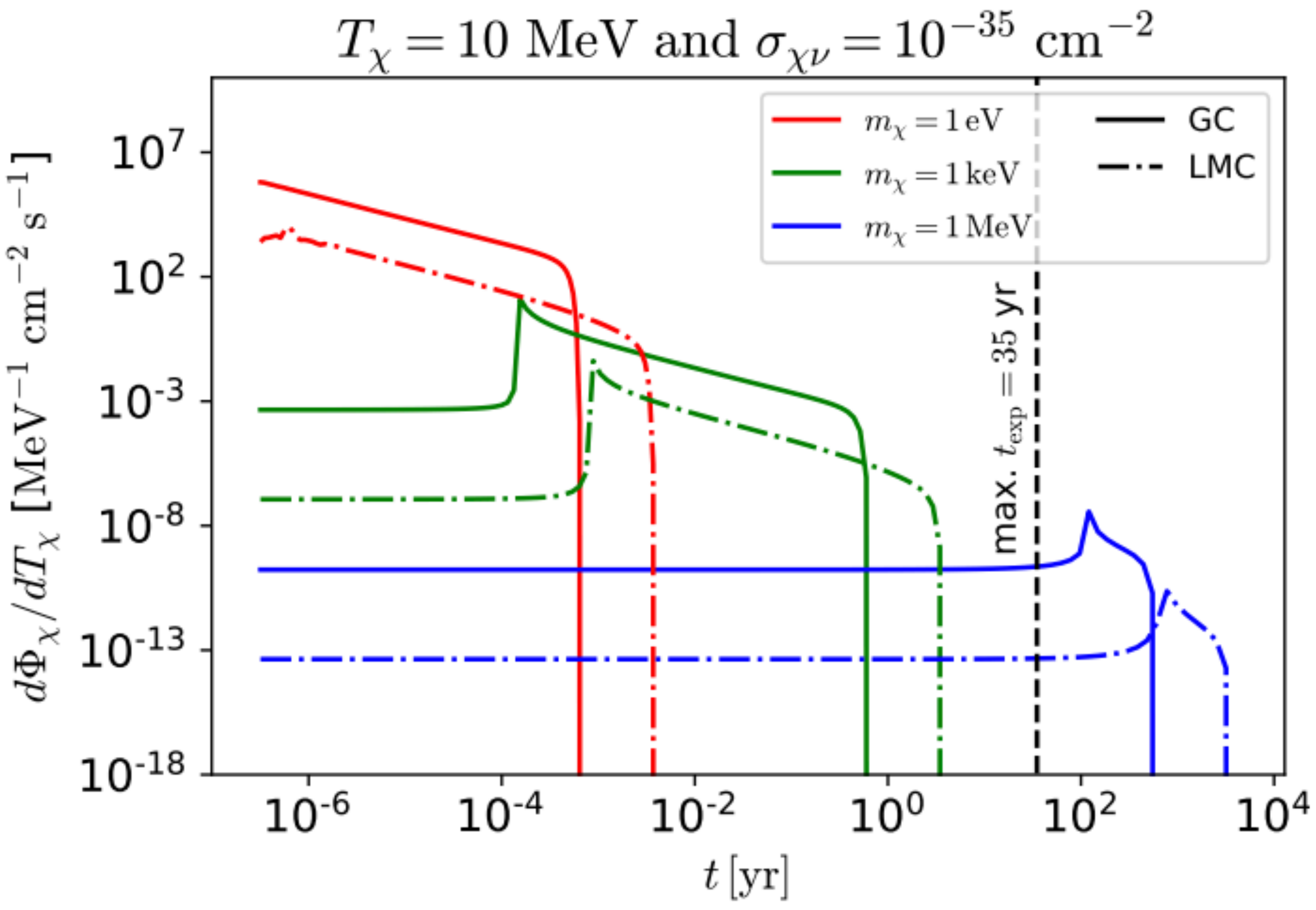

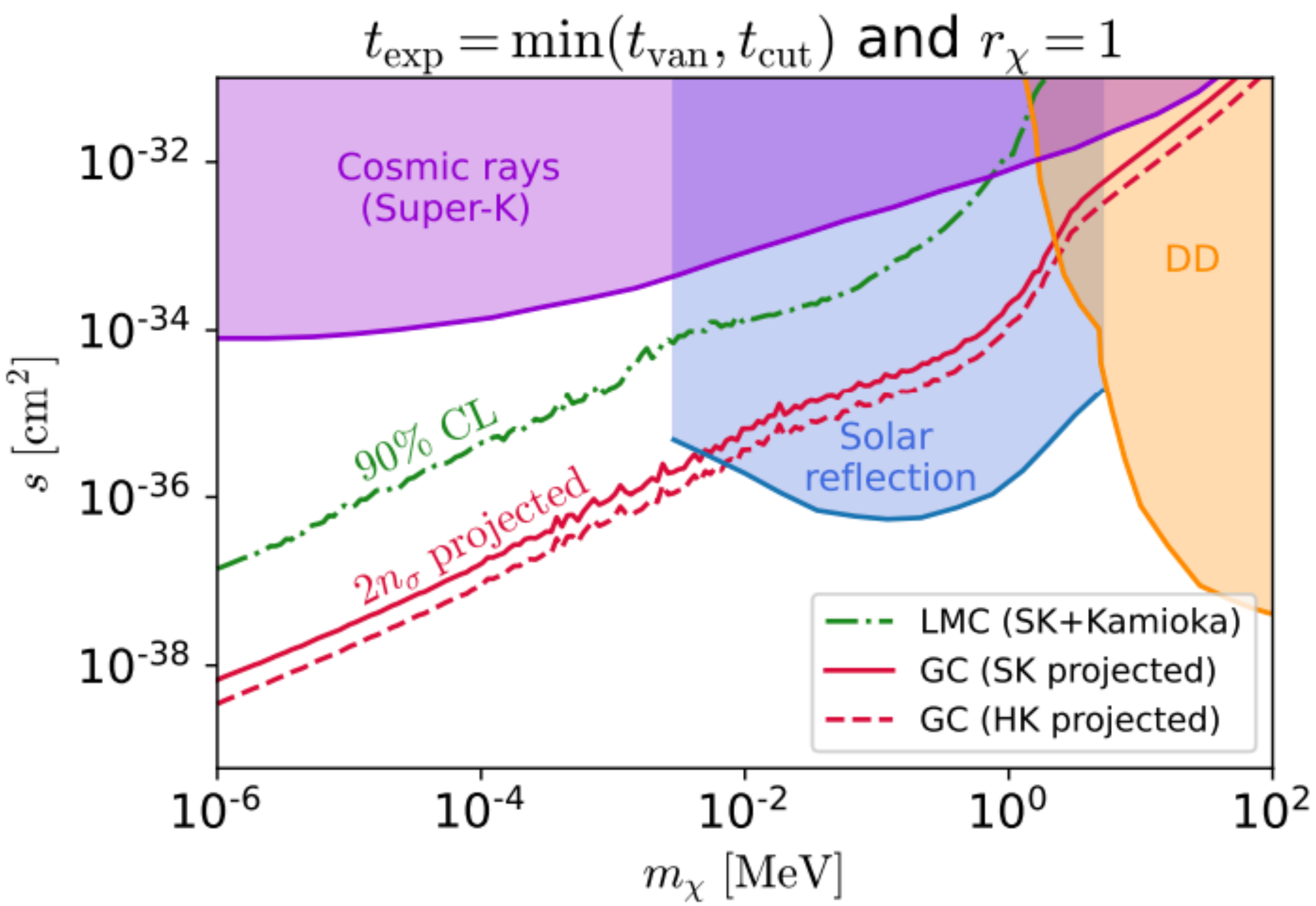

Lin et al, arXiv: 2206.06864

See also Lin et al, arXiv: 2404.08528

Atmospheric Dark Matter

Boosted Dark Matter from Cosmic Rays in the Atmosphere

- Heavy neutral leptons
- Hadrophilic dark matter
- Axion-like particles
- Long-lived neutralinos
- Monopoles
- Dark photon
- Millicharged particles
- …

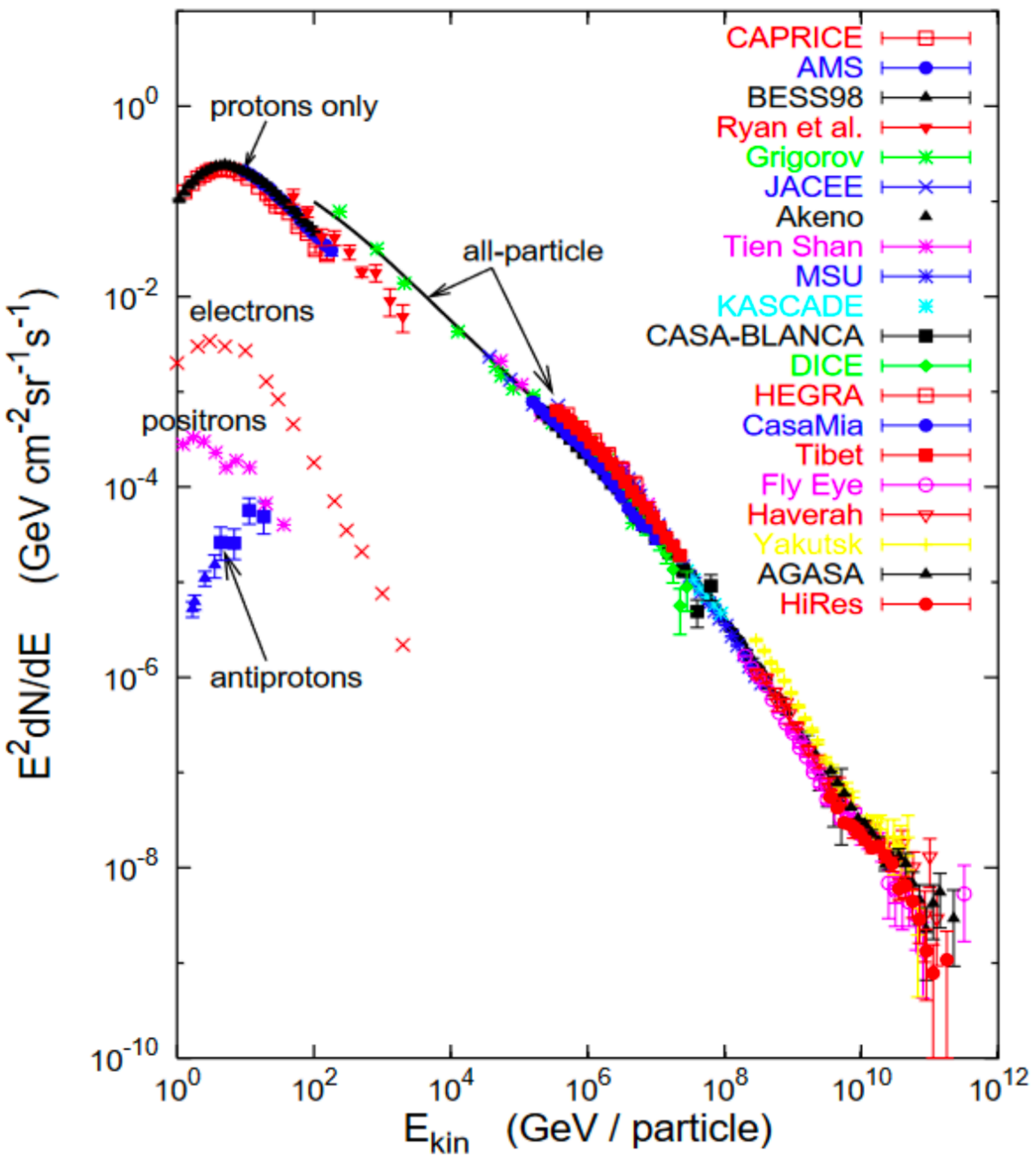

Dark Photon Kinetic Mixing

Extra $U(1)$? $SU(3)_c \times SU(2)_L \times U(1)_Y \times U(1)'$

Pospelov' 2008
Ackerman, Buckley, Carrol, Kamionkowsk' 2008
Arkani-Hame, Finkbeine, Slatyer, Weiner' 2008

$$\mathscr{L} = -\frac{1}{4}(F_{\mu\nu}F^{\mu\nu} - 2\epsilon F_{\mu\nu}F'^{\mu\nu} + F'_{\mu\nu}F'^{\mu\nu}) - J^\mu A_\mu$$

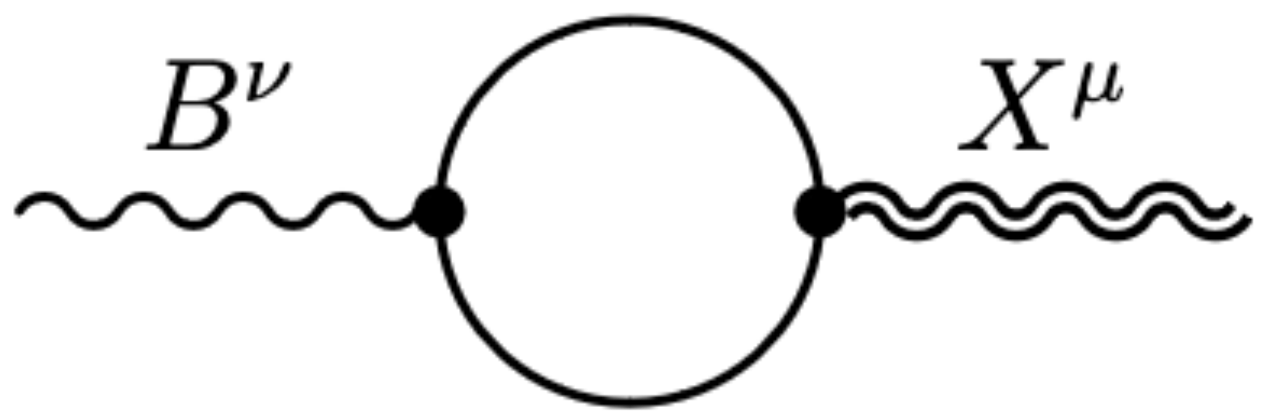

$$\epsilon = -\frac{g' g_X}{16\pi^2}\sum_i Y_i q_i \ln\frac{M_i^2}{\mu^2} \sim 10^{-1} - 10^{-3}$$

Millicharge Particles

Massless dark photon $\mathcal{L}_0 = -\frac{1}{4}F_{a\mu\nu}F_a^{\mu\nu} - \frac{1}{4}F_{b\mu\nu}F_b^{\mu\nu} - \frac{\varepsilon}{2}F_{a\mu\nu}F_b^{\mu\nu}$ $\mathcal{L} = e\, J_\mu A_b^\mu + e' J'_\mu A_a^\mu$

$$\begin{pmatrix} A_a^\mu \\ A_b^\mu \end{pmatrix} = \begin{pmatrix} \frac{1}{\sqrt{1-\varepsilon^2}} & 0 \\ -\frac{\varepsilon}{\sqrt{1-\varepsilon^2}} & 1 \end{pmatrix} \begin{pmatrix} \cos\theta & -\sin\theta \\ \sin\theta & \cos\theta \end{pmatrix} \begin{pmatrix} A'^\mu \\ A^\mu \end{pmatrix}$$

$$\begin{aligned} \mathcal{L}' &= \left[\frac{e'\cos\theta}{\sqrt{1-\varepsilon^2}} J'_\mu + e\left(\sin\theta - \frac{\varepsilon\cos\theta}{\sqrt{1-\varepsilon^2}}\right) J_\mu\right] A'^\mu \\ &+ \left[-\frac{e'\sin\theta}{\sqrt{1-\varepsilon^2}} J'_\mu + e\left(\cos\theta + \frac{\varepsilon\sin\theta}{\sqrt{1-\varepsilon^2}}\right) J_\mu\right] A^\mu \end{aligned}$$

$$\boxed{\mathcal{L}' = e' J'_\mu A'^\mu + \left[-\frac{e'\varepsilon}{\sqrt{1-\varepsilon^2}} J'_\mu + \frac{e}{\sqrt{1-\varepsilon^2}} J_\mu\right] A^\mu}$$

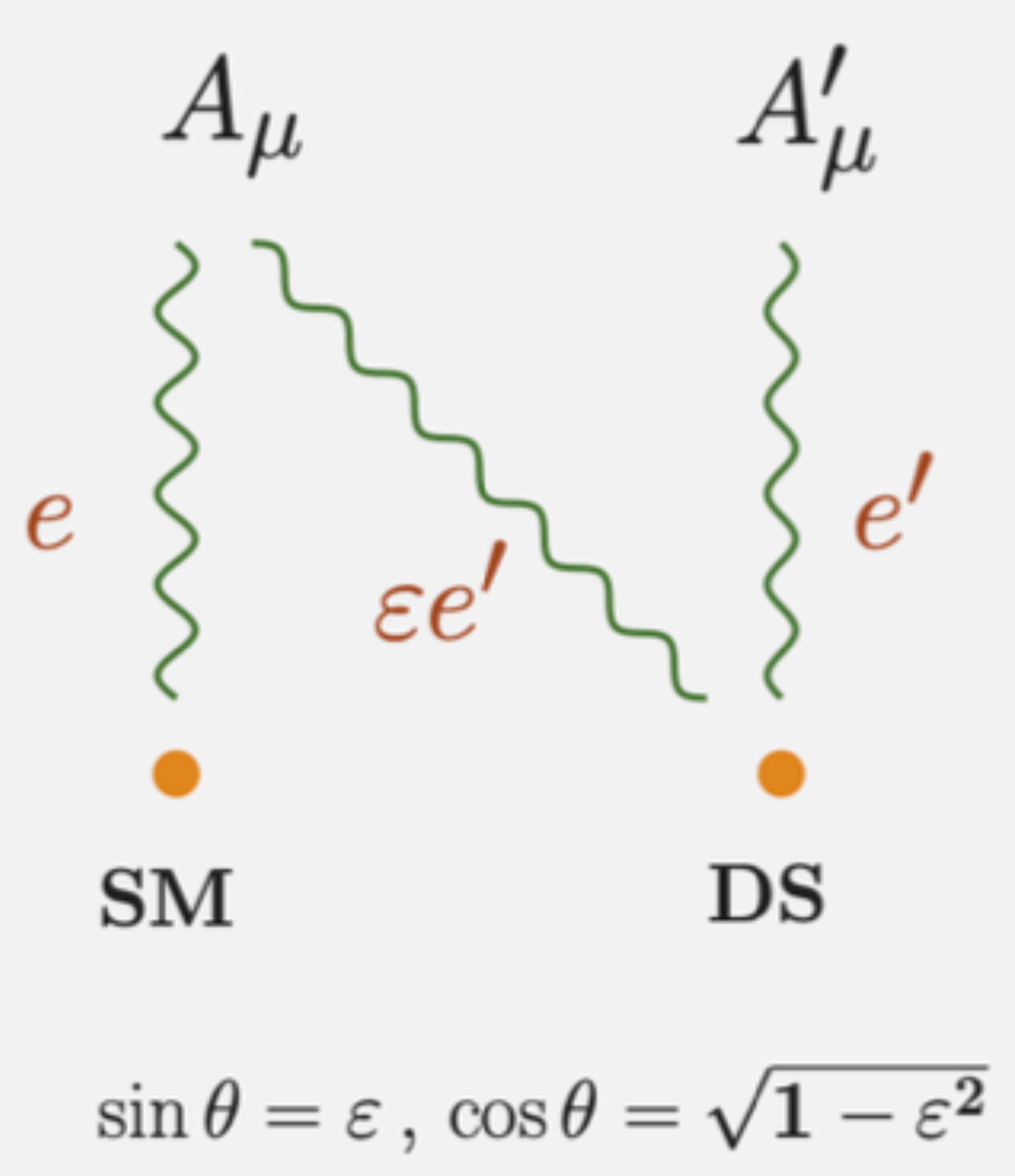

Fabbrichesi et al arXiv: 2005.01515

Millicharge Particles from Light Meson Decay

$$\Phi_{\mathfrak{m}}(\gamma_{\mathfrak{m}}) = \Omega_{\text{eff}} \int \mathcal{I}_{\text{CR}}(\gamma_{\text{cm}}) \frac{\sigma_{\mathfrak{m}}(\gamma_{\text{cm}})}{\sigma_{\text{in}}(\gamma_{\text{cm}})} P(\gamma_{\mathfrak{m}}|\gamma_{\text{cm}})\, \mathrm{d}\gamma_{\text{cm}}$$

$$\gamma_{\text{cm}} = \frac{1}{2}\sqrt{s}/m_p$$

$$P(\gamma_{\mathfrak{m}}|\gamma_{\text{cm}}) \approx \sum_{\alpha} \frac{1}{\sigma_{\mathfrak{m}}} \times \frac{\mathrm{d}\sigma_{\mathfrak{m}}}{\mathrm{d}x_F} \times \frac{\mathrm{d}x_F^{(\alpha)}}{\mathrm{d}\gamma_{\mathfrak{m}}}$$

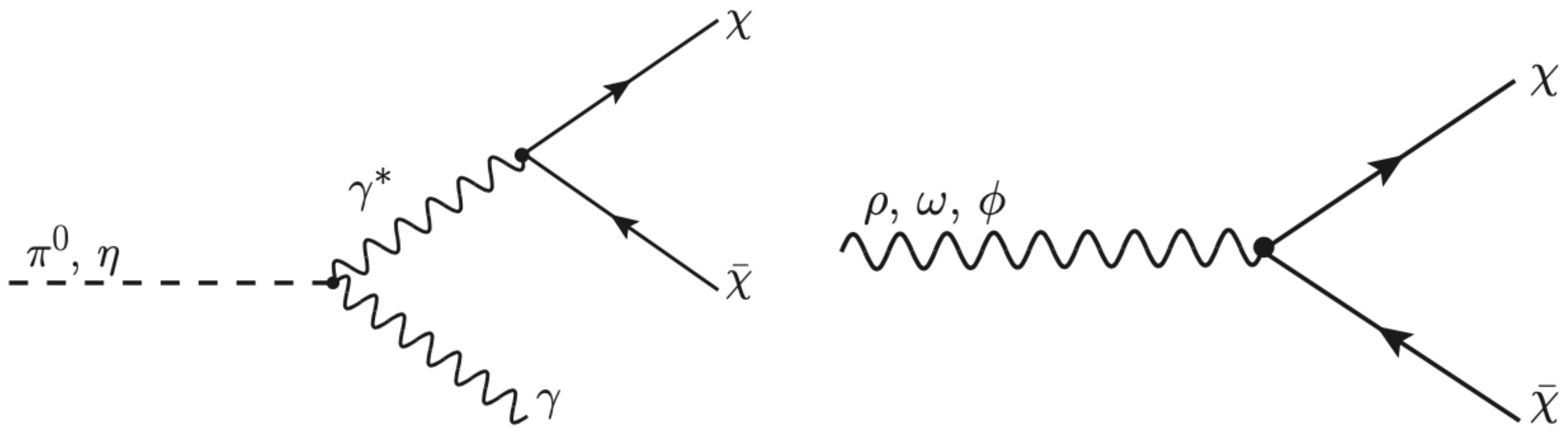

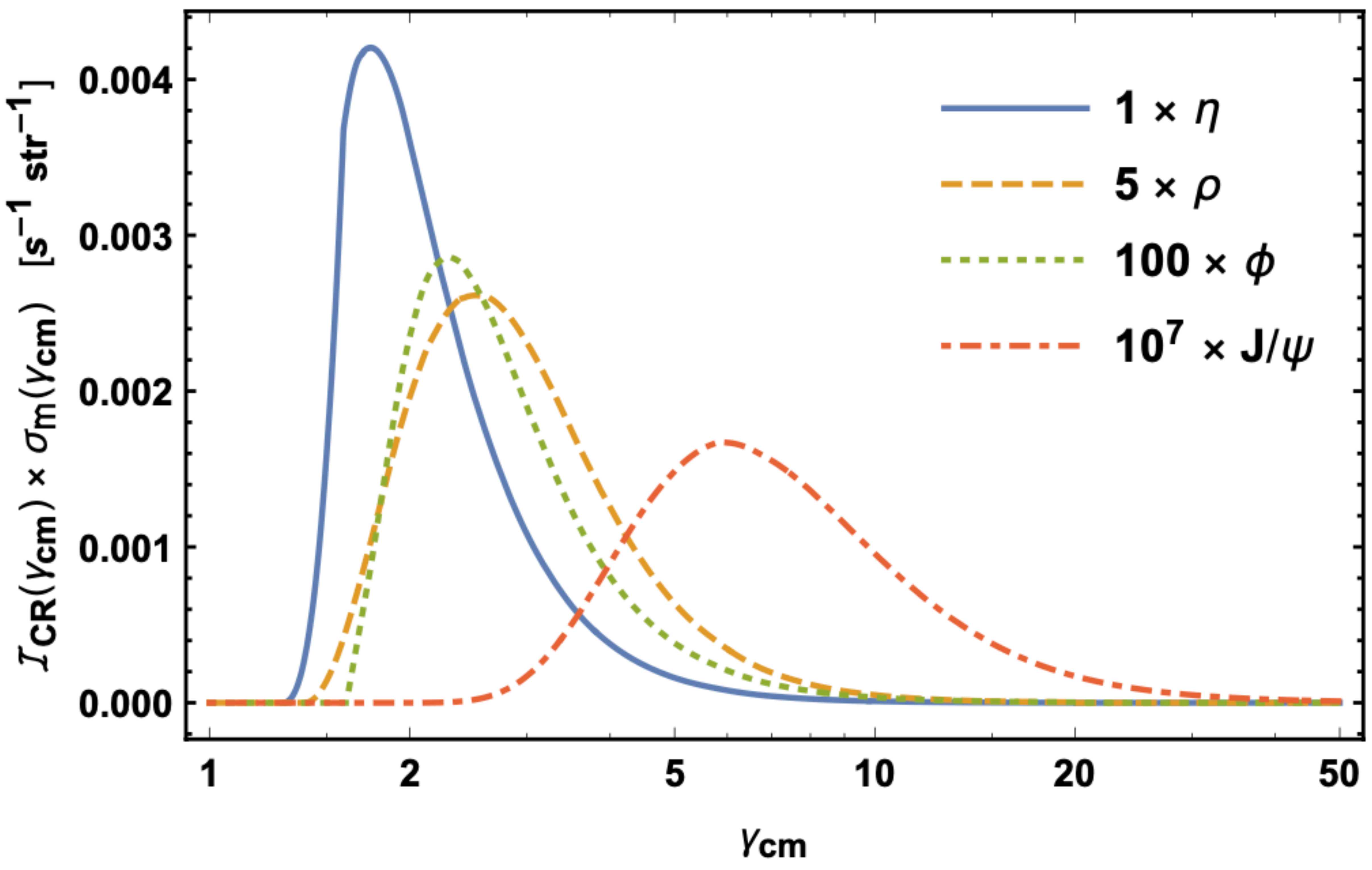

Plestid et al PRD/2002.11732

Millicharge Particles from Upsilon Meson Decay

Pythia8 simulations

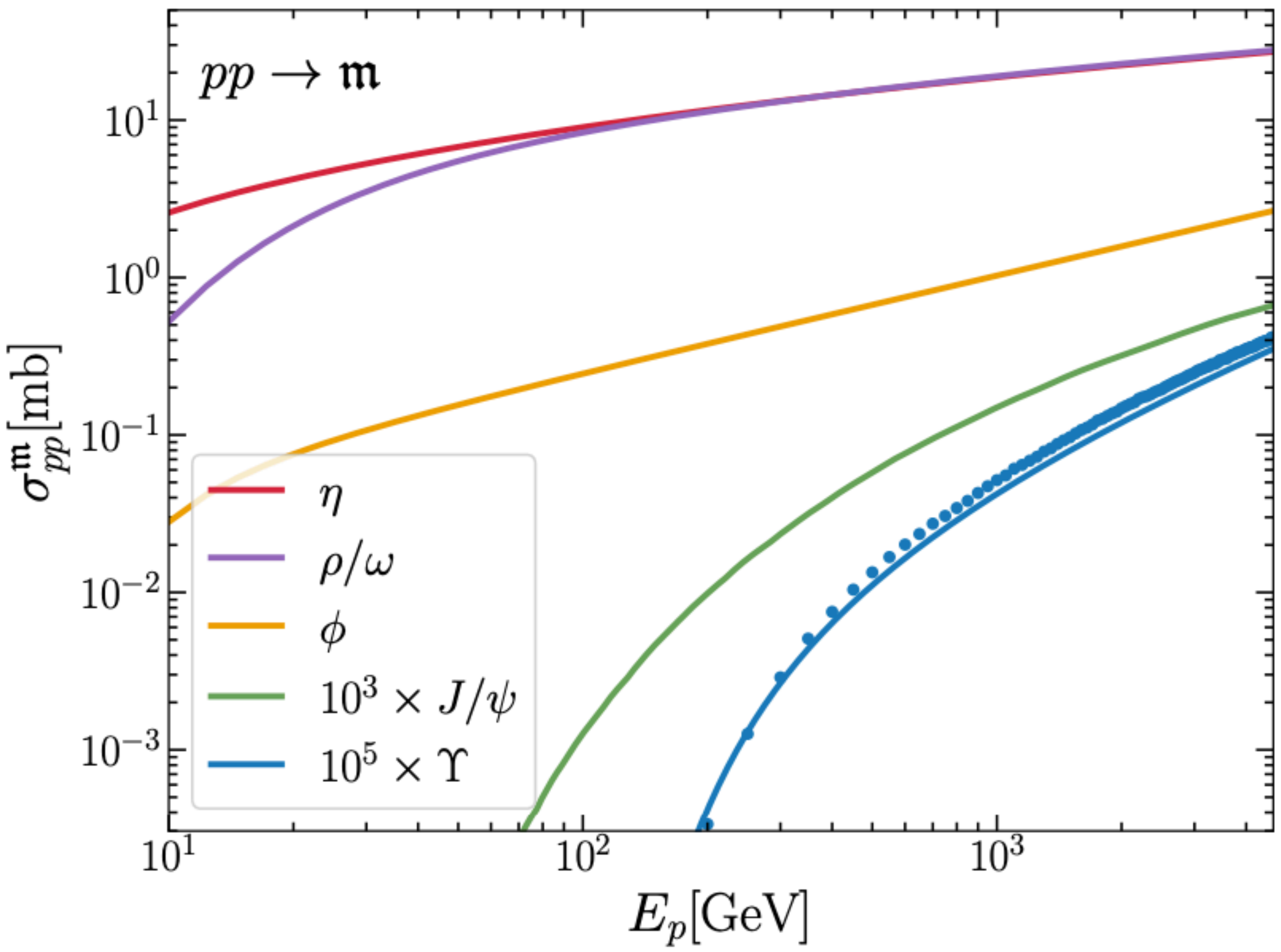

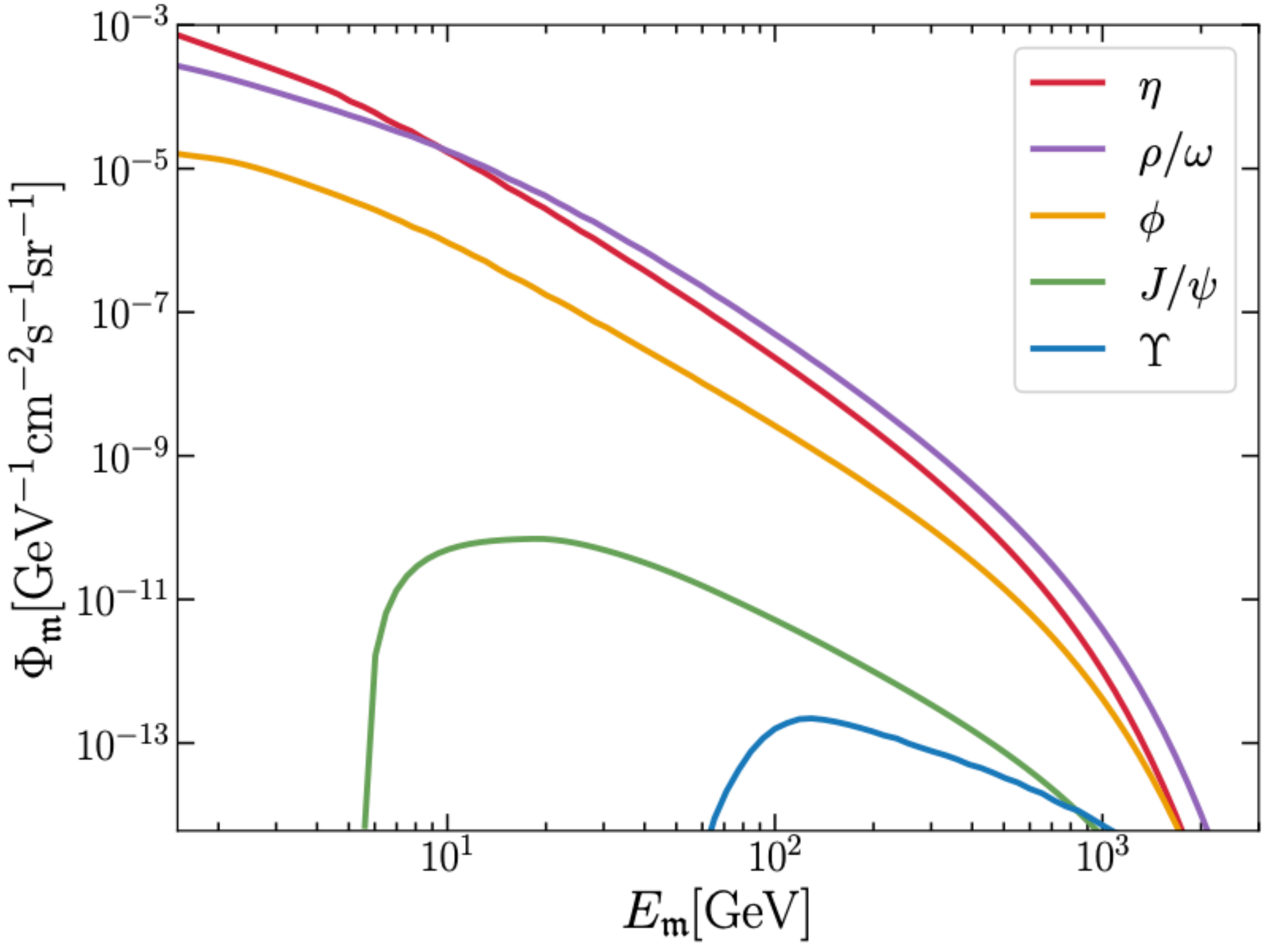

Wu, Hardy, **NS**, PRD/2406.01668

Millicharge Particles from Proton Bremsstrahlung

Fermi-Weizsacker-Williams (FWW) approximation with the splitting-kernel approach

$$d\sigma^{\rm PB}(s) \simeq d\mathscr{P}_{p\to\gamma^* p'} \times \sigma_{pN}(s')$$

Kernel

$$\frac{d^2\mathcal{P}^{\rm FWW}_{p\to\gamma^* p}}{dE_k\, d\cos\theta_k} = \left|\mathbf{J}(z,p_T^2)\right| \frac{d^2\mathcal{P}^{\rm FWW}_{p\to\gamma^* p}}{dz\, dp_T^2} = \left|\mathbf{J}(z,p_T^2)\right| |F_V(k)|^2\, \omega(z,p_T^2)$$

EM form factor

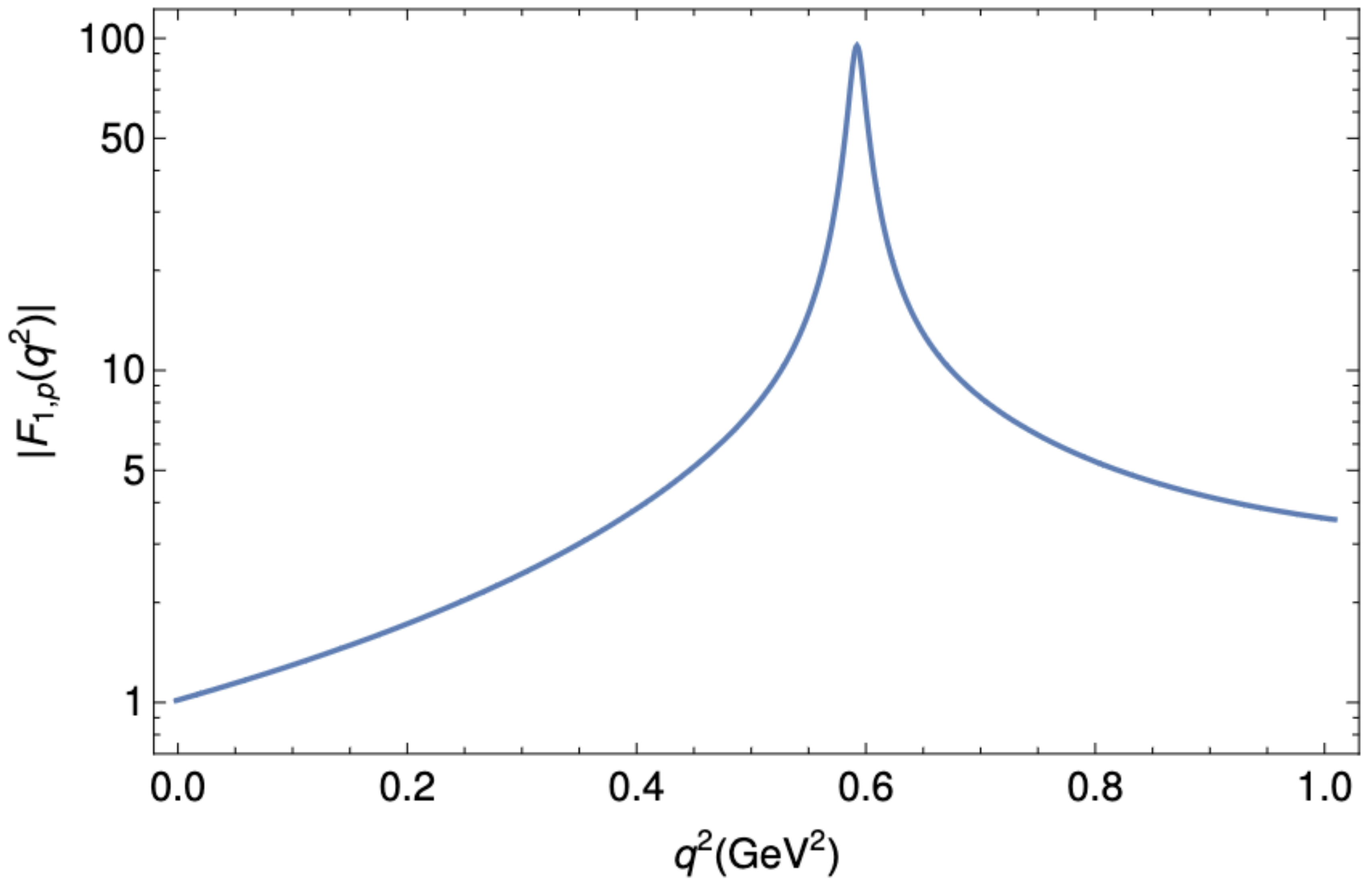

deNiverville et al PRD/1609.01770

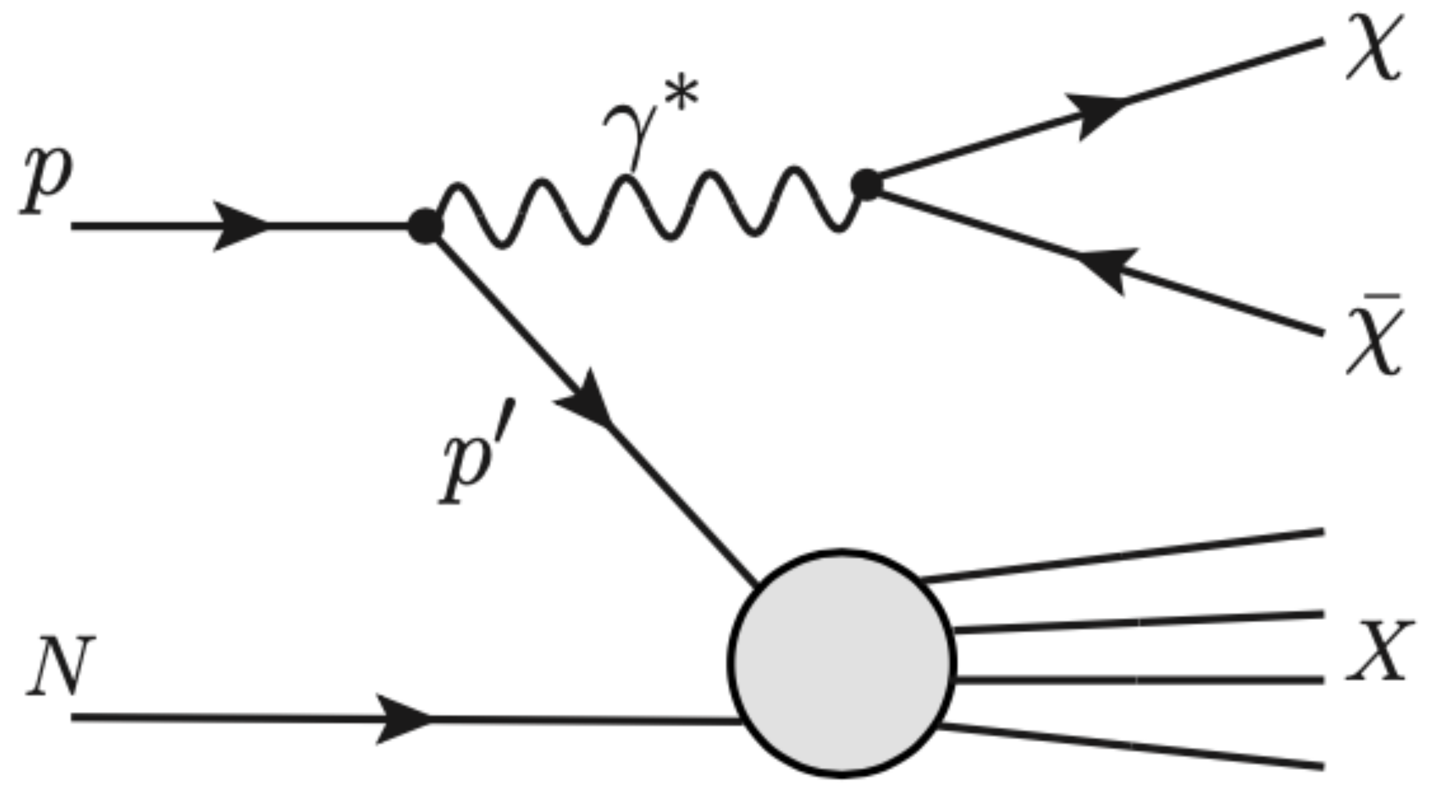

$$\Phi_\chi^{\rm PB} = \int dE_p \Phi_p \frac{\epsilon^2 e^2}{6\pi^2} \int \frac{dk^2}{k^2} \sqrt{1-\frac{4m_\chi^2}{k^2}} \left(1+\frac{2m_\chi^2}{k^2}\right)$$
$$\times \int dE_k \frac{1}{\sigma_{pN}} \frac{d\sigma^{\rm PB}}{dE_k} \frac{\Theta(E_\chi - E_{\rm min})\Theta(E_{\rm max}-E_\chi)}{E_{\rm max}-E_{\rm min}}$$

Du et al arXiv: 2211.11469

Du et al arXiv: 2308.05607

Millicharge Particles from Drell-Yan Process

Madgraph simulations

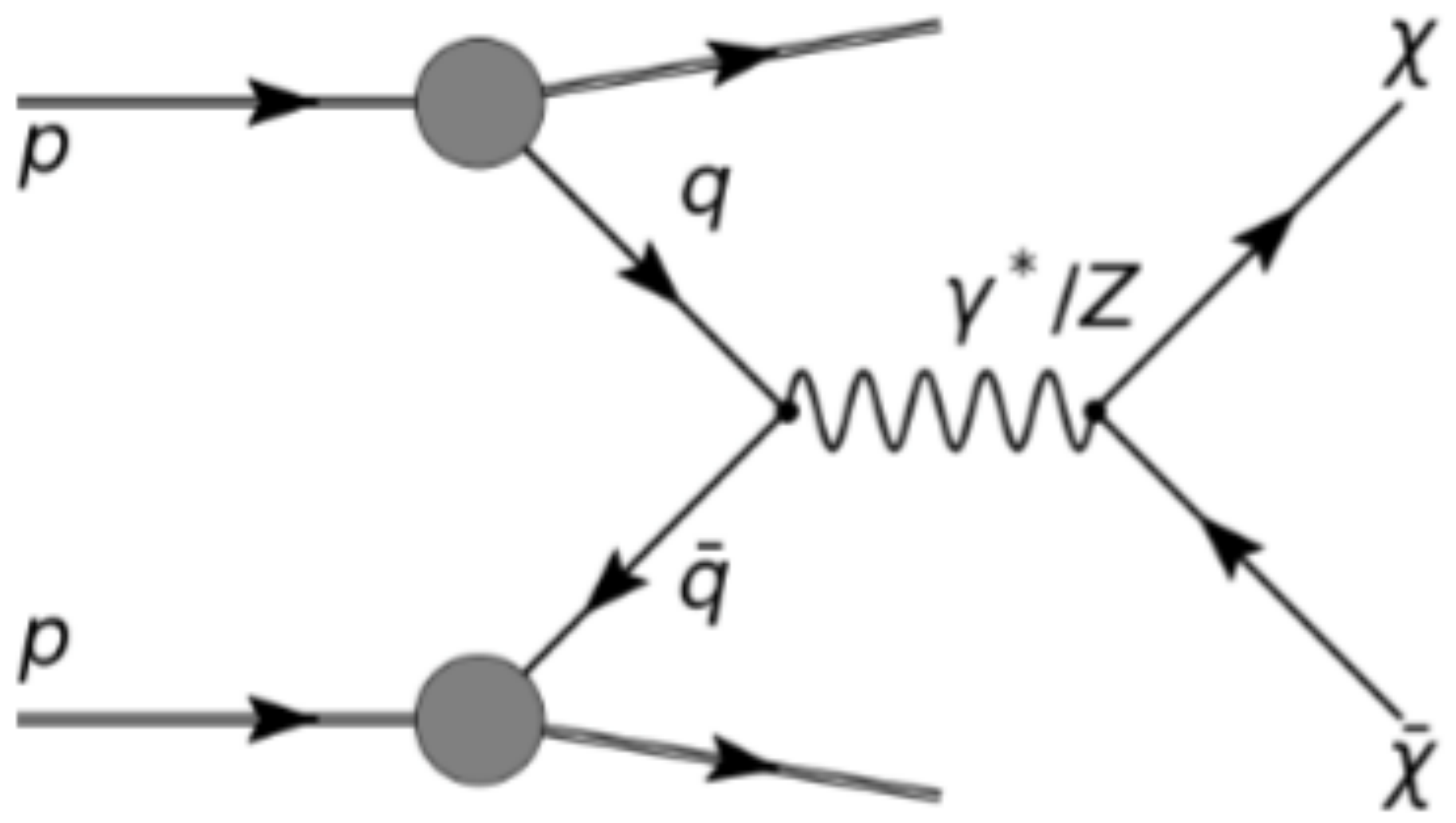

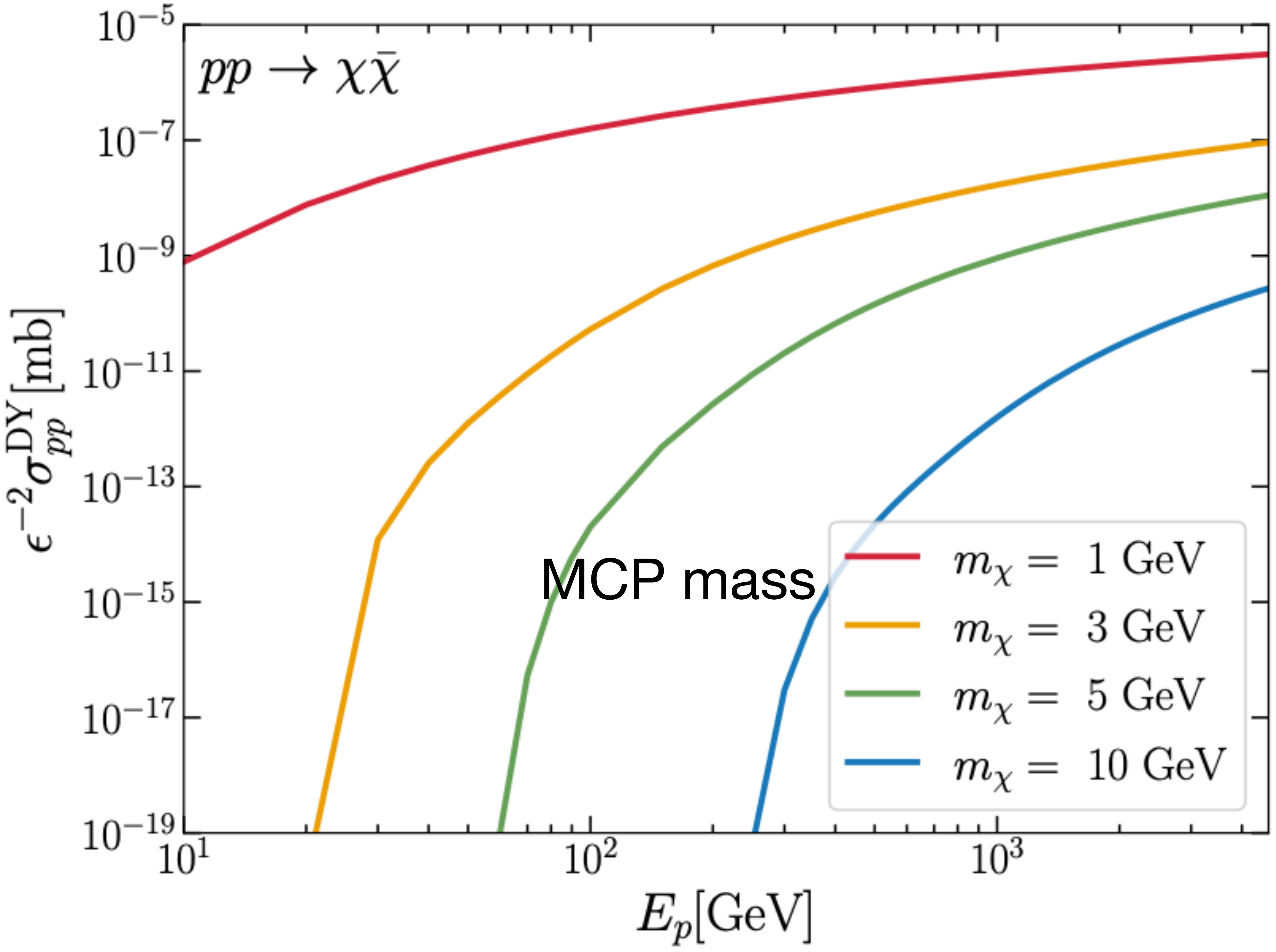

Wu, Hardy, **NS**, PRD/2406.01668

$$\hat{\sigma}\left(q(p_1)\,\bar{q}(p_2) \to l^+l^-\right) = \frac{4\pi\alpha^2}{3\hat{s}}\frac{1}{N_c}Q_q^2$$

Millicharge Particles Flux

Meson decay+Proton Bremsstrahlung+Drell-Yan

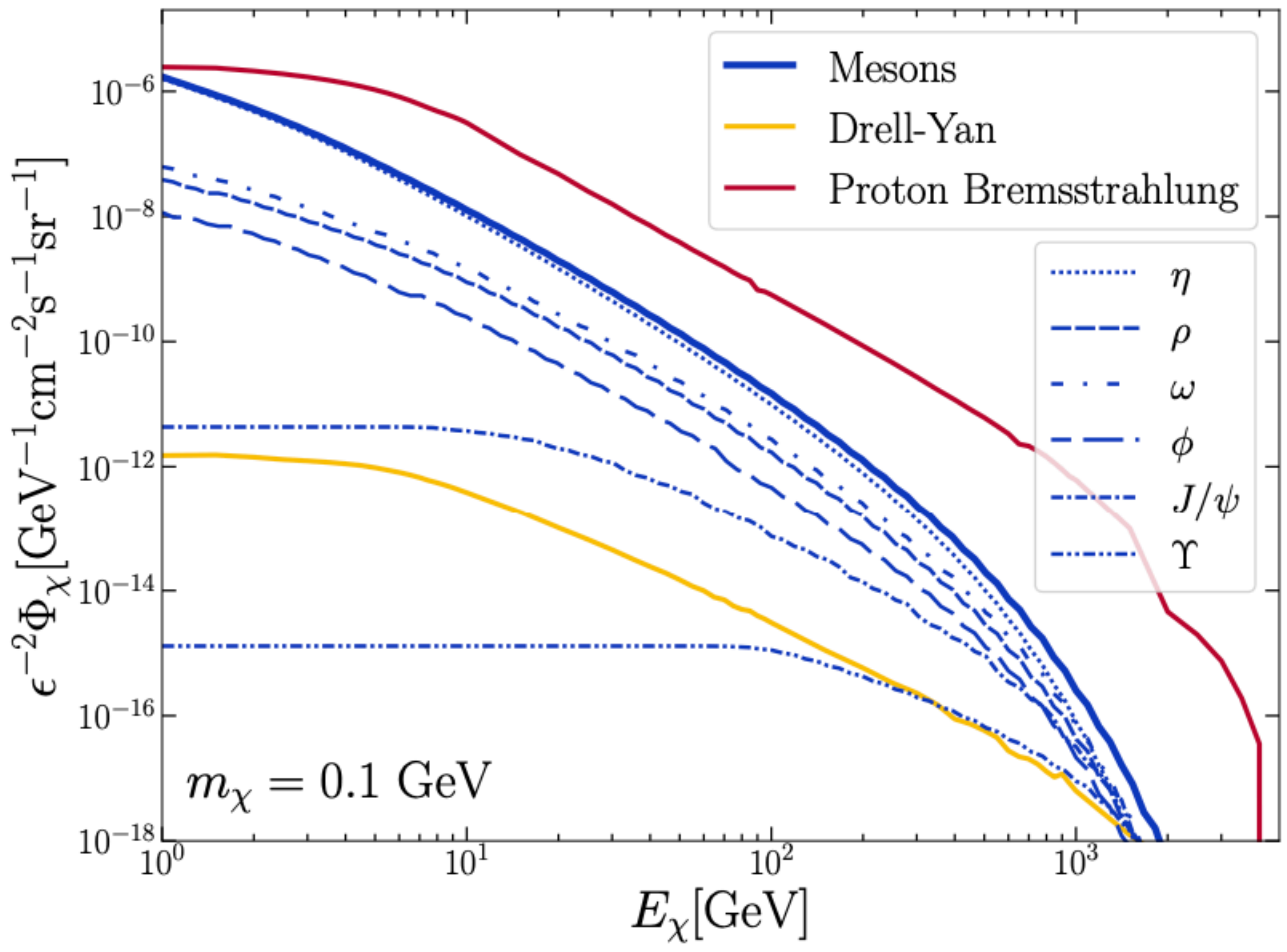

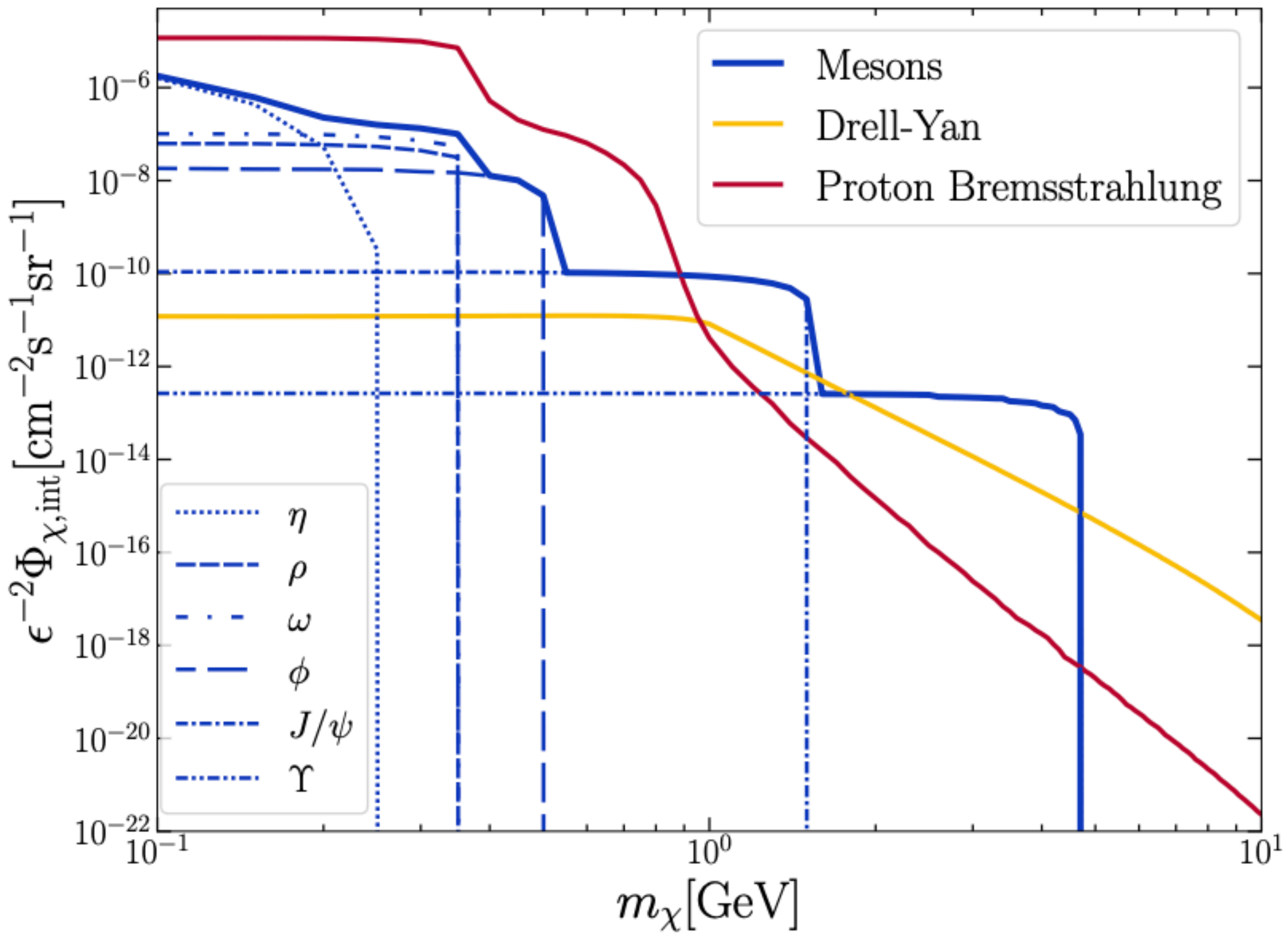

Wu, Hardy, **NS**, PRD/2406.01668

Earth Attenuation

$$-\frac{dE}{dX} = \varepsilon^2 \left(a_{\text{ion.}} + b_{\text{el.-brem.}}\varepsilon^2 E + b_{\text{inel.-brem.}}E + b_{\text{pair}}E + b_{\text{photo-had.}}E\right) \approx \varepsilon^2 \left(a + bE\right)$$

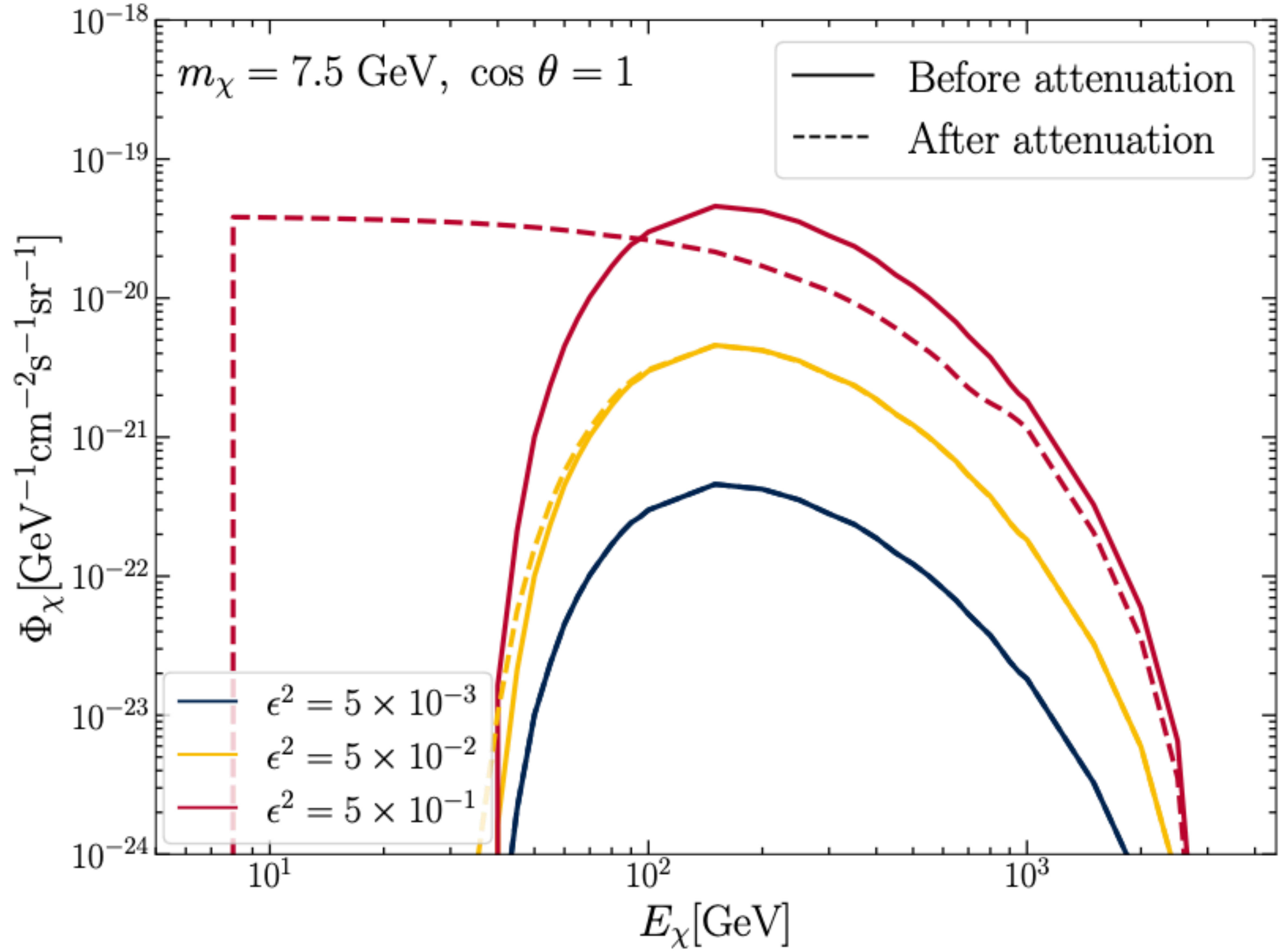

For $\epsilon^2 \gtrsim 10^{-2}$, the down-going flux becomes significantly attenuated

Wu, Hardy, **NS**, PRD/2406.01668

Single Scatter Constraint

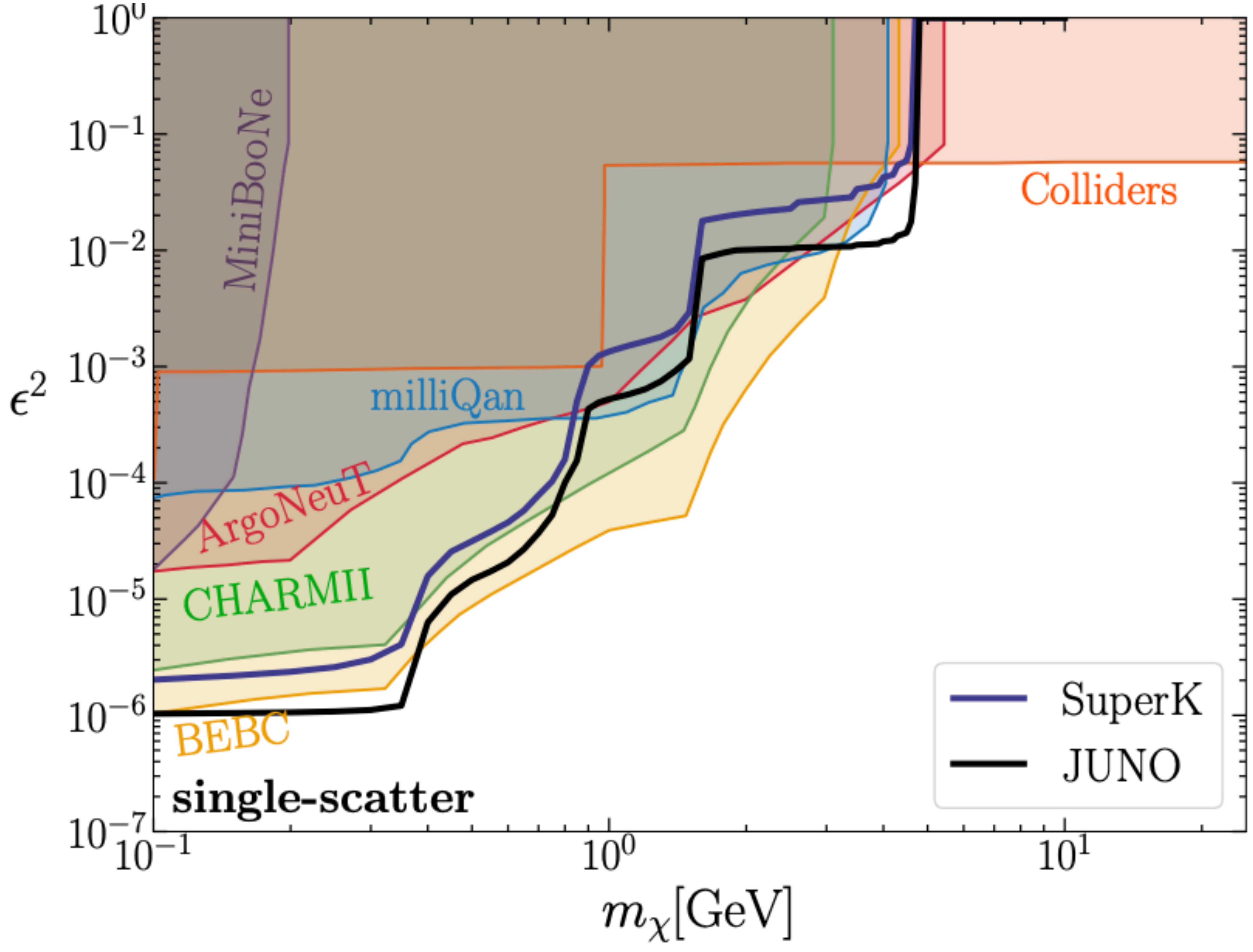

$$\frac{d\sigma_{\chi e}}{dE_r} = \pi\epsilon^2\alpha^2 \frac{(E_r^2 + 2E_\chi^2)m_e - ((2E_\chi + m_e)m_e + m_\chi^2)\ E}{E_r^2 m_e^2\left(E_\chi^2 - m_\chi^2\right)}$$

$$d\sigma_{\chi e}/dE_r \propto 1/E_r^2$$

$$\sigma_{\chi e} \simeq \frac{\pi\alpha_{EM}\epsilon^2}{m_e T_{\min}} = 2.6\times 10^{-25}\epsilon^2\ \mathrm{cm}^2 \frac{\mathrm{MeV}}{T_{\min}}$$

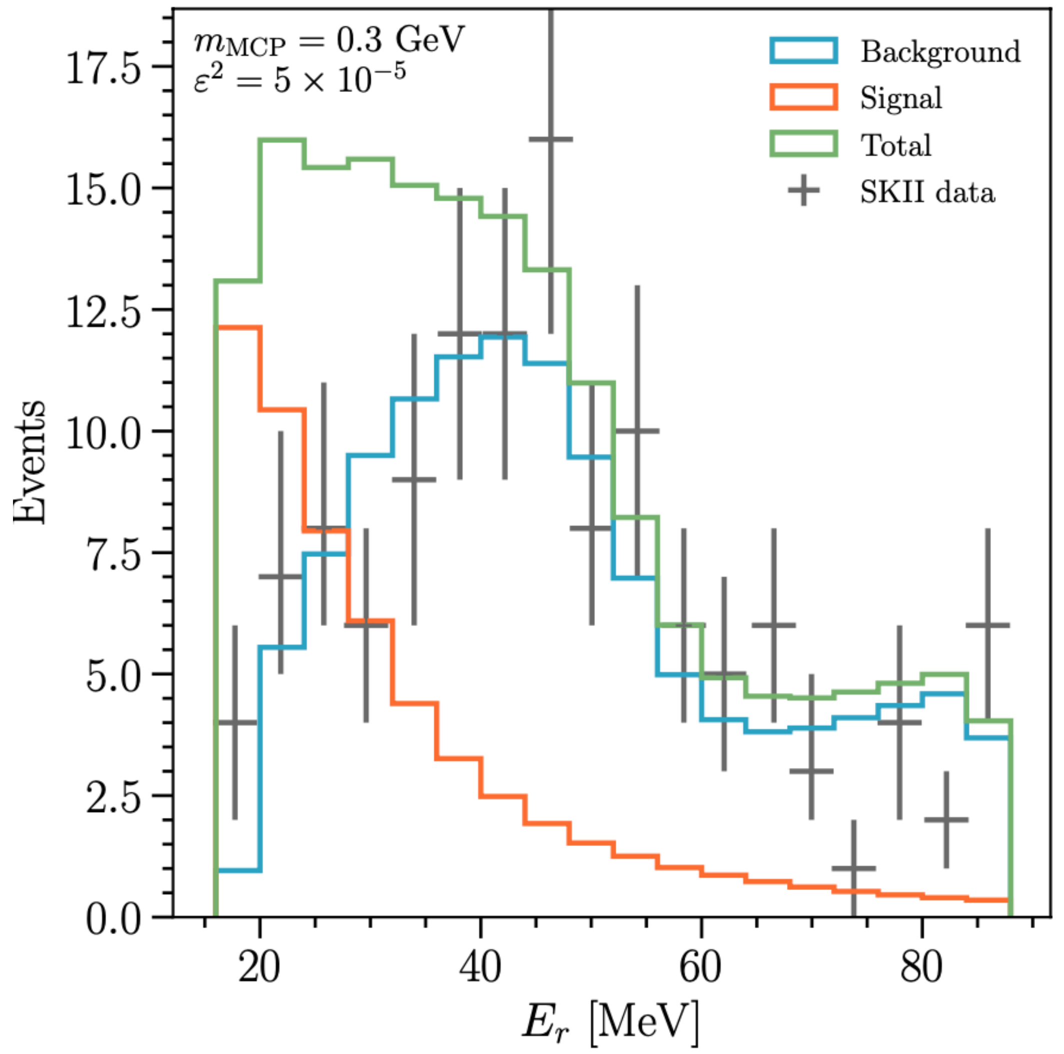

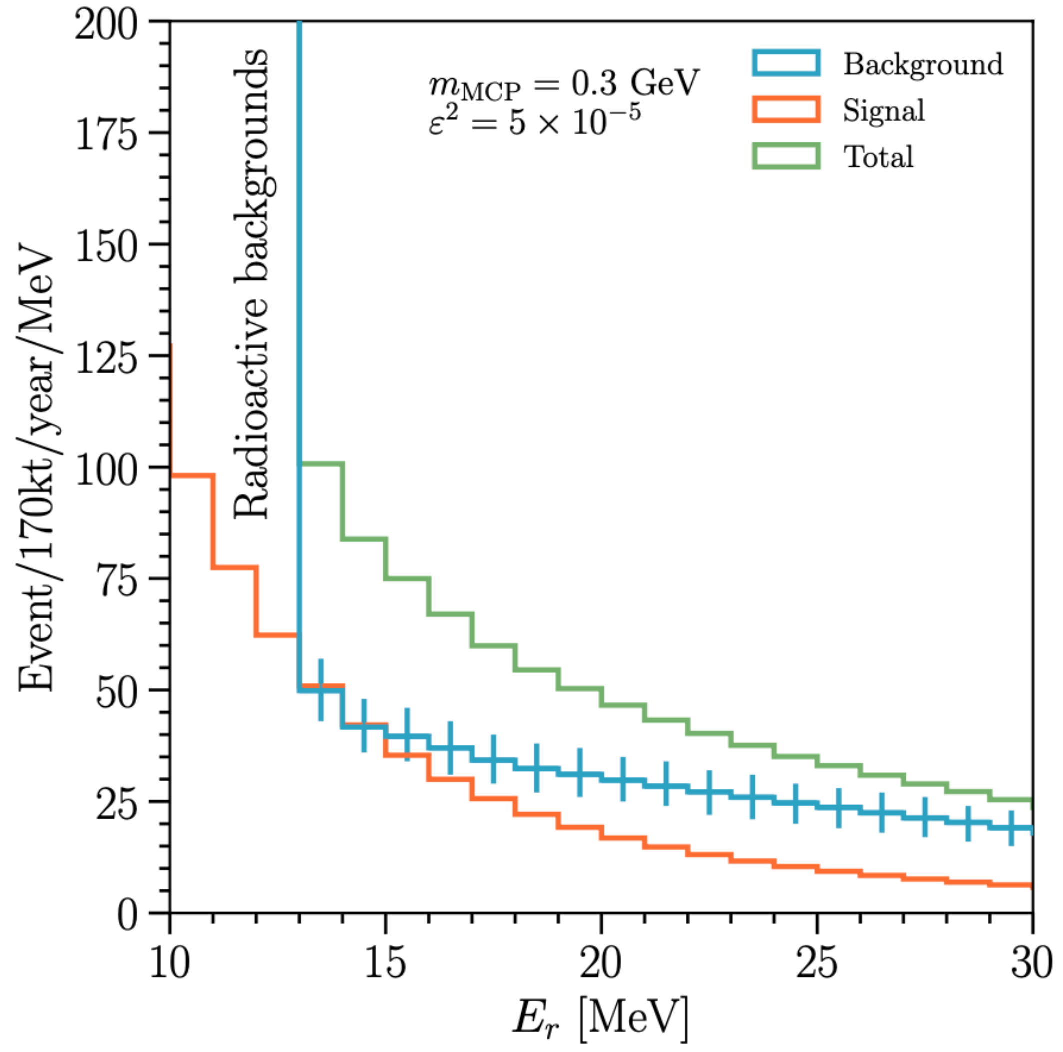

Assuming JUNO 10 MeV threshold+170 kton·yr exposure

Wu, Hardy, **NS**, PRD/2406.01668

Arguelles et al JHEP/2104.13924

Multiple Scatter Constraint

Single scatter probability $$P_1 = 1 - \exp\left(-\frac{L_D}{\lambda(T_{\min})}\right)$$

Multiple scatter probability $$P_{n\geq 2}(T_{\min}) = 1 - \exp\left(-\frac{L_D}{\lambda}\right)\left(1 + \frac{L_D}{\lambda}\right)$$

Number of observed events $$N_{\text{multi}} = N_{\text{single}} P_{n\geq 2}(T_{\min,\text{multi}}) / P_1(T_{\min,\text{single}})$$

$$N_{\text{single}}\left(m_\chi, \epsilon\right) = N_e T \int_{E_{i,\min}}^{E_{i,\max}} dE_r \epsilon_D(E_r) \times \int dE_\chi d\Omega \Phi_\chi^D \left(E_\chi, \Omega\right) \frac{d\sigma_{\chi e}}{dE_r}$$

Multiple Scatter Constraint

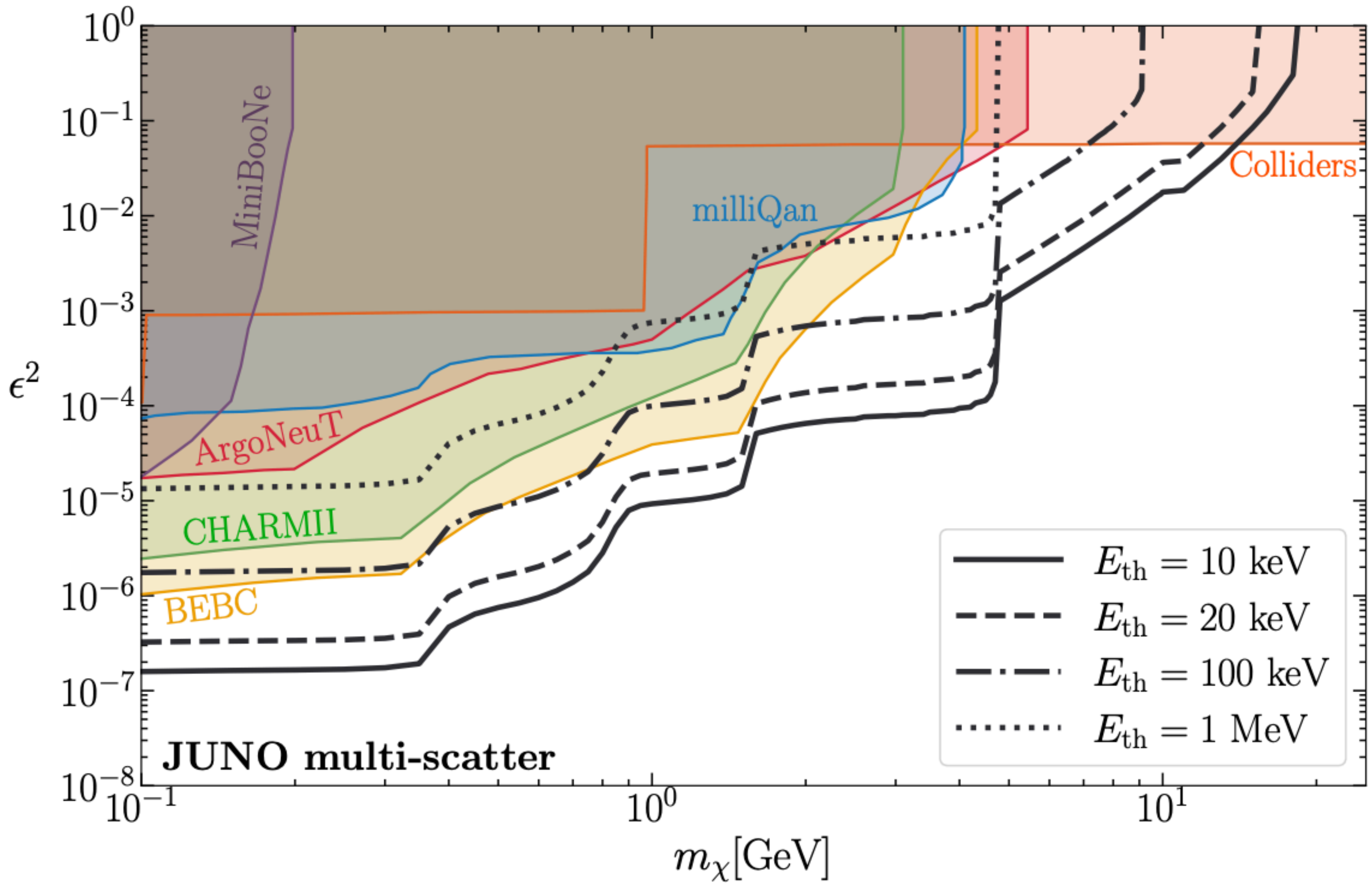

Assuming JUNO 170 kton·yr exposure

Wu, Hardy, **NS**, PRD/2406.01668

Contributions from Inelastic Scattering

Elastic scattering $\chi + A \rightarrow \chi + A$

$$\frac{d\sigma_{\rm ES}}{dE_R} = \frac{\bar{\sigma}_{\rm n} A^2 m_S^4 F^2(E_R)}{32\mu_{\rm n}^2 m_A (2m_A E_R + m_S^2)^2 (E_\chi^2 - m_\chi^2)} \times (4m_\chi^2 + 2m_A E_R)(4m_A^2 + 2m_A E_R),$$

Quasi-elastic scattering $\chi + A \rightarrow \chi + (A-1) + n/p$

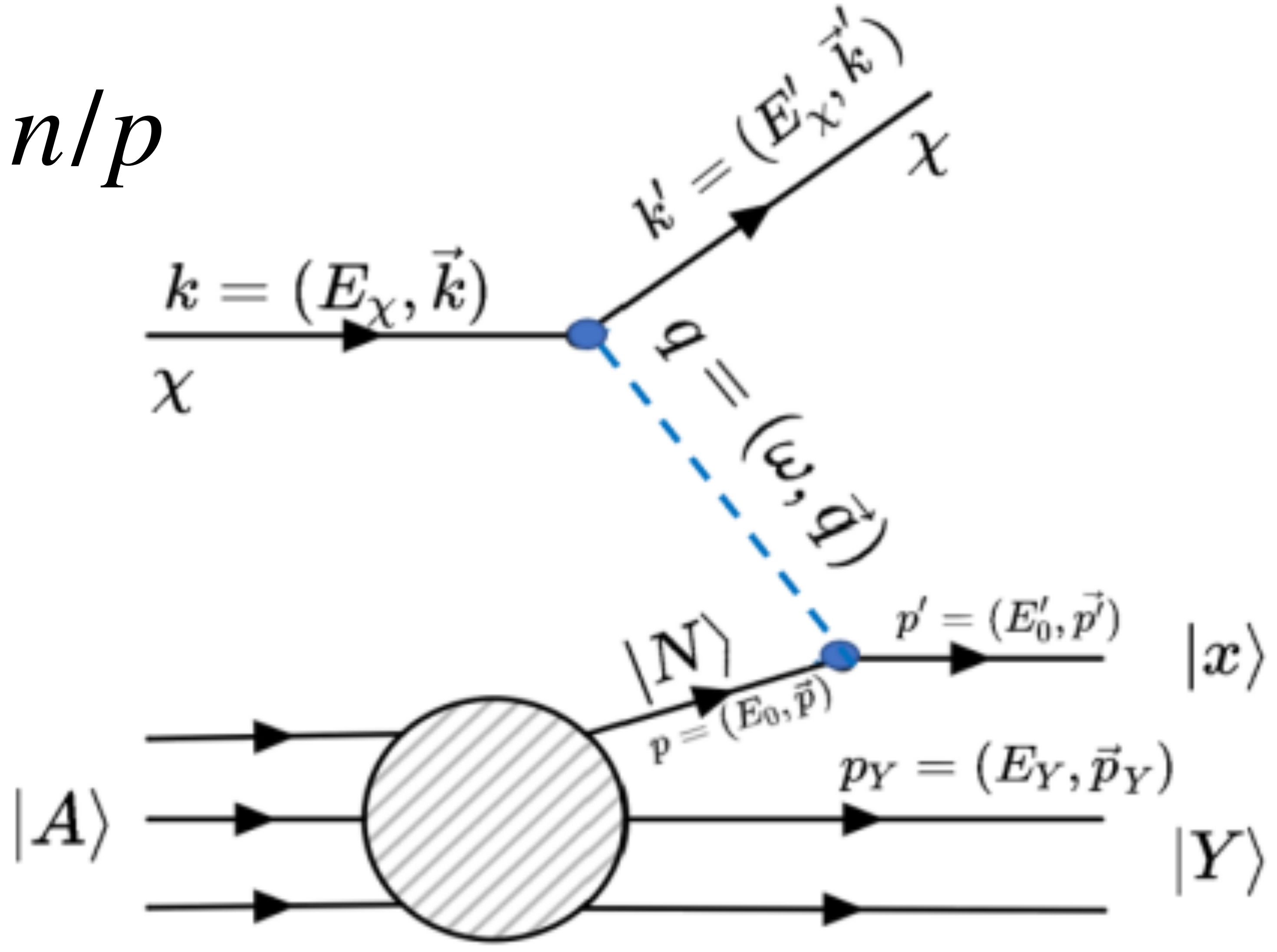

$$\frac{d\sigma_{\rm QE}}{dE'_\chi d\Omega} = \frac{\bar{\sigma}_{\rm n} m_S^4}{16\pi\mu_{\rm n}^2} \frac{|\vec{k}'|}{|\vec{k}|} \frac{\mathcal{X}_S W_S}{(Q^2 + m_S^2)^2},$$

Deep inelastic scattering $\chi + A \rightarrow \chi + X$

$$d\sigma_{\rm DIS} = \frac{d\nu dQ^2}{64\pi m_A^2 \nu (E_\chi^2 - m_\chi^2)} \int_0^1 \frac{f(\xi)}{\xi} d\xi \overline{|\mathcal{M}(\xi)|^2} \delta(\xi - x)$$
$$= \sum_q \frac{g_\chi^2 g_q^2 (4m_\chi^2 + Q^2)(4m_q^2 + Q^2) d\nu dQ^2}{32\pi m_A Q^2 (E_\chi^2 - m_\chi^2)(Q^2 + m_S^2)^2} f_{q/A}(x, Q^2),$$

Su et al, arXiv: 2212.02286

Contributions from Inelastic Scattering

$$R_{\sigma_i} = \frac{\sigma_i}{\sigma_{tot}}$$

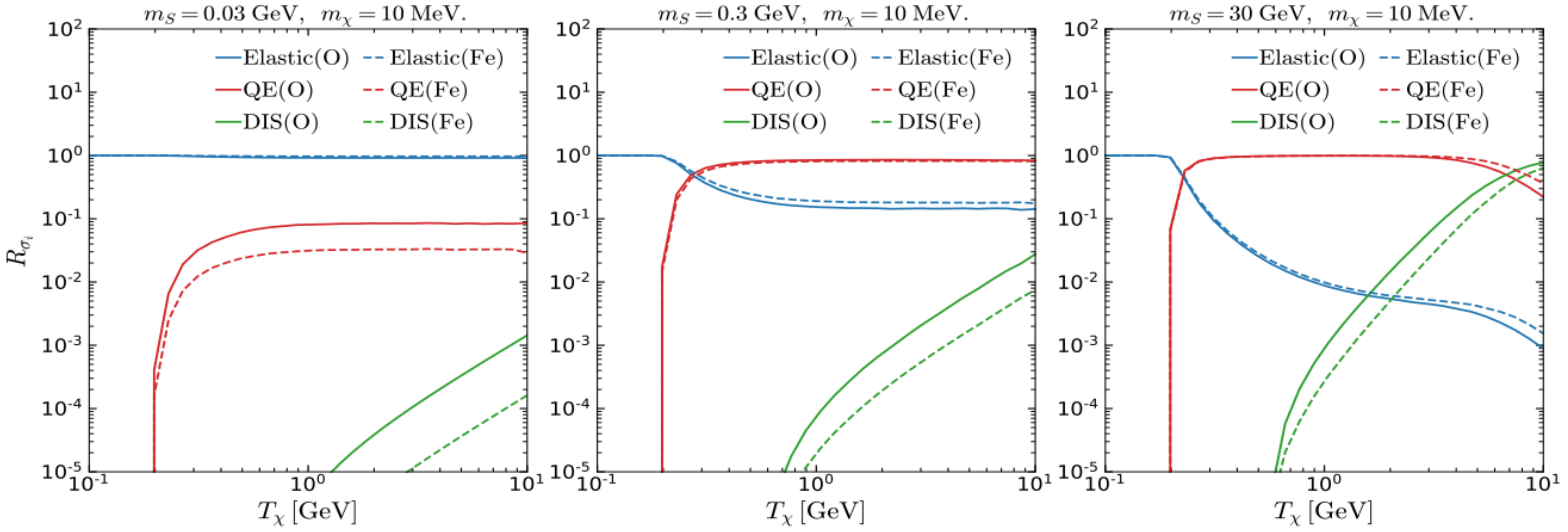

Su et al, arXiv: 2212.02286

New Limits from PandaX

PandaX Collaboration, arXiv: 2301.03010

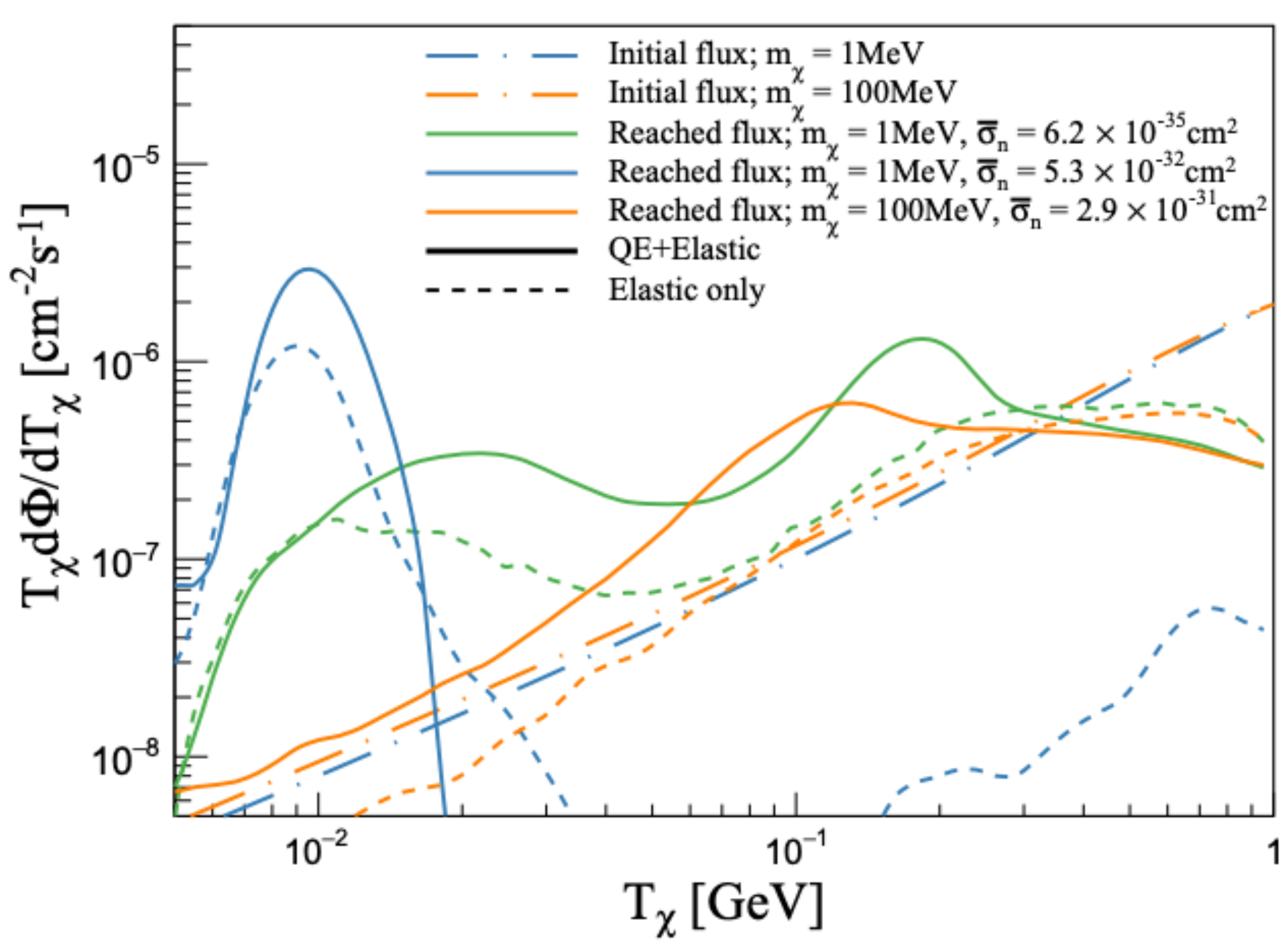

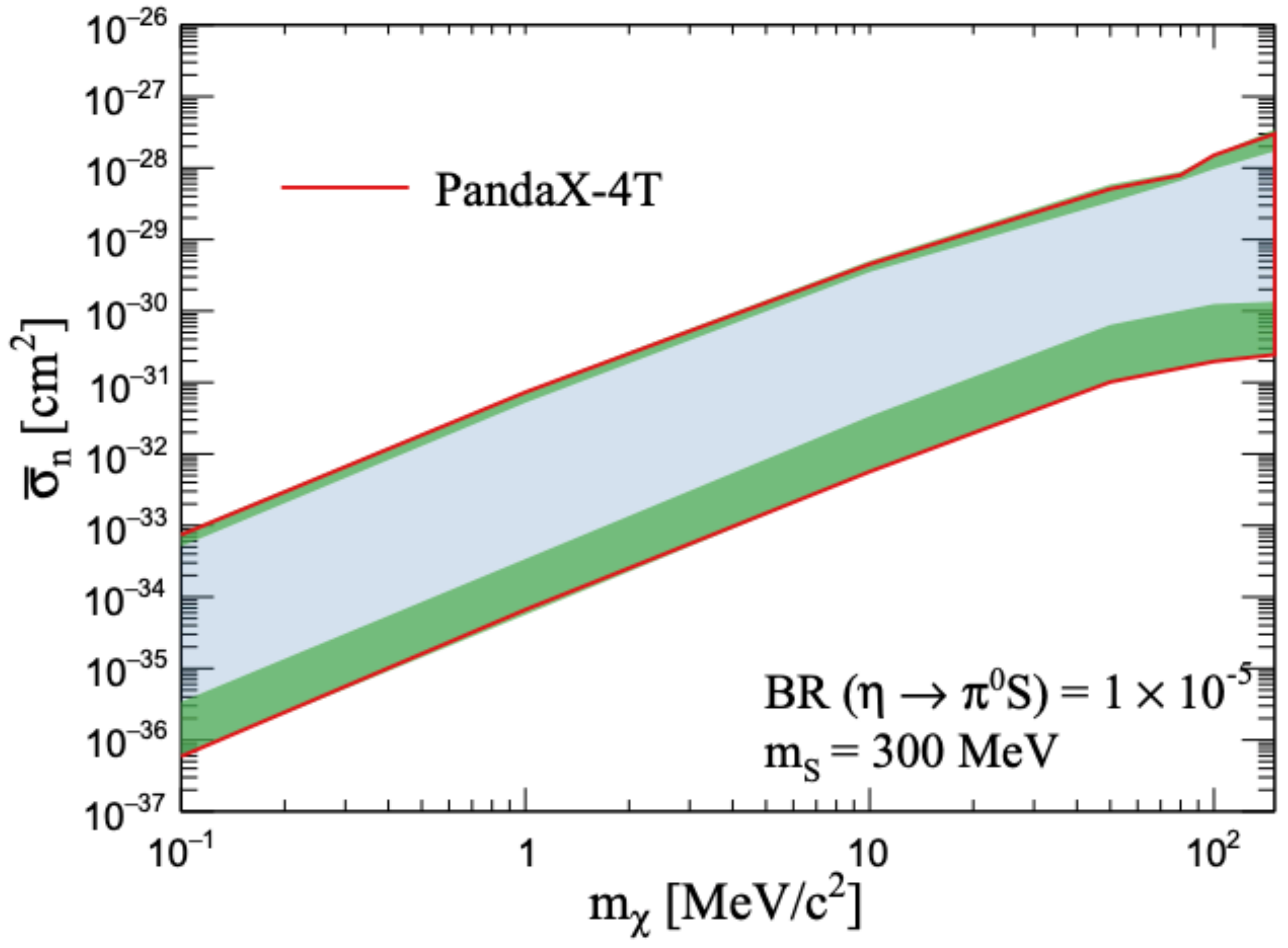

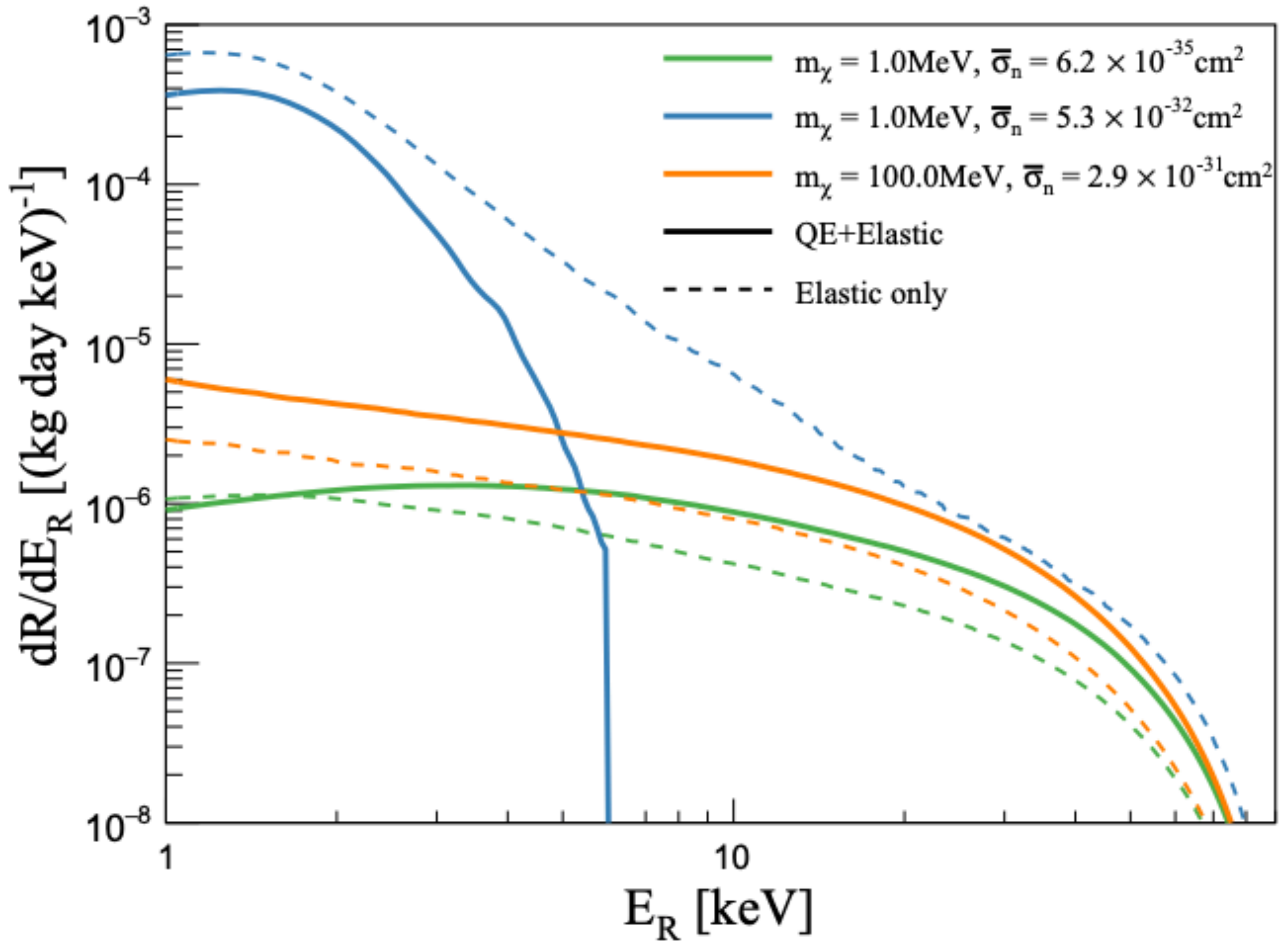

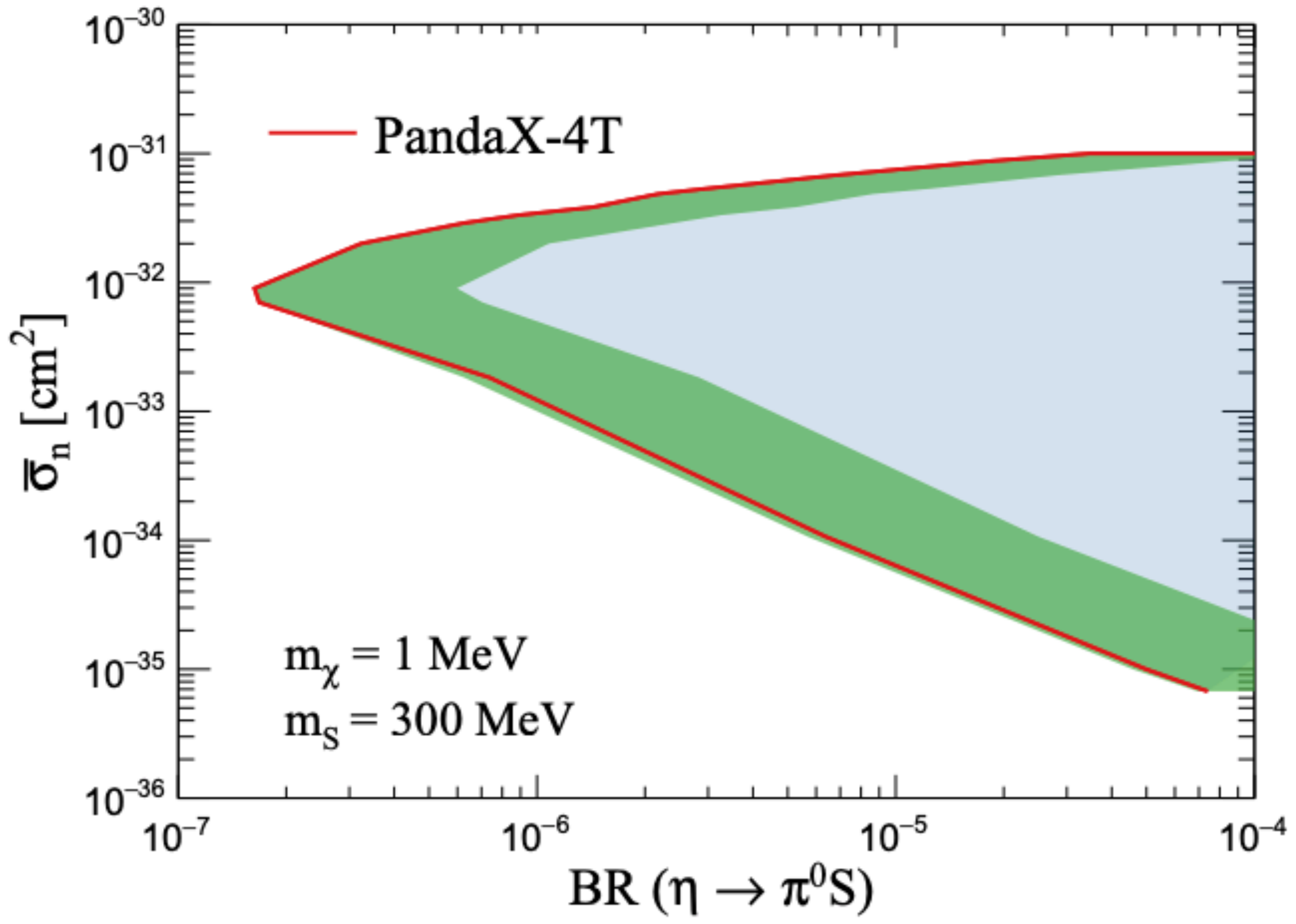

Constraints on WIMP Dark Matter

How to overcome the detection threshold?

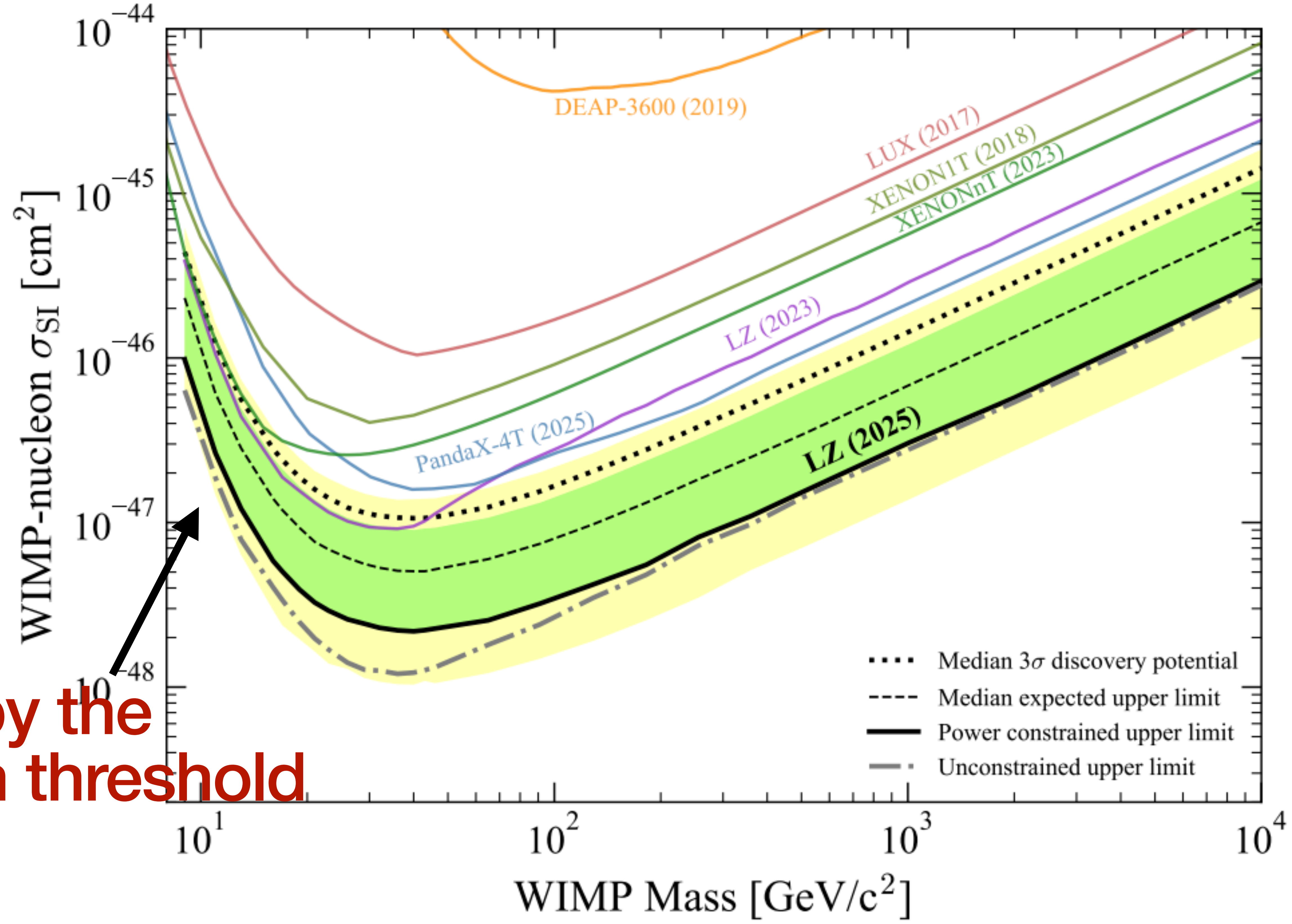

Limited by the detection threshold

- Boosted dark matter
- Atmospheric dark matter

Electron Recoil

For sub-GeV dark matter, $m_\chi \ll m_N$

$$q_{\max} = 2m_\chi v \sim \text{MeV} \qquad v \sim 300 \text{ km/s} \sim 10^{-3}c$$

$E_{R,\max} \sim 10 \text{ eV}$ for $m_\chi = 300 \text{ MeV}$ scattering on oxygen

$$E_{R,\max} \ll E_{k,\chi}$$

Detecting sub-GeV dark matter using nuclear recoil is difficult!

Kinematics of Light Dark Matter

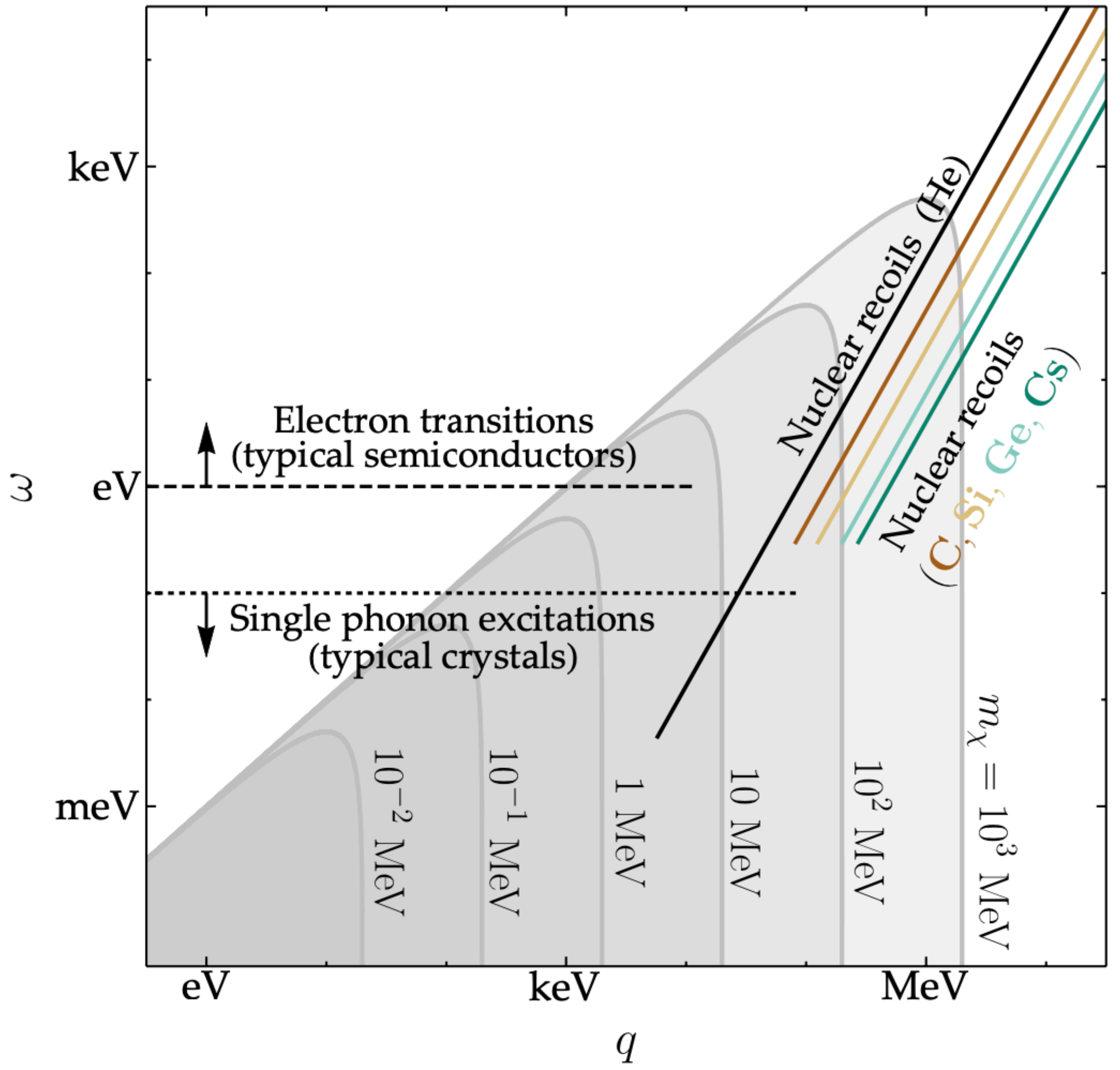

Trickle et al, arXiv: 1910.08092

- The maximum dark matter energy deposition depends on its mass
- The energy deposition reduces for lower mass dark matter

$$\omega_{\boldsymbol{q}} = \frac{1}{2}m_\chi v^2 - \frac{(m_\chi \boldsymbol{v} - \boldsymbol{q})^2}{2m_\chi} = \boldsymbol{q}\cdot\boldsymbol{v} - \frac{q^2}{2m_\chi}$$

$$\omega \leq E_k \sim m_{\mathrm{DM}} v^2 \sim 10^{-6} m_{\mathrm{DM}}$$

Look for electron recoil instead!

Electron Recoil

$$v > v_{min} = \frac{\Delta E_B + E_R}{q} + \frac{q}{2m_\chi}$$

$$\overline{\sigma}_e = \frac{16\pi\mu_{\chi e}^2 \alpha\epsilon^2\alpha_D}{(m_{A'}^2 + \alpha^2 m_e^2)^2} \simeq \begin{cases} \frac{16\pi\mu_{\chi e}^2\alpha\epsilon^2\alpha_D}{m_{A'}^4}, & m_{A'} \gg \alpha m_e \\ \frac{16\pi\mu_{\chi e}^2\alpha\epsilon^2\alpha_D}{(\alpha\, m_e)^4}, & m_{A'} \ll \alpha m_e \end{cases},$$

$$F_{DM}(q) = \frac{m_{A'}^2 + \alpha^2 m_e^2}{m_{A'}^2 + q^2} \simeq \begin{cases} 1\,, & m_{A'} \gg \alpha m_e \\ \frac{\alpha^2 m_e^2}{q^2}\,, & m_{A'} \ll \alpha m_e \end{cases}$$

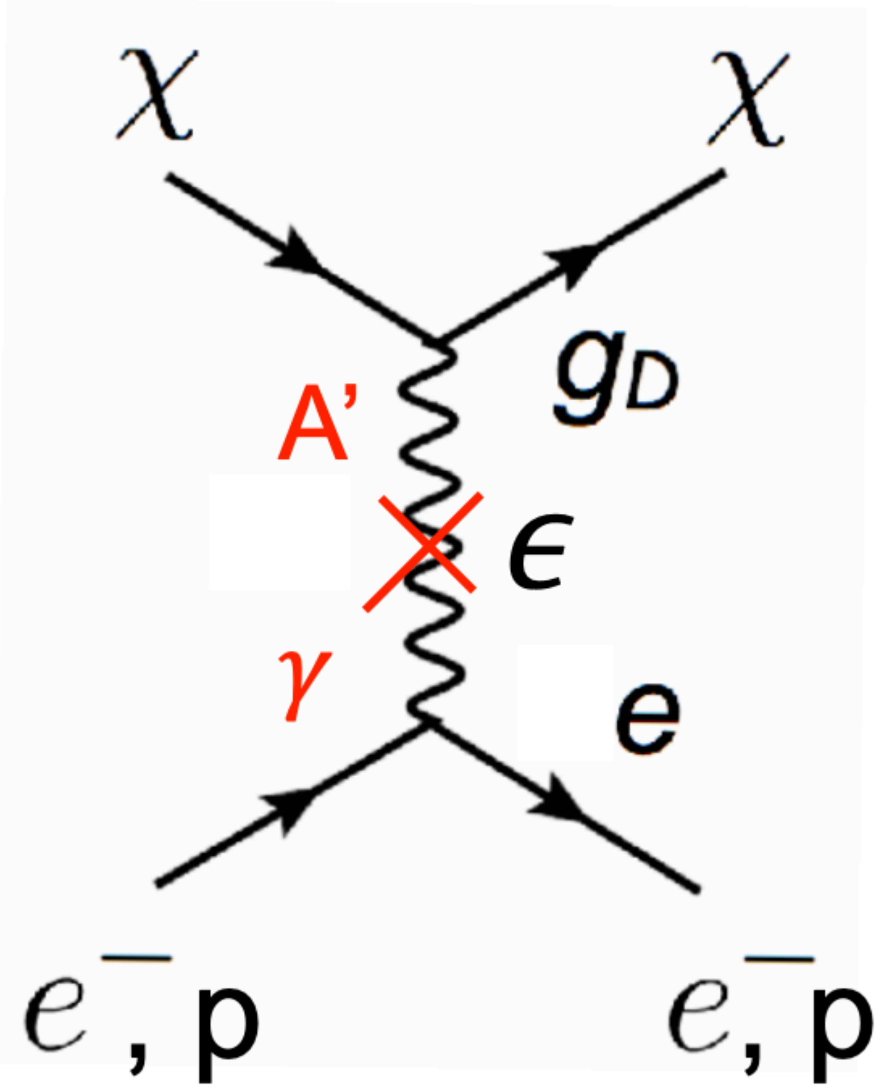

Essig et al, arXiv: 1509.01598

Essig et al, arXiv: 1108.5383

Electron Recoil

$$v > v_{min} = \frac{\Delta E_B + E_R}{q} + \frac{q}{2m_\chi}$$

$$\overline{\sigma}_e \equiv \frac{\mu_{\chi e}^2}{16\pi m_\chi^2 m_e^2} \overline{|\mathcal{M}_{\chi e}(q)|^2}\Big|_{q^2=\alpha^2 m_e^2},$$

$$\overline{|\mathcal{M}_{\chi e}(q)|^2} = \overline{|\mathcal{M}_{\chi e}(q)|^2}\Big|_{q^2=\alpha^2 m_e^2} \times |F_{\rm DM}(q)|^2$$

$$\frac{d\langle\sigma_{ion}^i v\rangle}{d\ln E_R} = \frac{\overline{\sigma}_e}{8\mu_{\chi e}^2}\int q\, dq \left|f_{ion}^i(k', q)\right|^2 \left|F_{\rm DM}(q)\right|^2 \eta(v_{\rm min})$$

Essig et al, arXiv: 1509.01598

Essig et al, arXiv: 1108.5383

Electron Recoil

Integral over momentum transfer

Dependence on DM velocity

$$\frac{dR^{ER}}{dE_e} = \bar{\sigma}_e \frac{\rho_\chi}{M_\chi} \frac{1}{8\mu_{e\chi}^2} \int q\,dq\, |F_{DM}(q)|^2 |f_{n,l}^{ion}(q, E_e)|^2 \eta(v_{min})$$

$$|f_{n,l}^{ion}(q, E_e)|^2 = \frac{k'^3}{4\pi^3} \sum_{n,l} |\langle \psi_{E_e} | e^{-i \sum_\alpha \mathbf{q} \cdot \mathbf{x}^\alpha} | \psi_{n,l} \rangle|^2$$

ionization form factor

Properties of the DM

Rate scales linearly with DM-electron cross section

DM Form Factor

- Choice of DM interaction mediator

Credit: Paolo Privitera

The Form Factors for Electron Recoil

Liquid noble

$$\left|f^{i}_{ion}(k',q)\right|^2 = \frac{2k'^3}{(2\pi)^3}\sum_{\substack{\text{degen.}\\ \text{states}}}\left|\int d^3x\,\tilde{\psi}^*_{k'l'm'}(\mathbf{x})\psi_i(\mathbf{x})e^{i\mathbf{q}\cdot\mathbf{x}}\right|^2$$

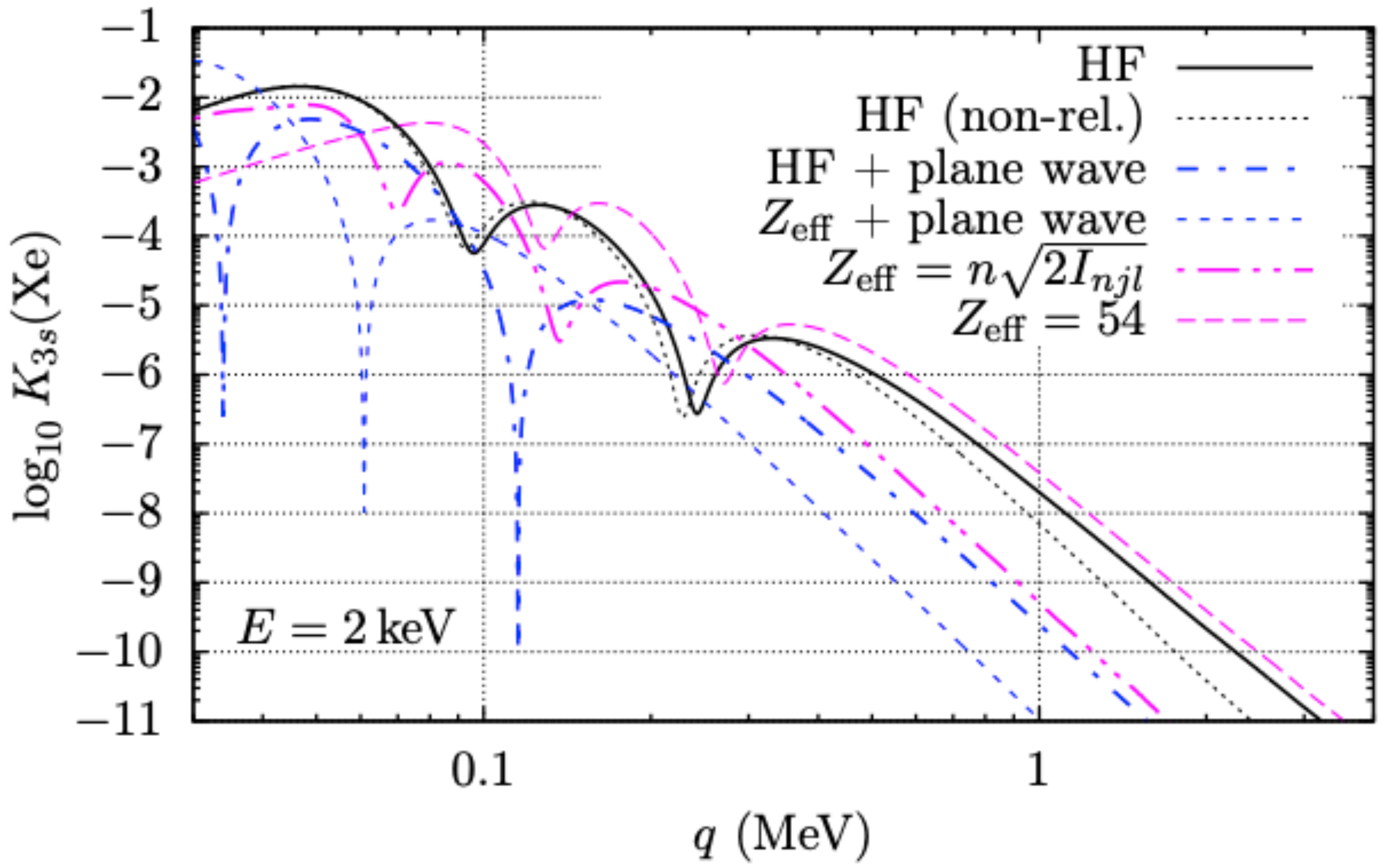

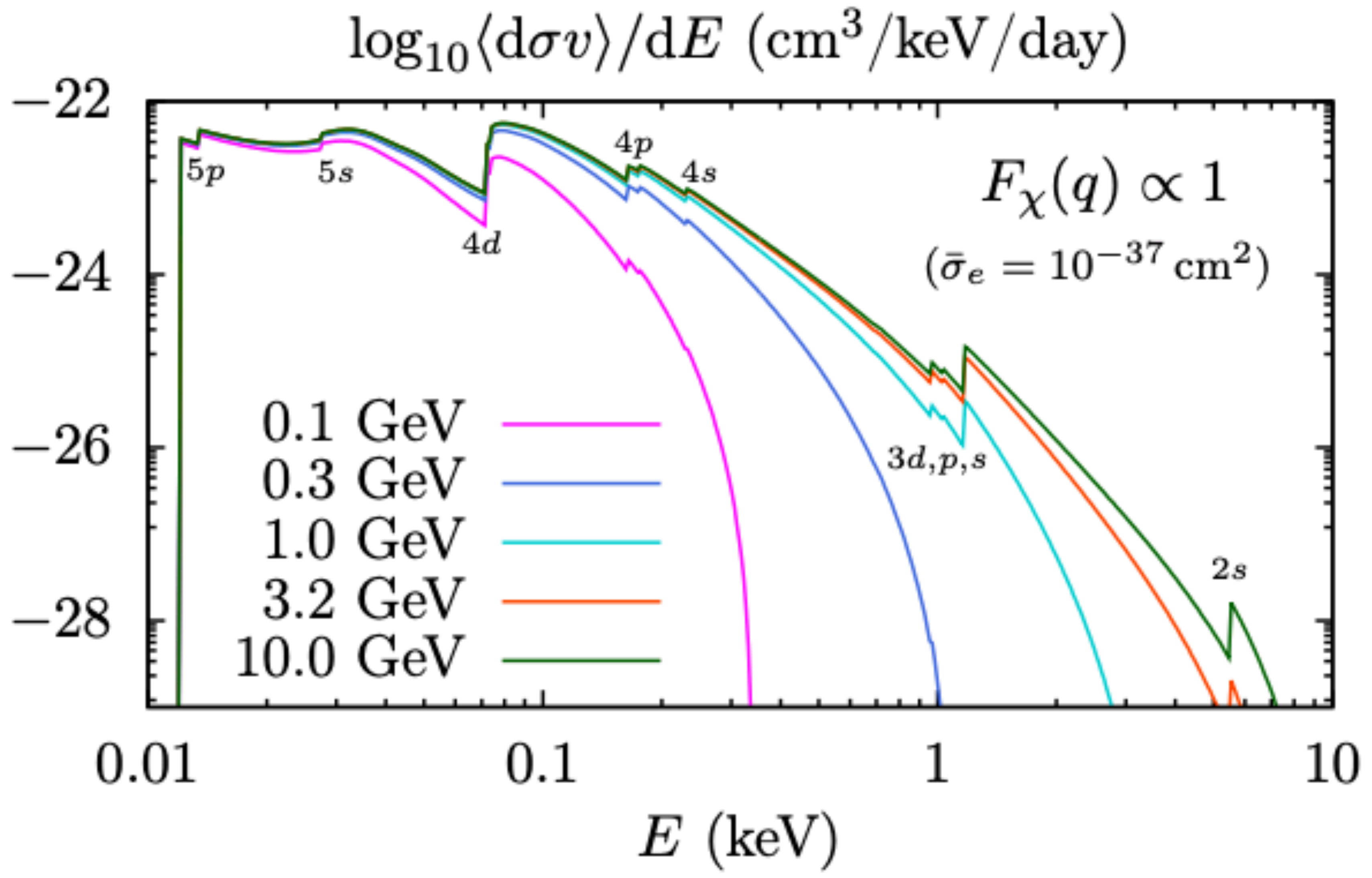

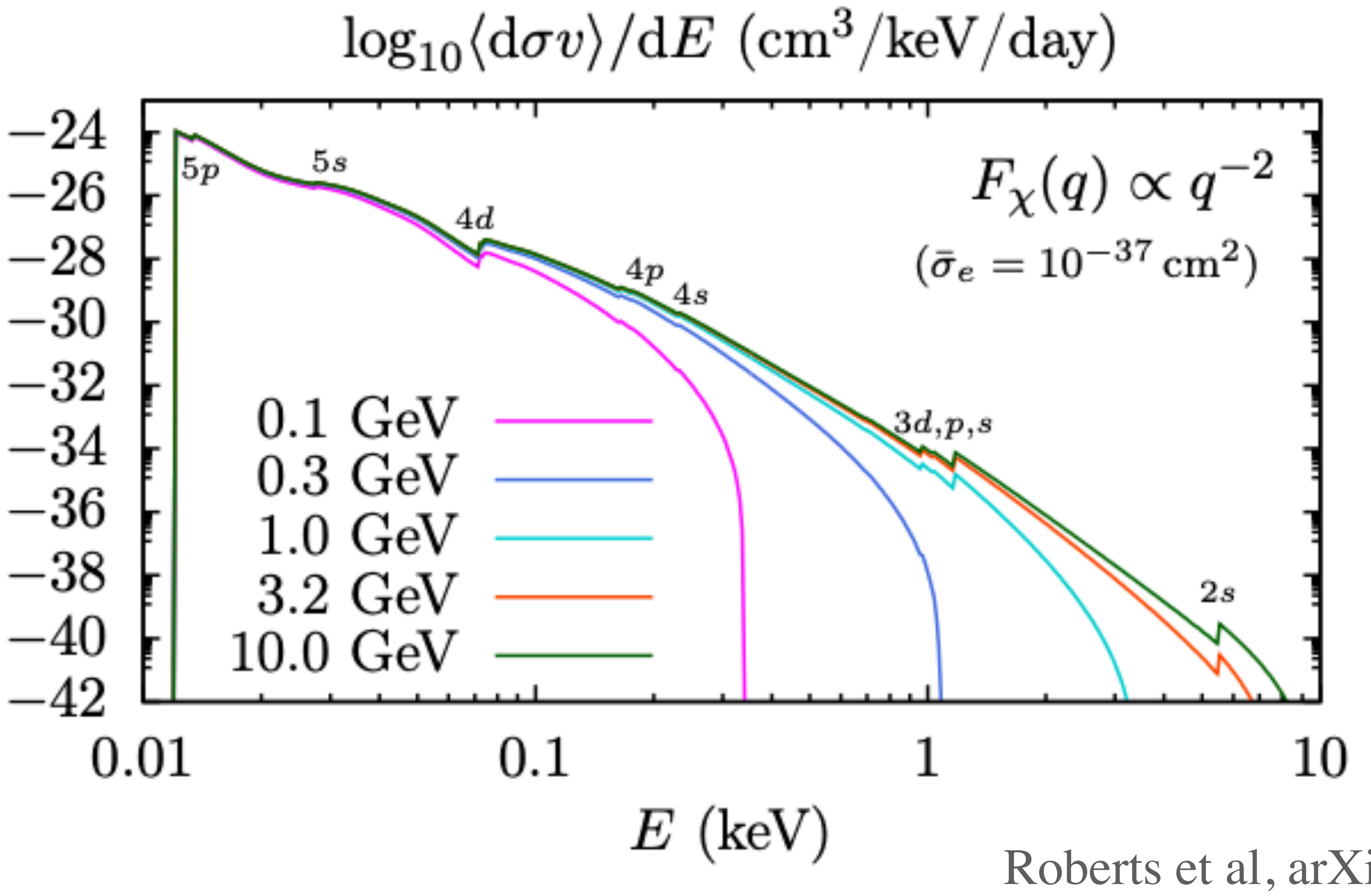

Roberts et al, arXiv: 1904.07127

The Form Factors for Electron Recoil

Semiconductor

$$\psi_{i\vec{k}}(\vec{x}) = \frac{1}{\sqrt{V}} \sum_{\vec{G}} u_i(\vec{k}+\vec{G}) e^{i(\vec{k}+\vec{G})\cdot\vec{x}}$$

$$\left|f_{\rm crystal}(q,E_e)\right|^2 = \frac{2\pi^2(\alpha m_e^2 V_{\rm cell})^{-1}}{E_e} \sum_{i\,i'} \int_{\rm BZ} \frac{V_{\rm cell}\, d^3k}{(2\pi)^3} \frac{V_{\rm cell}\, d^3k'}{(2\pi)^3} \times$$
$$E_e\, \delta(E_e - E_{i'\vec{k}'} + E_{i\vec{k}}) \sum_{\vec{G}'} q\, \delta(q - |\vec{k}' - \vec{k} + \vec{G}'|) \left|f_{[i\vec{k},i'\vec{k}',\vec{G}']}\right|^2$$

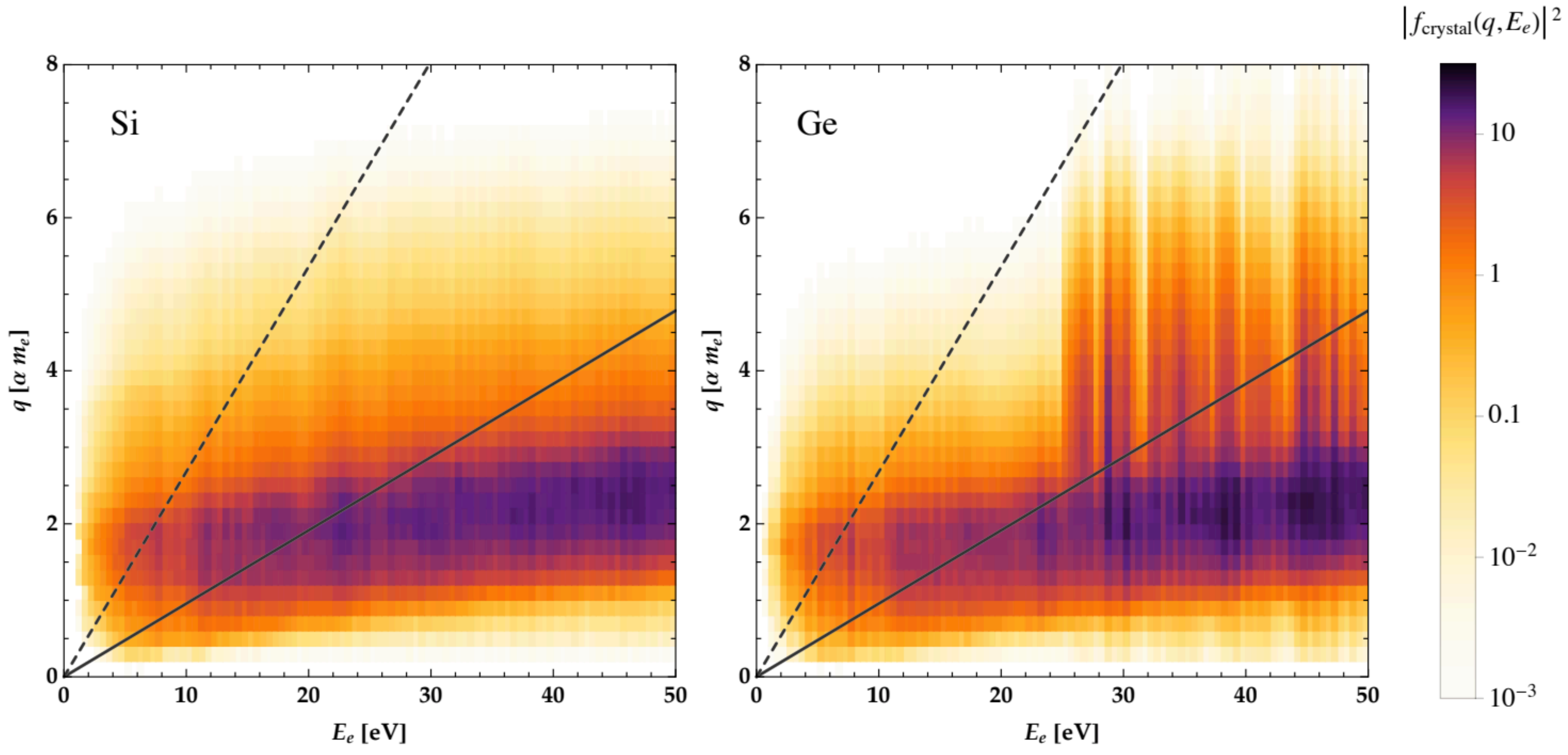

Essig et al, arXiv: 1509.01598

An Alternative Way

$$\mathrm{Im}\left(-\frac{1}{\epsilon(\mathbf{q},\omega)}\right) = \frac{\pi e^2}{q^2}\sum_f \left|\langle f|\hat{\rho}(\mathbf{q})|0\rangle\right|^2 \delta(\omega_f - \omega)$$

$$R = \frac{1}{\rho_T}\frac{\rho_\chi}{m_\chi}\frac{\bar{\sigma}_e}{\mu_{\chi e}^2}\frac{\pi}{\alpha_{em}}\int d^3v\, f_\chi(v)\int \frac{d^3\mathbf{k}}{(2\pi)^3} k^2 |F_{DM}(k)|^2 \int \frac{d\omega}{2\pi}\, \frac{1}{1-e^{-\beta\omega}}\, \mathrm{Im}\left[\frac{-1}{\epsilon_L(\omega,\mathbf{k})}\right]\delta\left(\omega + \frac{k^2}{2m_\chi} - \mathbf{k}\cdot\mathbf{v}\right)$$

- Dark matter that couples to charge density is similar to light
- Including the contribution from plasmons
- Can be determined experimentally with light response

Hochberg et al, arXiv: 2101.08263

Knapen et al, arXiv: 2101.08275

The Dielectric Function

$$\text{Im}\left(-\frac{1}{\epsilon(\mathbf{q},\omega)}\right) = \frac{\pi e^2}{q^2}\sum_f \left|\langle f|\hat{\rho}(\mathbf{q})|0\rangle\right|^2 \delta(\omega_f - \omega)$$

$$R = \frac{1}{\rho_T}\frac{\rho_\chi}{m_\chi}\frac{\bar{\sigma}_e}{\mu_{\chi e}^2}\frac{\pi}{\alpha_{em}}\int d^3v\, f_\chi(v)\int \frac{d^3\mathbf{k}}{(2\pi)^3}k^2|F_{DM}(k)|^2\int\frac{d\omega}{2\pi}\,\frac{1}{1-e^{-\beta\omega}}\,\text{Im}\left[\frac{-1}{\epsilon_L(\omega,\mathbf{k})}\right]\delta\left(\omega + \frac{k^2}{2m_\chi} - \mathbf{k}\cdot\mathbf{v}\right)$$

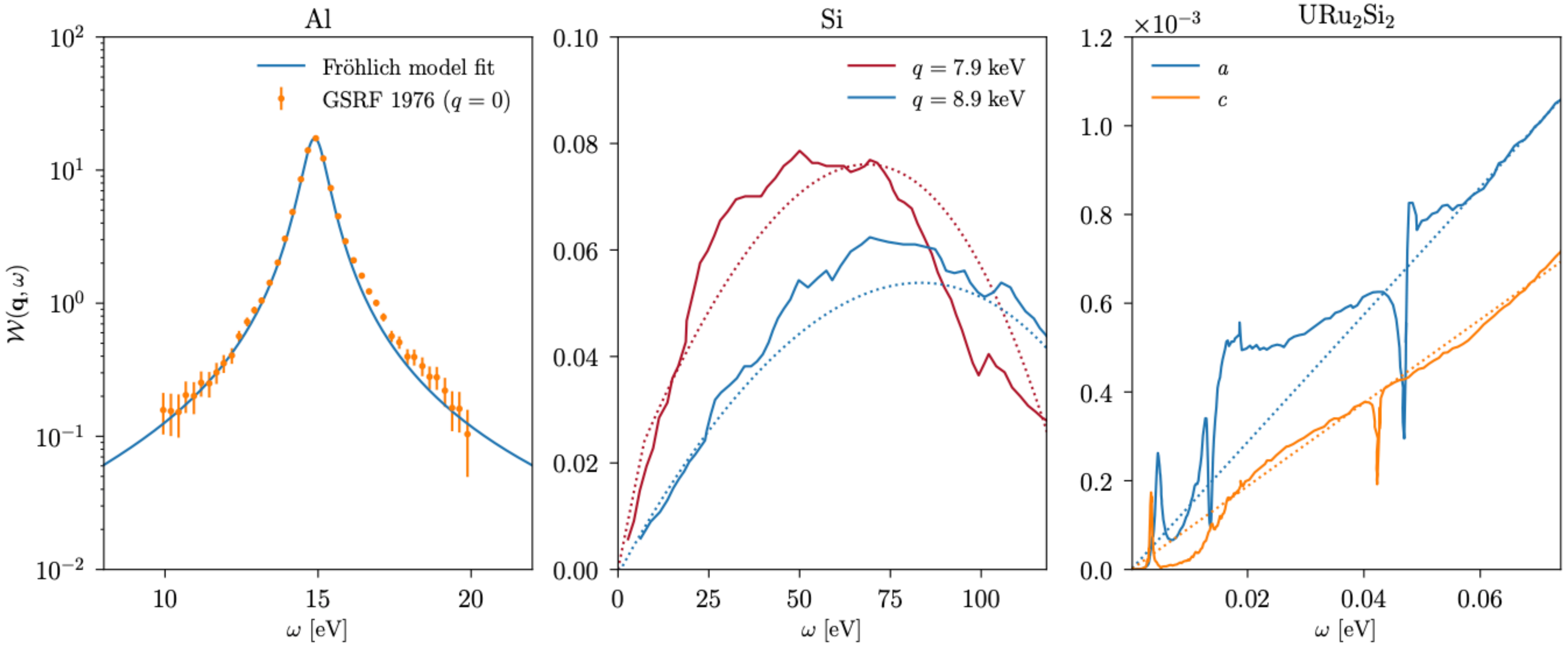

Hochberg et al, arXiv: 2101.08263

Knapen et al, arXiv: 2101.08275

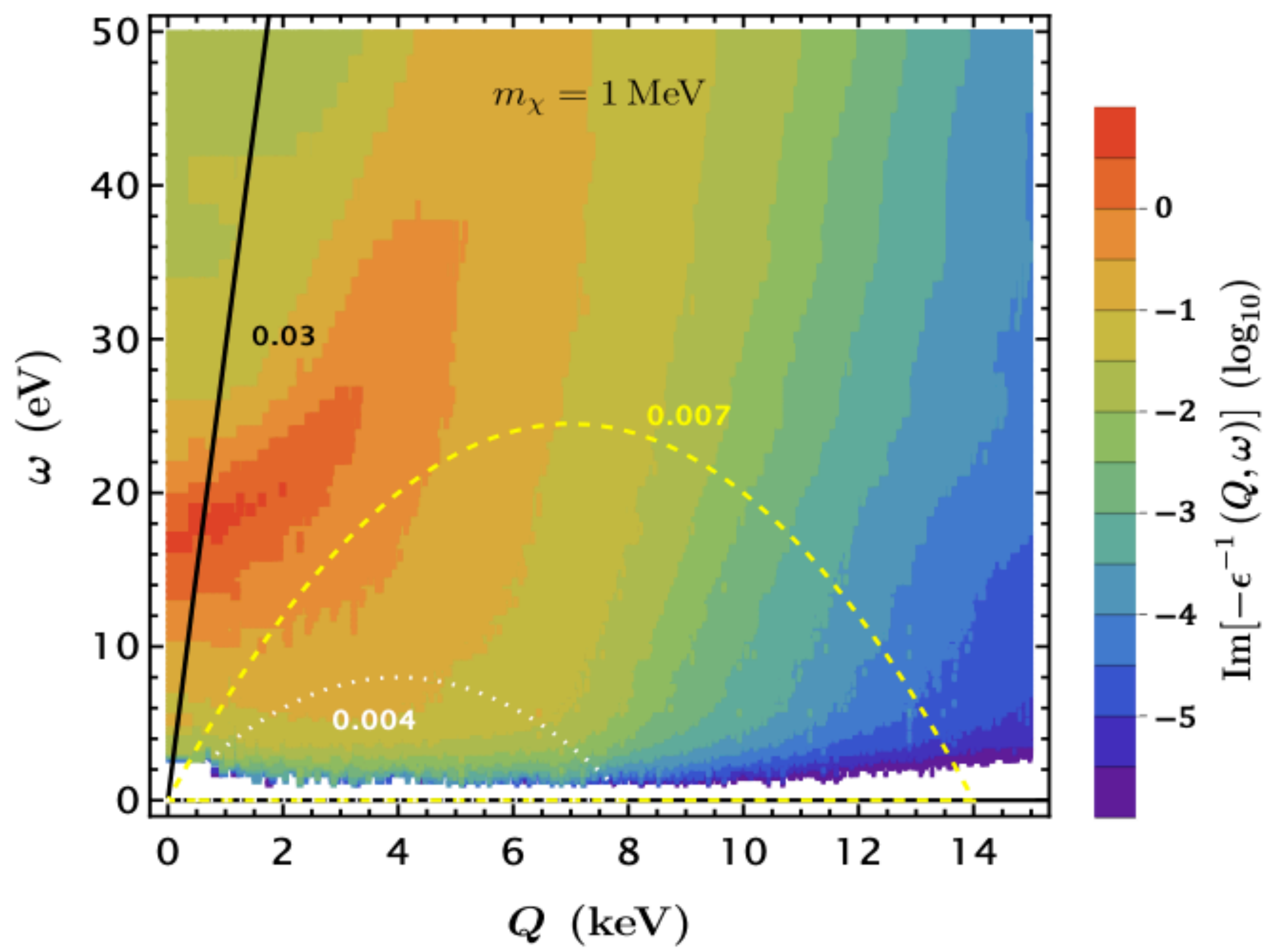

Liang et al, arXiv: 2401.11971

SENSEI/CDEX

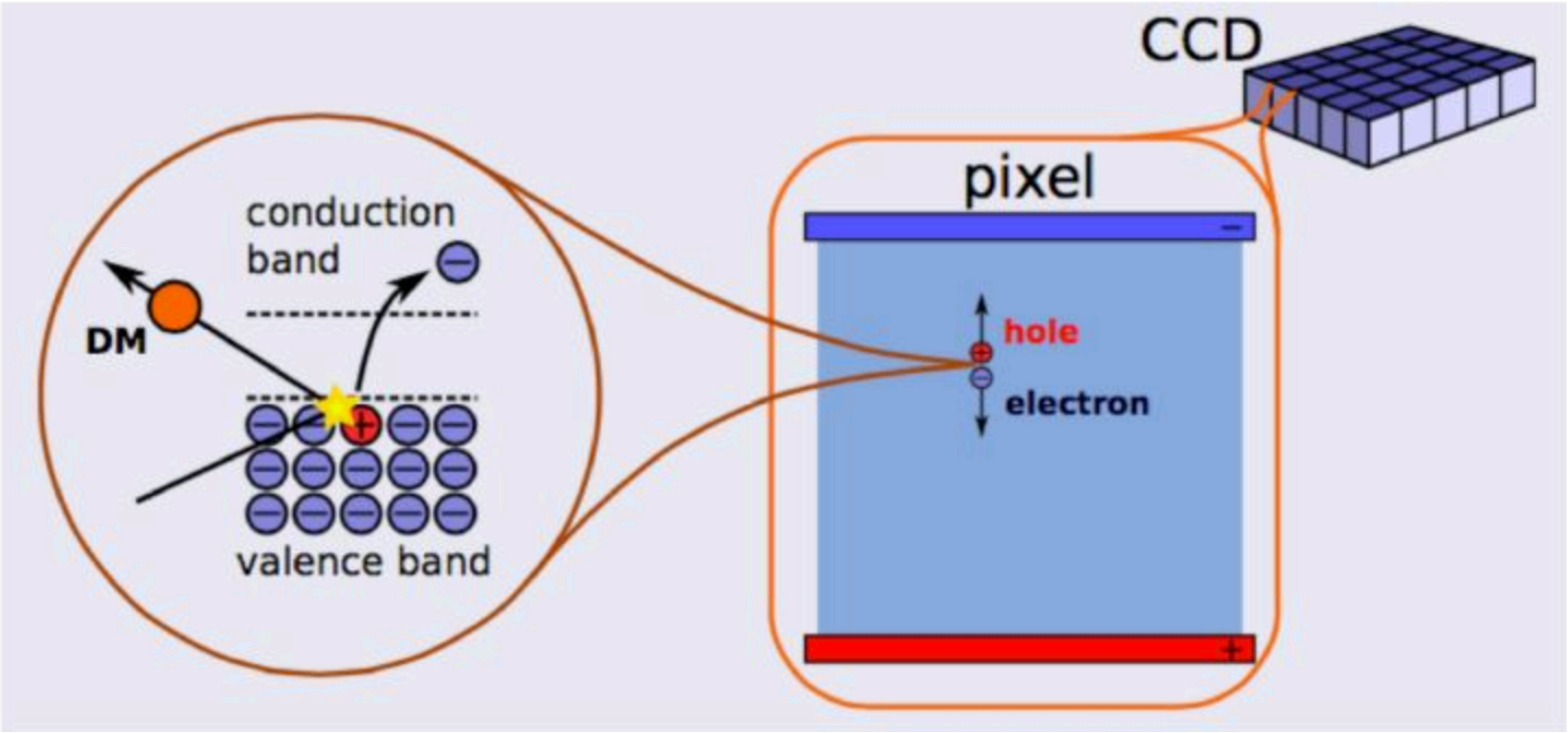

Yonit Hochberg

Electron-hole pair from ionization

Charge only

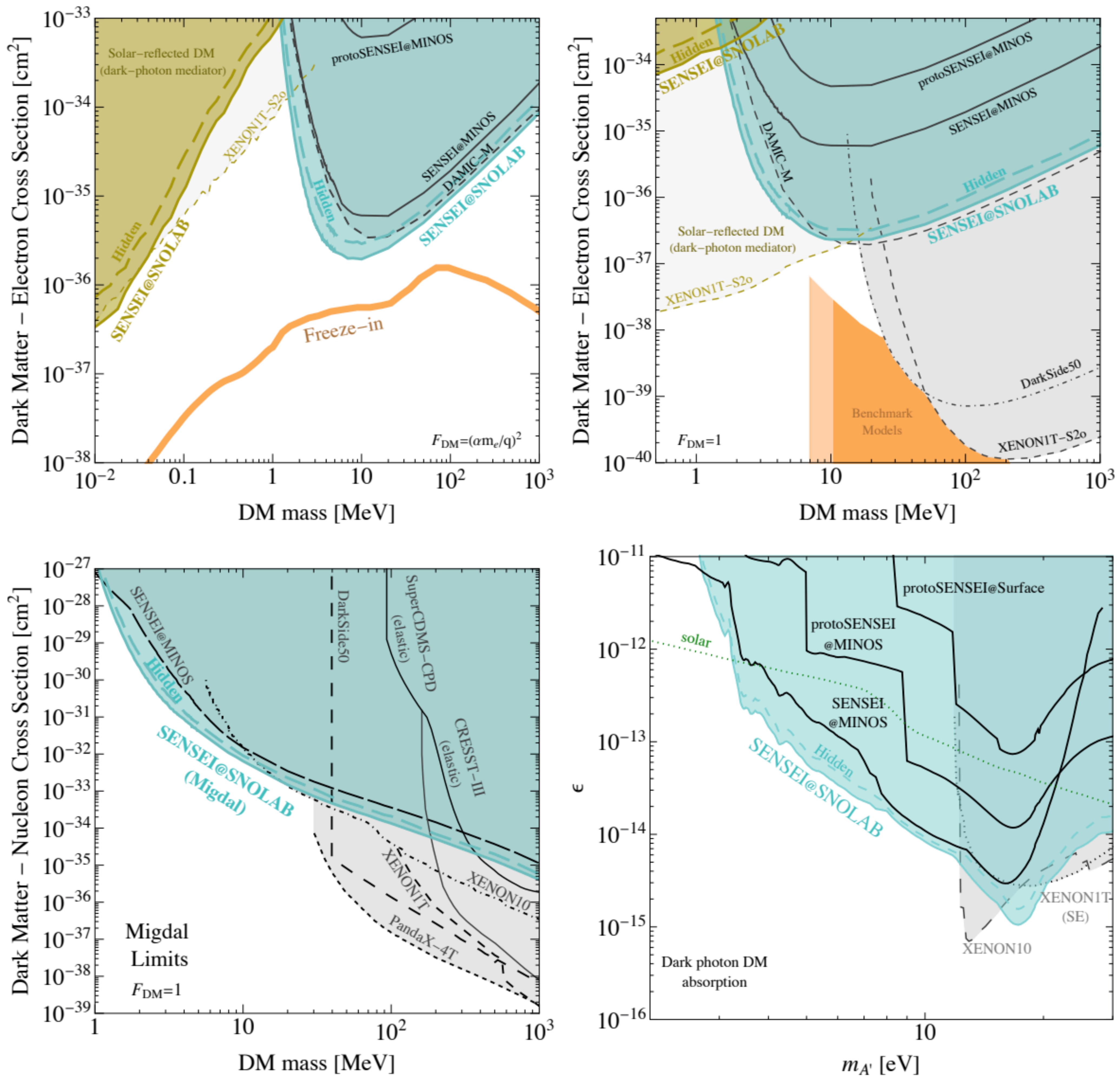

SENSEI@SNOLAB $E_{\rm th} \sim$ eV

2312.13342

Migdal Effect

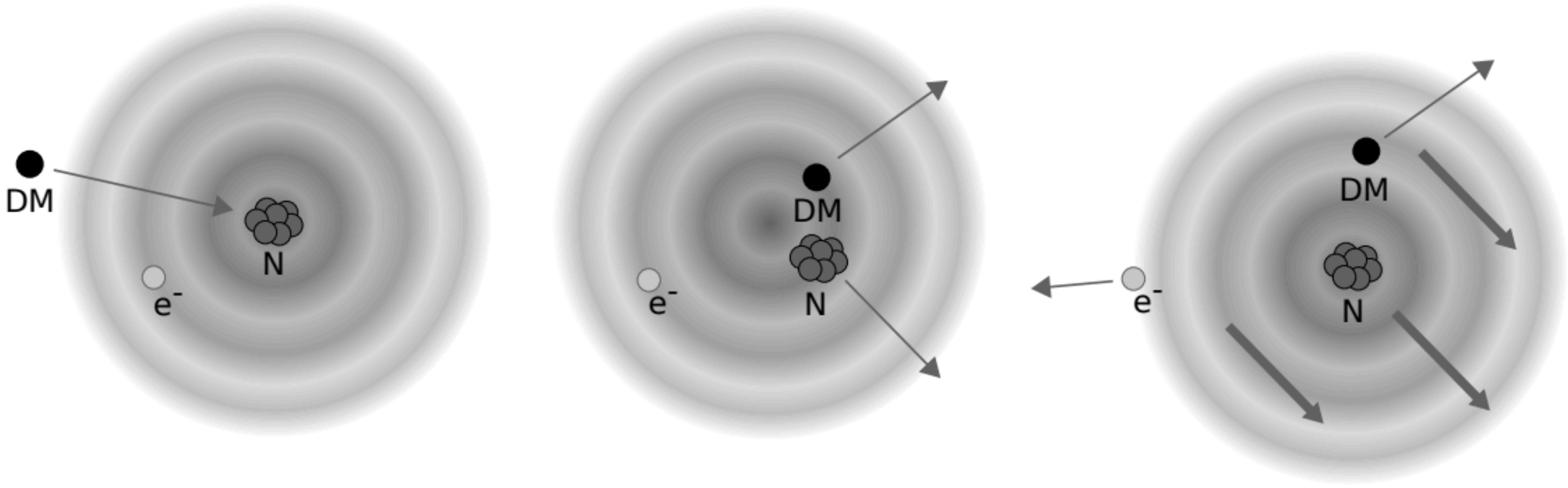

The nuclear gets recoil, but the electron cloud is left behind

Dolan et al, arXiv: 1711.09906

Migdal Effect

The nuclear gets recoil, but the electron cloud is left behind

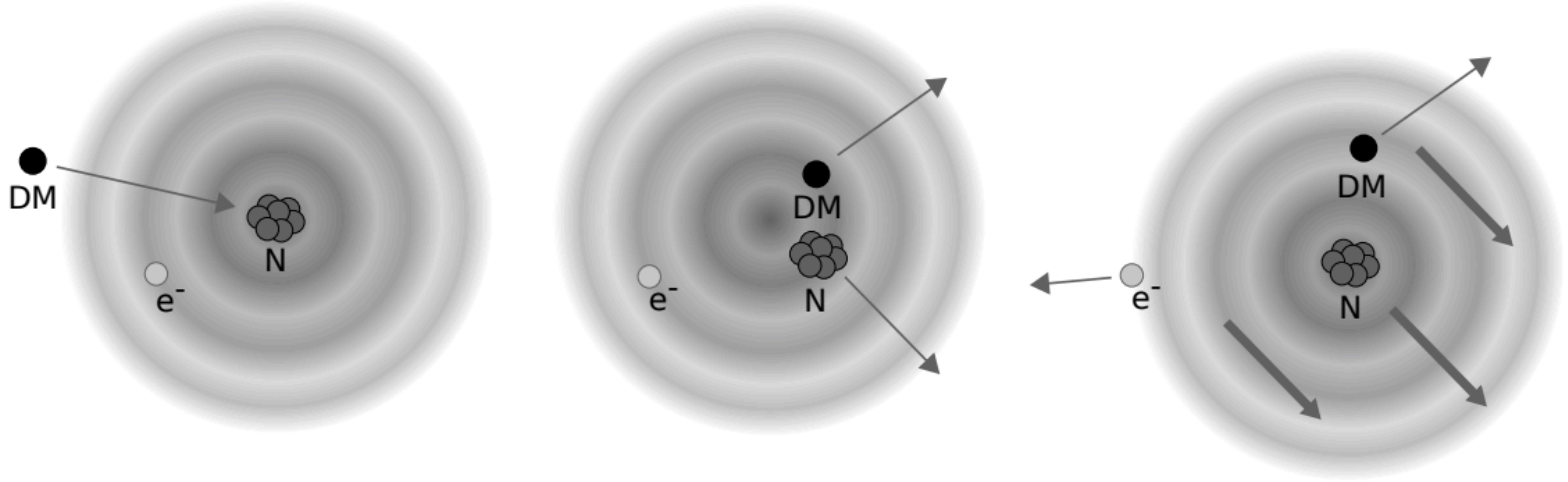

$$\frac{d^3 R_{\text{ion}}}{dE_R\, dE_e\, dv} = \frac{d^2 R_{\text{nr}}}{dE_R\, dv} \times |Z_{\text{ion}}(E_R, E_e)|^2$$

$$|Z_{\text{ion}}(E_R, E_e)|^2 = \sum_{nl} \frac{1}{2\pi} \frac{dp^c_{q_e}(nl \to E_e)}{dE_e}$$

Dolan et al, arXiv: 1711.09906

Migdal Effect

The nuclear gets recoil, but the electron cloud is left behind

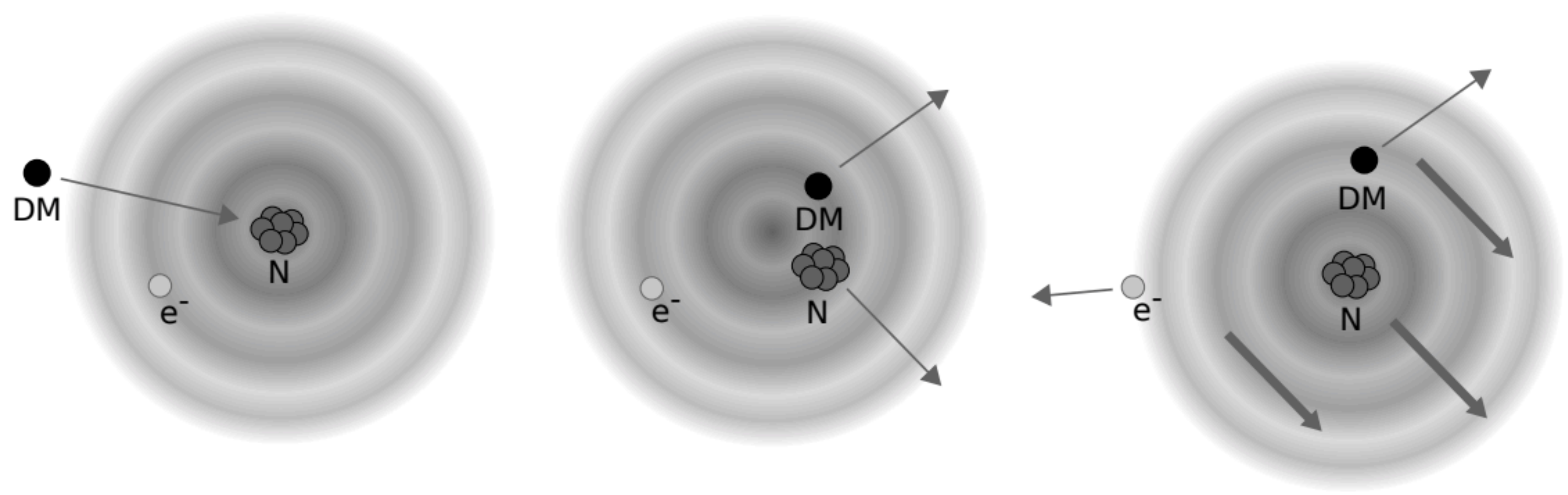

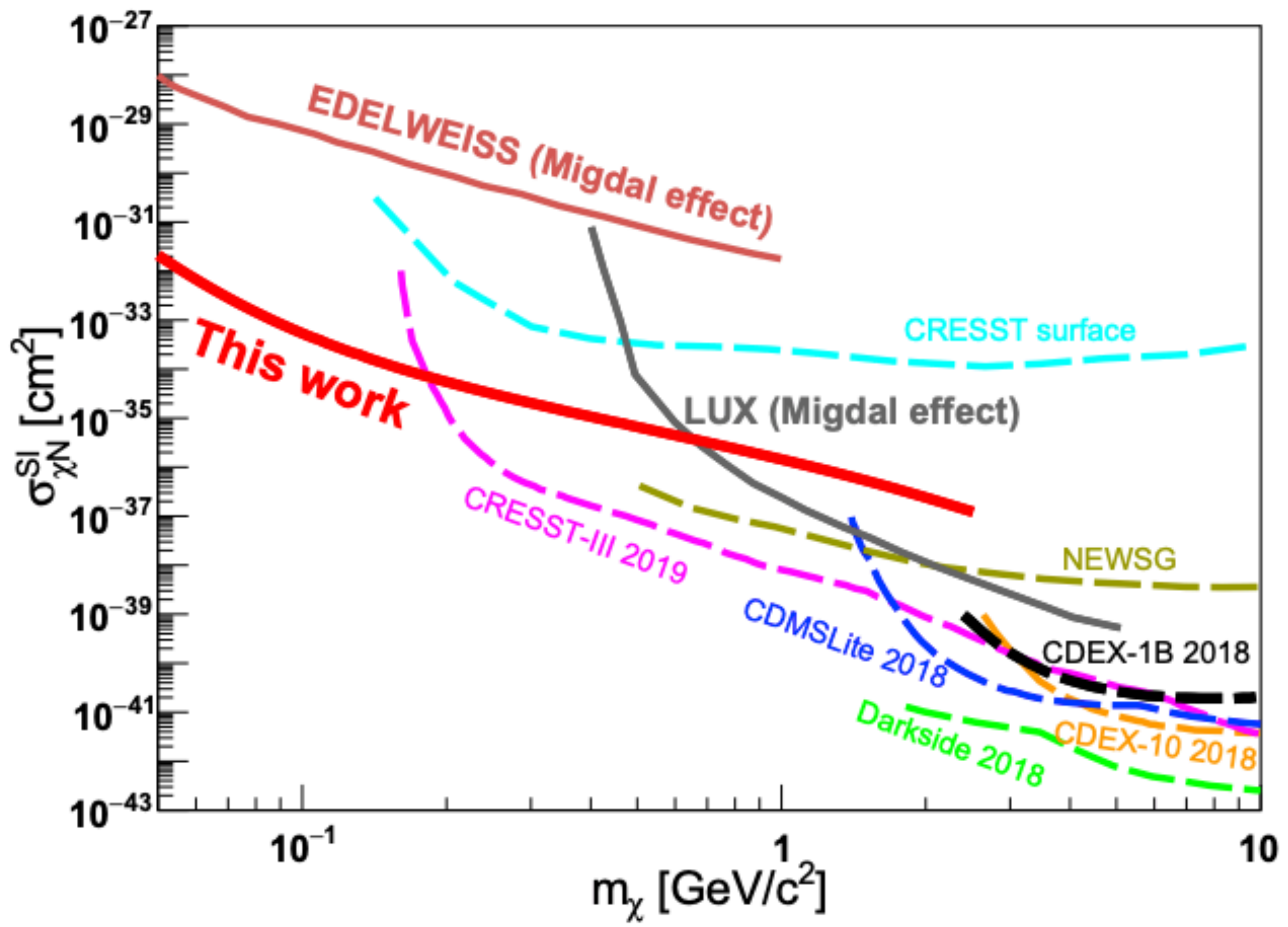

CDEX collaboration, arXiv: 1905.00354

Migdal Effect

nature

Explore content About the journal Publish with us

nature articles article

Article | Open access | Published: 14 January 2026

Direct observation of the Migdal effect induced by neutron bombardment

Difan Yi, Qian Liu, Shi Chen, Chunlai Dong, Huanbo Feng, Chaosong Gao, Wenqian Huang, Xinmei Jing, Lingquan Kong, Jin Li, Peirong Li, Enwei Liang, Ruiting Ma, Chenguang Su, Liangliang Su, Junwei Sun, Dong Wang, Junrun Wang, Zheng Wei, Zeen Yao, Yunlinchen Yu, Yu Zhang, Shiqiang Zhou, Zhuo Zhou, Bin Zhu, Jie Zuo, Hongbang Liu, Xiangming Sun, Lei Wu & Yangheng Zheng

— Show fewer authors

Nature **649**, 580–583 (2026) | Cite this article

Abstract

The search for dark matter focuses now on hypothetical light particles with masses ranging from MeV to GeV (refs. [1,2,3,4,5,6,7,8,9,10,11,12]). These particles would leave very faint signals experimentally. A potential avenue for enhancing experimental sensitivity to light matter relies on the Migdal effect[13,14,15], which involves the detectable ejection of electrons following the instantaneous accelerations of atoms colliding with neutral dark matter. However, although the Migdal effect could be equally generated in controlled experiments with neutral projectiles, a direct experimental observation of this effect is missing, casting doubt on the reliability of detection experiments relying on this effect. Here we report the direct observation of the Migdal effect in neutron–nucleus collisions, achieving a statistical significance of 5 standard deviations, which rests on 6 candidate events selected out of almost 10^6 recorded events. Our experiments have determined the ratio of the Migdal cross-section to the nuclear recoil cross-section to be $4.9^{+2.6}_{-1.9} \times 10^{-5}$, in which nuclear recoils exceed 35 keVee and electron recoils span 5–10 keV. These findings are consistent with theoretical predictions. This work resolves a long-standing gap in experimental validation, which not only strengthens the theoretical foundation of the Migdal effect but also paves the way for its application in light dark matter detection.

Constraints on WIMP Dark Matter

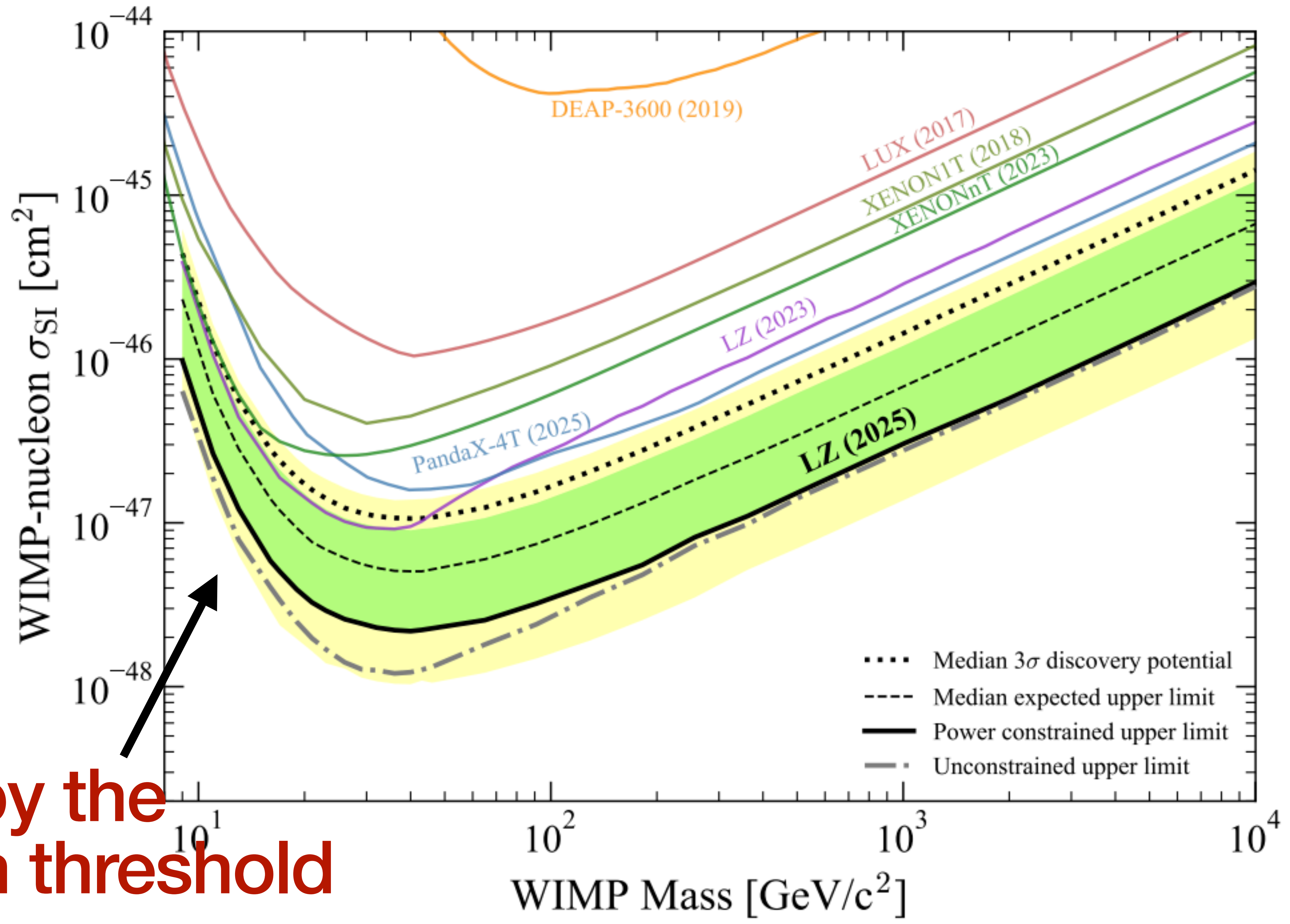

Limited by the detection threshold

How to overcome the detection threshold?

- Boosted dark matter
- Atmospheric dark matter
- Electron recoil
- Migdal effect

Kinematics of Light Dark Matter

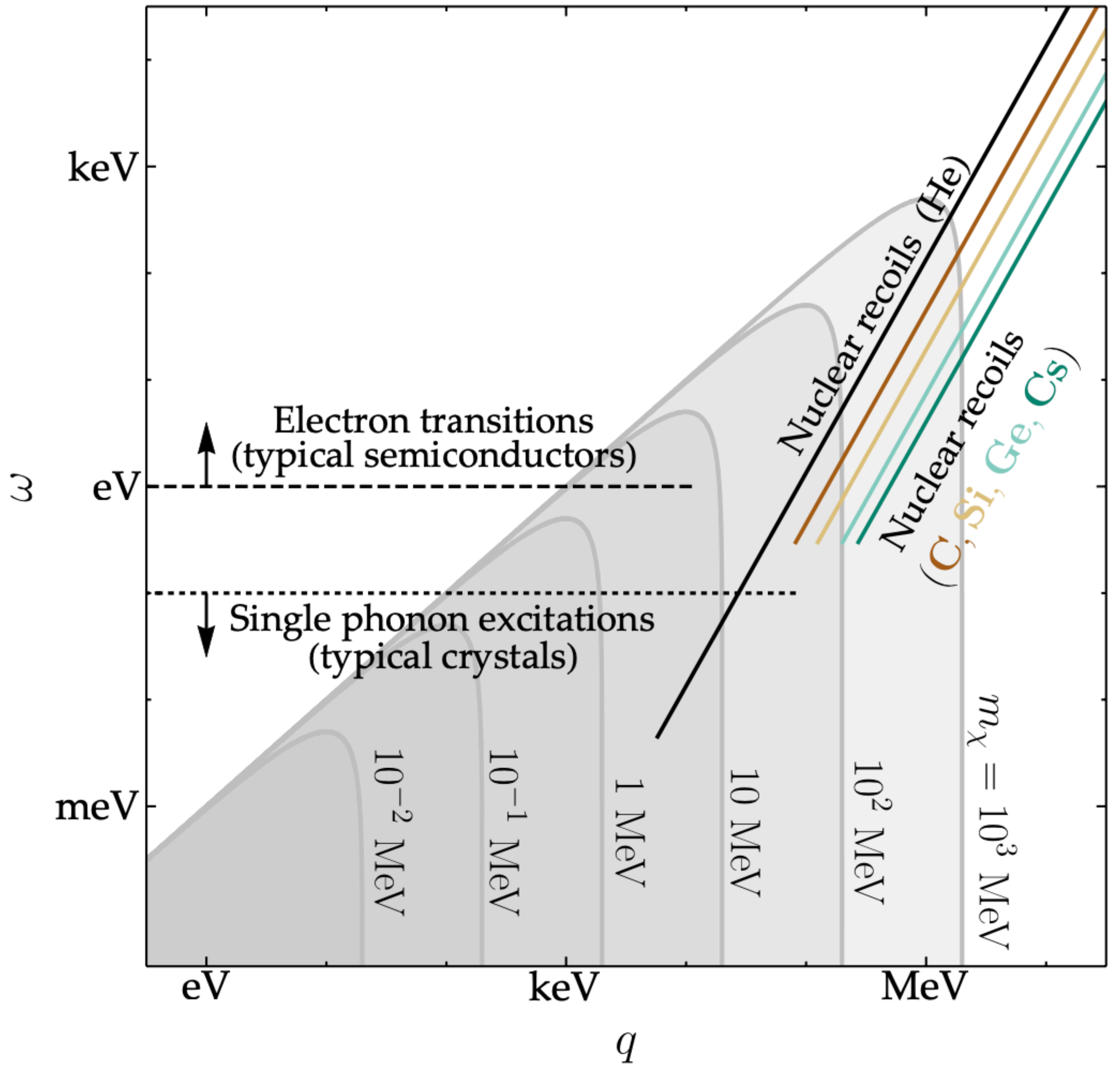

Trickle et al, arXiv: 1910.08092

- The maximum dark matter energy deposition depends on its mass
- The energy deposition reduces for lower mass dark matter

$$\omega_{\boldsymbol{q}} = \frac{1}{2}m_\chi v^2 - \frac{(m_\chi \boldsymbol{v} - \boldsymbol{q})^2}{2m_\chi} = \boldsymbol{q}\cdot\boldsymbol{v} - \frac{q^2}{2m_\chi}$$

$$\omega \leq E_k \sim m_{\rm DM} v^2 \sim 10^{-6} m_{\rm DM}$$

Look for phonon excitation!

从传统探测到低阈值轻暗物质探测

❑ 液氙闪烁探测器(LXe)

➢ 即时信号+延时信号

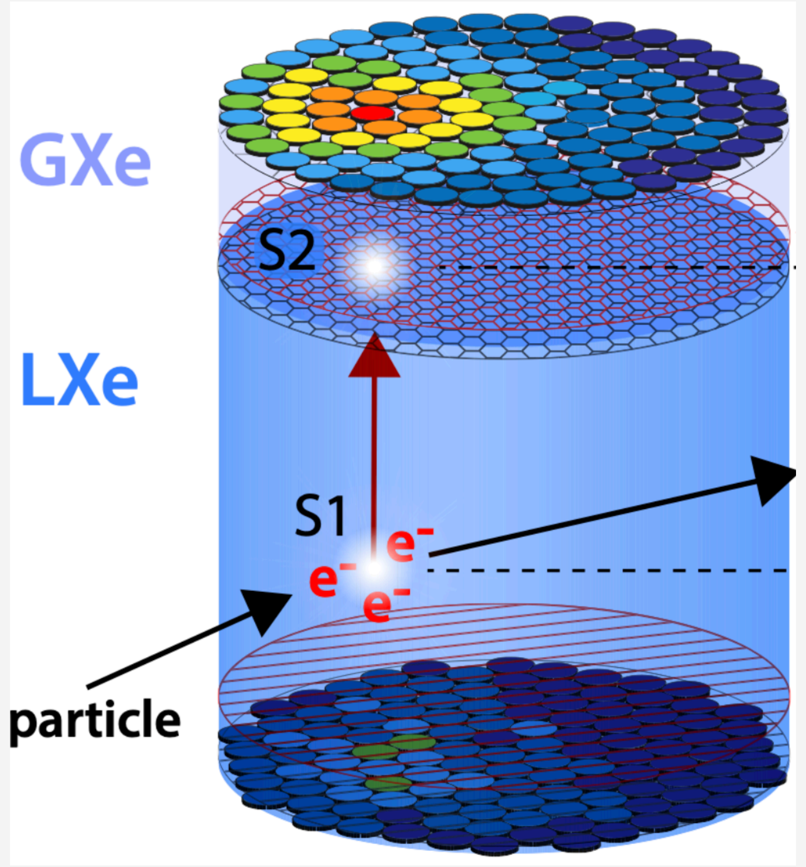

优点：探测器质量极大、粒子分辨能力强，探测WIMP极为灵敏

能量阈值高(keV)，不适合探测轻暗物质

❑ 半导体+转变边缘探测器(TES)

➢ 电荷信号+温度信号

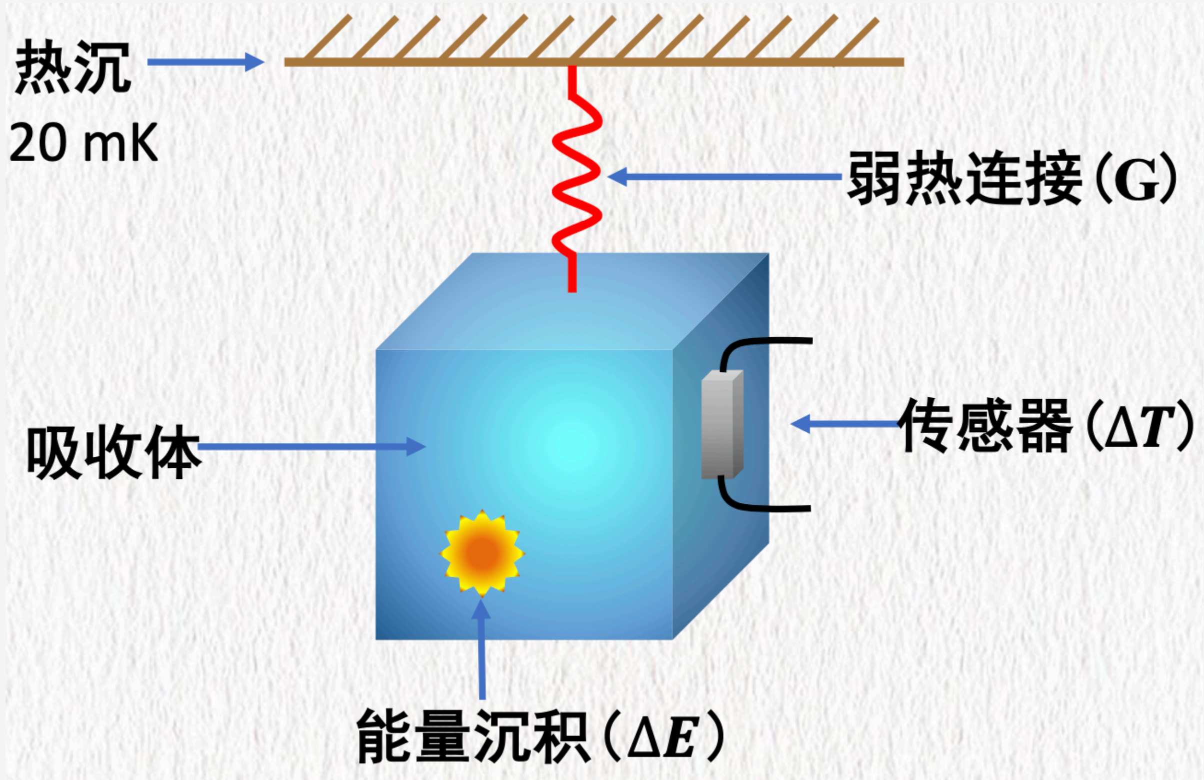

优点：粒子分辨能力较强，适合探测较轻的暗物质

能量阈值较高(eV)，不适合探测MeV以下轻暗物质，探测器质量较小

❑ 新一代量子传感器

➢ 超导准粒子信号

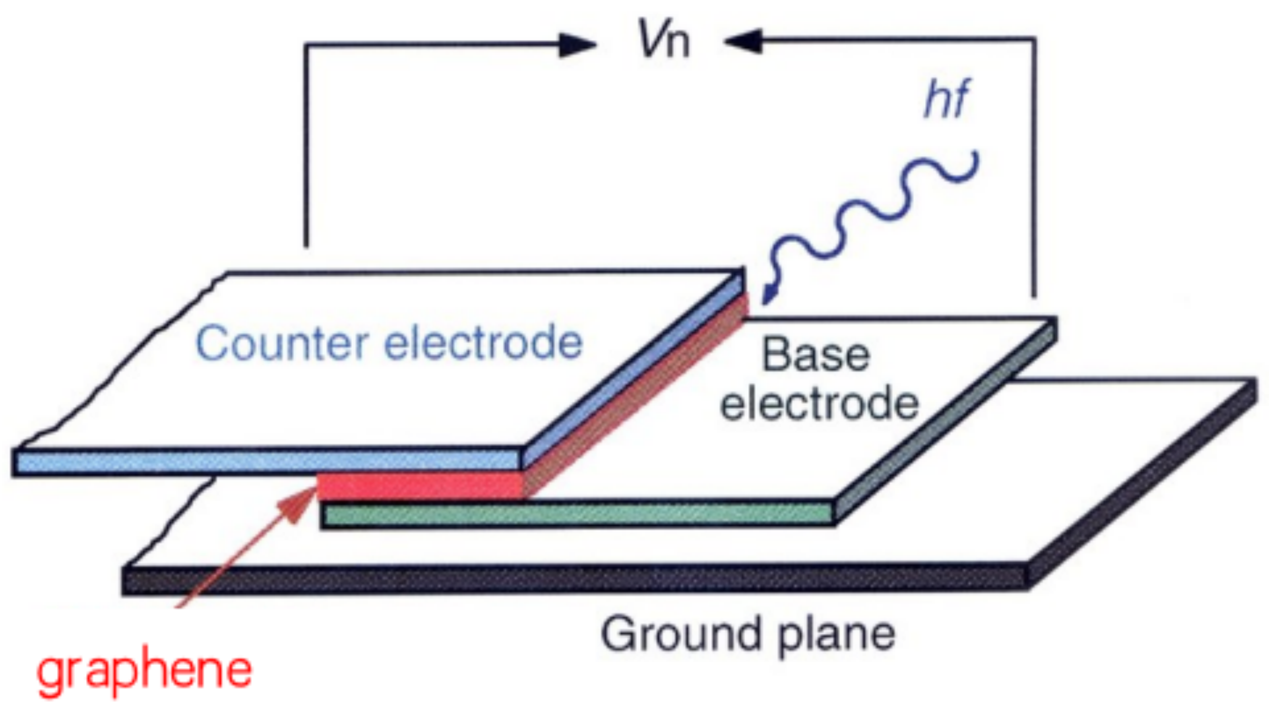

<u>能量阈值低、能量分辨率高</u>

低阈值(meV)、便于高度集成，适合探测质量MeV以下轻暗物质

SuperCDMS

PRD 104,032010 2021

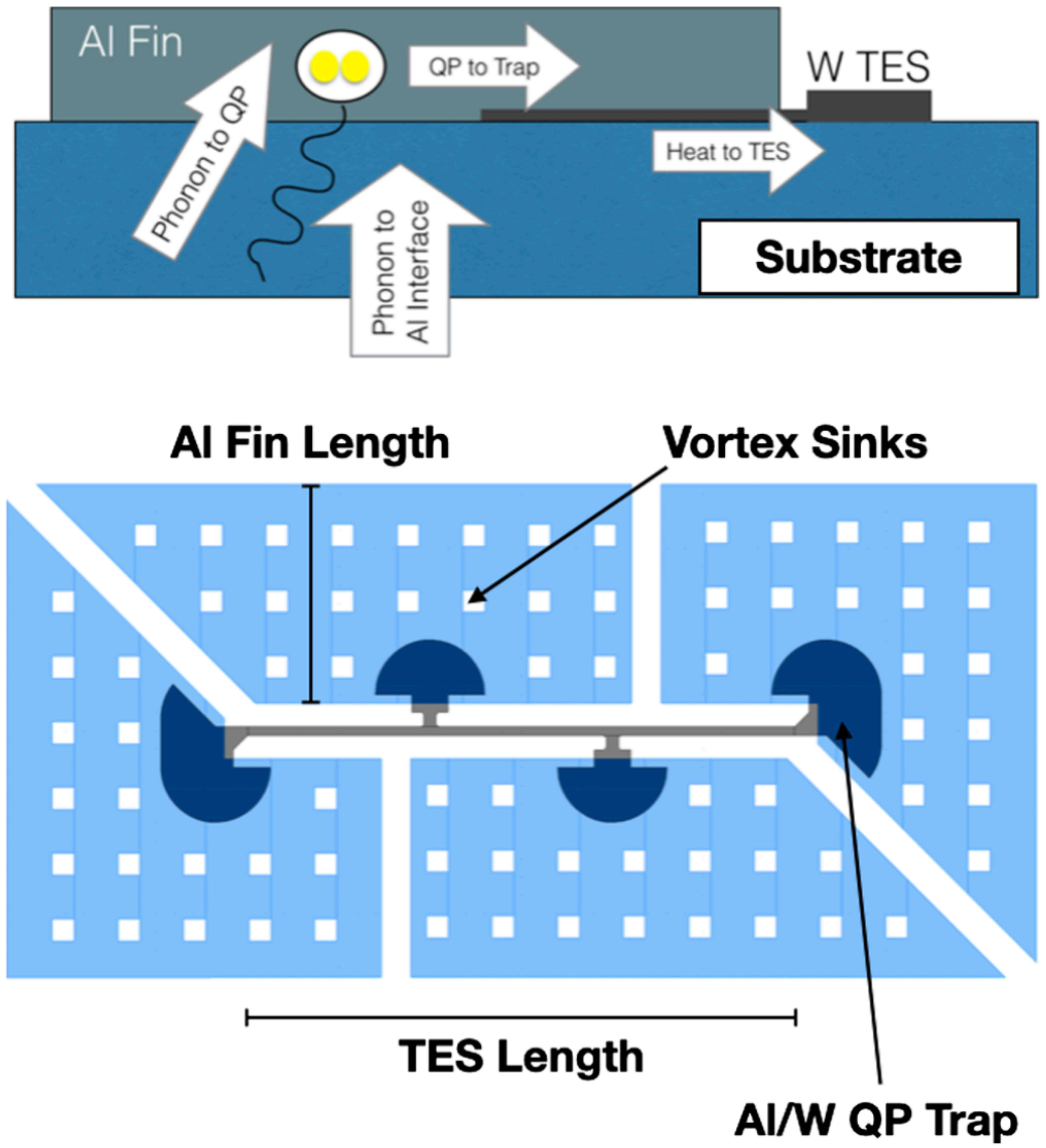

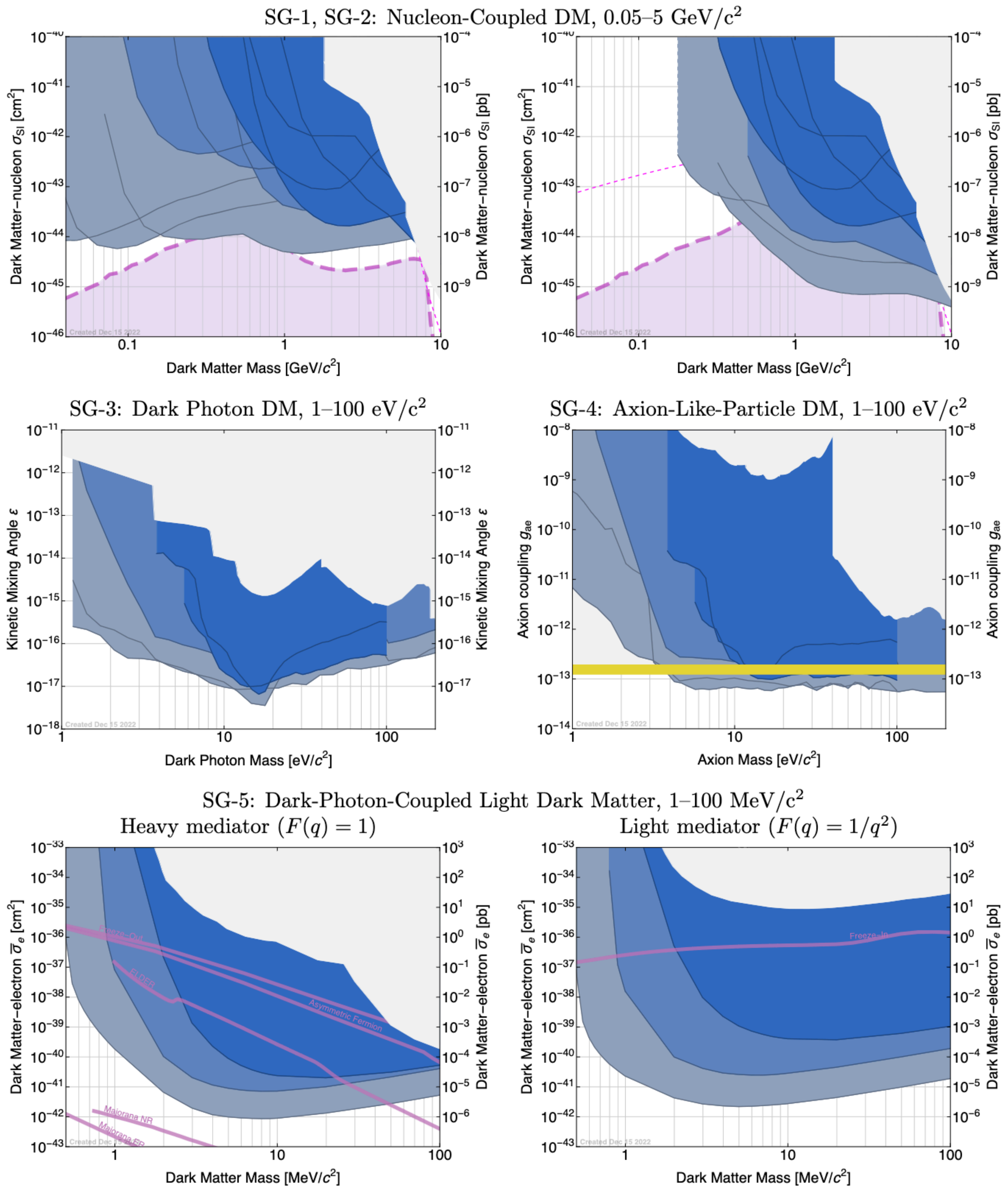

SuperCDMS-CPD phonon+charge

SuperCDMS@SNOLab

暗物质散射产生多声子，多声子加热转变边缘传感器

$E_{\mathrm{th}} \sim \mathrm{eV}$ 2203.08463

The Phonons

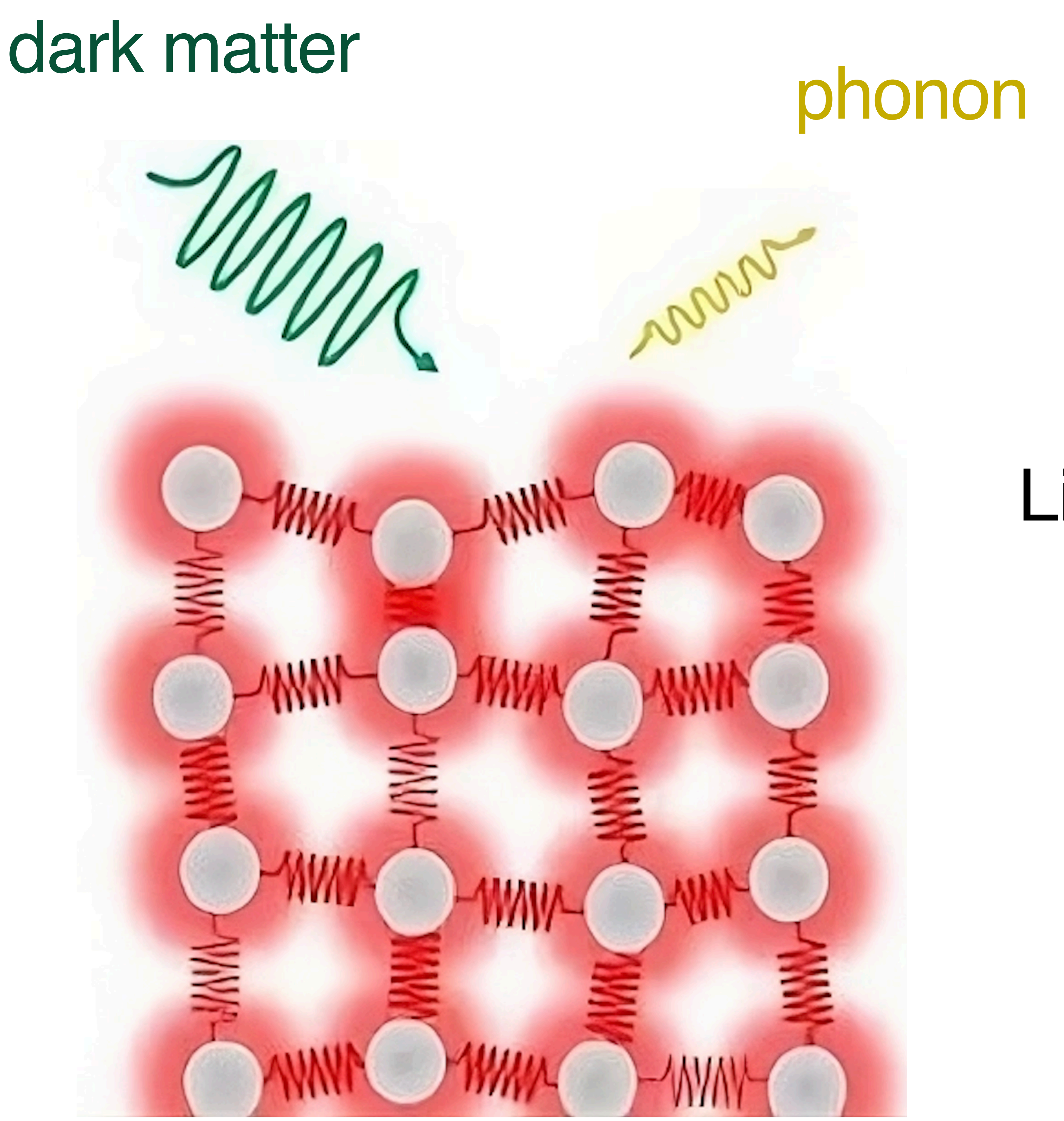

Light dark matter $\frac{1}{q} >$ lattice spacing

↓

phonon excitation

The Phonons

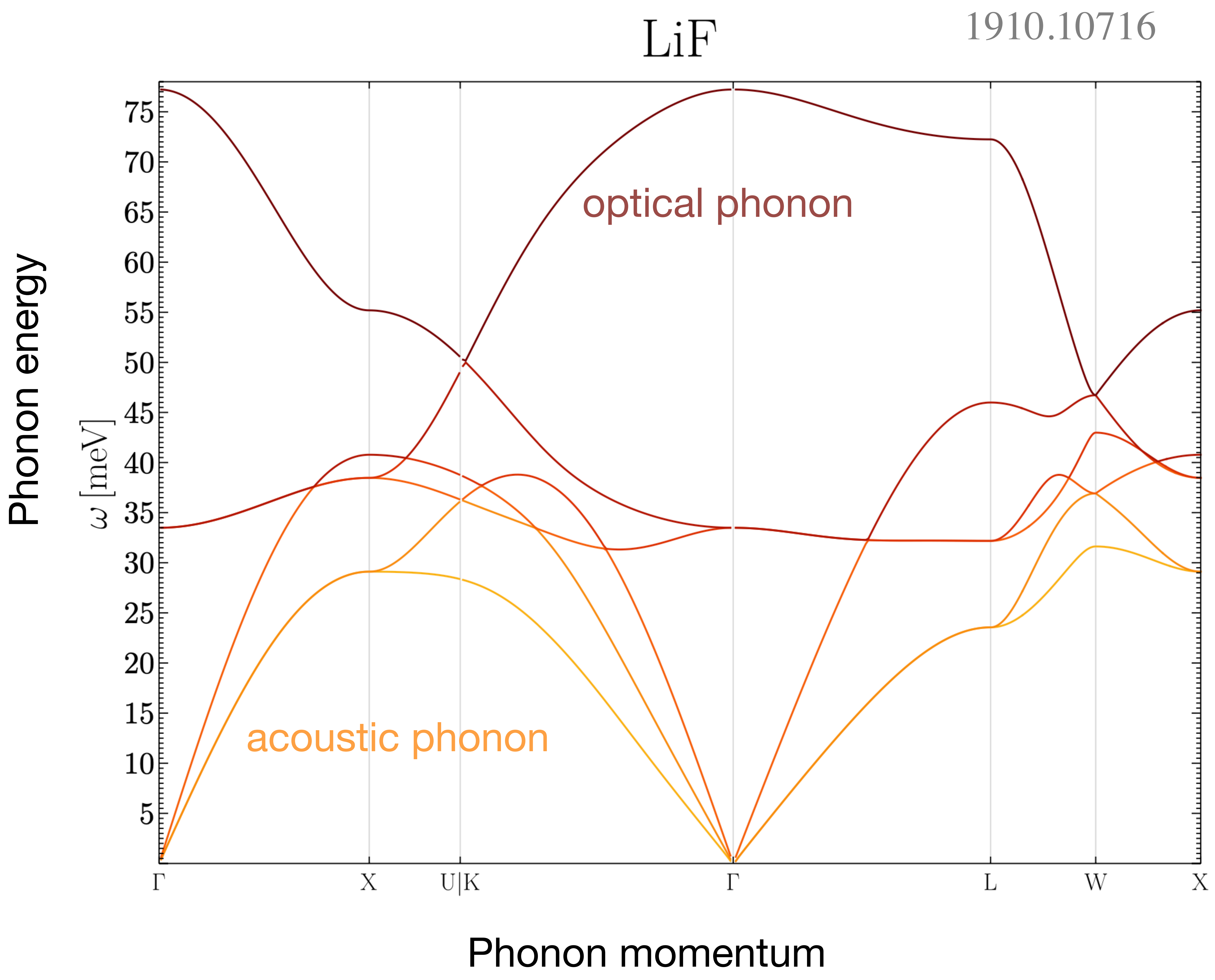

LiF
1910.10716
optical phonon
acoustic phonon
Phonon energy
ω [meV]
75
70
65
60
55
50
45
40
35
30
25
20
15
10
5
Γ
X
U|K
Γ
L
W
X
Phonon momentum

Dark Matter Scattering Rate

See also: 1910.08092, 2009.13534

$$\Gamma(\boldsymbol{v}) = V \int \frac{d^3q}{(2\pi)^3} \sum_f \left| \langle \boldsymbol{p}', f | \, \delta\hat{H} \, | \boldsymbol{p}, i \rangle \right|^2 2\pi\delta\big(E_f - E_i - \omega_{\boldsymbol{q}}\big)$$

$$R = \frac{1}{\rho_T} \frac{\rho_\chi}{m_\chi} \int d^3v \, f_\chi(\boldsymbol{v}) \, \Gamma(\boldsymbol{v})$$

$$R = \frac{1}{m_{\text{cell}}} \frac{\rho_\chi}{m_\chi} \frac{\pi\bar{\sigma}}{2\mu^2} \int \frac{d^3q}{(2\pi)^3} \mathcal{F}^2_{\text{med}}(q) \sum_\nu \frac{1}{\omega_{\nu,\boldsymbol{k}}} \left| \sum_j \frac{e^{-W_j(\boldsymbol{q})}}{\sqrt{m_j}} e^{i\boldsymbol{G}\cdot\boldsymbol{x}_j^0} \left(\boldsymbol{Y}_j \cdot \boldsymbol{\epsilon}^*_{\nu,\boldsymbol{k},j}\right) \right|^2 g(\boldsymbol{q}, \omega_{\nu,\boldsymbol{k}})$$

Cell mass

Mediator form factor

Phonon eigen energy

Material response

Dark matter velocity integral

Sensitivity to Light Dark Matter

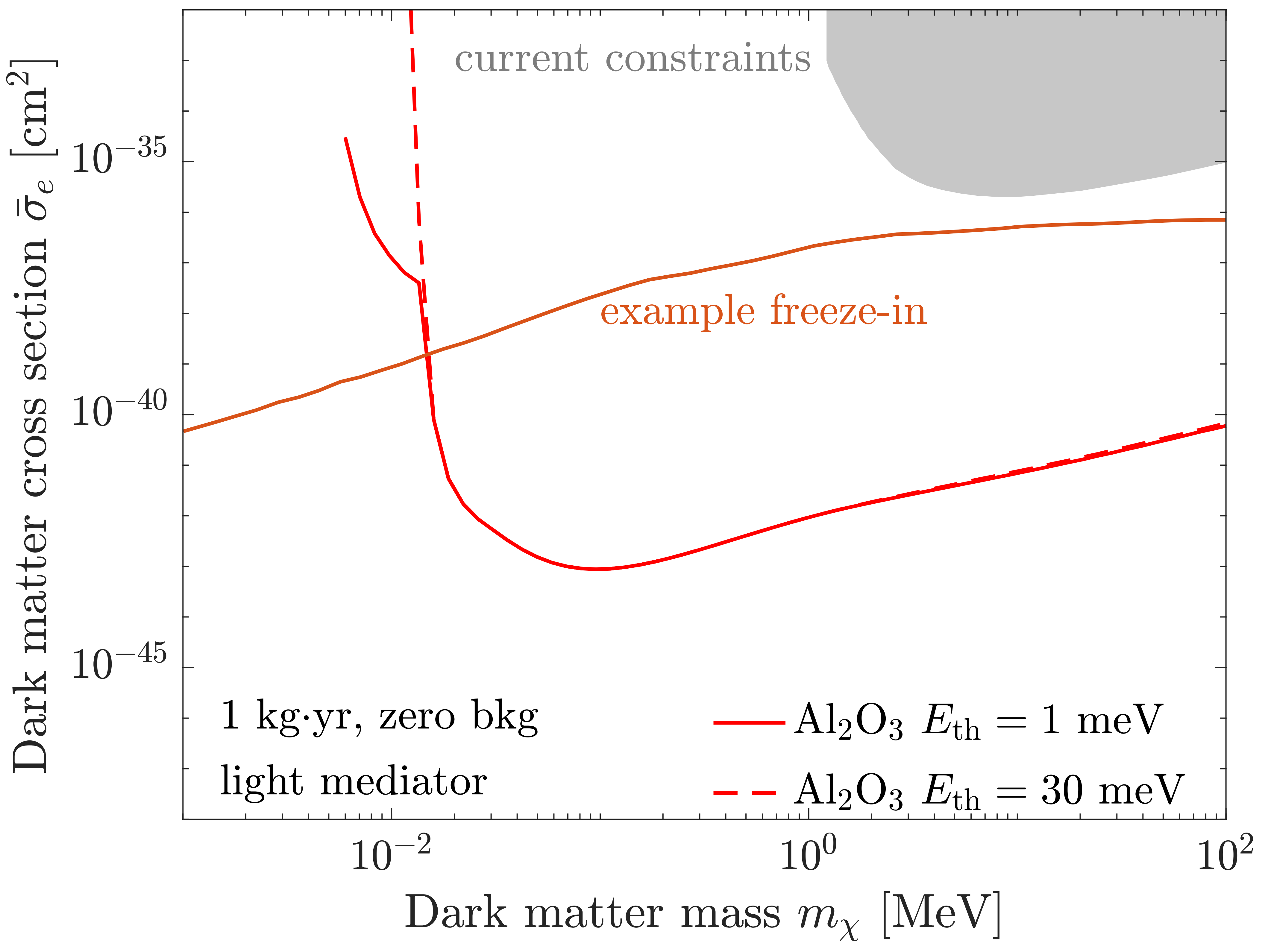

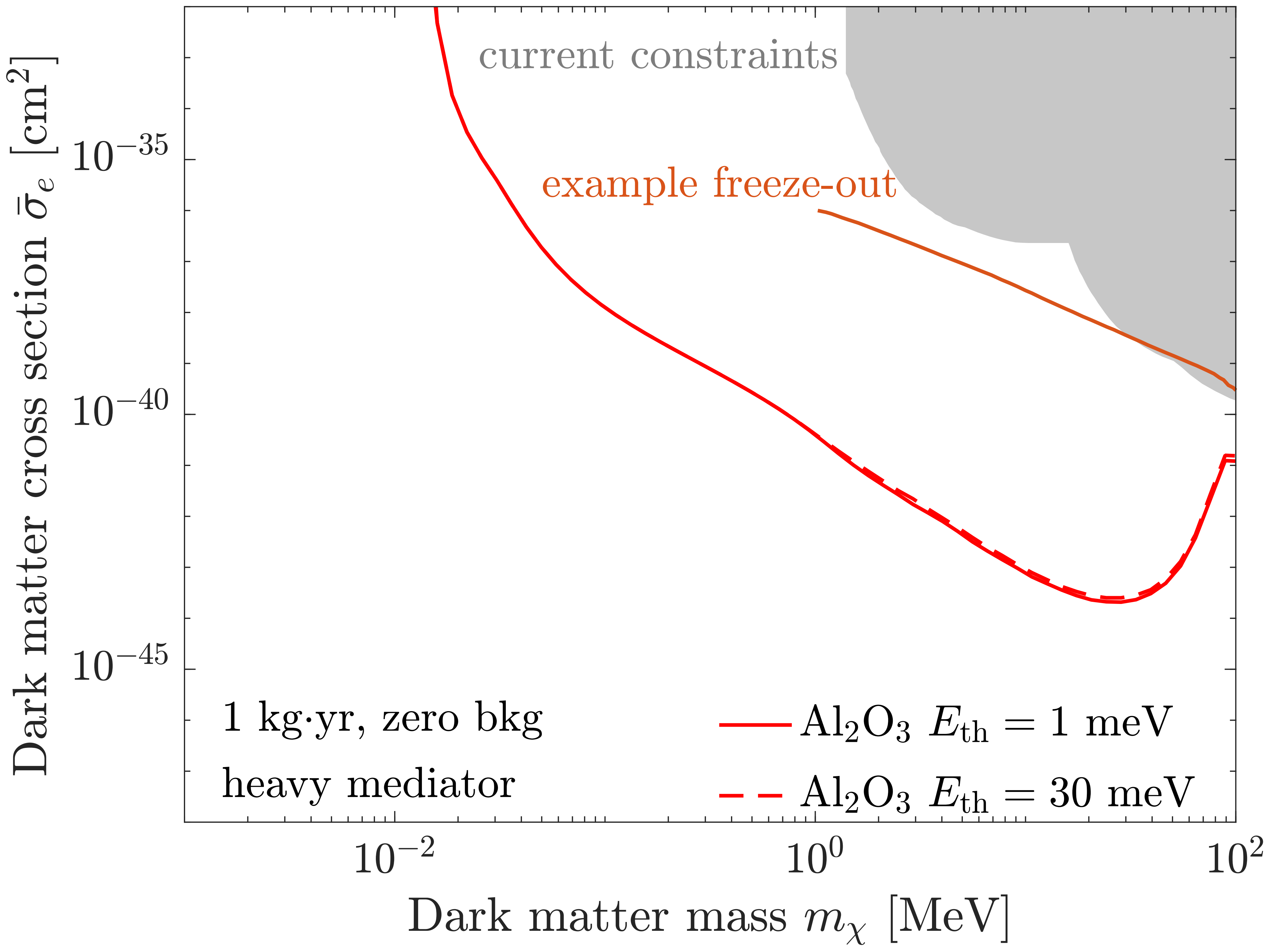

Light mediator $F_{\text{med}} = \frac{(\alpha m_e)^2}{q^2}$

Heavy mediator $F_{\text{med}} = 1$

暗物质是什么

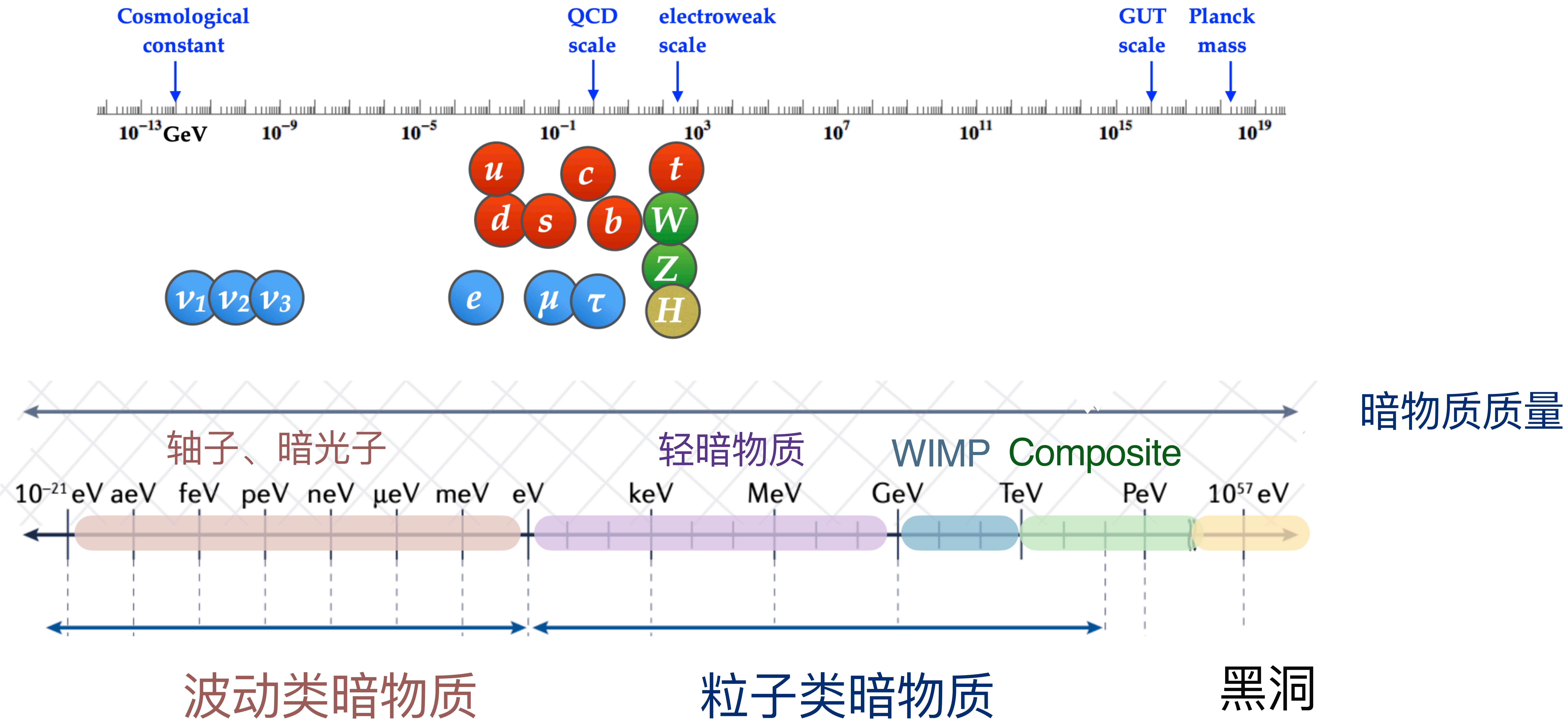
Cosmological constant
QCD scale
electroweak scale
GUT scale
Planck mass
10^-13 GeV
10^-9
10^-5
10^-1
10^3
10^7
10^11
10^15
10^19
u c t
d s b W
Z
ν1 ν2 ν3
e μ τ H
暗物质质量
轴子、暗光子
轻暗物质
WIMP
Composite
10^-21 eV aeV feV peV neV μeV meV eV keV MeV GeV TeV PeV 10^57 eV
波动类暗物质
粒子类暗物质
黑洞

Wave-like Dark Matter

The Strong CP Problem

The QCD theta-term $\mathscr{L} = \mathscr{L}_{\rm SM} - \theta \frac{g_s^2}{32\pi^2} G^a_{\mu\nu} \tilde{G}^a_{\mu\nu}$

$$F_{\mu\nu}\tilde{F}^{\mu\nu} \propto \vec{E} \cdot \vec{B}$$

The Strong CP Problem

The QCD theta-term $$\mathscr{L} = \mathscr{L}_{\mathrm{SM}} - \theta \frac{g_s^2}{32\pi^2} G^a_{\mu\nu} \tilde{G}^a_{\mu\nu}$$

$\downarrow$

$$F_{\mu\nu}\tilde{F}^{\mu\nu} \propto \vec{E} \cdot \vec{B}$$

E: even under time reversal (T/CP)

B: odd under time reversal (T/CP)

$G\tilde{G}$ violates CP conservation

The Strong CP Problem

The QCD theta-term $\mathscr{L} = \mathscr{L}_{\rm SM} - \theta \frac{g_s^2}{32\pi^2} G^a_{\mu\nu} \tilde{G}^a_{\mu\nu}$

$G\tilde{G}$ violates CP conservation

Theoretical prediction of neutron EDM

$$d_n \approx \bar{\theta} e m_\pi^2 / m_N^3 \approx 10^{-16}\, \bar{\theta}\, e\,\mathrm{cm}.$$

Experimental measurement

$$|d_n| \lesssim 1.8\ 10^{-26} e\,\mathrm{cm}$$

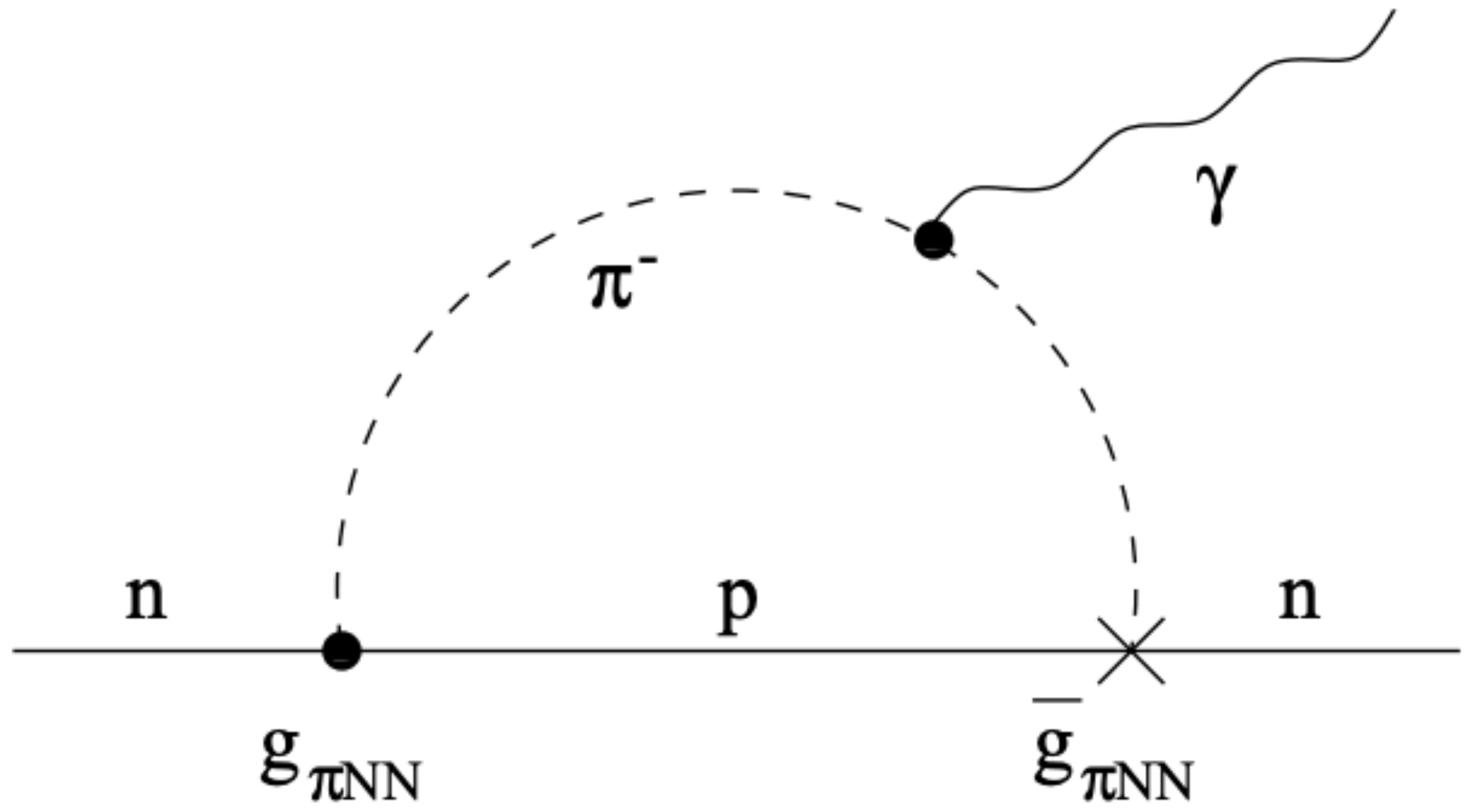

Pospelov et al, arXiv: hep-ph/9908508

Crewther et al, 1979

The Strong CP Problem

The QCD theta-term $\mathscr{L} = \mathscr{L}_{\mathrm{SM}} - \theta \frac{g_s^2}{32\pi^2} G^a_{\mu\nu} \tilde{G}^a_{\mu\nu}$

Theoretical prediction of neutron EDM

$$d_n \approx \bar{\theta} e m_\pi^2 / m_N^3 \approx 10^{-16}\, \bar{\theta}\, e\, \mathrm{cm}.$$

Promote θ to a dynamical field

Experimental measurement

$$|d_n| \lesssim 1.8\ 10^{-26} e\, \mathrm{cm}$$

The Strong CP Problem

$$\mathcal{L}_{\rm eff} \supset \frac{1}{2}\partial^\mu a\, \partial_\mu a + \frac{\alpha_s}{8\pi}\frac{a}{v_{\rm PQ}} G^a_{\mu\nu}\tilde{G}^{a\,\mu\nu}$$

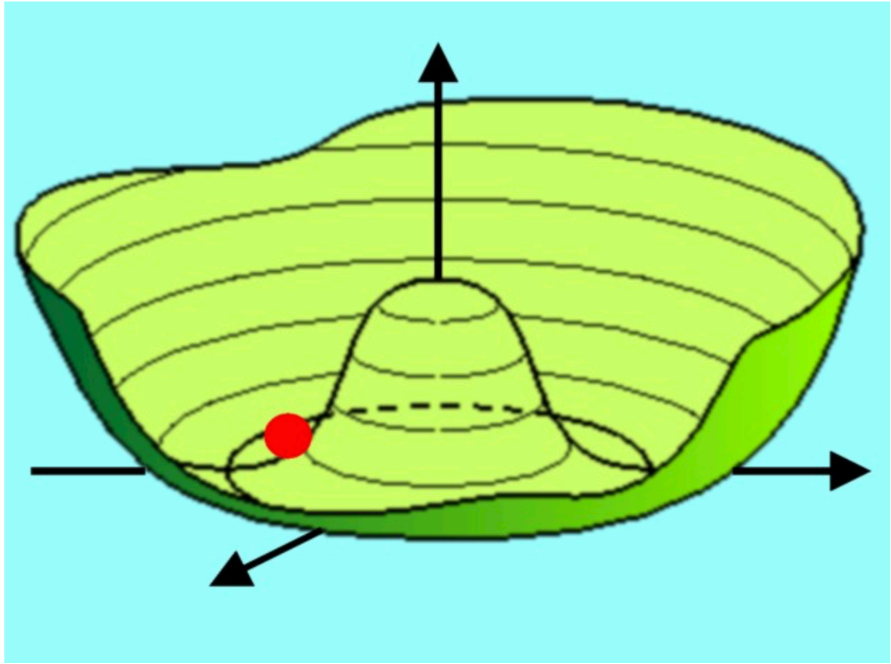

Di Vecchia et al, 1980

Leutwyler et al, 1992]

$$V(\theta) = m_\pi^2 f_\pi^2 \left(1 - \frac{\sqrt{1+z^2+2z\cos\theta}}{1+z}\right)$$

$$z \equiv m_u/m_d \approx 1/2$$

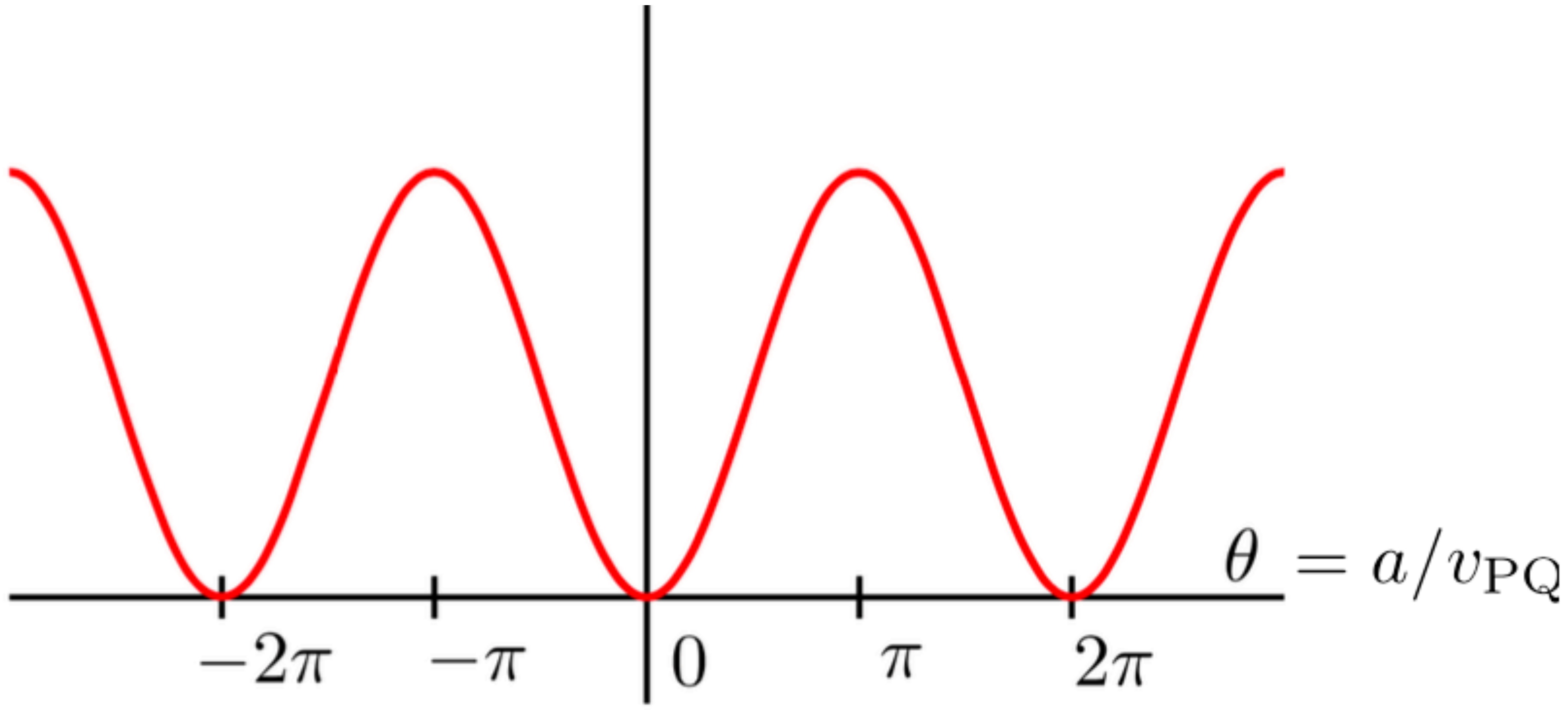

Credit: Ringwald

Promote θ to a dynamical field

The Strong CP Problem

$$\mathcal{L}_{\rm eff} \supset \frac{1}{2}\partial^\mu a\,\partial_\mu a + \frac{\alpha_s}{8\pi}\frac{a}{v_{\rm PQ}} G^a_{\mu\nu}\tilde{G}^{a\,\mu\nu}$$

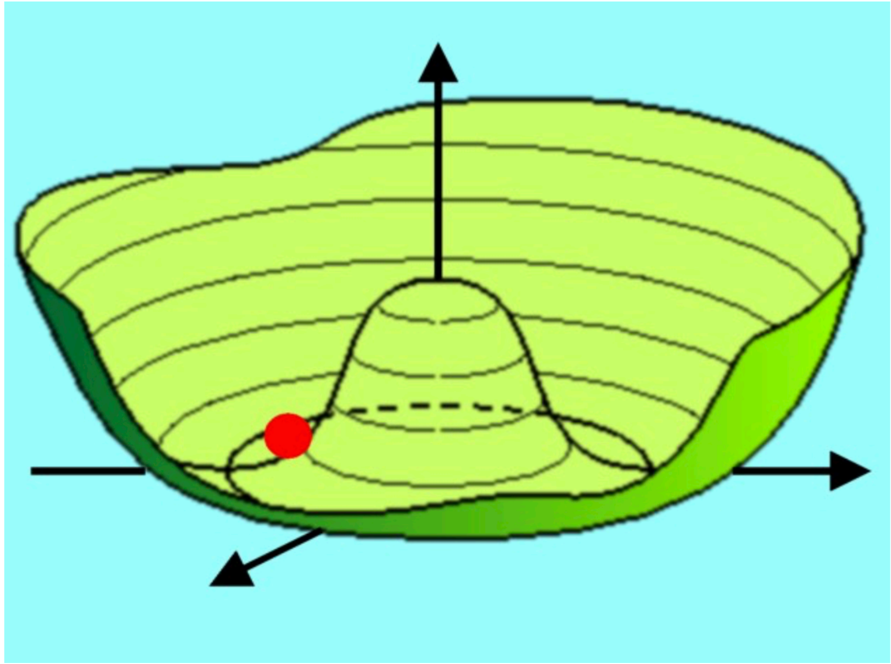

$$V(\theta) = m_\pi^2 f_\pi^2 \left(1 - \frac{\sqrt{1+z^2+2z\cos\theta}}{1+z}\right)$$

$$z \equiv m_u/m_d \approx 1/2$$

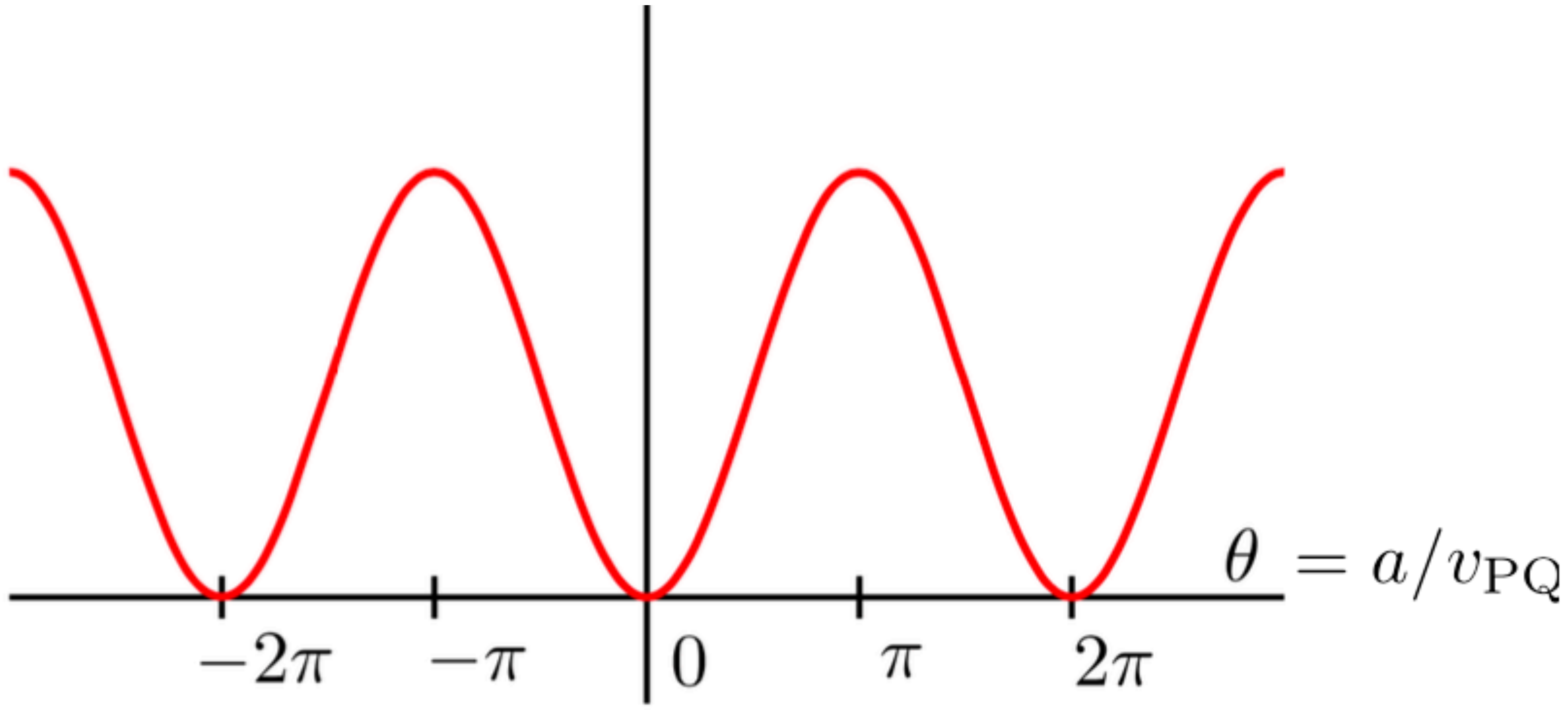

$\langle\theta(x)\rangle = 0 \;\Rightarrow$ **nEDM vanishes**

The Strong CP Problem

$$\mathcal{L}_{\rm eff} \supset \frac{1}{2}\partial^\mu a\,\partial_\mu a + \frac{\alpha_s}{8\pi}\frac{a}{v_{\rm PQ}}G^a_{\mu\nu}\tilde{G}^{a\,\mu\nu}$$

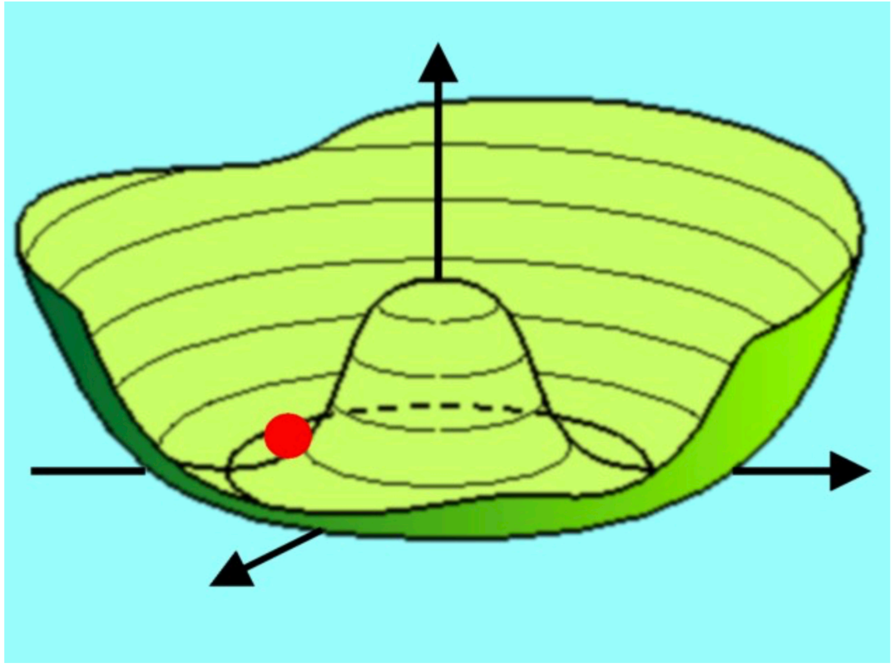

$$V(\theta) = m_\pi^2 f_\pi^2\left(1 - \frac{\sqrt{1+z^2+2z\cos\theta}}{1+z}\right)$$

$$z \equiv m_u/m_d \approx 1/2$$

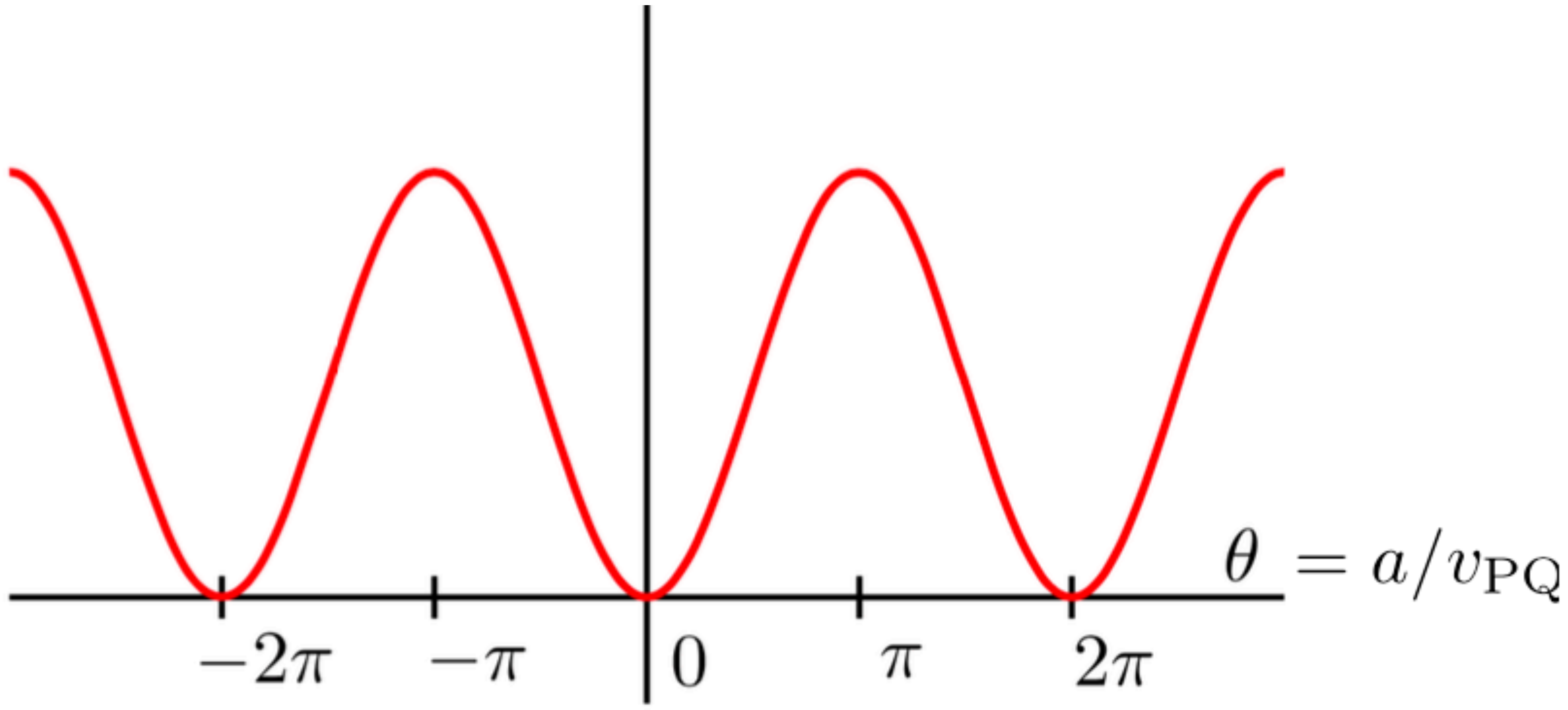

$$m_a = \frac{\sqrt{V''(0)}}{v_{\rm PQ}} = \frac{\sqrt{z}}{1+z}\frac{m_\pi f_\pi}{v_{\rm PQ}} \approx 6\ \mu{\rm eV}\left(\frac{10^{12}\,{\rm GeV}}{v_{\rm PQ}}\right)$$

The Effective Axion Coupling

$$\mathcal{L} \supset -\frac{1}{2}m_a^2 a^2 - \frac{i}{2}\frac{eC_{\rm NEDM}}{f_a}\, a\,\overline{\psi}_N \sigma_{\mu\nu}\gamma_5\psi_N F^{\mu\nu} + C_{a\gamma}\frac{\alpha}{8\pi}\frac{a}{f_a}F_{\mu\nu}\tilde{F}^{\mu\nu} + \frac{1}{2}C_{af}\frac{\partial_\mu a}{f_a}\overline{\psi}_f\gamma^\mu\gamma_5\psi_f$$

axion-nucleon coupling

axion-photon coupling

axion-fermion coupling

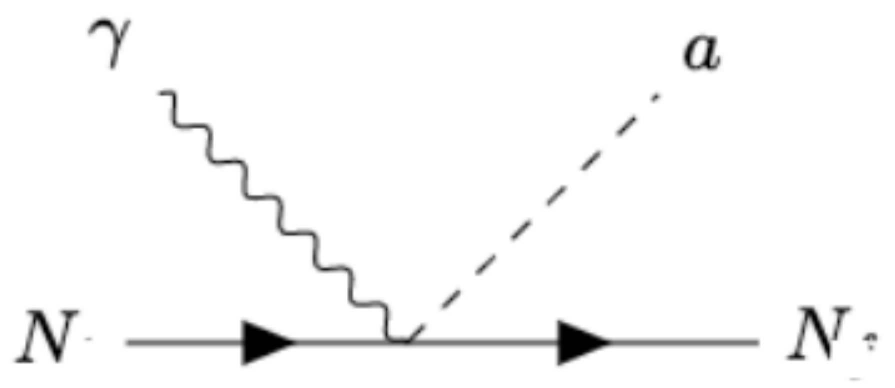

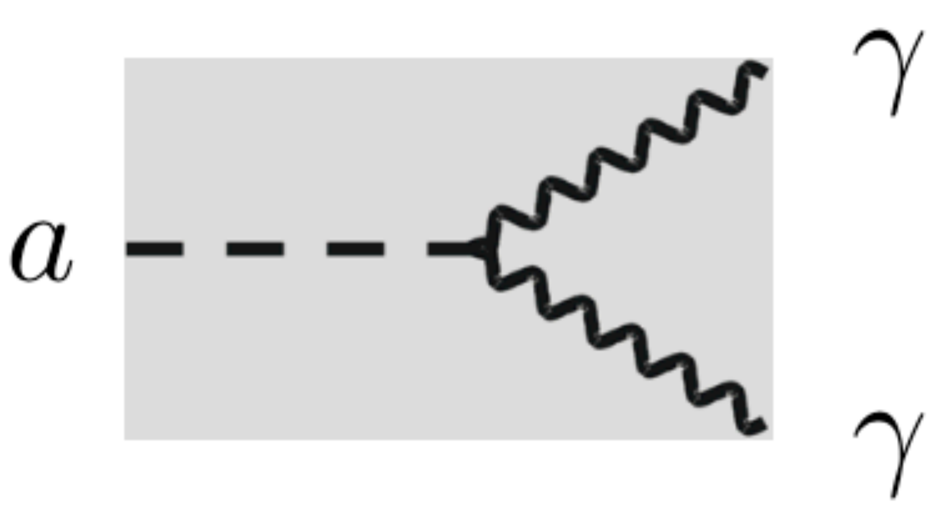

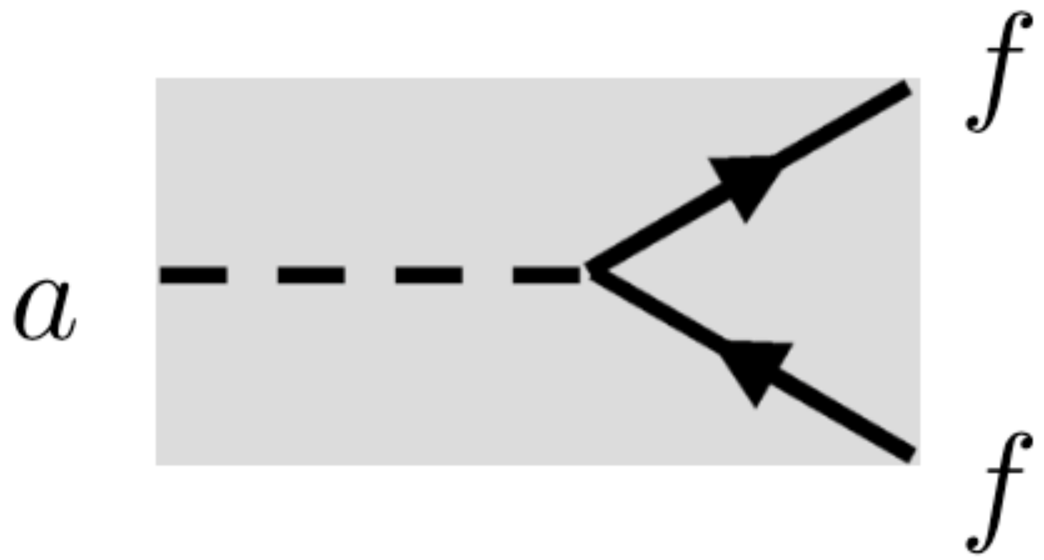

The Effective Axion Coupling

$$\mathcal{L} \supset -\frac{1}{2}m_a^2 a^2 - \frac{i}{2}\frac{eC_{\mathrm{NEDM}}}{f_a}\, a\,\overline{\psi}_N \sigma_{\mu\nu}\gamma_5 \psi_N F^{\mu\nu} + C_{a\gamma}\frac{\alpha}{8\pi}\frac{a}{f_a}F_{\mu\nu}\tilde{F}^{\mu\nu} + \frac{1}{2}C_{af}\frac{\partial_\mu a}{f_a}\overline{\psi}_f \gamma^\mu \gamma_5 \psi_f$$

$$g_{a\gamma\gamma} \equiv \frac{\alpha}{2\pi f_a}C_{a\gamma} \simeq \frac{\alpha}{2\pi f_\pi}\frac{m_a}{m_\pi}\frac{1+z}{\sqrt{z}}\left(\frac{E_{\mathcal{Q}}}{N_{\mathcal{Q}}} - \frac{2}{3}\frac{4+z}{1+z}\right)$$

Kaplan, 1985
Srednicki et al, 1985

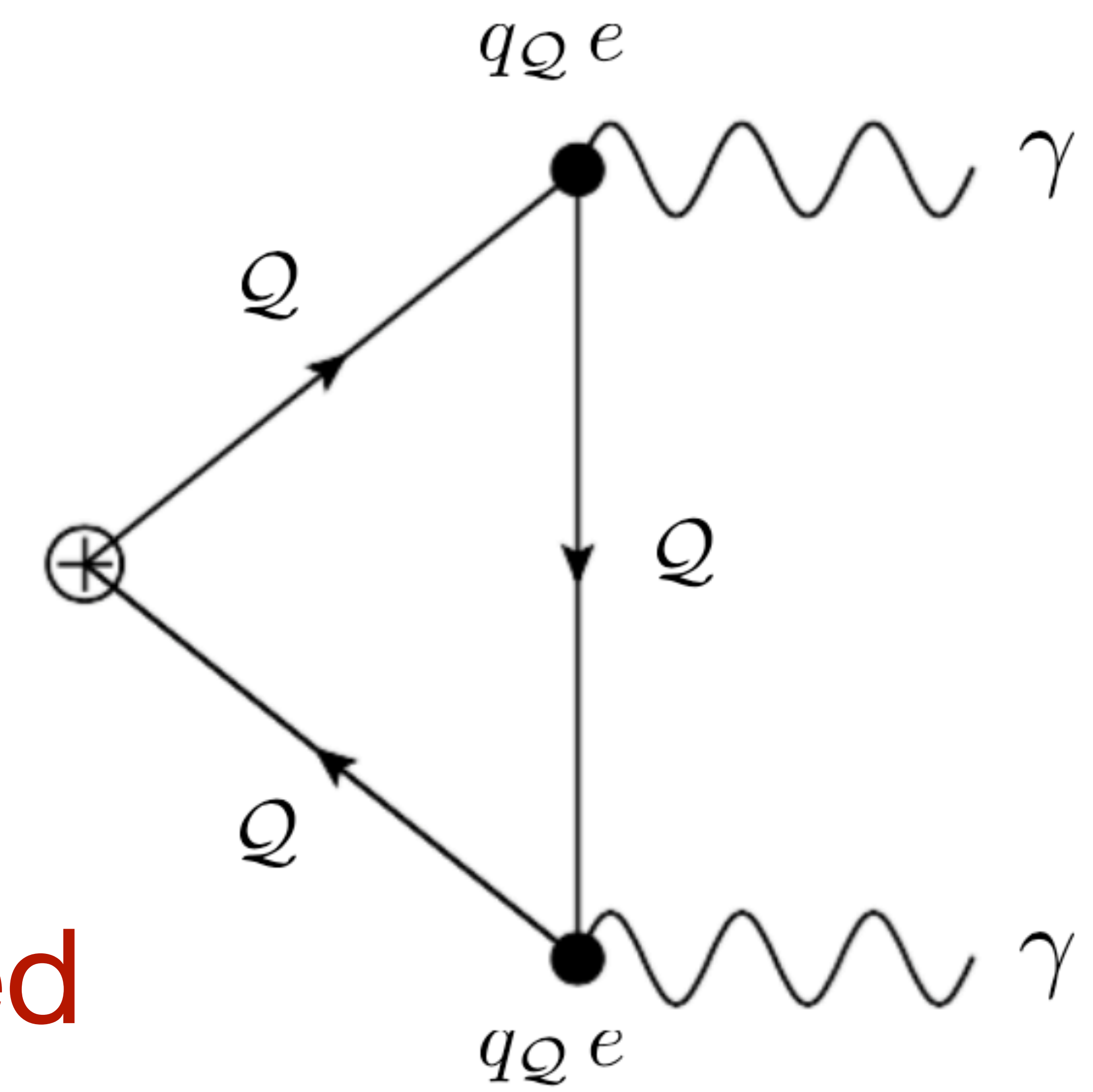

The QCD axion mass and coupling is tightly coupled

The Axion Experiments

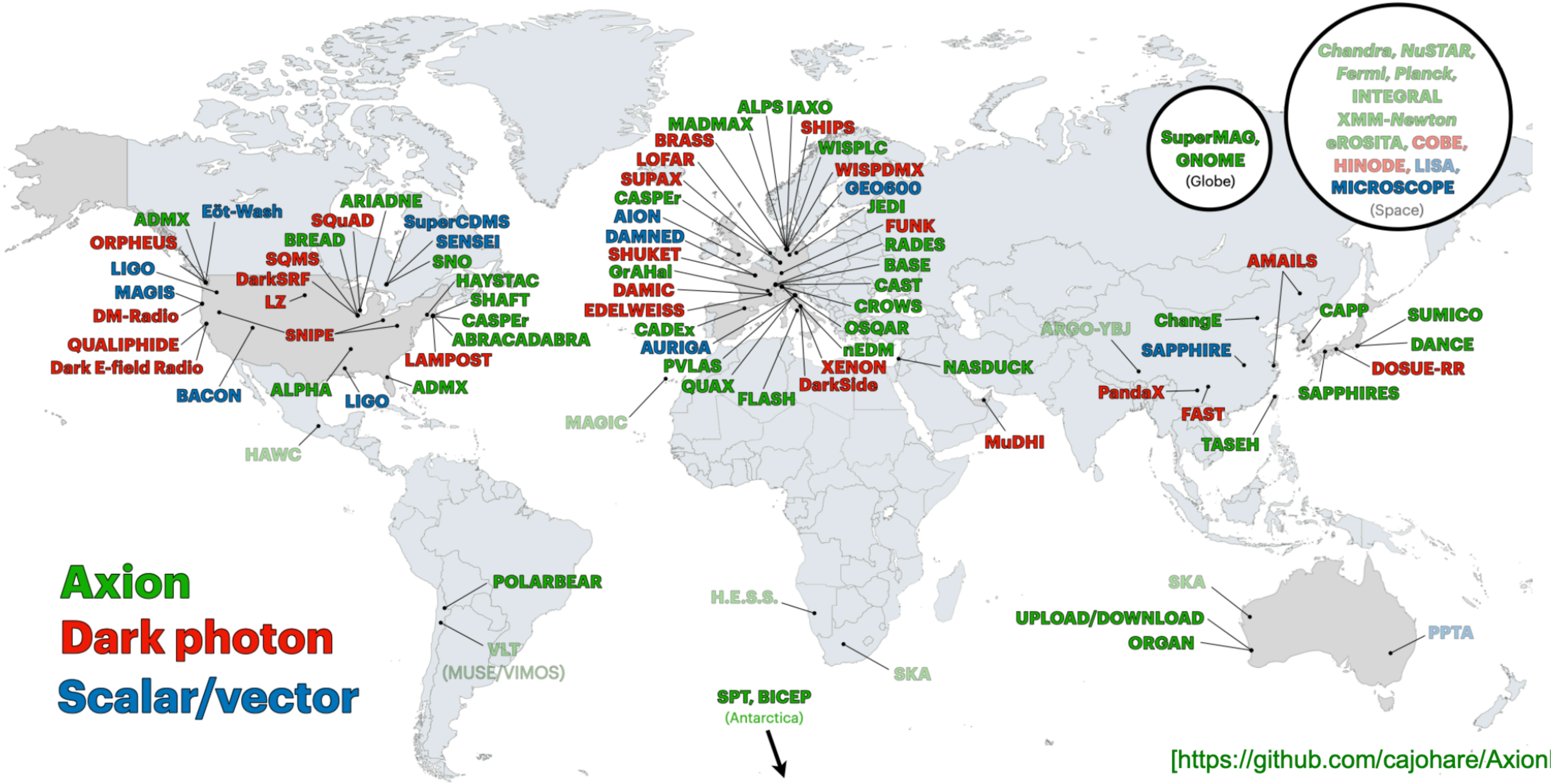

[https://github.com/cajohare/AxionLimits

The Misalignment Mechanism

A simple real scalar field

$$\mathcal{L} = \frac{1}{2}\partial_\mu \phi \partial^\mu \phi - \frac{1}{2} m_\phi^2 \phi^2 + \mathcal{L}_I$$

$$S = \int d^4x \sqrt{-g}(\frac{1}{2} g^{\mu\nu} \partial_\mu \phi \partial_\nu \phi g - V(\phi))$$

$$\ddot{\phi} + 3H\dot{\phi} + m_\phi^2 \phi = 0.$$

The Misalignment Mechanism

A simple real scalar field

$$\mathcal{L} = \frac{1}{2}\partial_\mu\phi\partial^\mu\phi - \frac{1}{2}m_\phi^2\phi^2 + \mathcal{L}_I$$

$$S = \int d^4x\sqrt{-g}(\frac{1}{2}g^{\mu\nu}\partial_\mu\phi\partial_\nu\phi g - V(\phi))$$

$$\ddot{\phi} + 3H\dot{\phi} + m_\phi^2\phi = 0.$$

Hubble friction

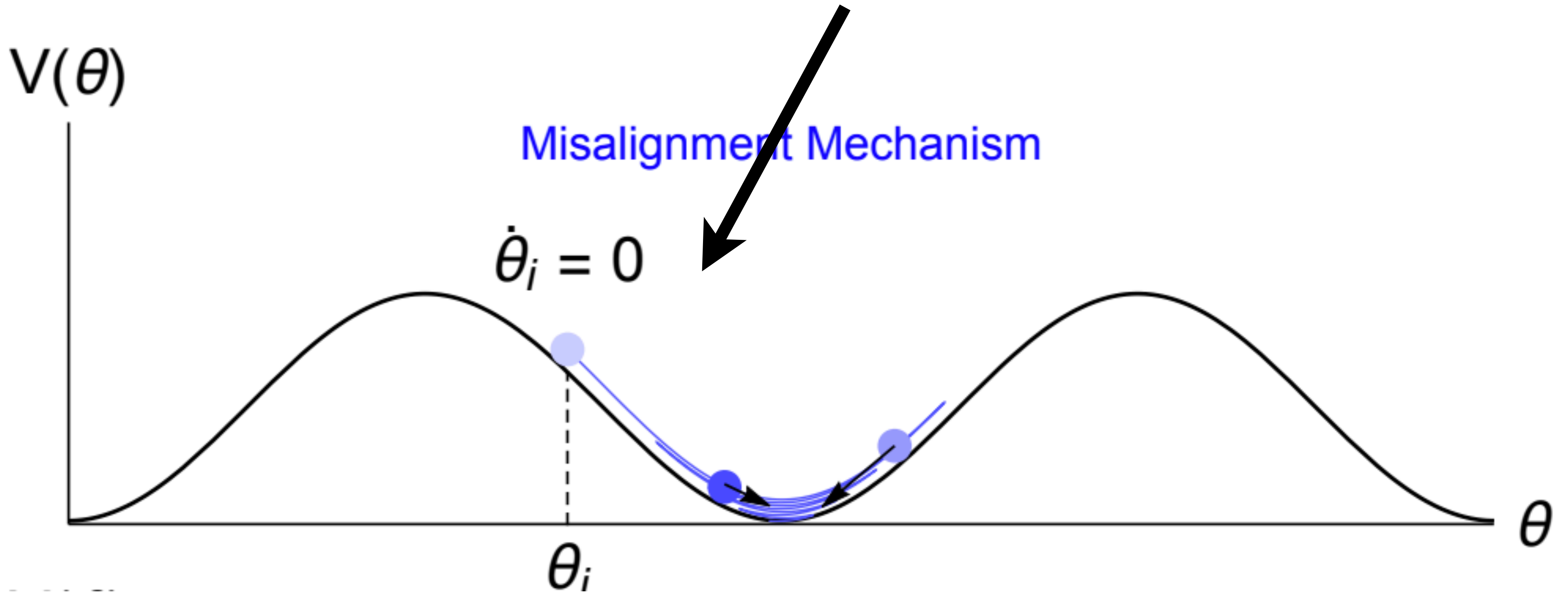

$H \gg m_\phi$, the field is frozen

The Misalignment Mechanism

A simple real scalar field

$$\mathcal{L} = \frac{1}{2}\partial_\mu\phi\partial^\mu\phi - \frac{1}{2}m_\phi^2\phi^2 + \mathcal{L}_I$$

$$S = \int d^4x\sqrt{-g}(\frac{1}{2}g^{\mu\nu}\partial_\mu\phi\partial_\nu\phi g - V(\phi))$$

$$\ddot{\phi} + 3H\dot{\phi} + m_\phi^2\phi = 0.$$

$H \ll m_\phi$ $\quad \phi \simeq \phi_1 \left(\frac{m_1 a_1^3}{m_\phi a^3}\right)^{1/2} \cos\left(\int_{t_1}^{t} m_\phi \, dt\right)$

Hubble friction

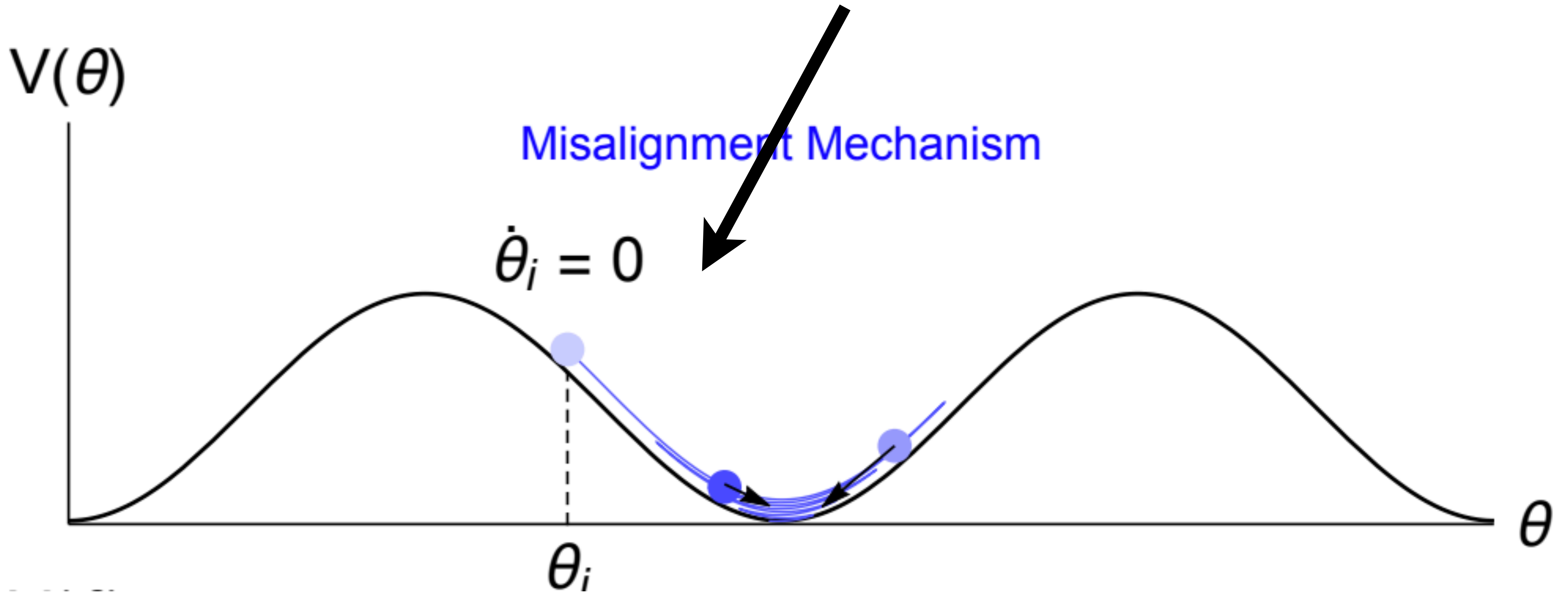

$H \gg m_\phi$, the field is frozen

$H \ll m_\phi$, the field oscillates

The Misalignment Mechanism

$$H \ll m_\phi \quad \phi \simeq \phi_1 \left(\frac{m_1 a_1^3}{m_\phi a^3}\right)^{1/2} \cos\left(\int_{t_1}^{t} m_\phi \, dt\right)$$

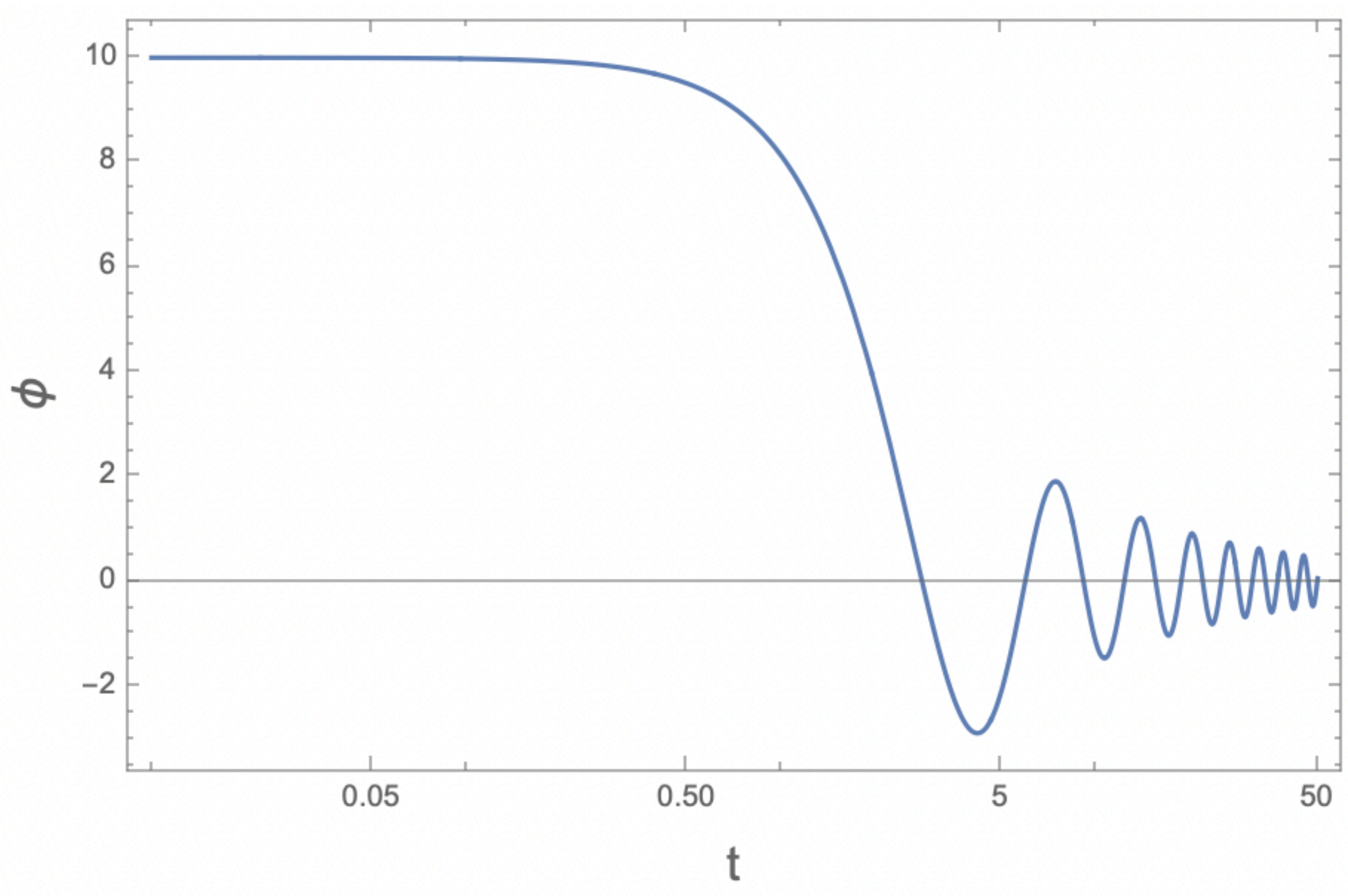

Hubble friction

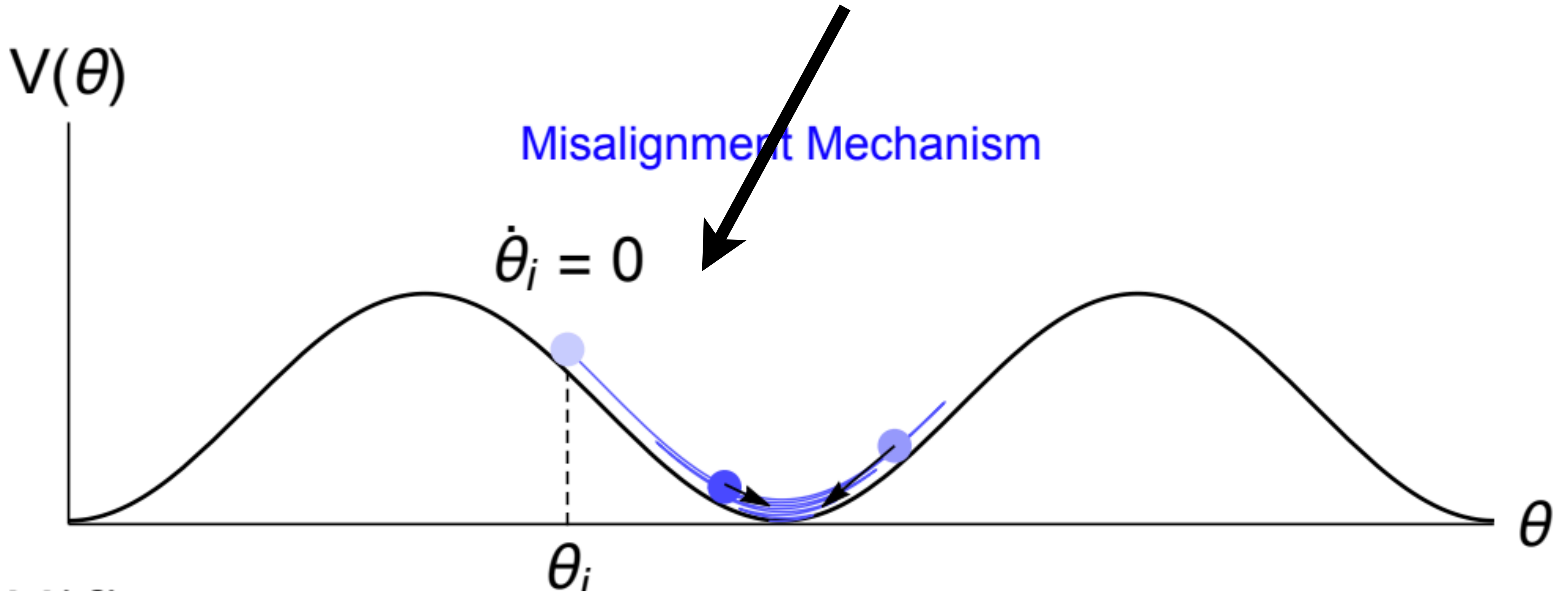

$H \gg m_\phi$, the field is frozen

$H \ll m_\phi$, the field oscillates

The Misalignment Mechanism

$$H \ll m_\phi \quad \phi \simeq \phi_1 \left(\frac{m_1 a_1^3}{m_\phi a^3}\right)^{1/2} \cos\left(\int_{t_1}^{t} m_\phi \, dt\right)$$

$$\mathcal{A}(t) = \dot{\phi}_1 (m_1 a_1^3 / m_\phi a^3)^{1/2}$$

$$\rho_\phi = \frac{1}{2}\dot{\phi}^2 + \frac{1}{2} m_\phi^2 \phi^2 = \frac{1}{2} m_\phi^2 \mathcal{A}^2 + \ldots$$

$$p_\phi = \frac{1}{2}\dot{\phi}^2 - \frac{1}{2} m_\phi^2 \phi^2 = -\frac{1}{2} m_\phi^2 \mathcal{A}^2 \cos(2\alpha) - \mathcal{A}\dot{\mathcal{A}} m_\phi \sin(2\alpha) + \dot{\mathcal{A}}^2 \cos^2(\alpha)$$

$$\langle p_\phi \rangle = \langle \dot{\mathcal{A}}^2 \cos^2(\alpha) \rangle = \frac{1}{2}\dot{\mathcal{A}}^2$$

$$w = \langle p \rangle / \langle \rho \rangle \simeq 0$$

The oscillating field behaves like matter

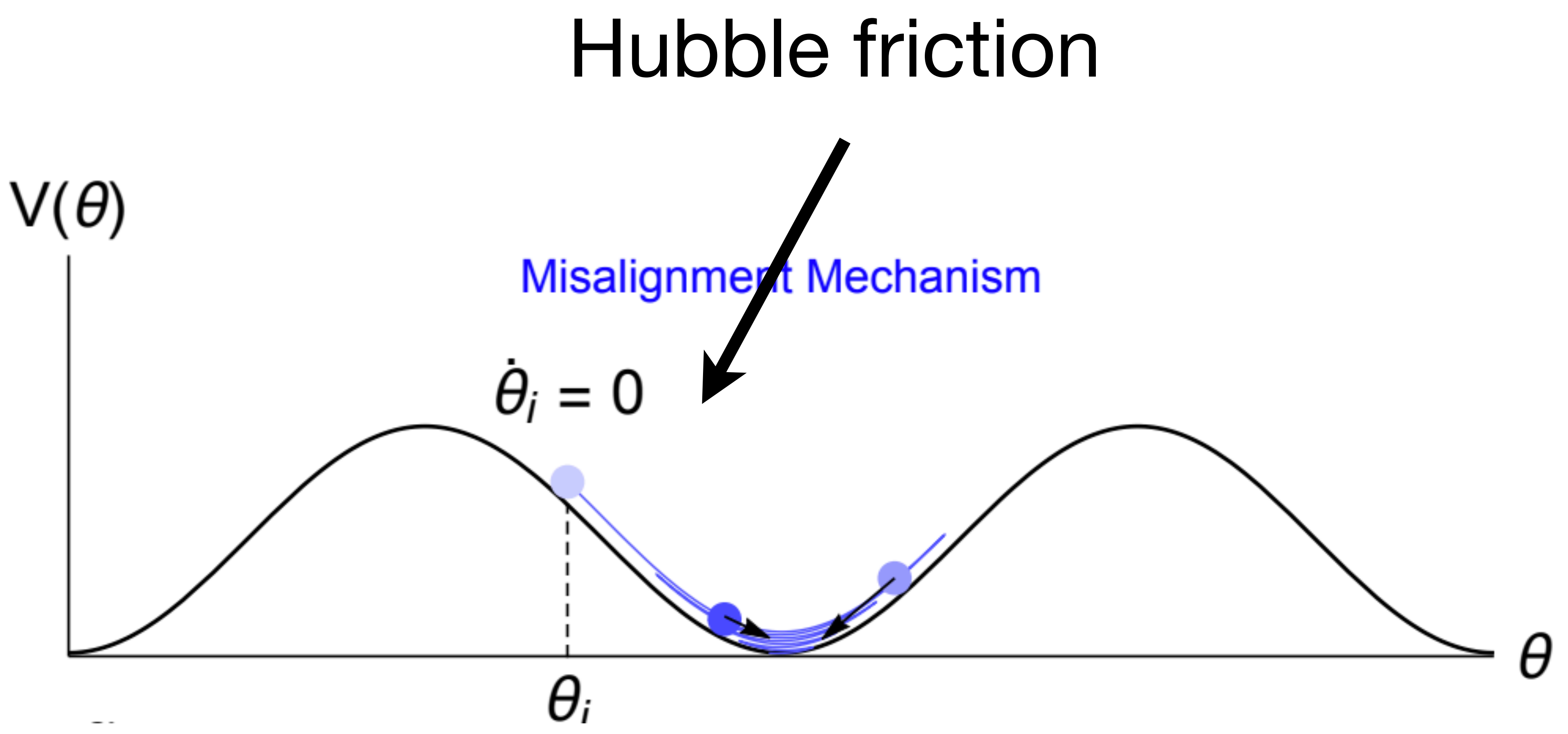

$H \gg m_\phi$, the field is frozen

$H \ll m_\phi$, the field oscillates

The Misalignment Mechanism

$$H \ll m_\phi \quad \phi \simeq \phi_1 \left(\frac{m_1 a_1^3}{m_\phi a^3}\right)^{1/2} \cos\left(\int_{t_1}^{t} m_\phi \, dt\right)$$

$$\mathcal{A}(t) \;=\; \phi_1 (m_1 a_1^3 / m_\phi a^3)^{1/2}$$

$$\rho_\phi = \frac{1}{2}\dot{\phi}^2 + \frac{1}{2} m_\phi^2 \phi^2 = \frac{1}{2} m_\phi^2 \mathcal{A}^2 + \ldots$$

$$N = \rho a^3 / m_\phi = \frac{1}{2} m_1 a_1^3 \phi_1^2$$

$$\rho_\phi(t_0) = m_0 \frac{N}{a_0^3} \simeq \frac{1}{2} m_0 m_1 \phi_1^2 \left(\frac{a_1}{a_0}\right)^3$$

The oscillating field behaves like matter

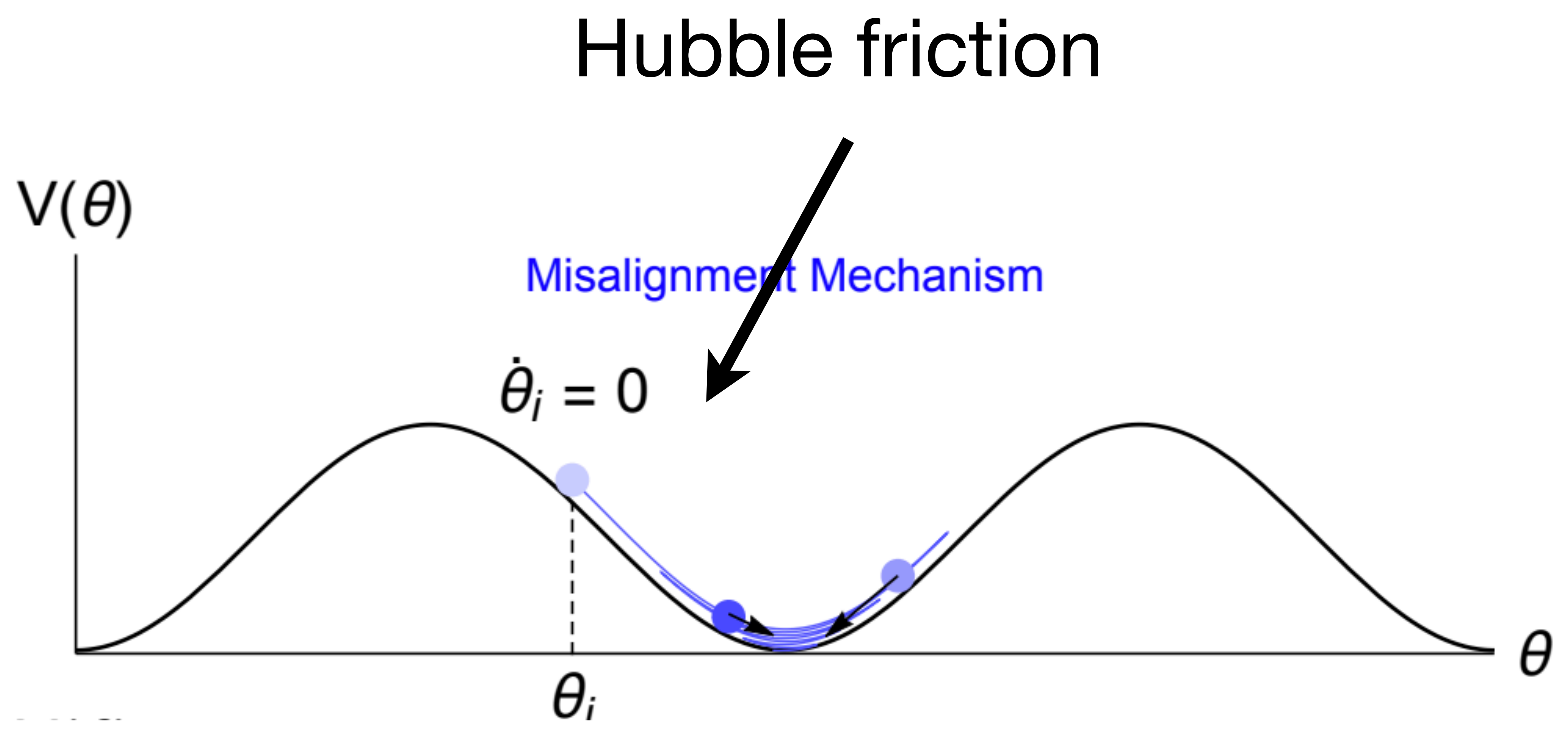

$H \gg m_\phi$, the field is frozen

$H \ll m_\phi$, the field oscillates

See e.g. Arias et al, arXiv: 1201.5902

The Axion Haloscope

Sikivie, 1983

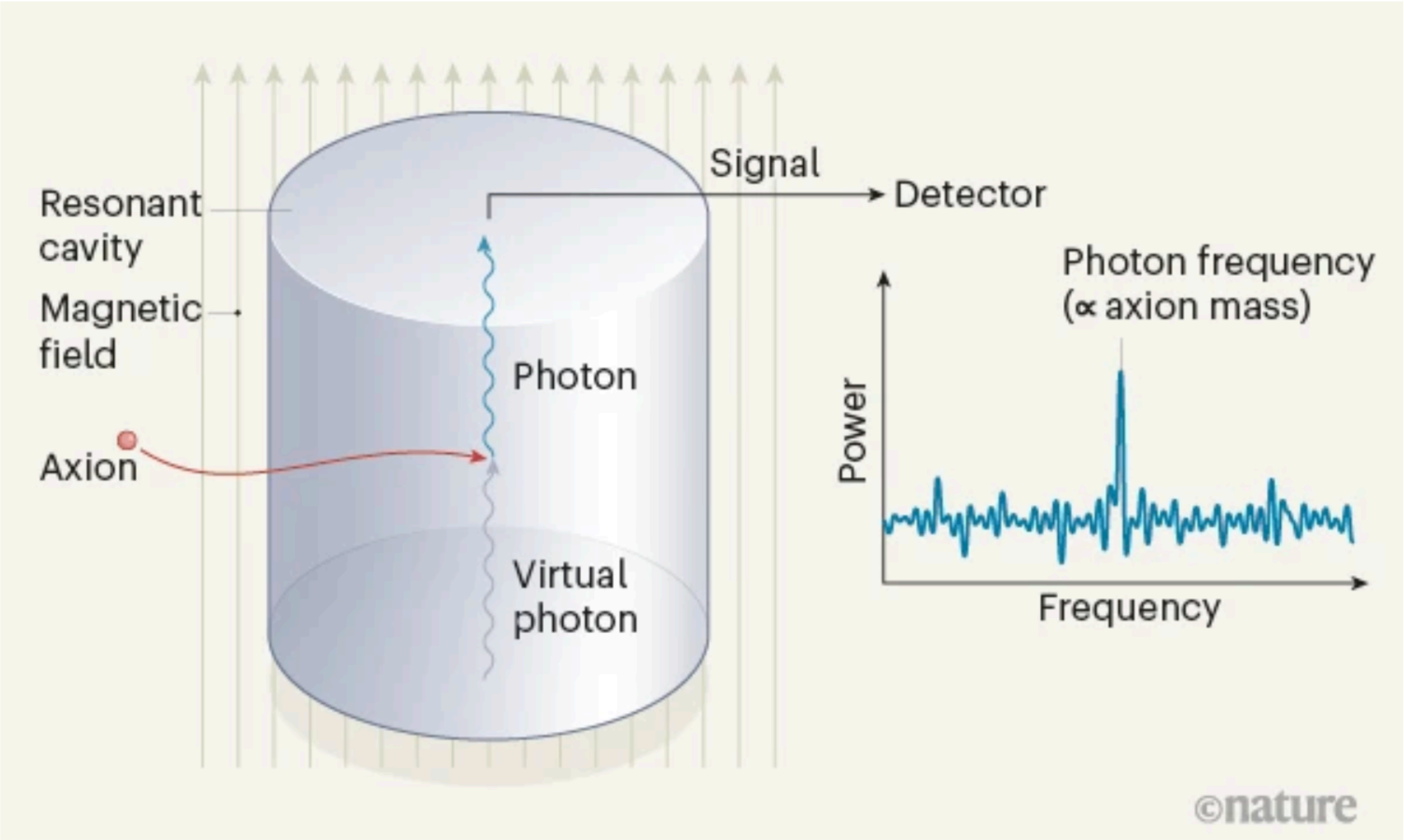

Irastorza, Nature, 2021

$$\mathcal{L} \supset \frac{g_{a\gamma}}{4}\, a\, F_{\mu\nu}\tilde{F}^{\mu\nu} \equiv g_{a\gamma}\, a\, \mathbf{E}\cdot\mathbf{B}$$

$$g_{a\gamma\gamma} a(t,x)\, \mathbf{B_0}\cdot\mathbf{E}$$

$$\ddot{\mathbf{E}} - \nabla^2\mathbf{E} = g_{a\gamma\gamma}\ddot{a}(t)\mathbf{B}_0$$

Axion could convert to photons in the cavity when applying strong magnetic field

The Axion Haloscope

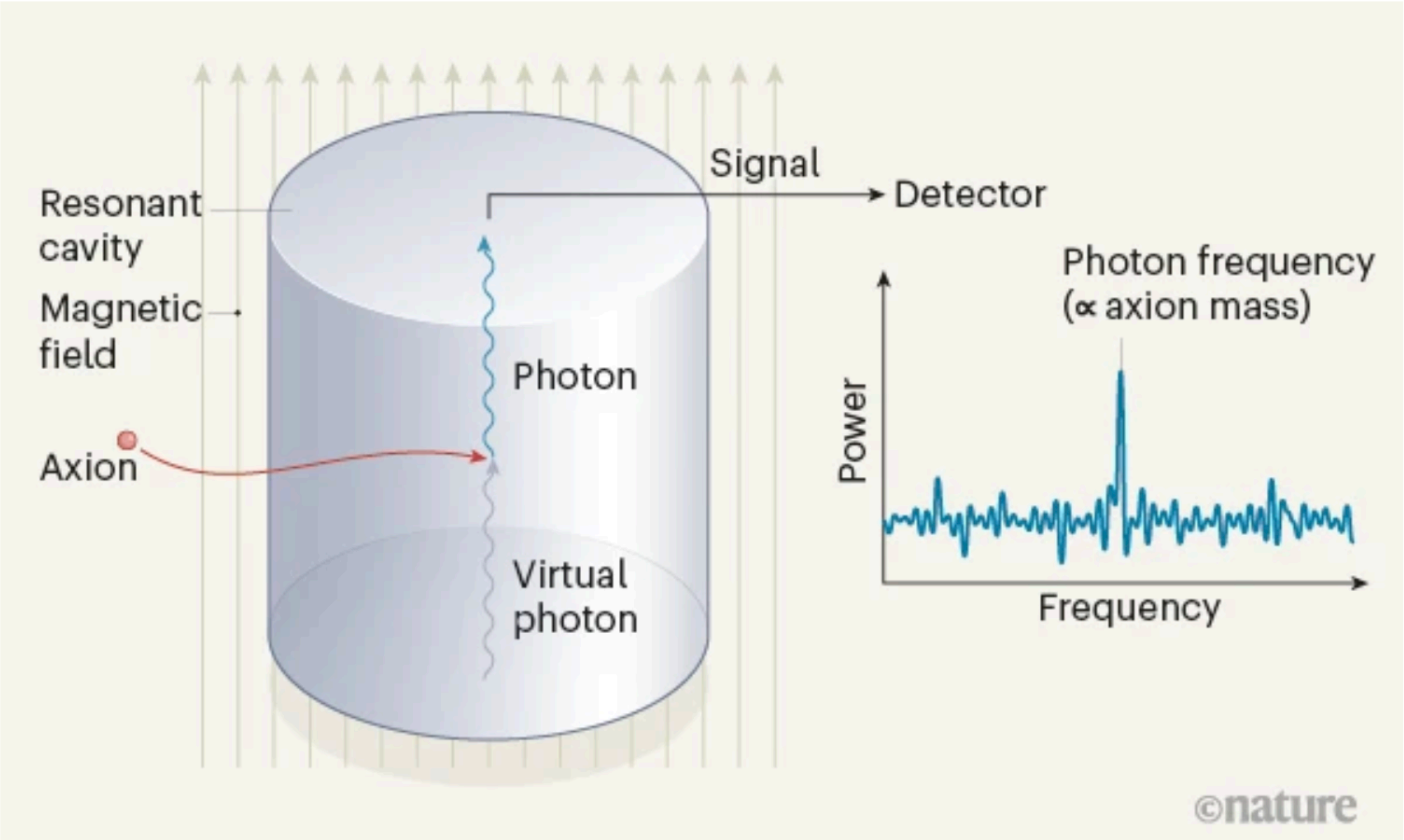

Irastorza, Nature, 2021

$$\mathcal{L} \supset \frac{g_{a\gamma}}{4}\, a\, F_{\mu\nu}\tilde{F}^{\mu\nu} \equiv g_{a\gamma}\, a\, \mathbf{E}\cdot\mathbf{B}$$

Sikivie, 1983

$$P_{\rm out} \sim g_{a\gamma}^2\, \rho_{\rm a}\, B_0^2\, V\, Q$$

Quality factor $\sim 10^5$

Axion could convert to photons in the cavity when applying strong magnetic field

Dark Matter Haloscopes

https://raw.githubusercontent.com/cajohare/AxionLimits

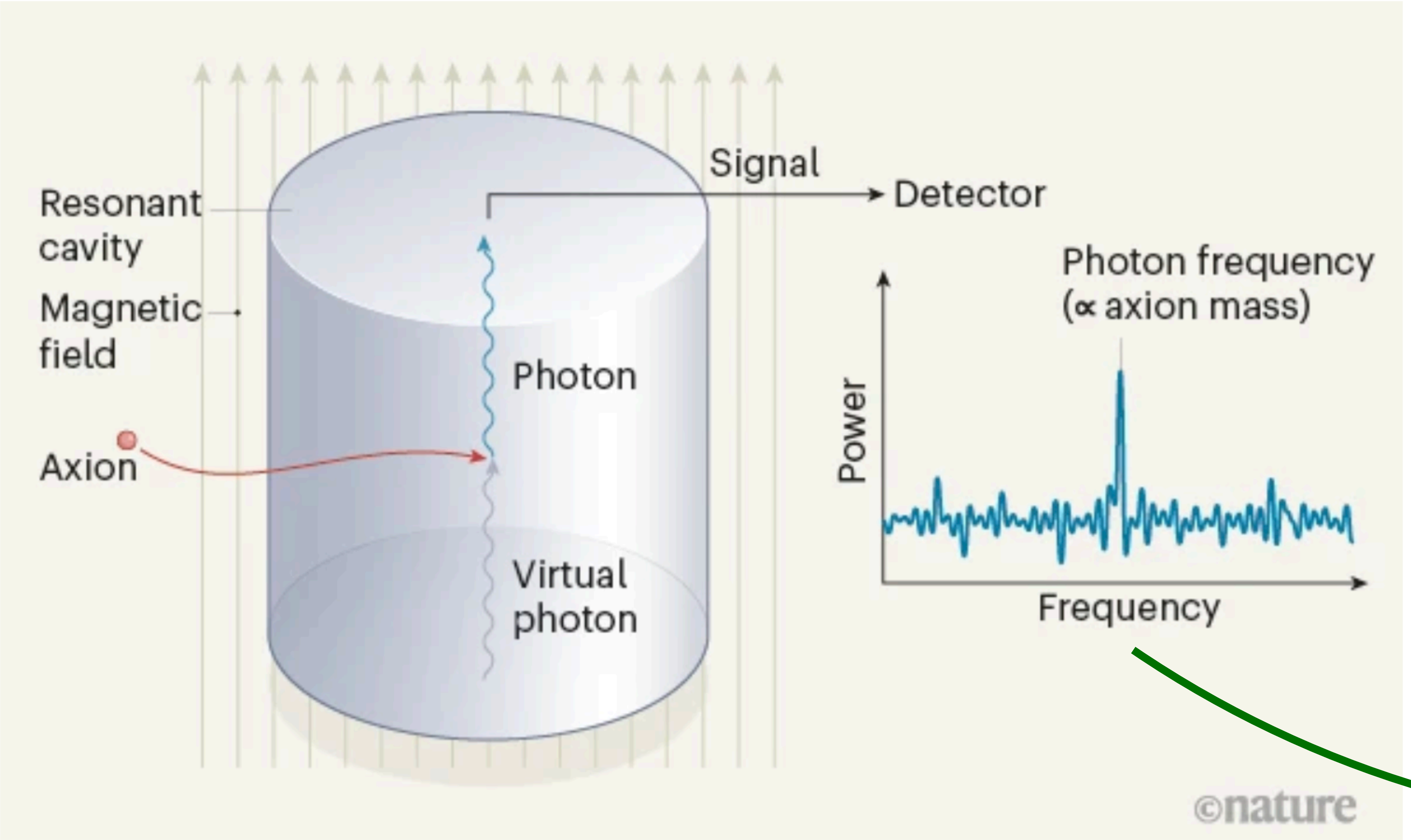

Irastorza, Nature 2021

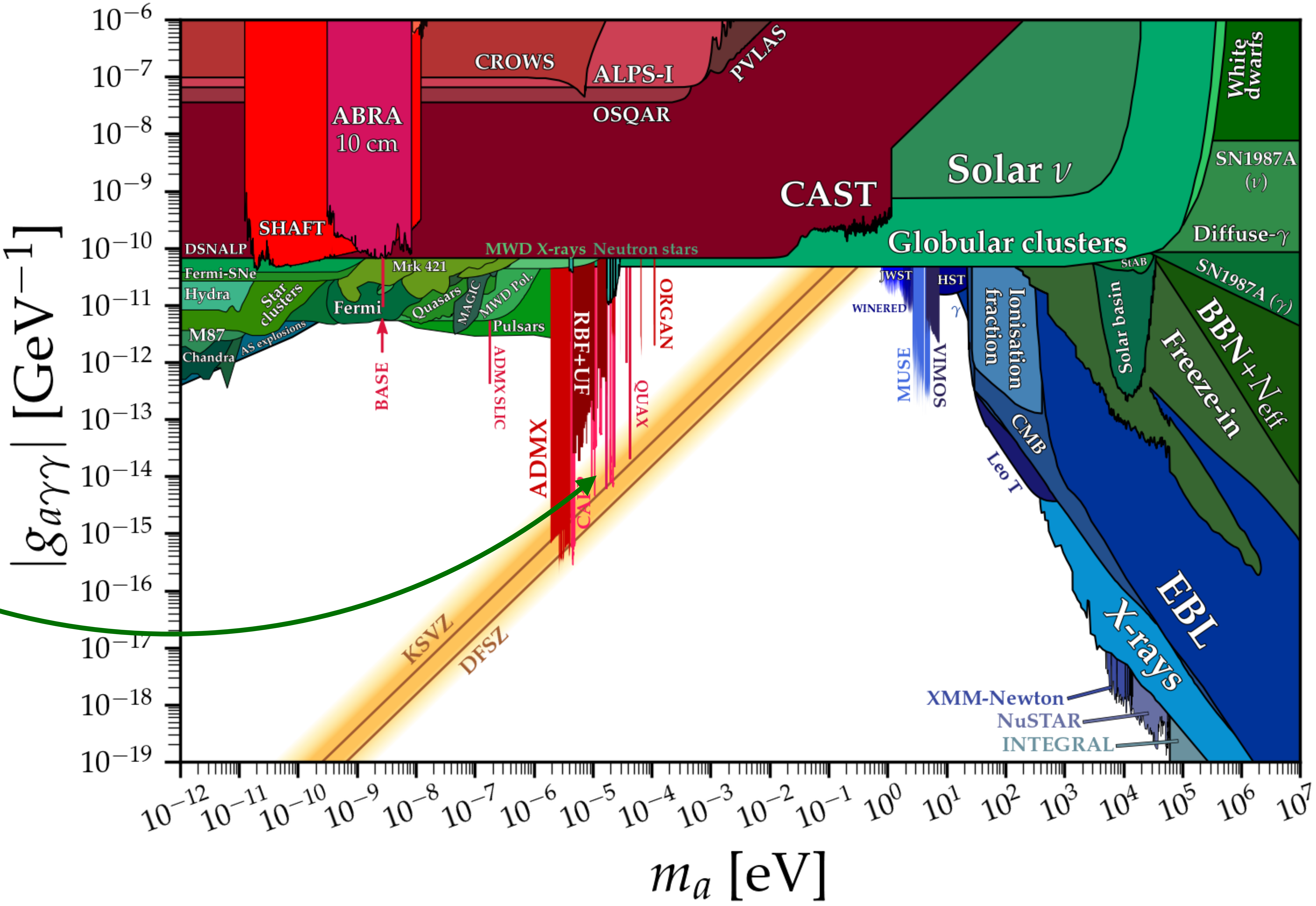

Future Dark Matter Haloscopes

https://raw.githubusercontent.com/cajohare/AxionLimits

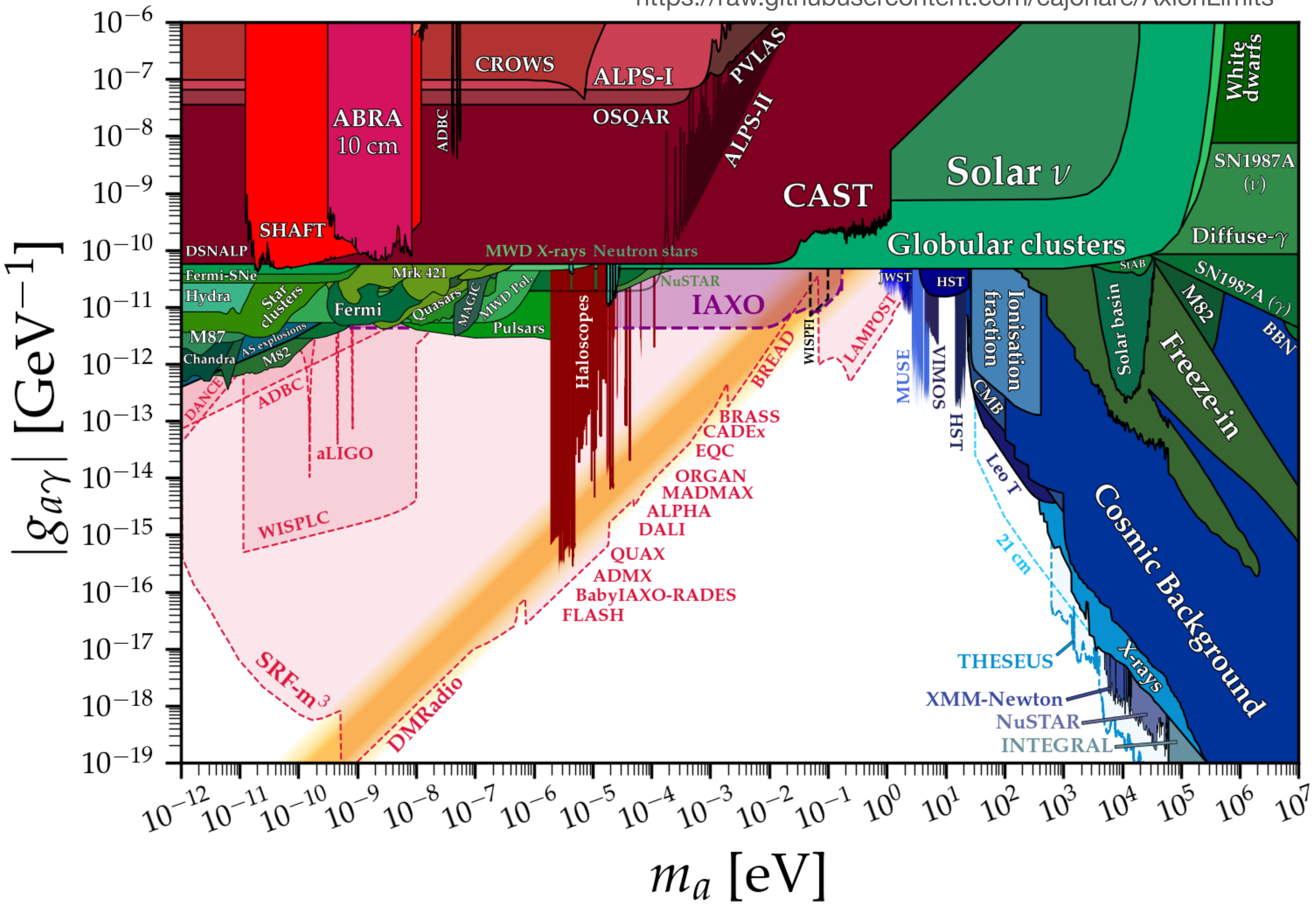

Indirect Detection

The Gamma Signal

detector area

$$\frac{dN_\gamma}{dEdtdV} = \left(\frac{dN_\gamma}{dE}\right)_0 \frac{A}{4\pi r^2} \times \begin{cases} \frac{1}{2}\langle\sigma v_{\mathrm{rel}}\rangle n(\vec{r})^2 & \text{annihilation} \\ \frac{n(\vec{r})}{\tau} & \text{decay} \end{cases}$$

dark matter properties

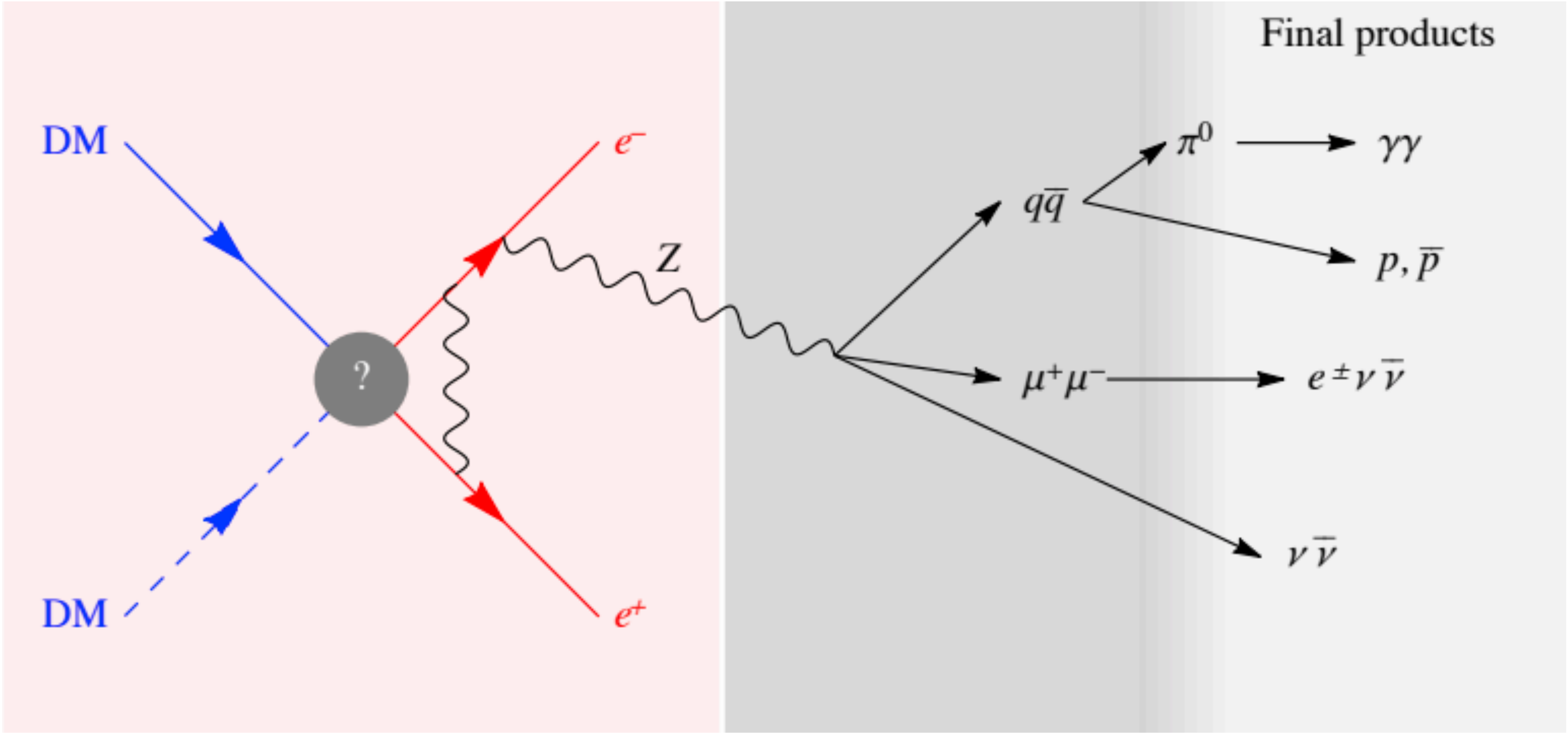

See e.g. Tracy Slatyer, arXiv: 1710.05137

The Gamma Signal

$$\frac{dN_\gamma}{dE\,dt\,d\Omega} = \frac{A}{4\pi}\left(\frac{dN_\gamma}{dE}\right)_0 \times \begin{cases} \frac{\langle \sigma v_{\rm rel}\rangle}{2m_{\rm DM}^2} \int_0^\infty \rho(\vec{r})^2 dr & \text{annihilation} \\ \frac{1}{m_{\rm DM}\tau} \int_0^\infty dr\,\rho(\vec{r}) & \text{decay} \end{cases}$$

Integrate along the line of sight

The Gamma Signal

$$\frac{dN_\gamma}{dEdt} = \frac{A}{4\pi}\left(\frac{dN_\gamma}{dE}\right)_0 \times \begin{cases} \frac{\langle\sigma v_{\rm rel}\rangle}{2m_{\rm DM}^2}\int dr d\Omega \rho(\vec{r})^2 & \text{annihilation} \\ \frac{1}{m_{\rm DM}\tau}\int_0^\infty dr d\Omega \rho(\vec{r}) & \text{decay} \end{cases}$$

Integrate over the solid angle

The Gamma Signal

$$\frac{1}{A}\frac{dN_\gamma}{dEdt} = \frac{\langle \sigma v_{\rm rel}\rangle}{m_{\rm DM}^2}\left(\frac{dN_\gamma}{dE}\right)_0 J_{\rm ann}$$

only particle physics

only dark matter distribution

$$J_{\rm ann} \equiv \frac{1}{8\pi}\int dr\, d\Omega\, \rho(\vec{r})^2,$$

Homework Exercise: J factor for the Milky Way

$$J_{\rm ann} \equiv \frac{1}{8\pi} \int dr d\Omega \rho(\vec{r})^2$$

Navarro-Frenk-White (NFW) $$\rho_{\rm NFW}(r) = \frac{\rho_0}{r/r_s(1+r/r_s)^2}$$

Einasto $$\rho_{\rm Ein}(r) = \rho_0 \exp\left[-\frac{2}{\gamma}\left(\left(\frac{r}{r_s}\right)^\gamma - 1\right)\right]$$

Burkert $$\rho_{\rm Burk}(r) = \frac{\rho_0}{(1+r/r_s)(1+(r/r_s)^2)}$$

$J \sim 10^{22}\ \mathrm{GeV^2/cm^5}$ within 1 degree of the galactic center using NFW

The Extragalactic Gamma Signal

physical volume

$$\frac{dN}{dE dV_0} = \int_\infty^0 dz \frac{dt}{dz} \frac{dN_\gamma(z)}{dE} \frac{\langle \sigma v_{\rm rel} \rangle}{2} n(z)^2 \frac{dV_z}{dV_0}$$

comoving volume

The Extragalactic Gamma Signal

$$\frac{dN}{dEdV_0} = \int_{\infty}^{0} dz \frac{dt}{dz} \frac{dN_\gamma(z)}{dE} \frac{\langle \sigma v_{\rm rel} \rangle}{2} n(z)^2 \frac{dV_z}{dV_0}$$

$$\frac{dN}{dEdV_0} = \int_0^\infty dz \frac{(1+z)^3}{H(z)} \rho(z=0)^2 \left[\left(\frac{dN_\gamma}{dE'} \right)_0 \Big|_{E'=E(1+z)} \frac{\langle \sigma v_{\rm rel} \rangle}{2 m_{\rm DM}^2} \right]$$

The Extragalactic Gamma Signal

$$\frac{dN}{dEdV_0} = \int_{\infty}^{0} dz \frac{dt}{dz} \frac{dN_\gamma(z)}{dE} \frac{\langle \sigma v_{\rm rel} \rangle}{2} n(z)^2 \frac{dV_z}{dV_0}$$

$$\frac{dN}{dEdV_0} = \int_0^\infty dz \frac{(1+z)^3}{H(z)} \rho(z=0)^2 \left[\left(\frac{dN_\gamma}{dE'} \right)_0 \Bigg|_{E'=E(1+z)} \frac{\langle \sigma v_{\rm rel} \rangle}{2m_{\rm DM}^2} \right]$$

$$\frac{dN_\gamma}{dEdAdt} = \int \frac{d\Omega}{4\pi} \int dz \left(\frac{dN_\gamma}{dE'} \right)_0 \Bigg|_{E'=E(1+z)} \frac{1}{H(z)(1+z)^3} \times \begin{cases} \frac{\langle \sigma v_{\rm rel} \rangle}{2m_{\rm DM}^2} \rho(z,\theta,\phi)^2 & \text{annihilation} \\ \frac{1}{m_{\rm DM}\tau} \rho(z,\theta,\phi) & \text{decay} \end{cases}$$

The Extragalactic Gamma Signal

More rigorously,

attenuation

$$\frac{d\Phi_{\rm EG\gamma}}{dE_\gamma}(E_\gamma) = c\frac{1}{E_\gamma}\int_0^\infty dz' \frac{1}{H(z')(1+z')^4}\, j_{\rm EG\gamma}(E'_\gamma, z')\; e^{-\tau(E_\gamma,z')}$$

$$j^{\rm prompt}_{\rm EG\gamma}(E'_\gamma, z') = E'_\gamma \begin{cases} \dfrac{1}{2}B(z')\left(\dfrac{\bar\rho(z')}{M_{\rm DM}}\right)^2 \sum_f \langle\sigma v\rangle_f \dfrac{dN^f_\gamma}{dE_\gamma}(E'_\gamma) & \text{(annihilation)} \\ \dfrac{\bar\rho(z')}{M_{\rm DM}} \sum_f \Gamma_f \dfrac{dN^f_\gamma}{dE_\gamma}(E'_\gamma) & \text{(decay)} \end{cases}$$

Clustering effect

$$B(z, M_{\rm min}) = 1 + \frac{\Delta_c}{3\bar\rho_{m,0}}\int_{M_{\rm min}}^\infty dM\, M\frac{dn}{dM}(M,z)\, f\left[c(M,z)\right]$$

Cirelli et al, arXiv: 1012.4515

The Extragalactic Gamma Signal

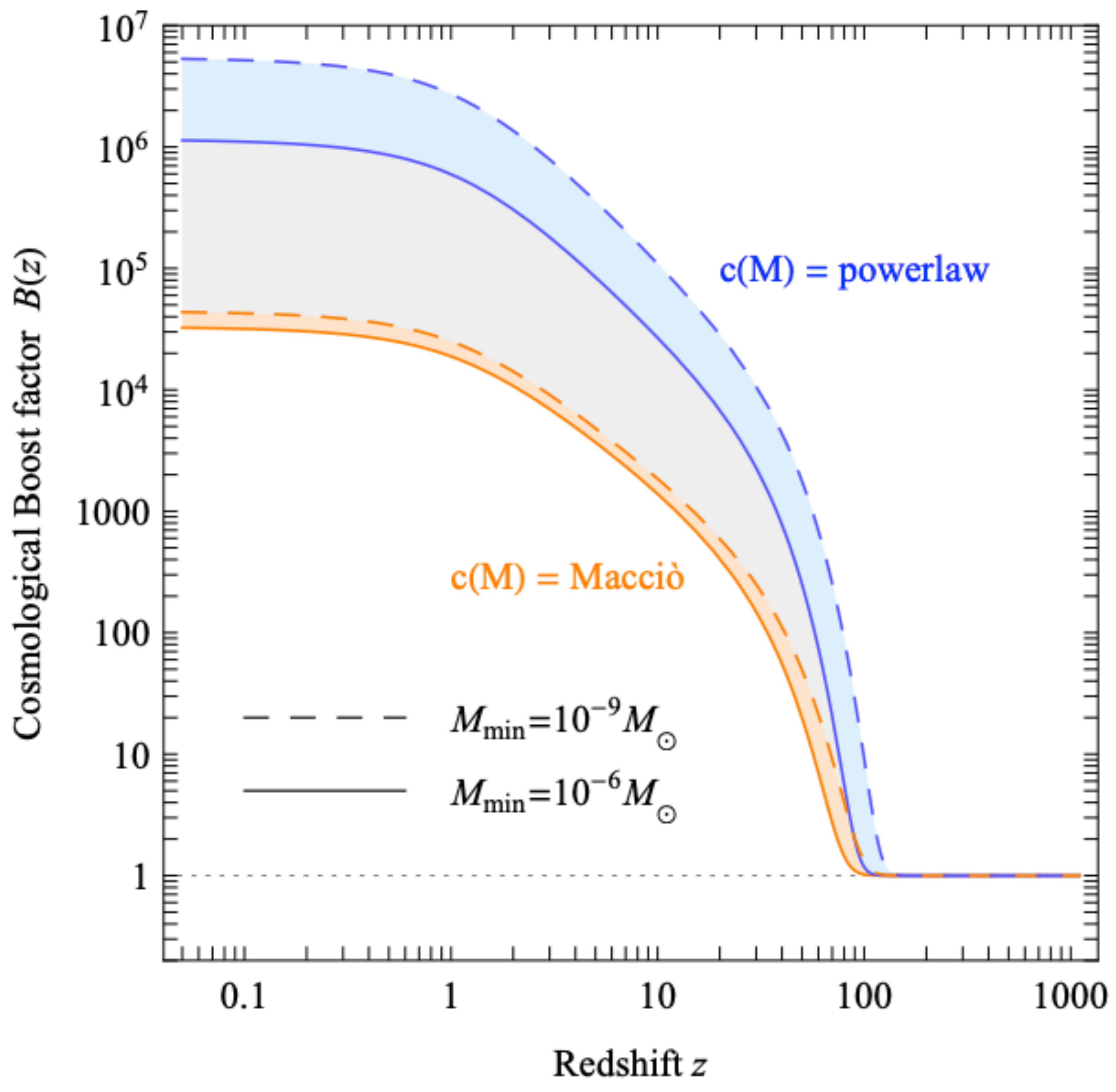

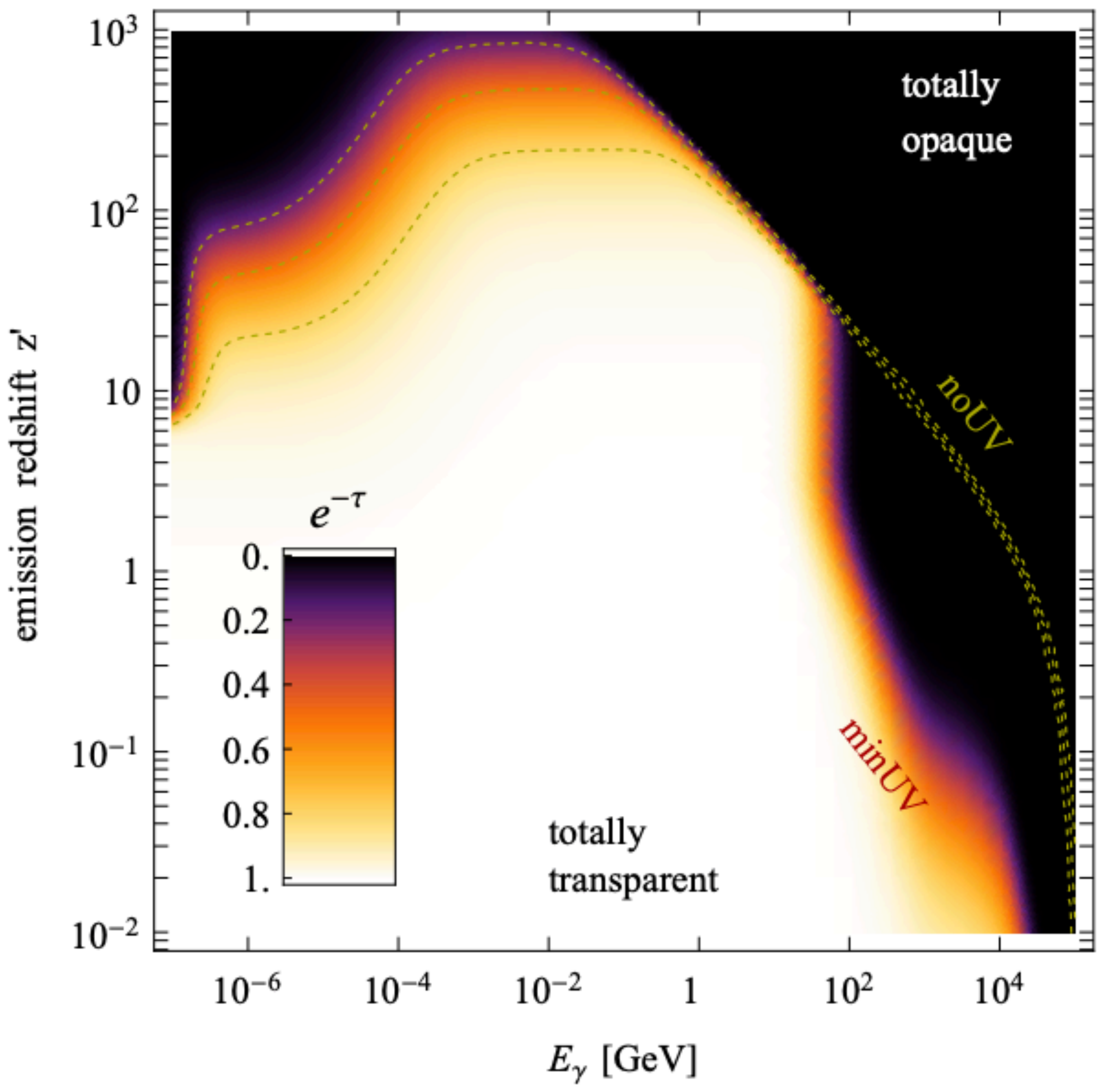

Cirelli et al, arXiv: 1012.4515

Primordial Black Hole Dark Matter

Primordial Black Hole Dark Matter

- Primordial perturbations reenter the horizon, if the overdensity is larger than the critical value, $\delta > \delta_c$, the overdense regions may collapse into black holes

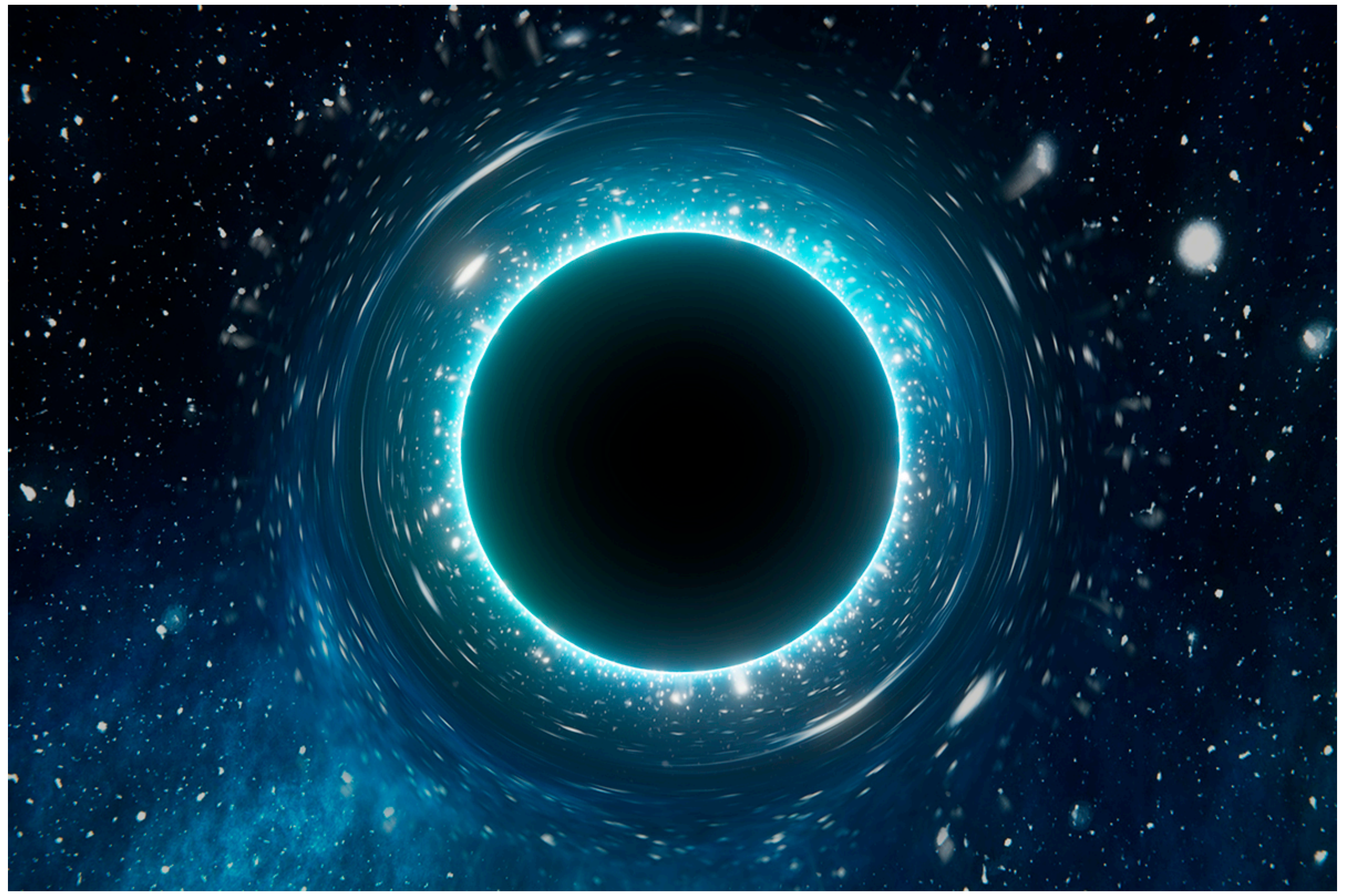

Primordial Black Hole Dark Matter

- Primordial perturbations reenter the horizon, if the overdensity is larger than the critical value, $\delta > \delta_c$, the overdense regions may collapse into black holes

$$M_{\mathrm{PBH}}(k) = \gamma \frac{4\pi}{3} \rho H^{-3} \Big|_{k=aH}$$

$$M_{\mathrm{PBH}}(k) \sim 5 \times 10^{15} \mathrm{g} \left(\frac{g_{\star,0}}{g_{\star,i}} \right)^{\frac{1}{6}} \left(\frac{10^{15}\ \mathrm{Mpc}^{-1}}{k} \right)^2$$

Primordial Black Hole Dark Matter

- Primordial perturbations reenter the horizon, if the overdensity is larger than the critical value, $\delta > \delta_c$, the overdense regions may collapse into black holes

$$M_{\rm PBH}(k) \sim 5 \times 10^{15}{\rm g} \left(\frac{g_{\star,0}}{g_{\star,i}}\right)^{\frac{1}{6}} \left(\frac{10^{15}\ {\rm Mpc}^{-1}}{k}\right)^{2}$$

Initial BH fraction $\beta(M_{\rm PBH}) = \dfrac{\rho_{{\rm PBH},i}}{\rho_{{\rm total},i}}$

$$\beta(M_{\rm PBH}) = \frac{\Omega_{\rm PBH,0}(M_{\rm PBH})}{\Omega_{r,0}^{\frac{3}{4}}\ \gamma^{\frac{1}{2}}} \left(\frac{g_{\star,i}}{g_{\star,0}}\right)^{\frac{1}{4}} \left(\frac{M_{\rm PBH}}{M_{H0}}\right)^{\frac{1}{2}}$$

$$f_{\rm PBH} = \frac{\beta(M_{\rm PBH})\Omega_{r,0}^{\frac{3}{4}}\gamma^{\frac{1}{2}}}{\Omega_{\rm CDM,0}} \left(\frac{g_{\star,i}}{g_{\star,0}}\right)^{-\frac{1}{4}} \left(\frac{M_{\rm PBH}}{M_{H0}}\right)^{-\frac{1}{2}}$$

Primordial Black Hole Dark Matter

- Primordial perturbations reenter the horizon, if the overdensity is larger than the critical value, $\delta > \delta_c$, the overdense regions may collapse into black holes

$$M_{\rm PBH}(k) \sim 5 \times 10^{15}{\rm g} \left(\frac{g_{\star,0}}{g_{\star,i}}\right)^{\frac{1}{6}} \left(\frac{10^{15}\ {\rm Mpc}^{-1}}{k}\right)^2$$

Initial BH fraction $$\beta(M_{\rm PBH}) = \frac{\rho_{{\rm PBH},i}}{\rho_{{\rm total},i}}$$

$$\beta(M_{\rm PBH}) = {\rm Erfc}\left(\frac{\delta_c}{\sqrt{2}\sigma(R)}\right)$$

$$\sigma^2(R) = \int \tilde{W}^2(kR)\mathcal{P}_\delta(k)\frac{dk}{k}$$

$$\mathcal{P}_\delta(k) = 4\left(\frac{1+w}{5+3w}\right)^2 \mathcal{P}_\mathcal{R}(k)$$

Primordial Black Hole Dark Matter

- Primordial perturbations reenter the horizon, if the overdensity is larger than the critical value, $\delta > \delta_c$, the overdense regions may collapse into black holes

$$M_{\rm PBH}(k) \sim 5\times 10^{15}{\rm g}\left(\frac{g_{\star,0}}{g_{\star,i}}\right)^{\frac{1}{6}}\left(\frac{10^{15}\ {\rm Mpc}^{-1}}{k}\right)^{2}$$

Initial BH fraction $\beta(M_{\rm PBH}) = \frac{\rho_{{\rm PBH},i}}{\rho_{{\rm total},i}}$

$$\beta(M_{\rm PBH}) = {\rm Erfc}\left(\frac{\delta_c}{\sqrt{2}\sigma(R)}\right)$$

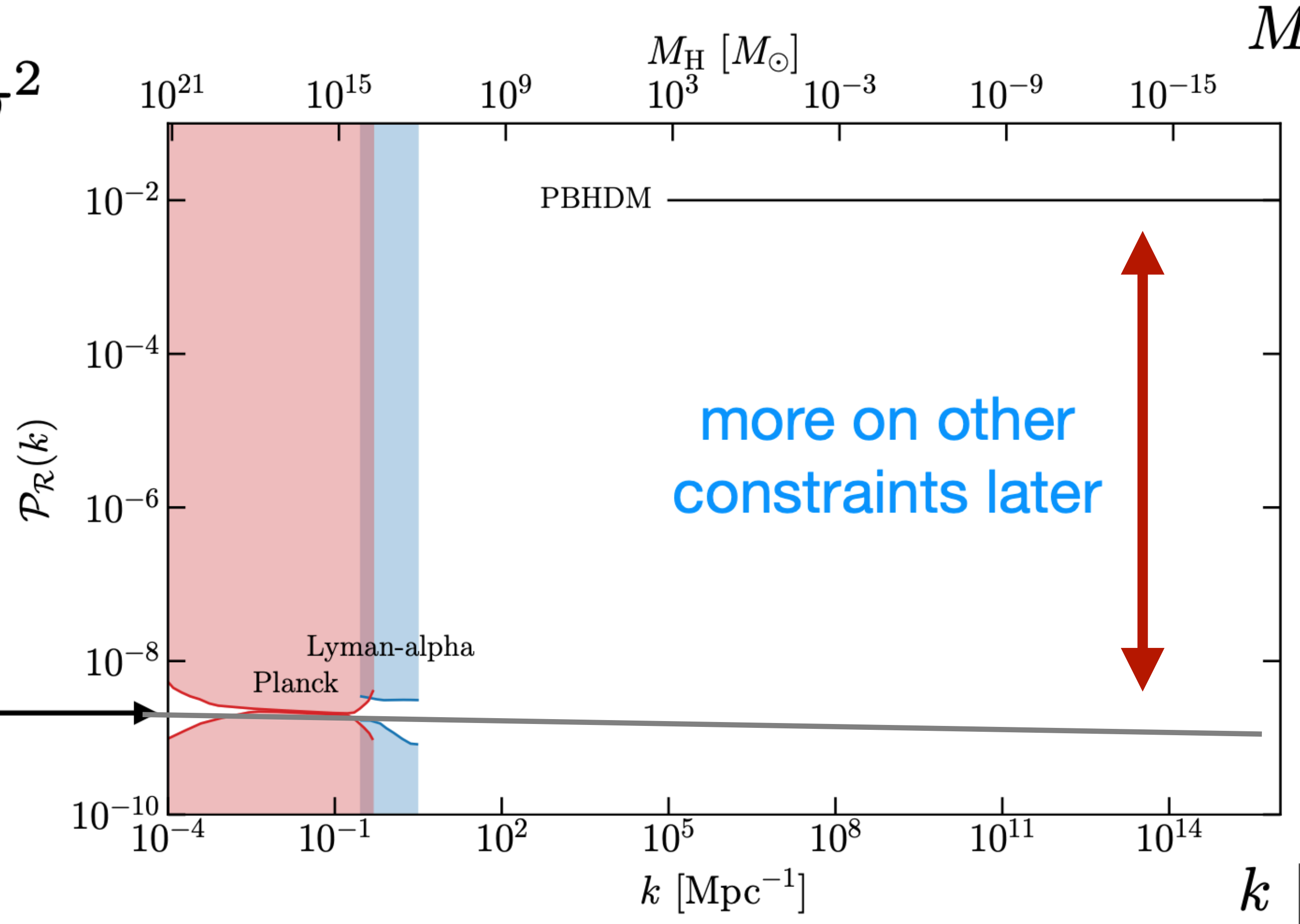

At $k \sim 0.05\ {\rm Mpc}^{-1}$, $P_R \sim 2.1\times 10^{-9}$, much less than the requirement $\mathcal{O}(10^{-2})$, curvature perturbation needed!

See e.g. arXiv:2208.14279

Constraints on PBH Dark Matter

Carr, Kohri, Sendouda, Yokoyama, arXiv:2002.12778

Galactic Gamma Ray

$$\frac{d\Phi_\gamma}{dEd\Omega} = \frac{1}{4\pi}\frac{dN}{dEdt}\frac{f_{\bullet,0}}{M}\frac{1}{\Delta\Omega}\mathcal{D}(\Omega),$$

$$\mathcal{D}(\Omega) \equiv \int_{\text{l.o.s.}\Delta\Omega} \rho_{DM}(\vec{x})d\Omega dx,$$

$$\frac{d\Phi_{511}}{d\Omega} = 2(1-0.75 f_P)\frac{dN_{e^+}}{dt}\frac{1}{4\pi}\frac{1}{M}\frac{1}{\Delta\Omega}\mathcal{D}(\Omega)$$

fraction of positronium

25% annihilation to 2 gamma,
75% to 3 gamma

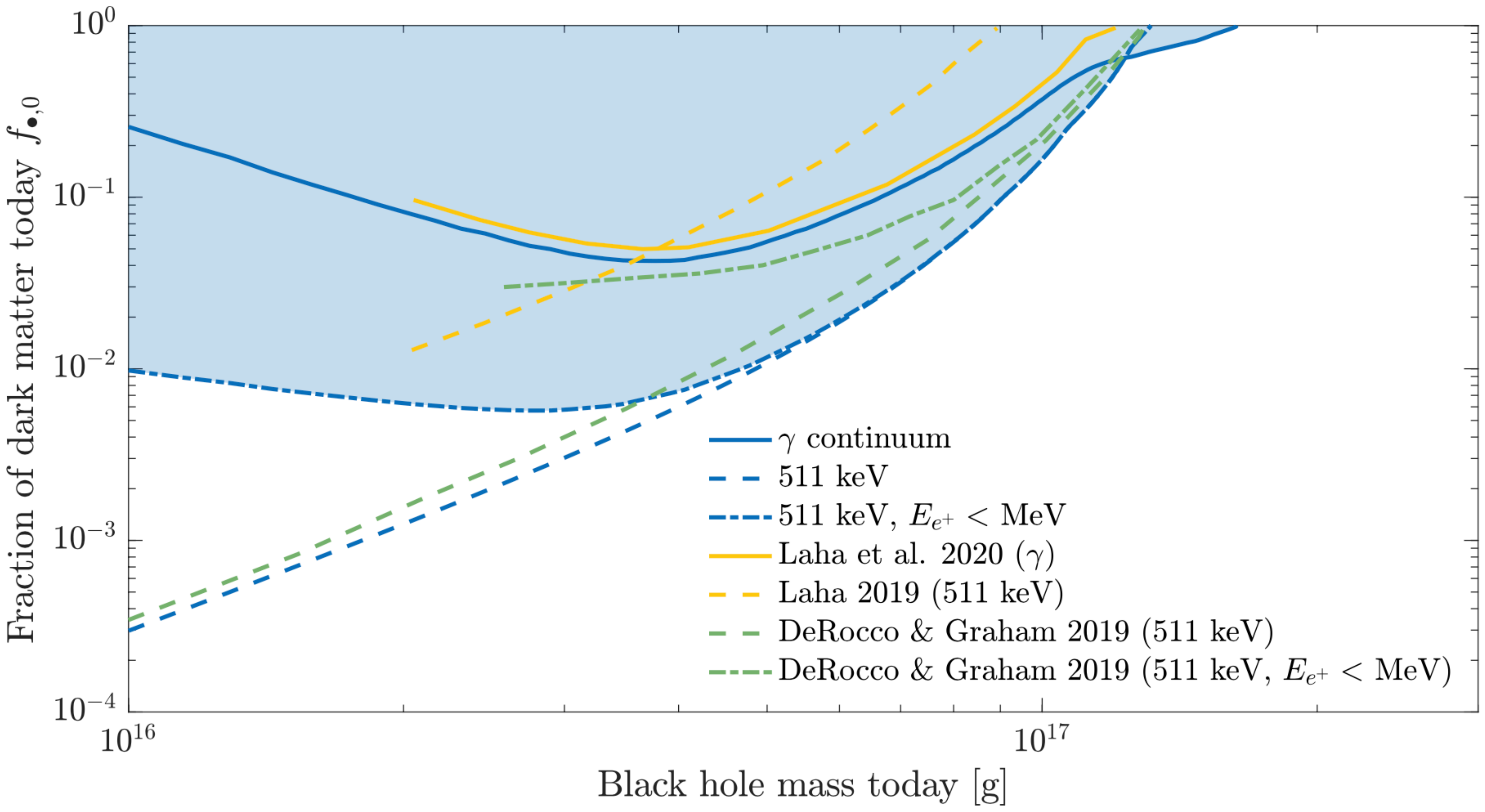

Friedlander, Mack, **NS**, Schon, Vincent, PRD/2201.11761

Isotropic Gamma Ray Background

direct evaporation

positron annihilation

$$\frac{d^2N_\gamma}{dEdt}(E,M) = \frac{d^2N_{\gamma,\mathrm{evap}}}{dEdt}(E,M) + \frac{d^2N_{\gamma,\mathrm{pos}}}{dEdt}(E,M) + \frac{d^2N_{\gamma,\mathrm{ics}}}{dEdt}(E,M).$$

Inverse Compton scattering

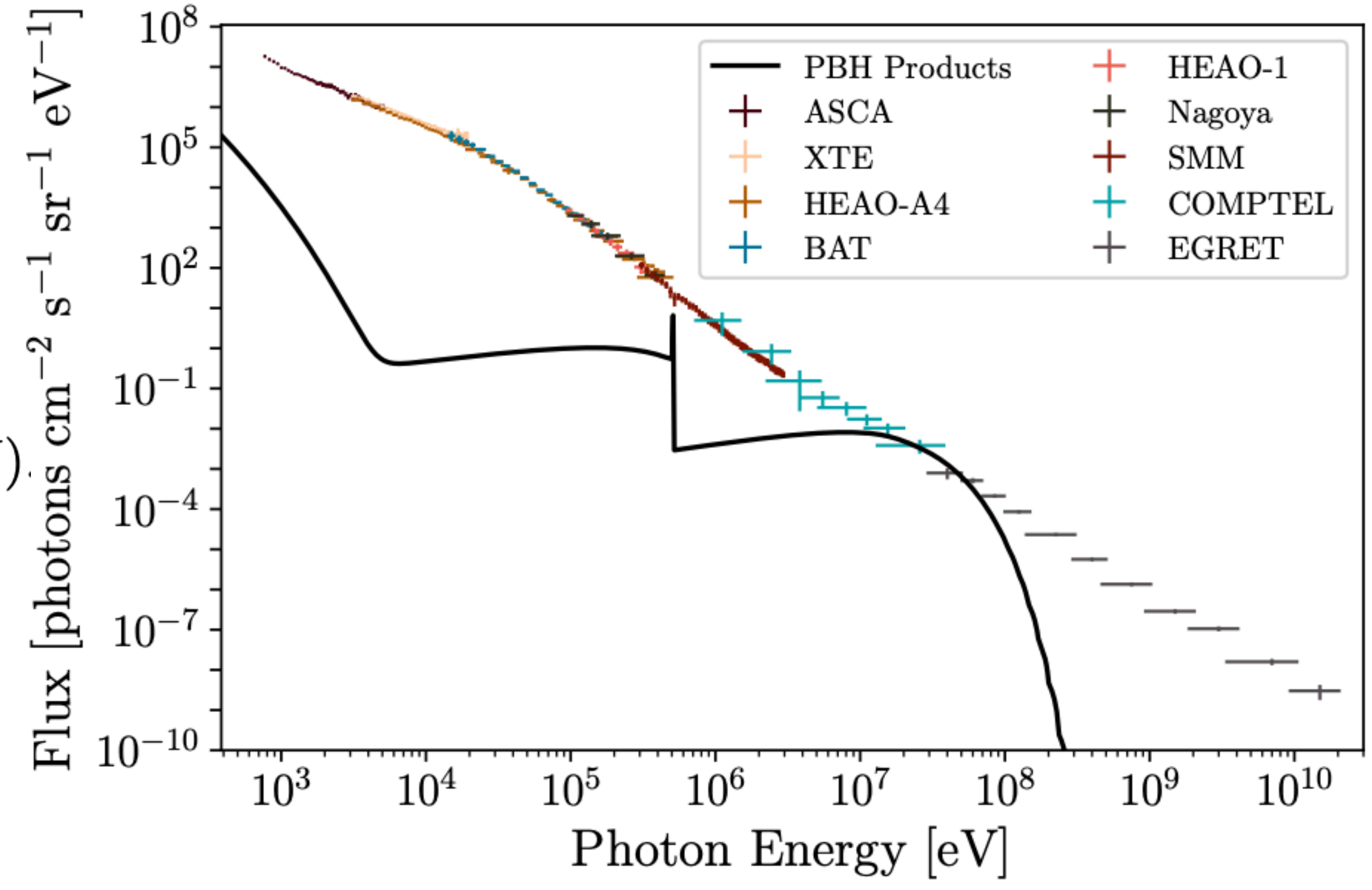

A Snapshot of 4D BH Constraints

CosmoLED
https://github.com/songningqiang/CosmoLED

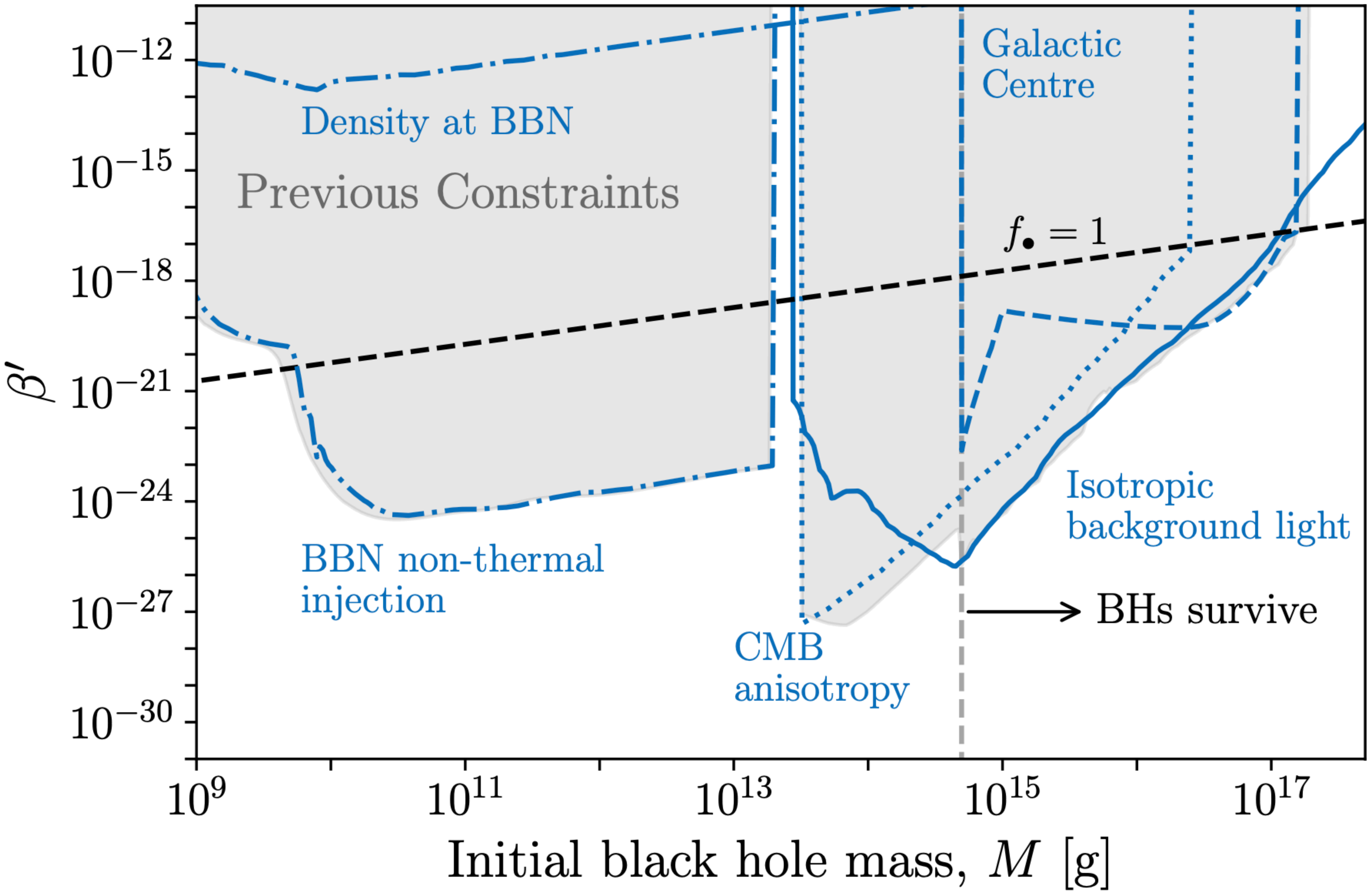

Axion-photon Conversion

Axion-photon Conversion

- CP conserved in QCD ⇒ axion
- $\mathcal{L}_{a\gamma\gamma} = \frac{1}{4} g_{a\gamma\gamma} a F_{\mu\nu} \tilde{F}^{\mu\nu}$
- Resonant conversion from axion to photon in plasma when $m_a \sim \omega_p$

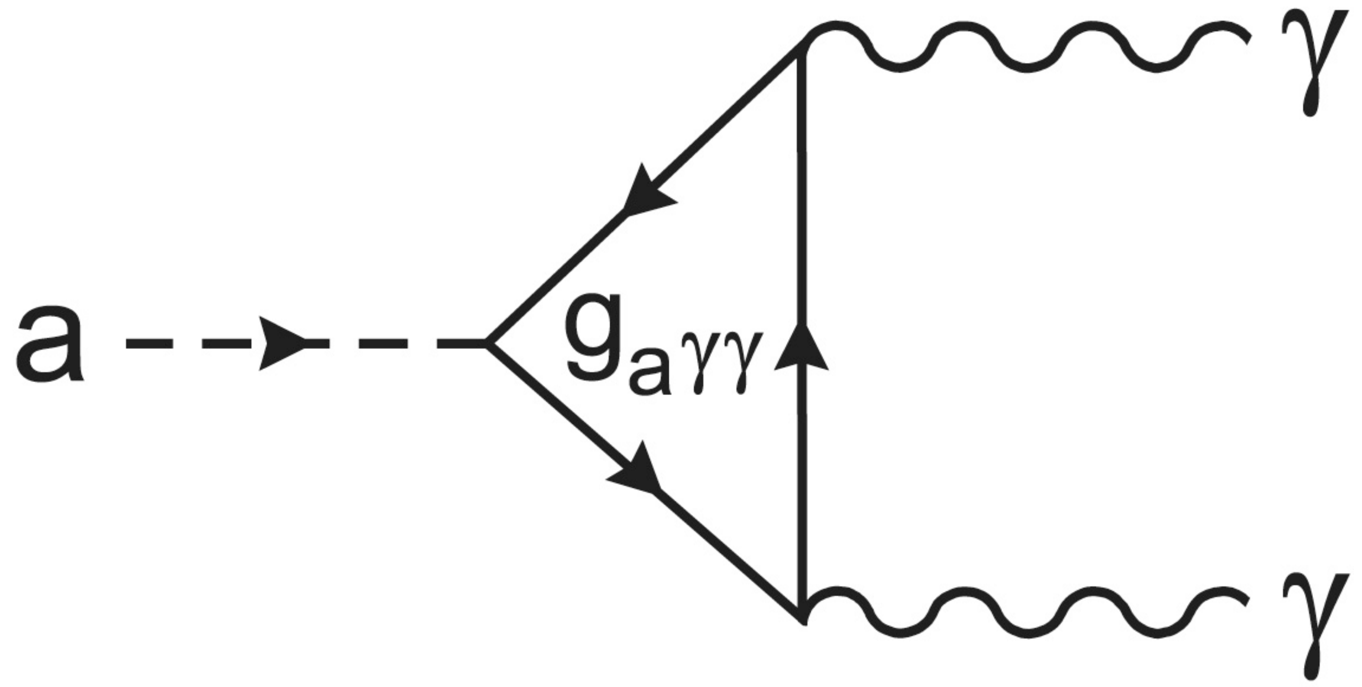

$\omega^2 = k^2 + m_a^2$

$\omega^2 \sim k^2 + \omega_p^2$

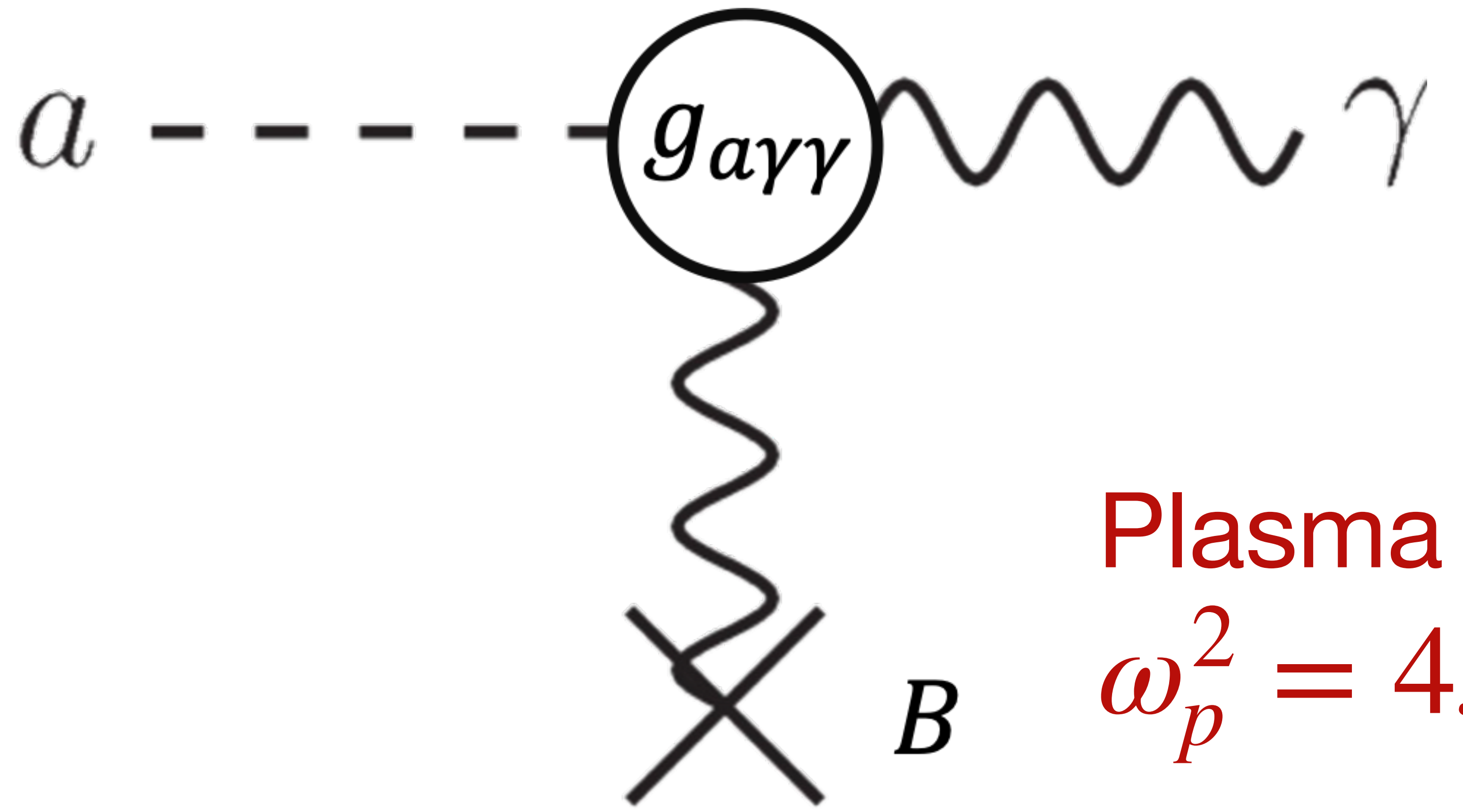

Plasma frequency
$\omega_p^2 = 4\pi\alpha n_e / m_e$

Axion Conversion in Neutron Star

- Magnetized neutron star atmosphere—magnetosphere

$$n_{\rm GJ}(\mathbf{r}_{\rm NS}) = \frac{2\mathbf{\Omega}\cdot\mathbf{B}_{\rm NS}}{e}\frac{1}{1-\Omega^2 r^2 \sin^2\theta_{\rm NS}}$$

$$B_z = \frac{B_0}{2}\left(\frac{r_0}{r}\right)^3\left[3\cos\theta\,\hat{\mathbf{m}}\cdot\hat{\mathbf{r}} - \cos\theta_m\right]$$

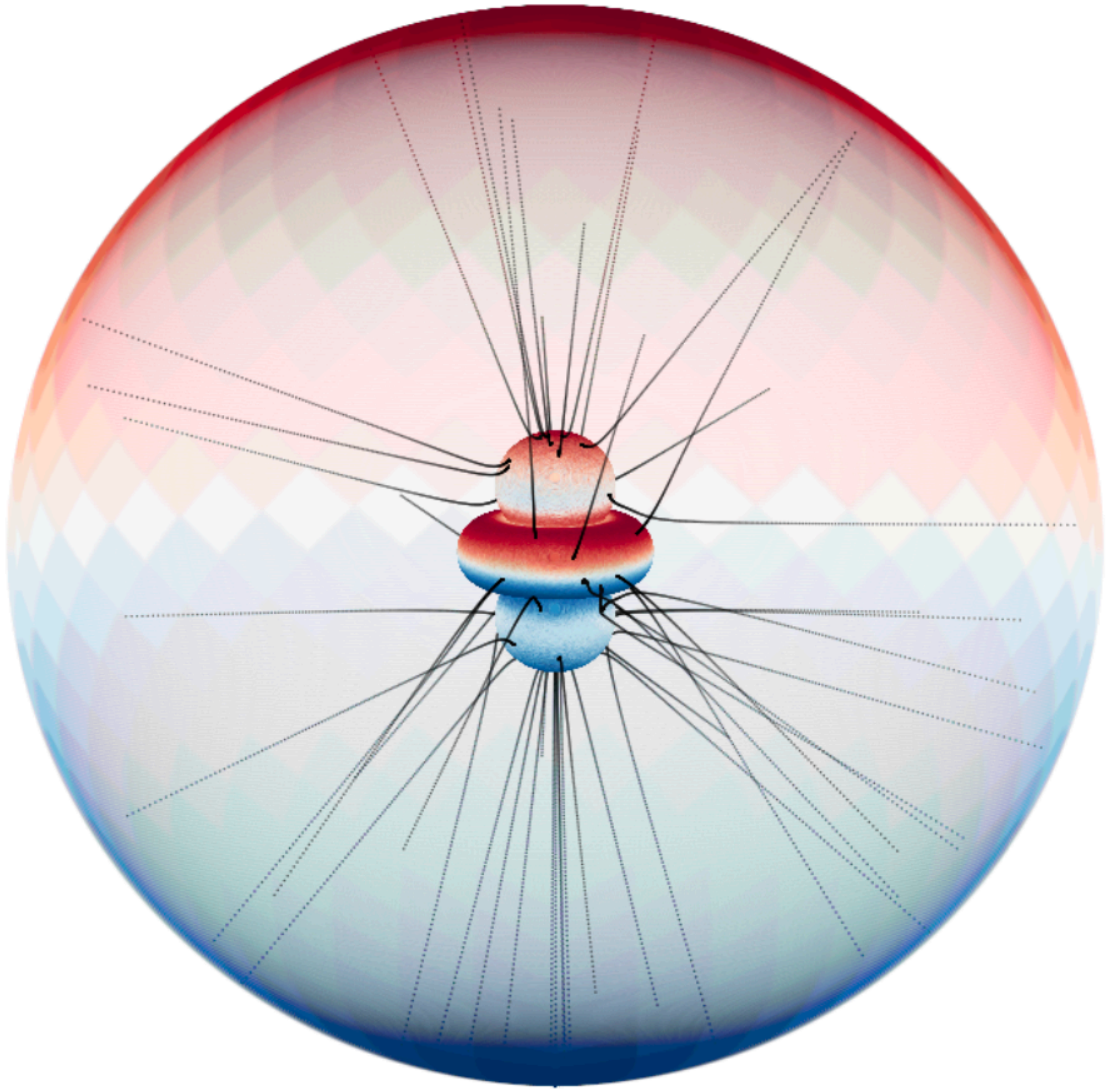

Witte et al 2104.07670

Homework Exercise: Axion Conversion in Neutron Star

$$n_{\rm GJ}(\mathbf{r}_{\rm NS}) = \frac{2\mathbf{\Omega}\cdot\mathbf{B}_{\rm NS}}{e}\frac{1}{1-\Omega^2 r^2\sin^2\theta_{\rm NS}}$$

$$-\partial_t^2 a + \nabla^2 a = m_a^2 a - g_{a\gamma\gamma}\mathbf{E}\cdot\mathbf{B},$$
$$-\nabla^2\mathbf{E} + \nabla(\nabla\cdot\mathbf{E}) = \omega^2\mathbf{D} + \omega^2 g_{a\gamma\gamma} a\mathbf{B},$$

$$B_z = \frac{B_0}{2}\left(\frac{r_0}{r}\right)^3\left[3\cos\theta\,\hat{\mathbf{m}}\cdot\hat{\mathbf{r}} - \cos\theta_m\right]$$

$$\left[-i\frac{d}{dr} + \frac{1}{2k}\begin{pmatrix} m_a^2 - \xi\,\omega_p^2 & \Delta_B \\ \Delta_B & 0\end{pmatrix}\right]\begin{pmatrix}\tilde{A}_\parallel \\ \tilde{a}\end{pmatrix} = 0\,,$$

$$\mathbf{D} = R^{yz}_{\tilde\theta}\cdot\begin{pmatrix}\epsilon & ig & 0 \\ -ig & \epsilon & 0 \\ 0 & 0 & \eta\end{pmatrix}\cdot R^{yz}_{-\tilde\theta}\cdot\begin{pmatrix}E_x \\ E_y \\ E_z\end{pmatrix},$$

$$\xi = \frac{\sin^2\tilde\theta}{1-\frac{\omega_p^2}{\omega^2}\cos^2\tilde\theta}\,,\qquad \Delta_B = B g_{a\gamma\gamma} m_a\frac{\xi}{\sin\tilde\theta}\,,$$

$$-\partial_z^2\begin{pmatrix}E_y \\ a\end{pmatrix} = \begin{pmatrix}\frac{\omega^2-\omega_p^2}{1-\frac{\omega_p^2}{\omega^2}\cos^2\tilde\theta} & \frac{g_{a\gamma\gamma}B_t\omega^2}{1-\frac{\omega_p^2}{\omega^2}\cos^2\tilde\theta} \\ \frac{g_{a\gamma\gamma}B_t}{1-\frac{\omega_p^2}{\omega^2}\cos^2\tilde\theta} & \omega^2 - m_a^2\end{pmatrix}\cdot\begin{pmatrix}E_y \\ a\end{pmatrix},$$

$$p_{a\gamma}^\infty \approx \frac{1}{2v_c}\,g_{a\gamma\gamma}^2 B(r_c)^2 L^2$$

$$\rho_{\rm DM}^{r_c} = \rho_{\rm DM}^\infty\frac{2}{\sqrt{\pi}}\frac{1}{v_0}\sqrt{\frac{2GM_{\rm NS}}{r_c}} + \cdots.$$

$$\frac{d\mathcal{P}(\theta,\theta_m t)}{d\Omega} \approx 2\times p_{a\gamma}^\infty\,\rho_{\rm DM}^{r_c} v_c r_c^2\,,$$

Hook et al 1804.03145

Millar et al 2107.07399

Witte et al 2104.07670

Radio Observation Constraint

Radio flux limit from the galactic center

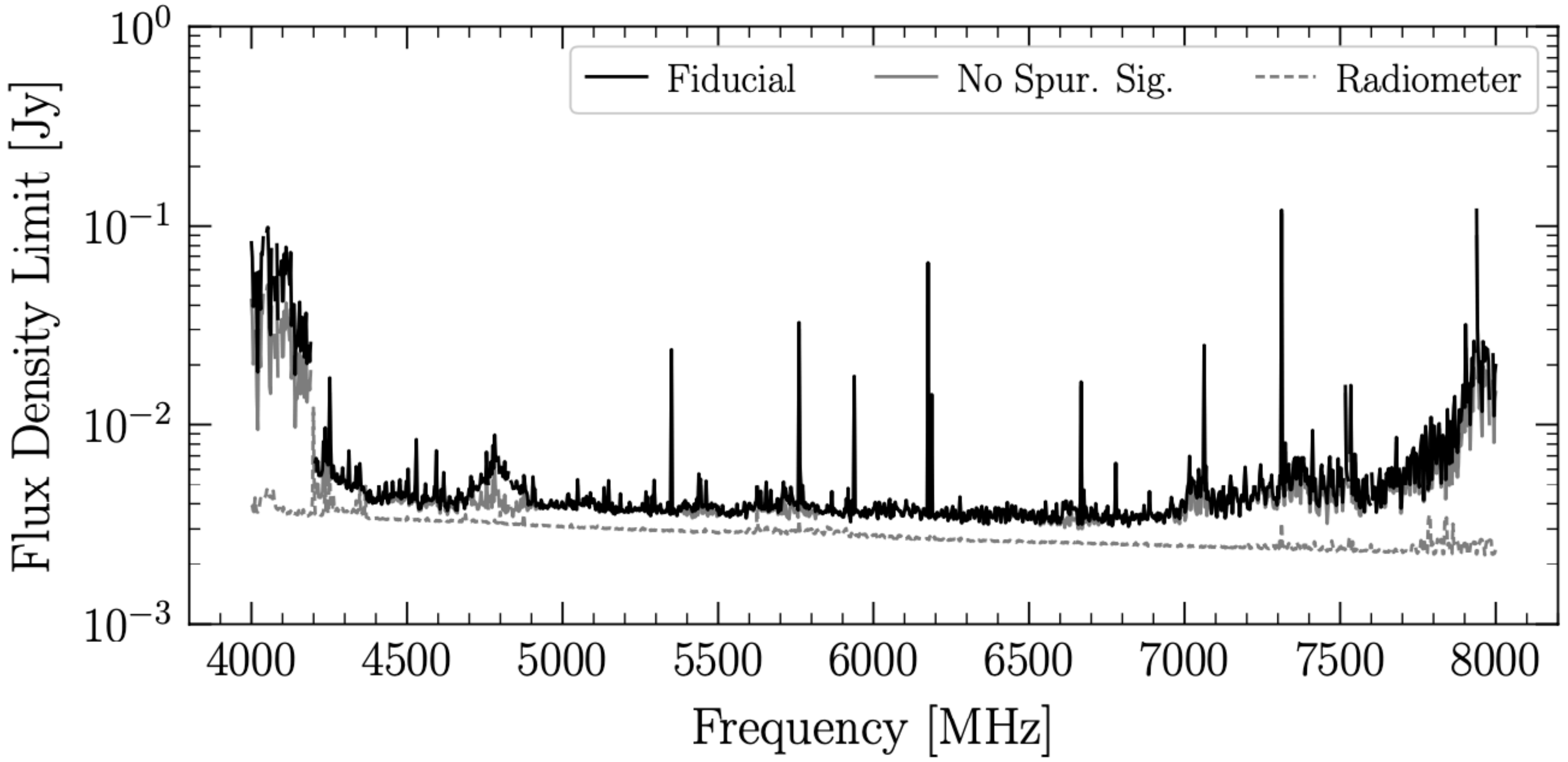

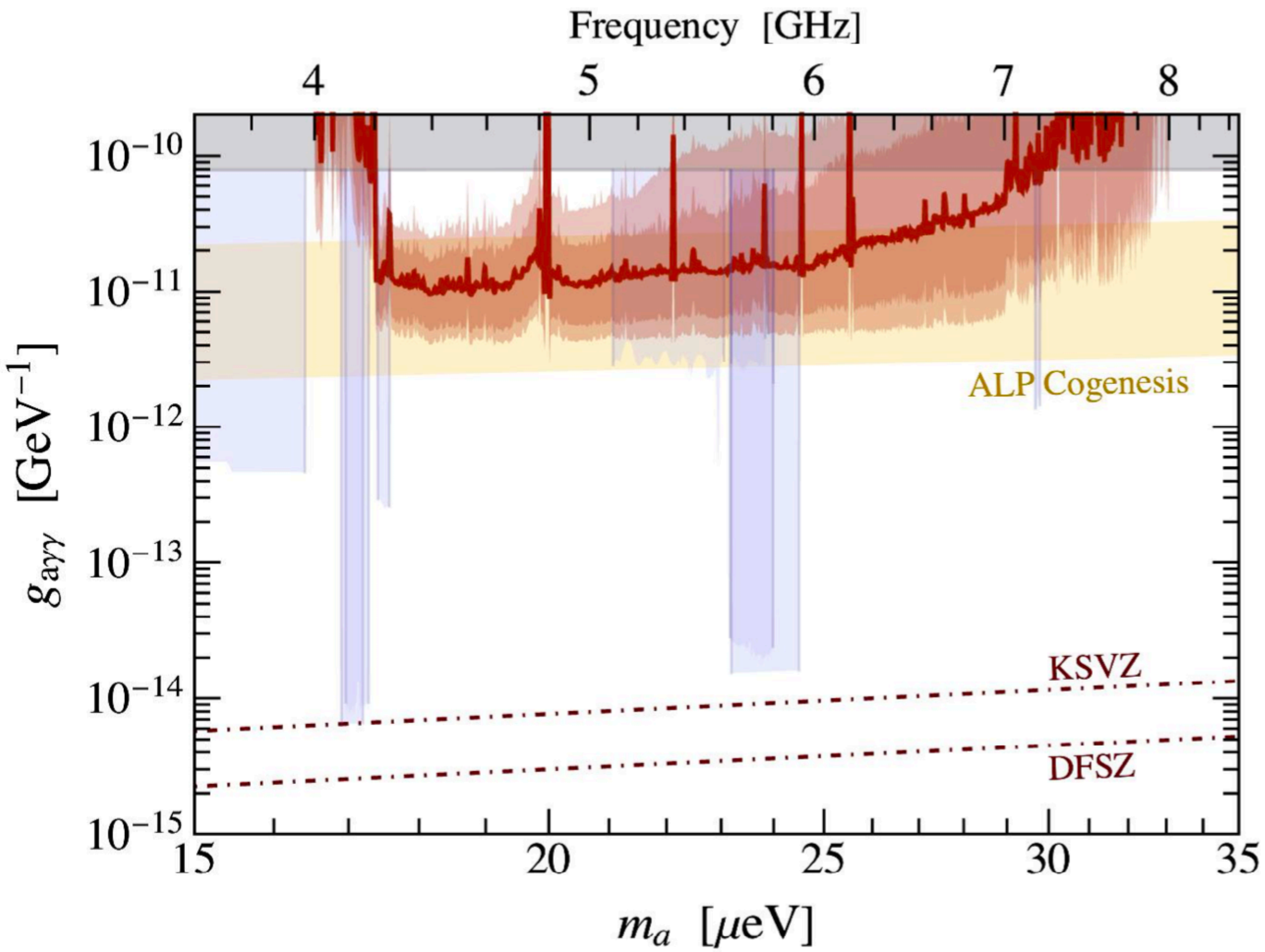

Axion mass

Foster et al 2202.08274

Optical Polarization Signal

- CP conserved in QCD ⇒ axion
- $\mathscr{L}_{a\gamma\gamma} = \frac{1}{4} a F_{\mu\nu} \tilde{F}^{\mu\nu}$

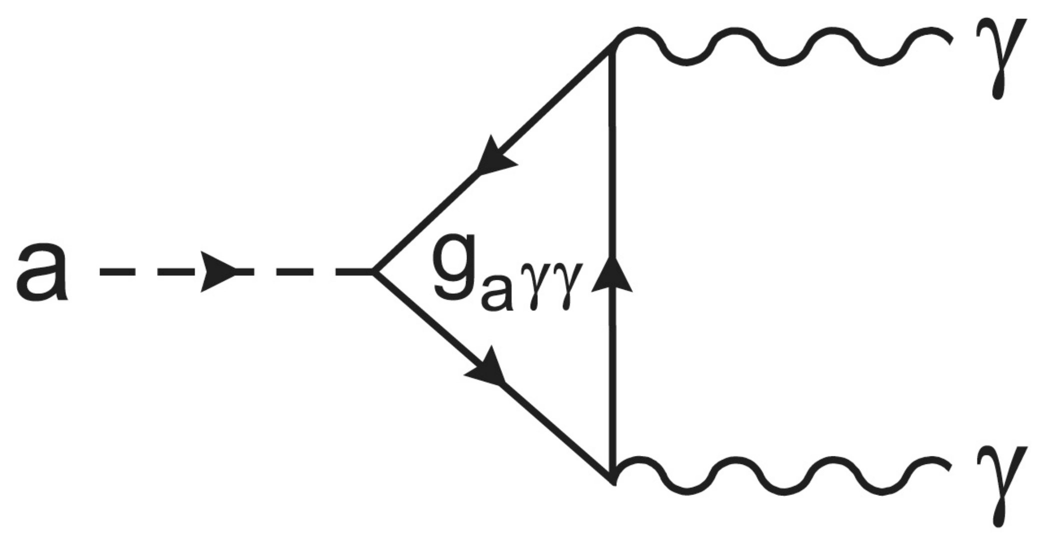

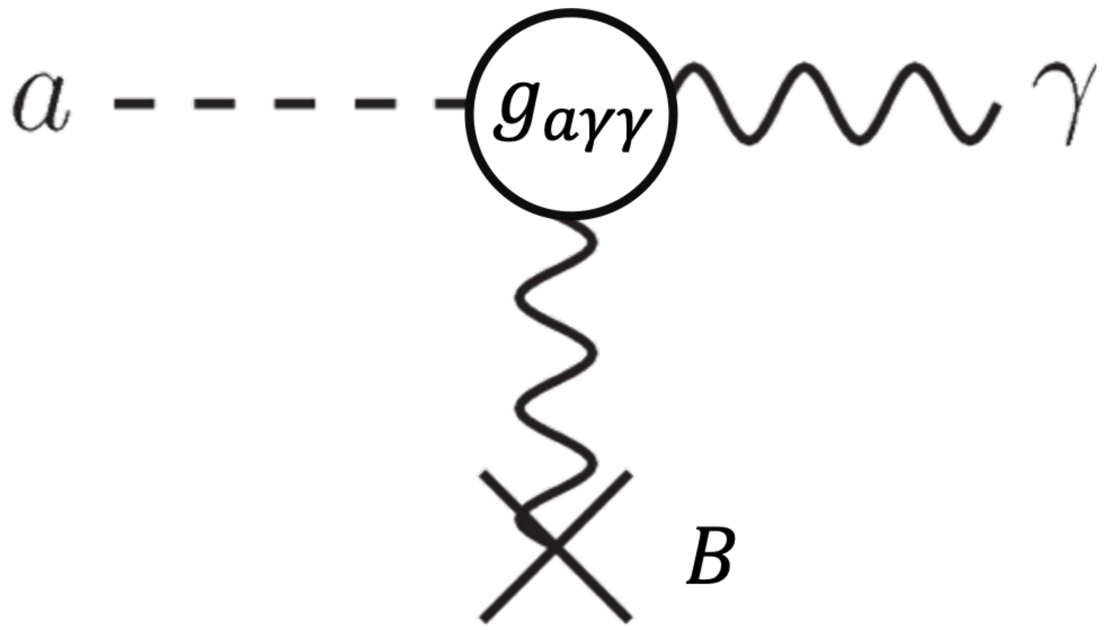

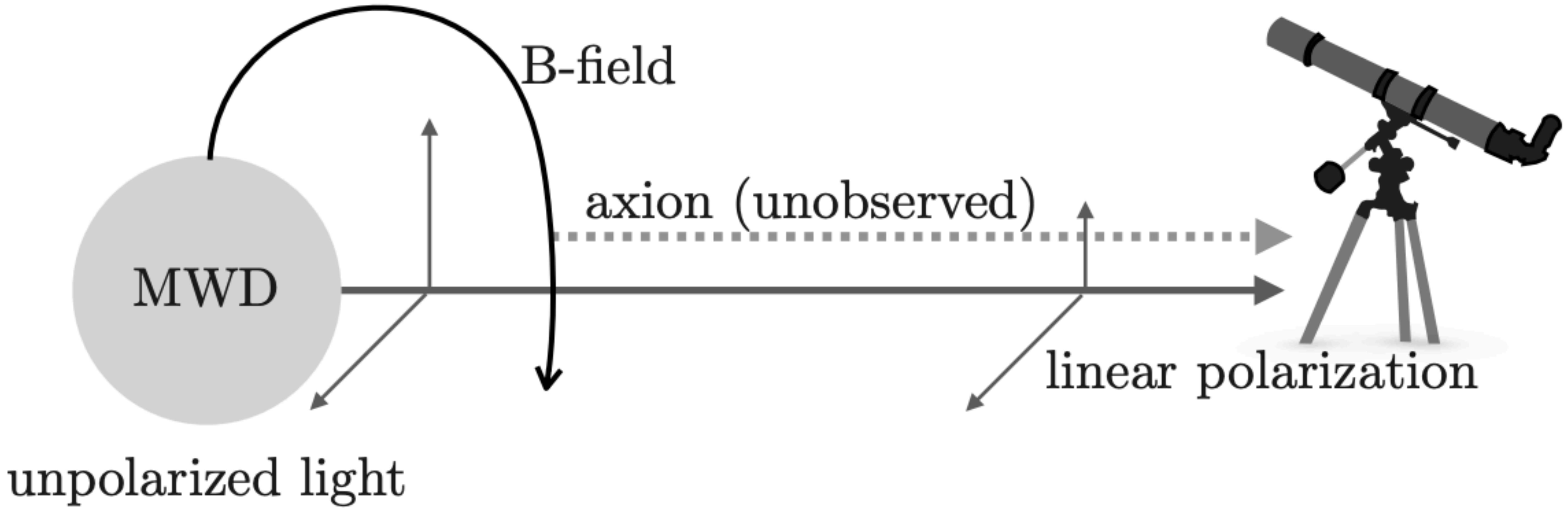

- Photon only converts to axion in the direction parallel to magnetic field, inducing polarization signals

Optical Polarization Signal

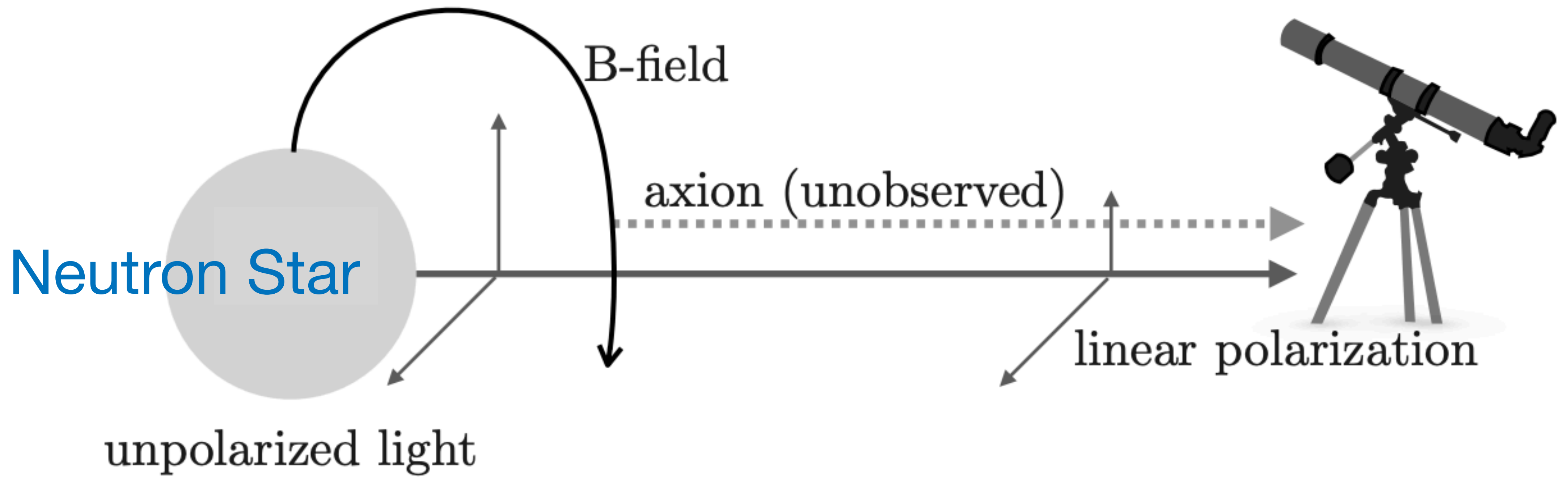

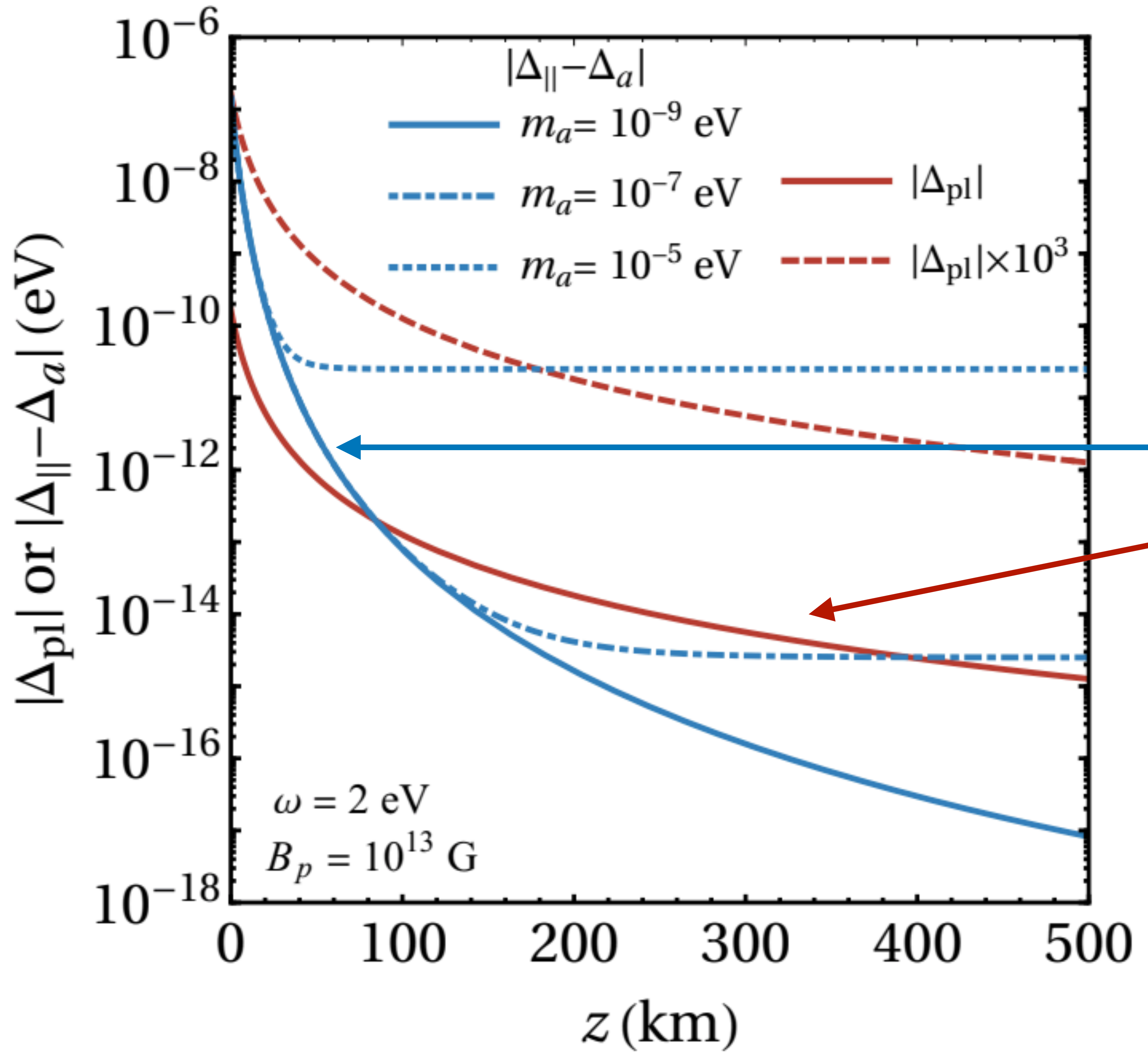

$$\Delta_{\|} + \Delta_{pl} - \Delta_a = 0$$

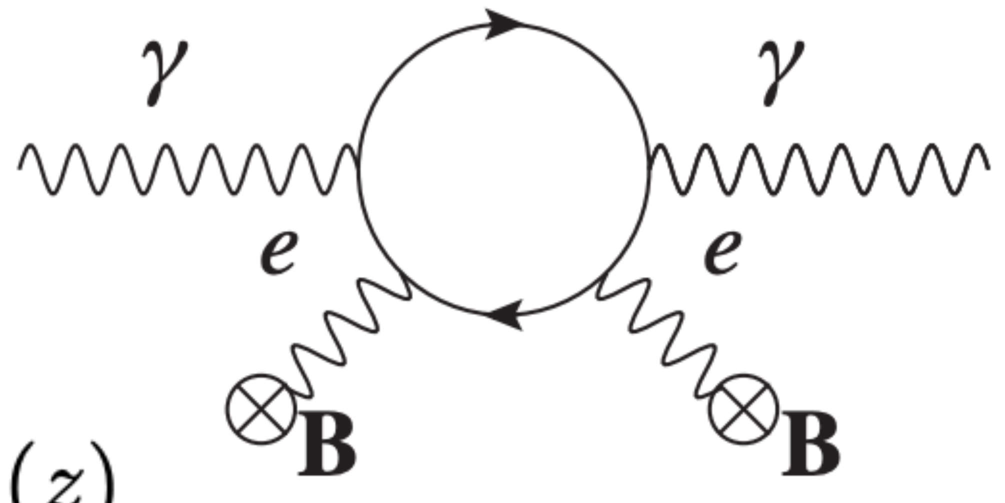

$$\Pi_L(z) = \frac{I_\perp(z) - (1 - P^{res}_{\gamma\to a}) I^{nonres}_{\|}(z)}{I_\perp(z) + (1 - P^{res}_{\gamma\to a}) I^{nonres}_{\|}(z)}$$

$$\approx \frac{P^{res}_{\gamma\to a} + 2|\mathrm{Re}(A_{\|,2})|}{2 - (P^{res}_{\gamma\to a} + 2|\mathrm{Re}(A_{\|,2})|)},$$

- Photon only converts to axion in the direction parallel to magnetic field, inducing polarization signals
- Resonant conversion occurs when vacuum polarization matches plasma

NS, Liangliang Su, Lei Wu, arXiv: 2402.15144

Optical Polarization Signal

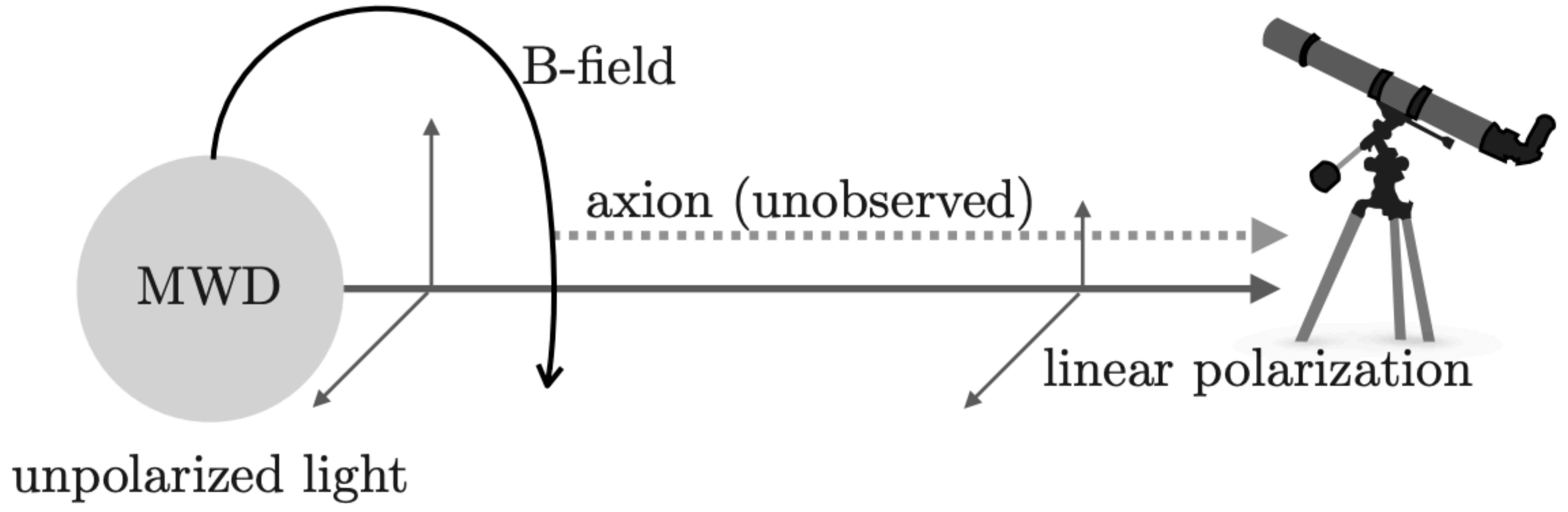

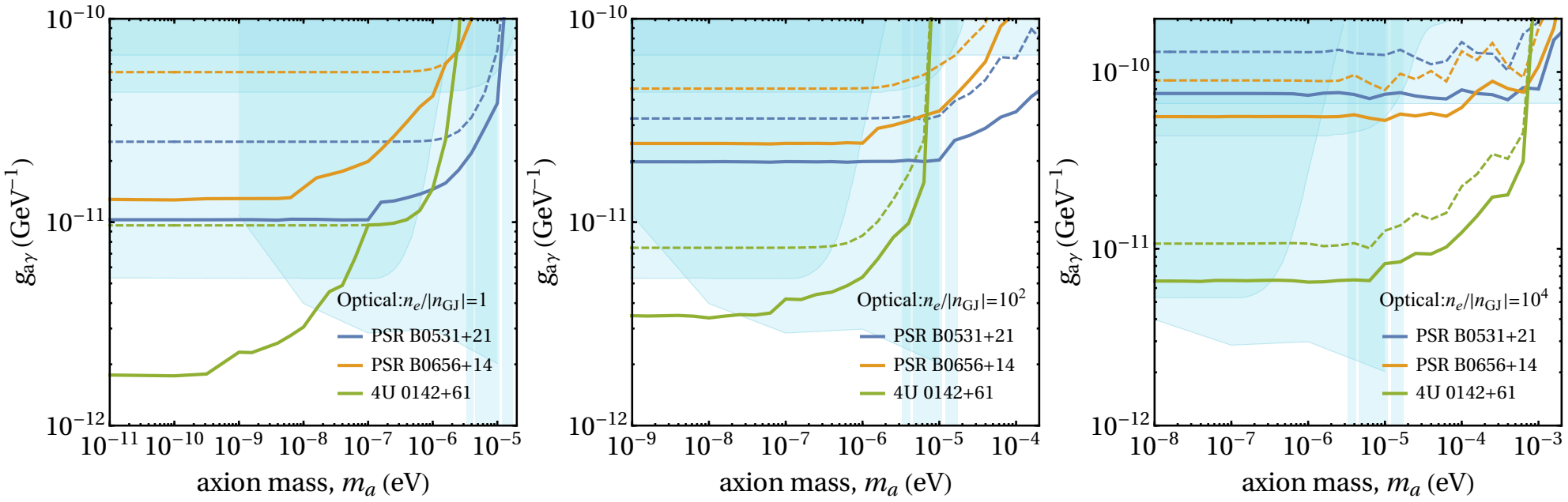

- Photon only converts to axion in the direction parallel to magnetic field, inducing polarization signals
- Optical polarization signals from neutron stars could place the most stringent limits

NS, Liangliang Su, Lei Wu, arXiv: 2402.15144

Summary

- Introduction
- Direct detection of dark matter
- Astrophysical probes of dark matter

Thanks

Back up

Inelastic Dark Matter

The WIMP Miracle?

- Dark matter with weak interactions freezes out to the correct relic abundance

$$\Omega h^2 \simeq \left(\frac{3 \times 10^{-26} \mathrm{cm}^3/\mathrm{s}}{\langle \sigma v \rangle} \right)$$

- Dark matter scatters though the Z boson mediator

$$\sigma_{\chi p} = \frac{g^4 m_\chi^2 m_p^2}{4\pi (m_\chi + m_p)^2} \frac{1}{m_Z^4} \sim 10^{-39}\ \mathrm{cm}^2$$

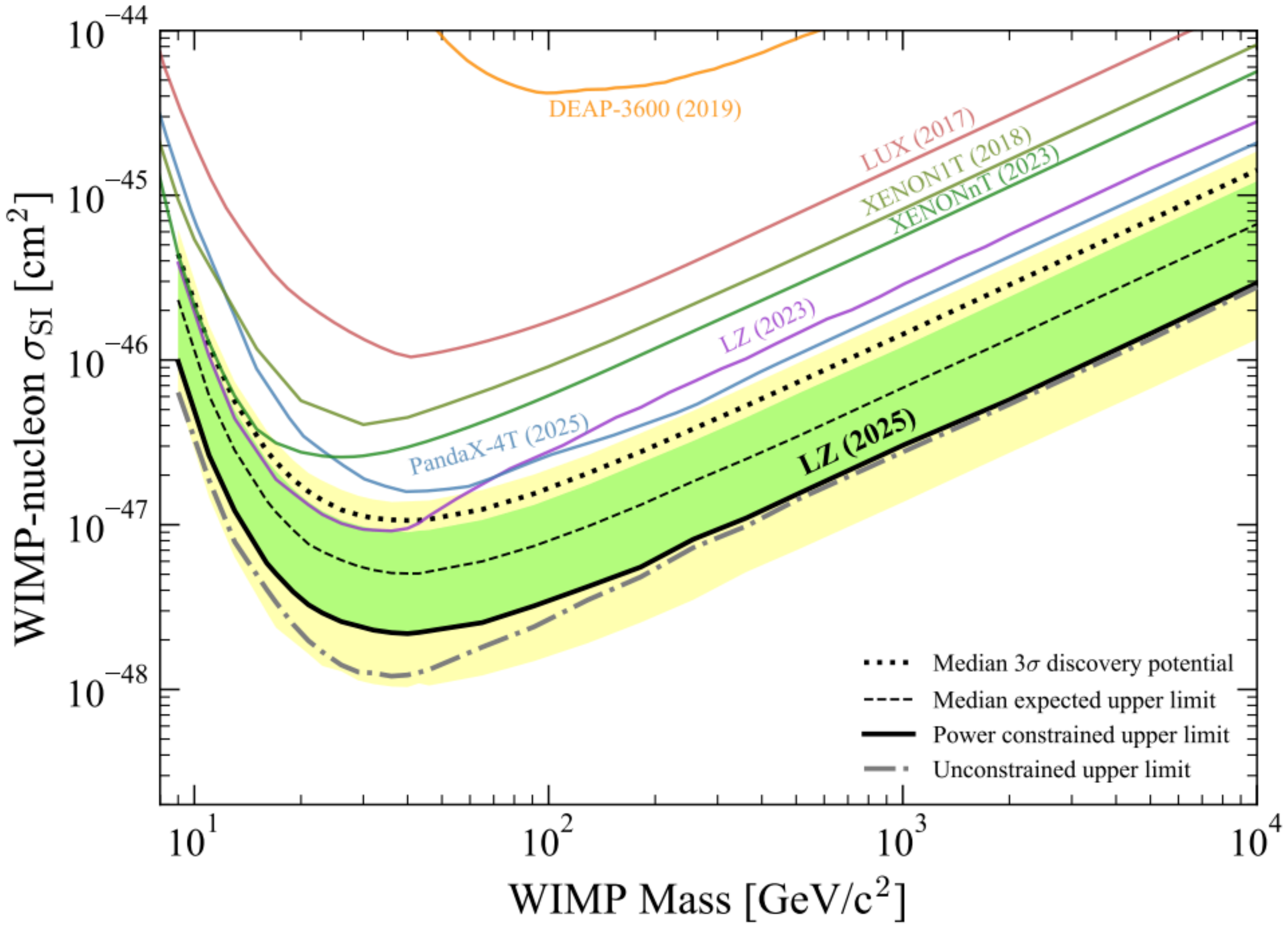

Are there ways around?

Feb 22, 2019, 02:00am EST | 57,704 views

The 'WIMP Miracle' Hope For Dark Matter Is Dead

Ethan Siegel Senior Contributor
Starts With A Bang Contributor Group ⓘ
Science
The Universe is out there, waiting for you to discover it.

WIMPs on Death Row

Posted on July 21, 2016 by woit

One of the main arguments given for the idea of supersymmetric extensions of the standard model has been what SUSY enthusiasts call the "WIMP Miracle" (WIMP=Weakly Interacting Massive Particle). This is the claim that such SUSY models include a stable very massive weakly interacting particle that could provide an explanation for dark matter.

Inelastic Dark Matter

- Off-diagonal mass term $\begin{pmatrix} M & v \\ v & M \end{pmatrix}$

- After diagonalization $M_{\chi_1} = M + v$, $M_{\chi_2} = M - v$

- $\delta \equiv M_{\chi_2} - M_{\chi_1} \ll M_\chi$

- Example: dark photon-mediated DM

$$\mathscr{L} \supset \bar{\psi}(iD_\mu\gamma^\mu - m_\psi)\psi + (y\phi\bar{\psi}^T C^{-1}\psi + h.c.)$$

Bramante, **NS**, PRL/2006.14089
Batell, Pospelov, Ritz, 0903.3396

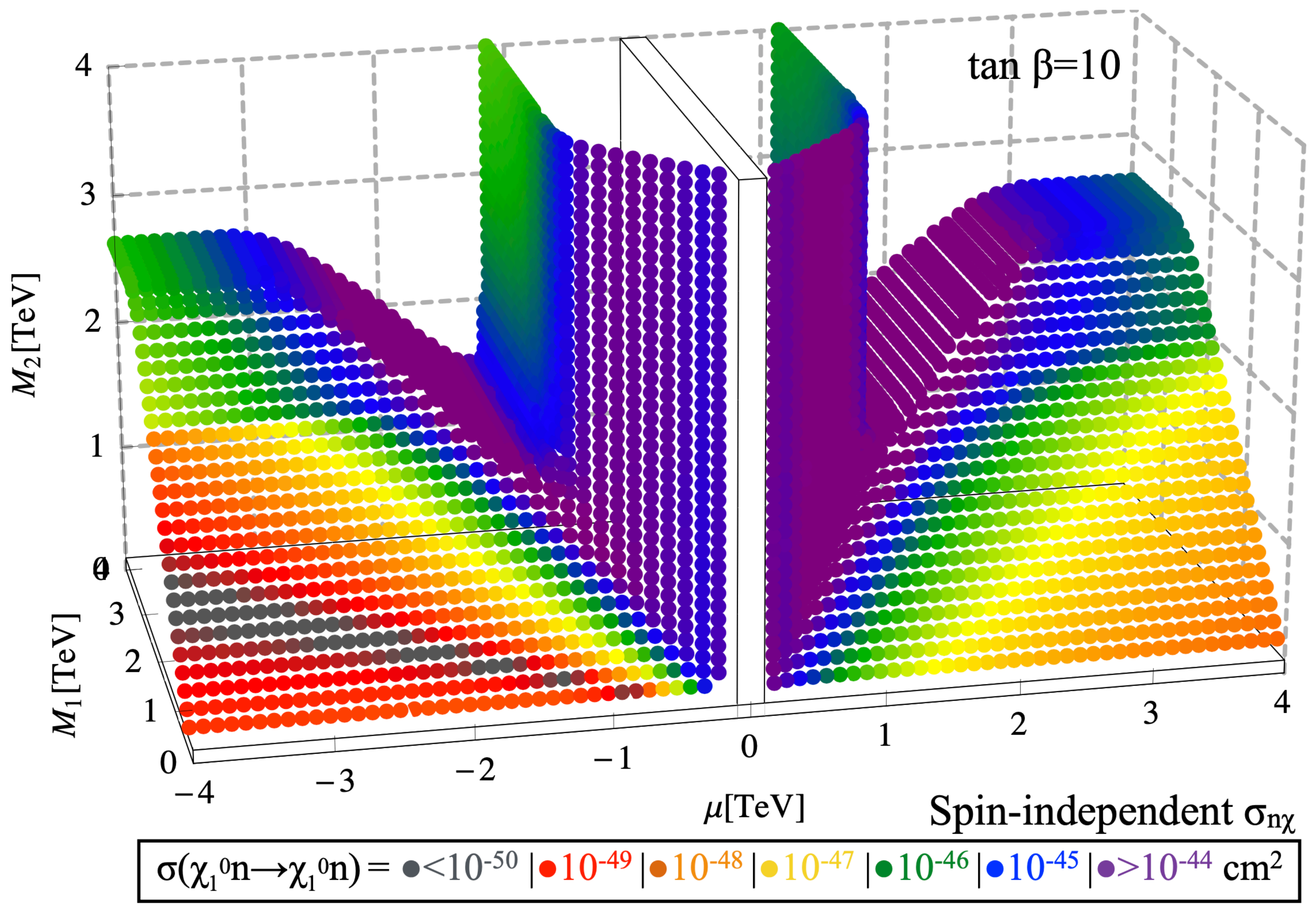

Neutralino DM, see Bramante et al, 1510.03460, 1412.4789

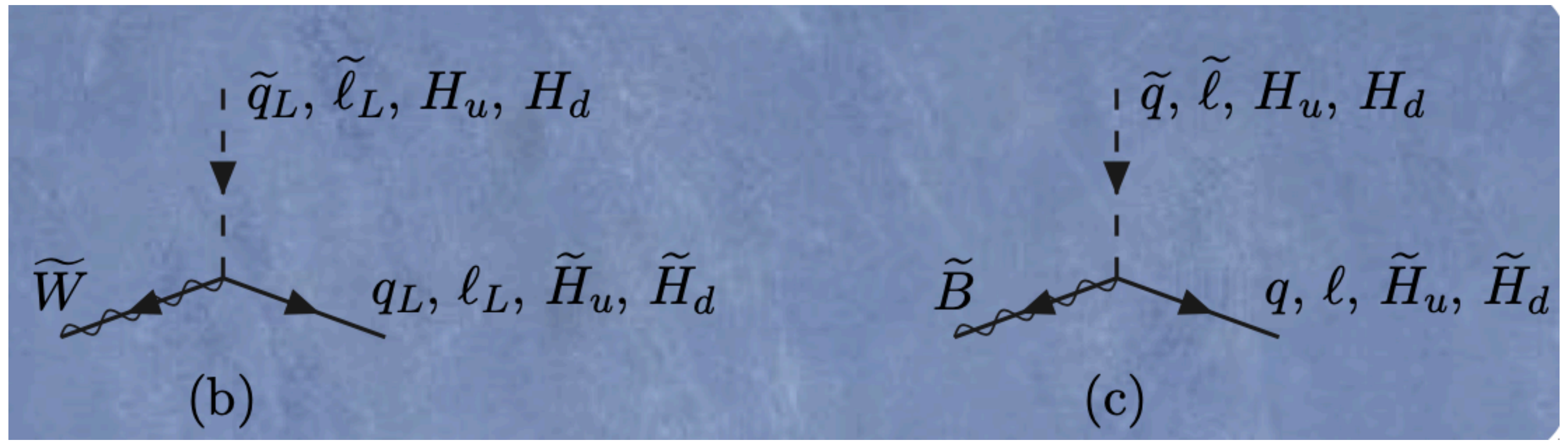

Inelastic Dark Matter

- Off-diagonal mass term $\begin{pmatrix} M & v \\ v & M \end{pmatrix}$
- After diagonalization $M_{\chi_1} = M + v$, $M_{\chi_2} = M - v$
- $\delta \equiv M_{\chi_2} - M_{\chi_1} \ll M_\chi$
- Example: dark photon-mediated DM

$$\mathcal{L} \supset \bar{\psi}(iD_\mu \gamma^\mu - m_\psi)\psi + (y\phi\bar{\psi}^T C^{-1}\psi + h.c.)$$

Bramante, **NS**, PRL/2006.14089
Batell, Pospelov, Ritz, 0903.3396

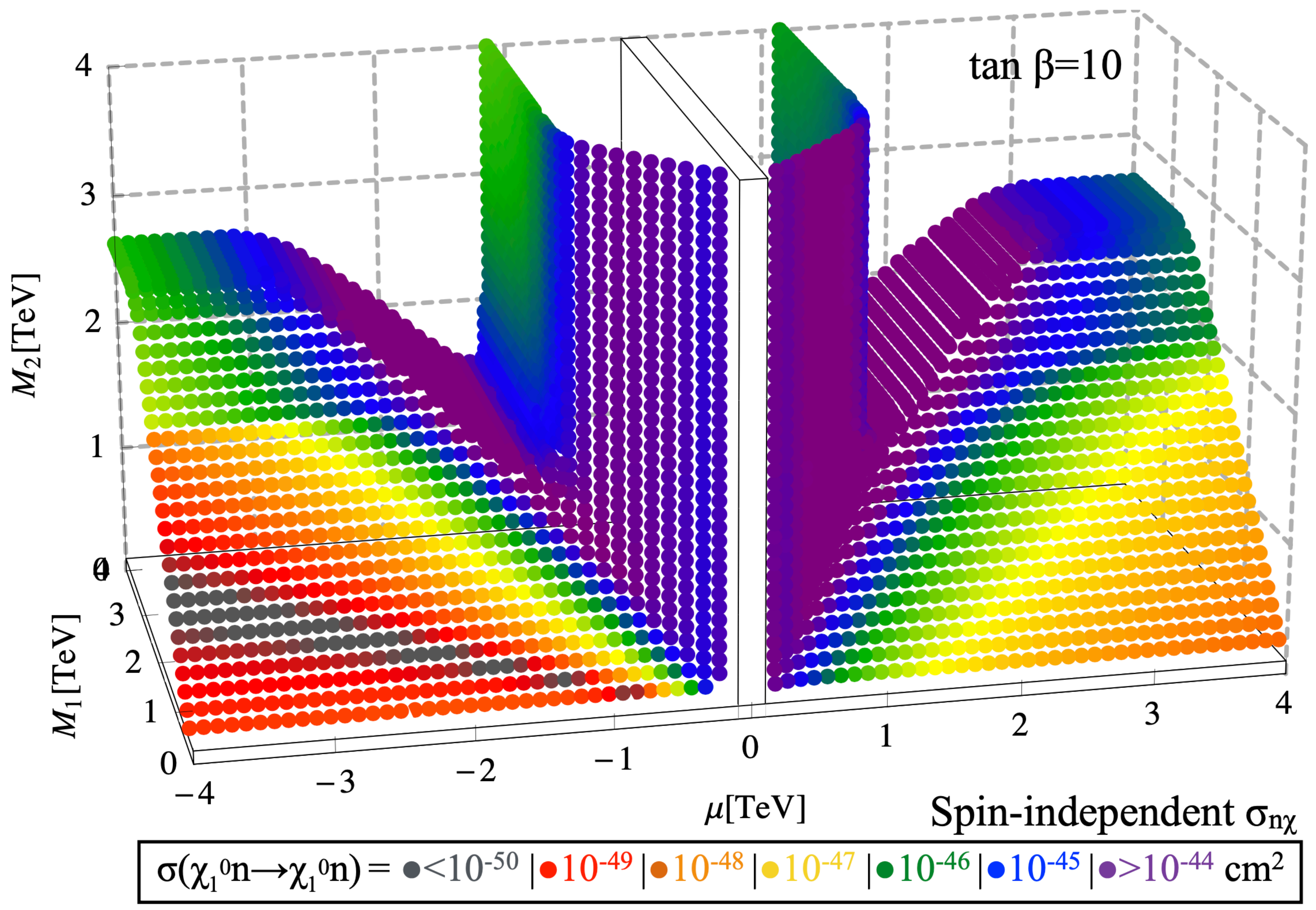

Neutralino DM, see Bramante et al, 1510.03460, 1412.4789

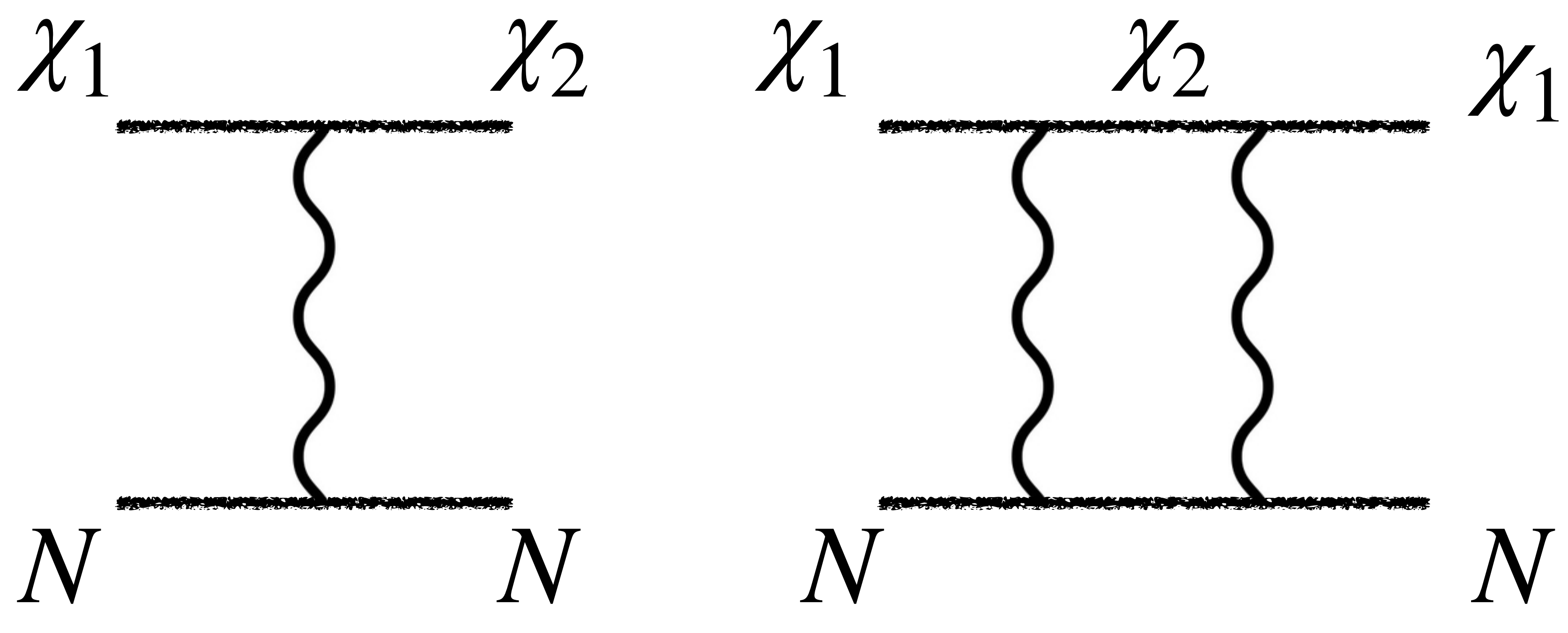

kinematically suppressed loop suppressed

Homework Exercise: Kinematics in Nuclear Recoil

$\delta \equiv M_{\chi_2} - M_{\chi_1}$

- $$\frac{\vec{q}_i^{\,2}}{2M_{\chi_1}} = \frac{\vec{q}_f^{\,2}}{2M_{\chi_2}} + \frac{\vec{q}^{\,2}}{2M_A} + \delta$$
- $$q_{\min/\max} = \mu_{\chi A} v \left[1 \mp \sqrt{1 - 2\frac{\delta}{\mu_{\chi A} v^2}} \right]$$
- Minimum velocity $v_{\min} = \sqrt{2\frac{\delta}{\mu_{\chi A}}}$

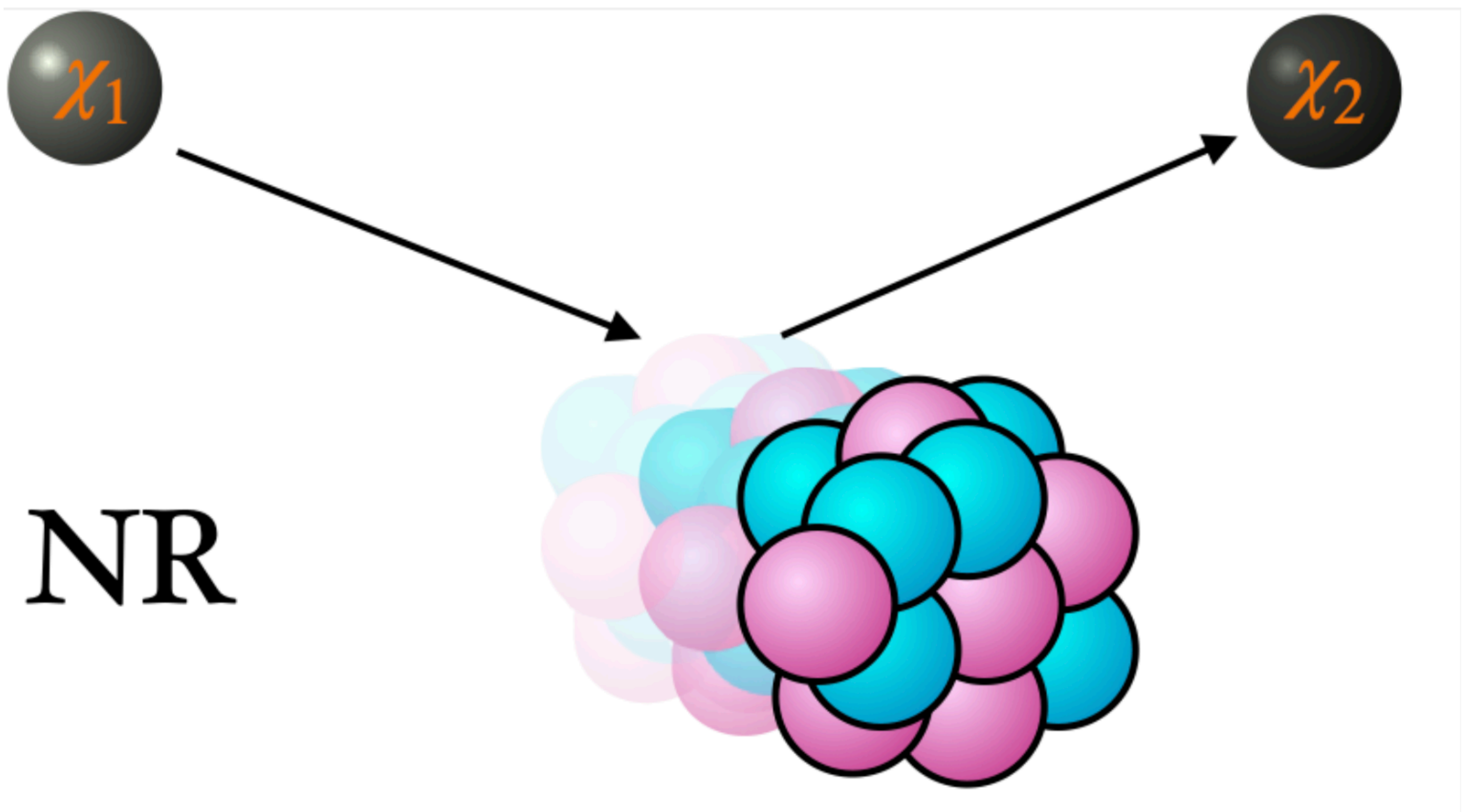

NR

Why not XENON

- Xenon not heavy enough
- Xenon experiments only sensitive to low energy deposition ($E_R \lesssim 40$ keV)

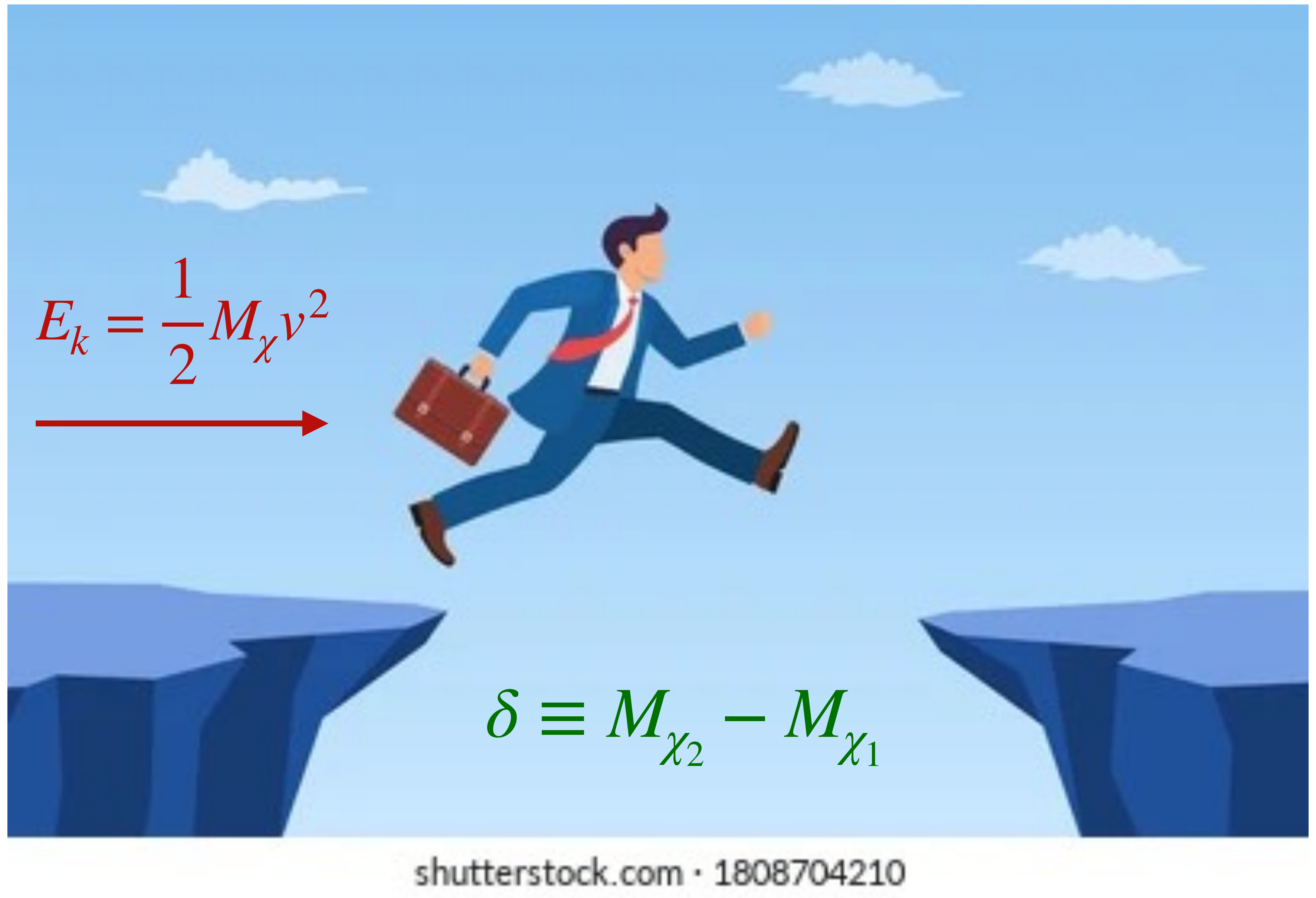

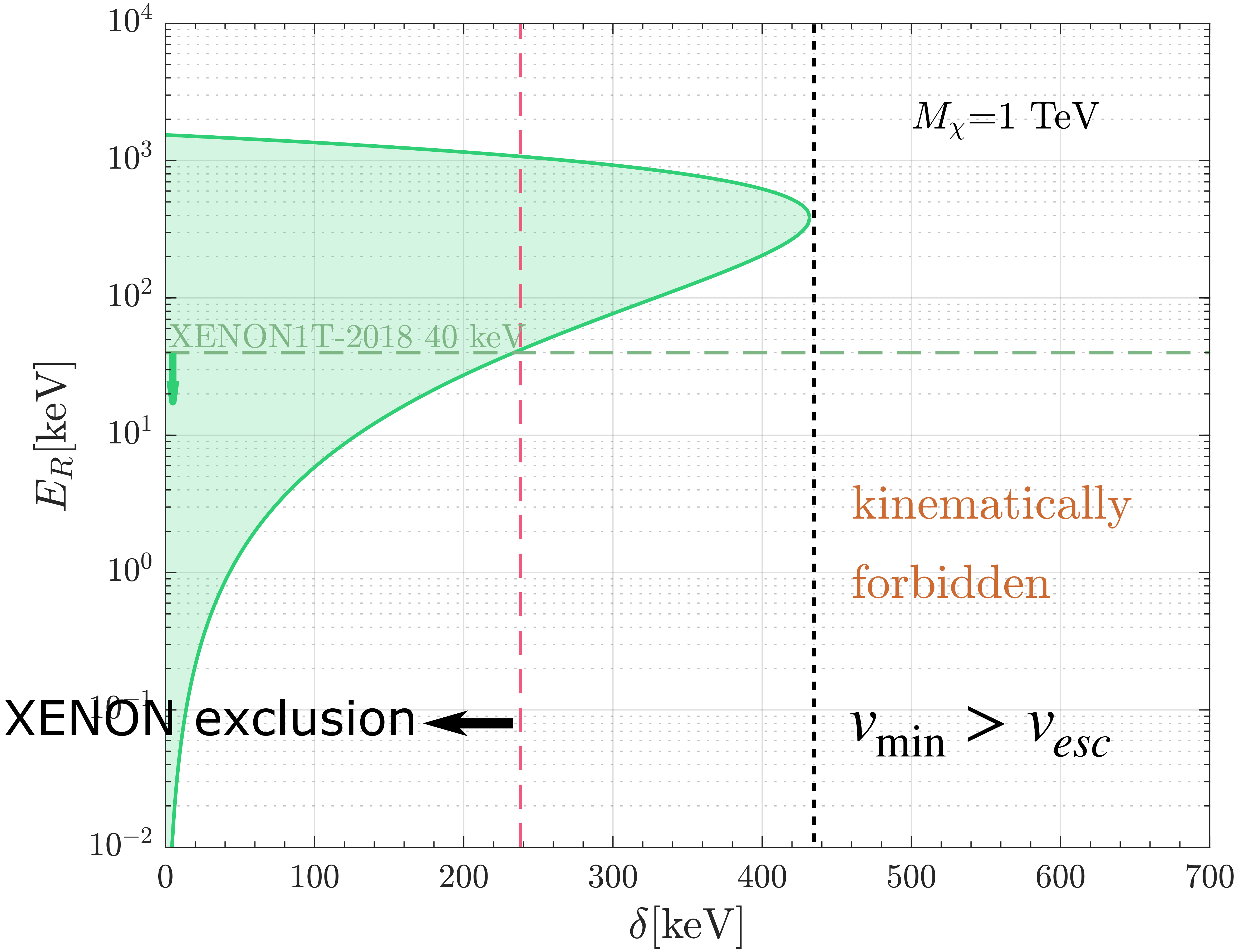

Two Criteria

- Heavy nuclear target

$$\delta_{\max} = \frac{1}{2}\mu_{\chi A}(v_e + v_{esc})^2$$

- High energy deposition acceptance

$$E_{accept} > E_R^{\min} \sim \text{MeV}$$

Target nuclei with $A \sim 200$

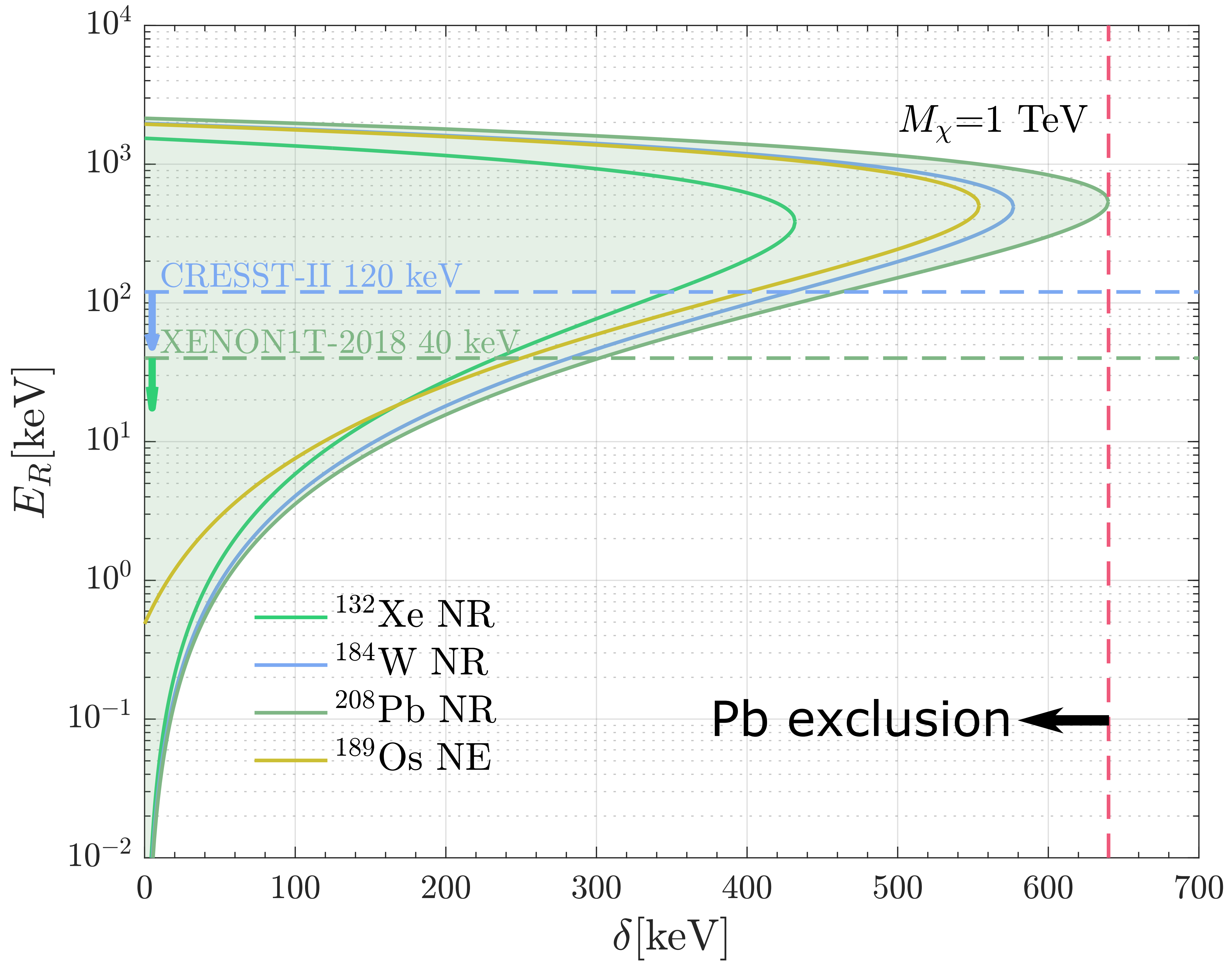

NS, Nagorny, Vincent, PRD/2104.09517

Dark Matter Capture

Earth Heating

- Dark matter scatters with Earth matter, slows down and gets trapped

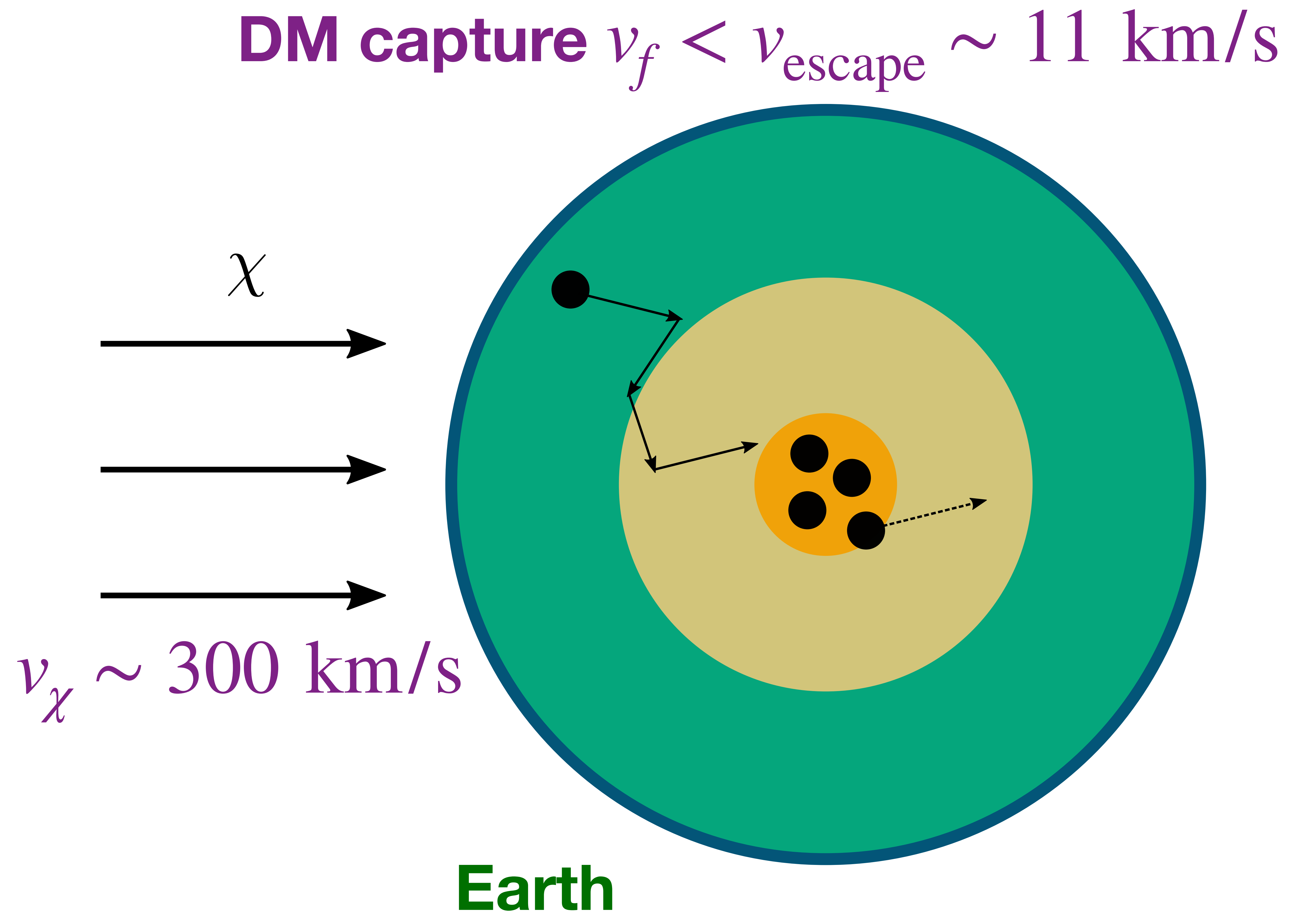

Earth Heating

- Dark matter scatters with Earth matter, slows down and gets trapped

- Dark matter scatters with thermal nuclei and escapes from the Earth

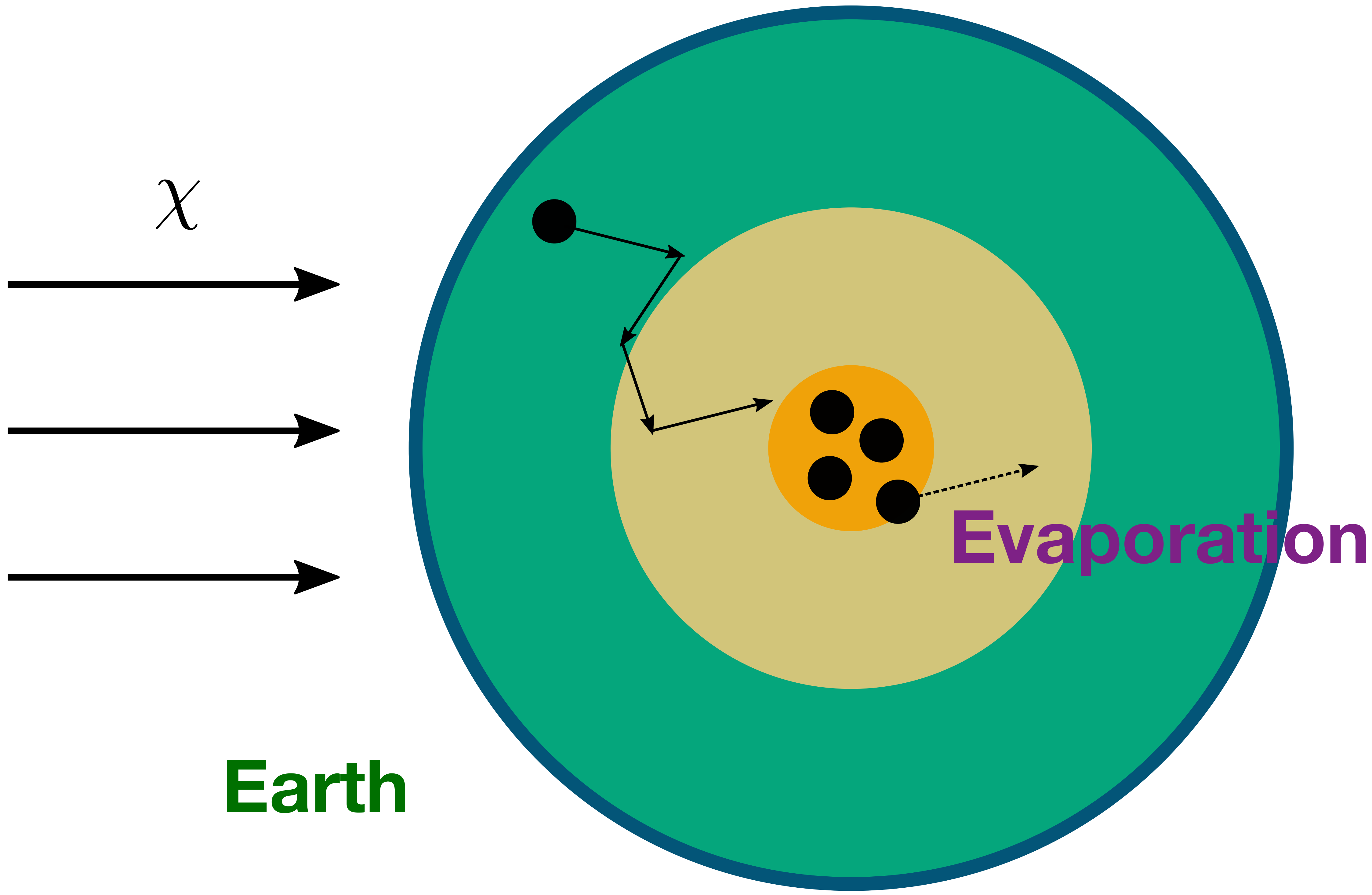

Earth Heating

- Dark matter scatters with Earth matter, slows down and gets trapped
- Dark matter scatters with thermal nuclei and escapes from the Earth
- Dark matter annihilate to Standard Model particles, heating the Earth

DM Heating $\lesssim$ 44 TW

Kamland, Borexino
geoneutrino observation

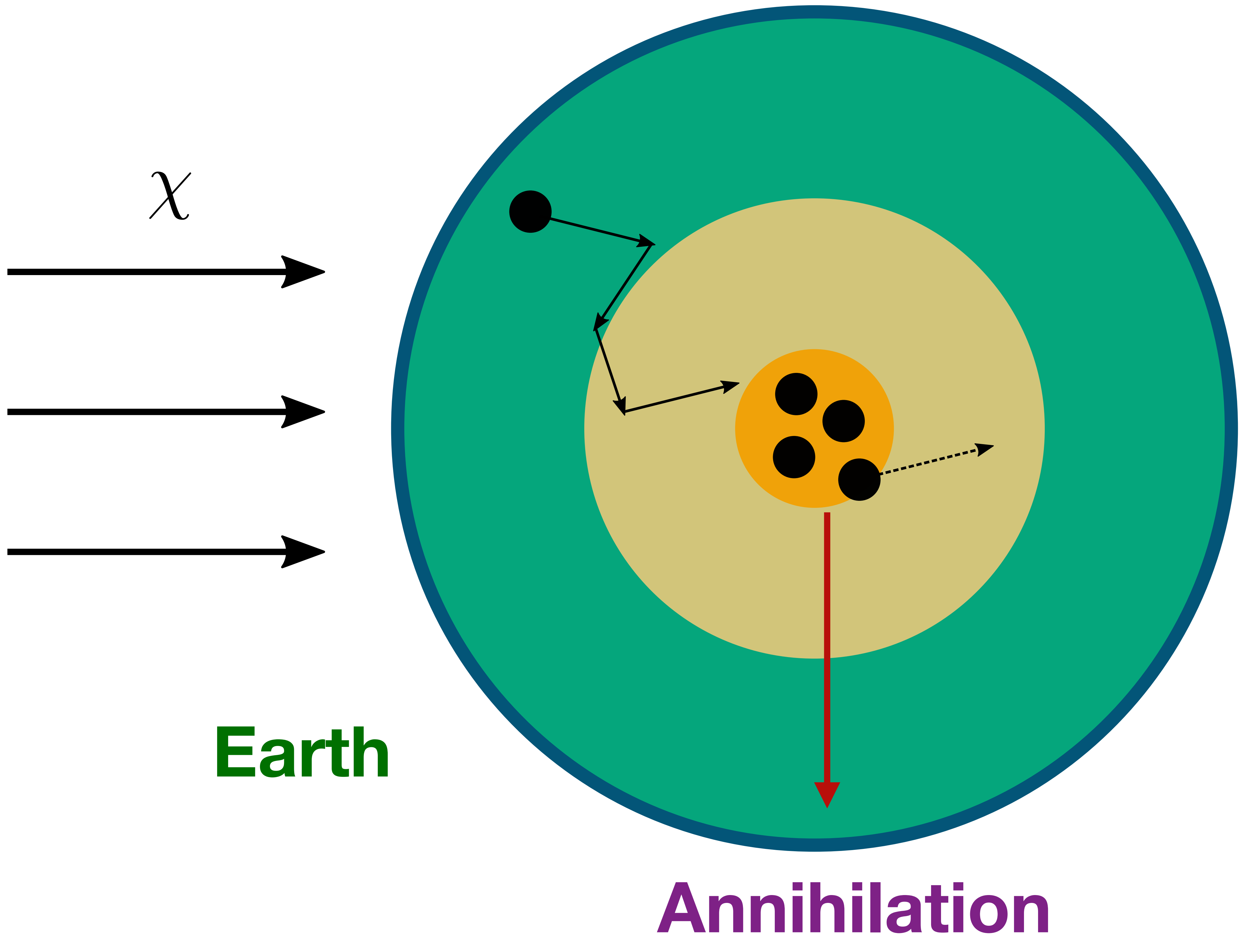

Monte Carlo

DaMaSCUS_EarthCapture
https://github.com/songningqiang/DaMaSCUS-EarthCapture

Top of atmosphere

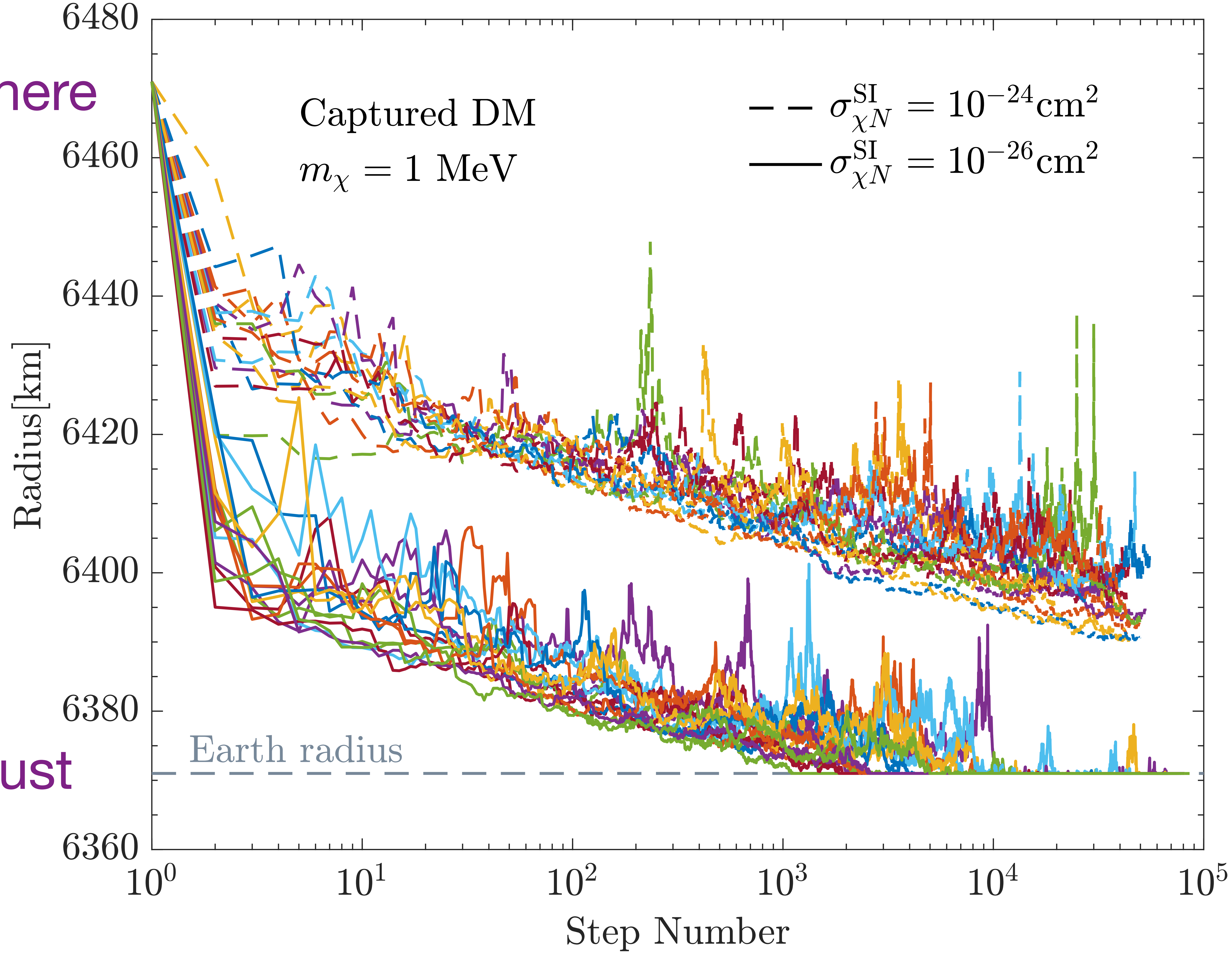

Top of Earth crust

Number of scattering

See also DaMaSCUS
https://github.com/temken/DaMaSCUS

Monte Carlo

DaMaSCUS_EarthCapture
https://github.com/songningqiang/DaMaSCUS-EarthCapture

Top of atmosphere

Top of Earth crust

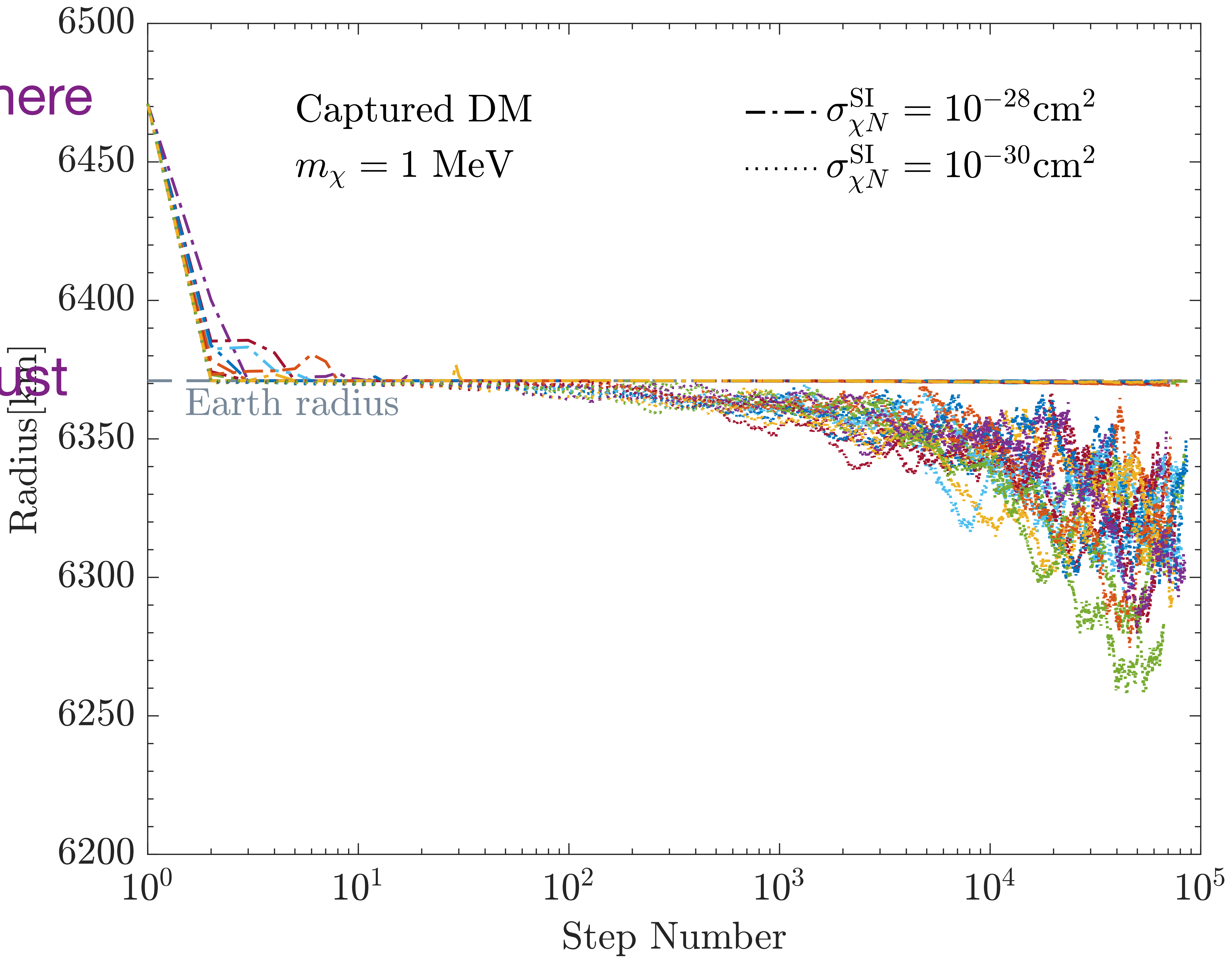

Number of scattering

Capture Fraction

DaMaSCUS_EarthCapture
https://github.com/songningqiang/DaMaSCUS-EarthCapture

Capture fraction

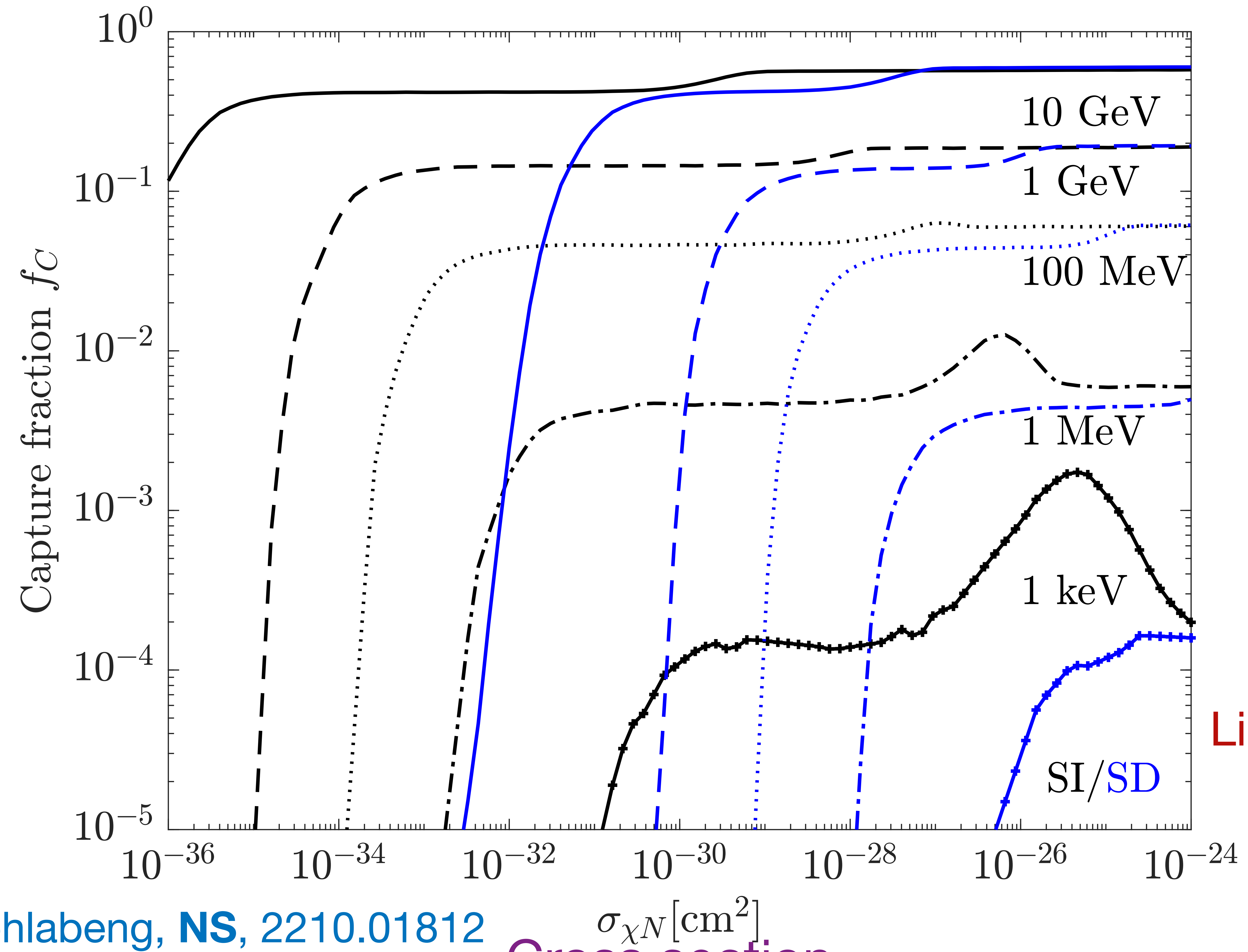

Lighter DM

Cross section

Bramante, Kumar, Mohlabeng, **NS**, 2210.01812

Dark Matter Evaporation

$$E_{\oplus} = \sum_j \int_0^{R_{\oplus}} 4\pi r^2 n_{\chi}(r) s(r) dr \times \int_0^{v_e(r)} 4\pi u_{\chi}^2 f_{\oplus} du_{\chi} \int_{v_e(r)}^{\infty} R_j^{+}(u_{\chi} \to v) dv$$

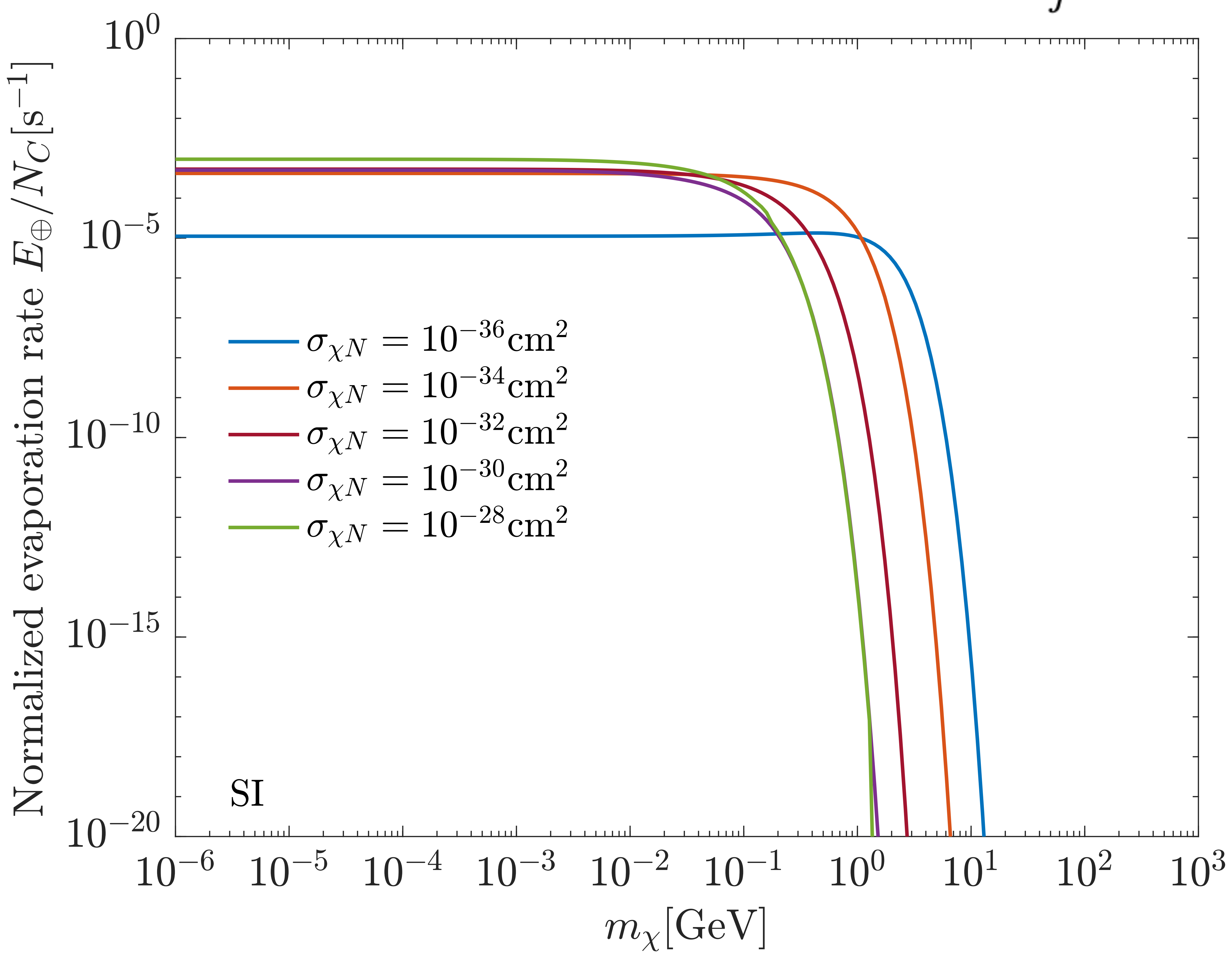

Dark matter mass

Multi scatter

Dark matter scatters with thermal nuclei and escapes from the Earth

Garani 1702.02768

Dark Matter Annihilation

Assuming dark matter annihilates to SM final states

Normalized annihilation rate
$$A_\oplus = \frac{\langle \sigma v \rangle_{\chi\chi}}{N_C^2} \int_0^{R_{\oplus,\mathrm{atm}}} n_\chi^2 4\pi r^2 dr \qquad \langle \sigma v \rangle_{\chi\chi} \simeq 3 \times 10^{-26}\ \mathrm{cm}^3/\mathrm{s}$$

DM in the Earth
$$\frac{dN_C}{dt} = C_\oplus - \left(\frac{E_\oplus}{N_C}\right) N_C - A_\oplus N_C^2$$

Total annihilation rate
$$\Gamma_\oplus(t) = (1/2) A_\oplus N_C(t)^2$$

Capture Evaporation Annihilation

Earth Heating Constraints

DM Heating $\leq$ 44 TW

Cross section

Spin-Independent 100%

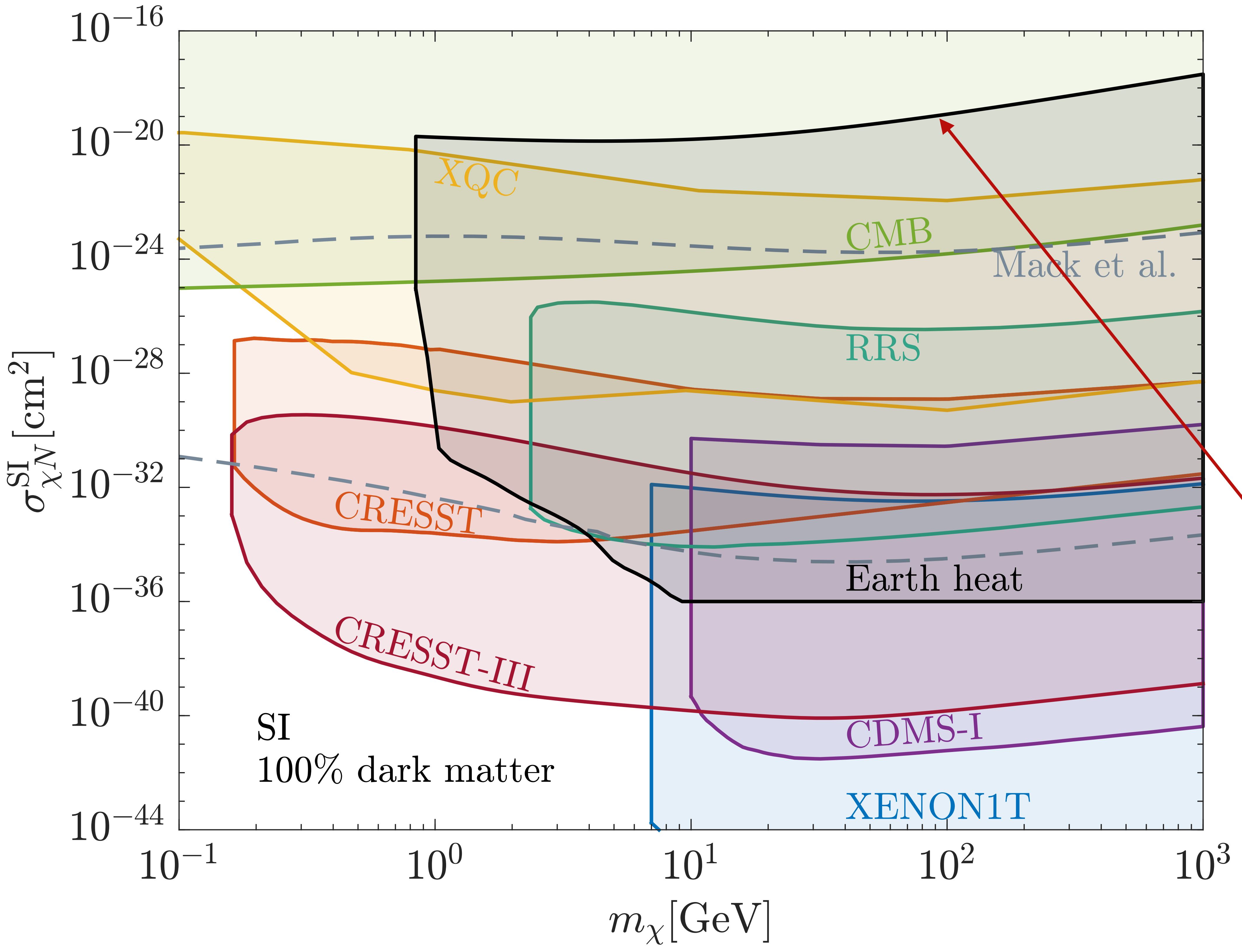

Dark matter mass

Spin-Independent 5%

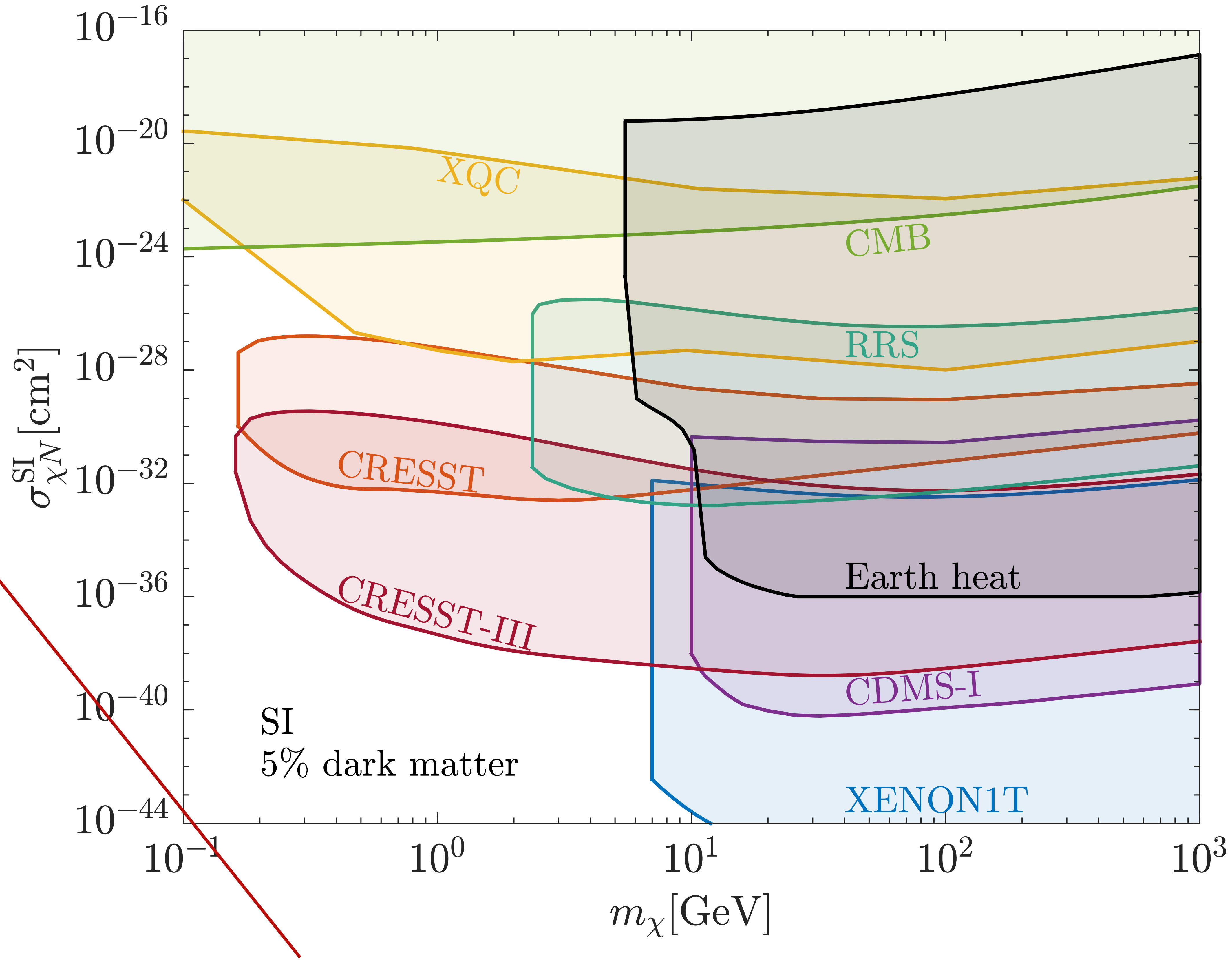

Less than 10% DM annihilation when drifting down to Earth crust

Bramante, Kumar, Mohlabeng, **NS**, 2210.01812

Heating Constraints - Spin-Dependent

Spin-Dependent 100%

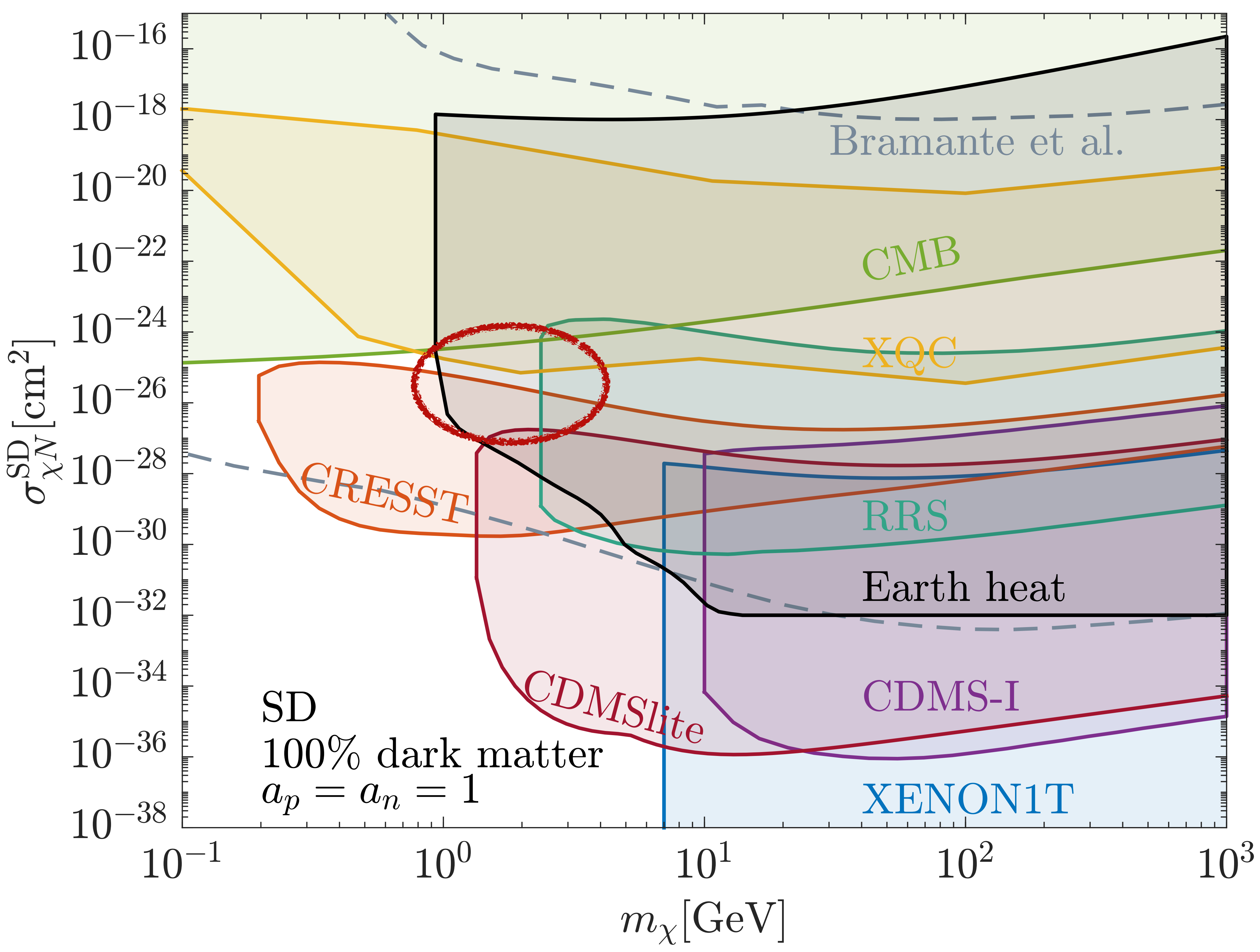

Spin-Dependent 5%

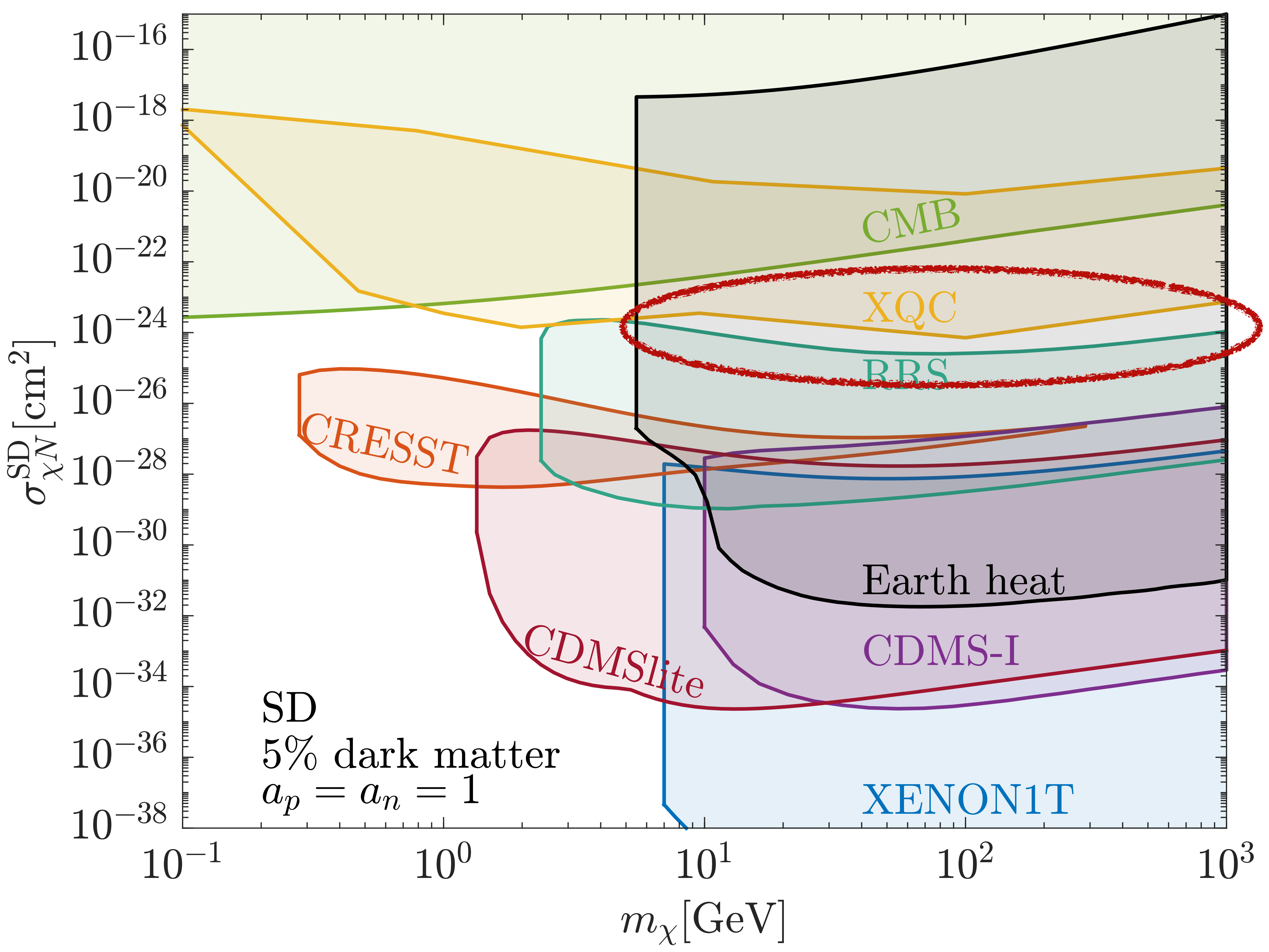

Bramante, Kumar, Mohlabeng, **NS**, 2210.01812

Scintillating Bolometers

- Simultaneous double readout of heat (H) and scintillation light (L)

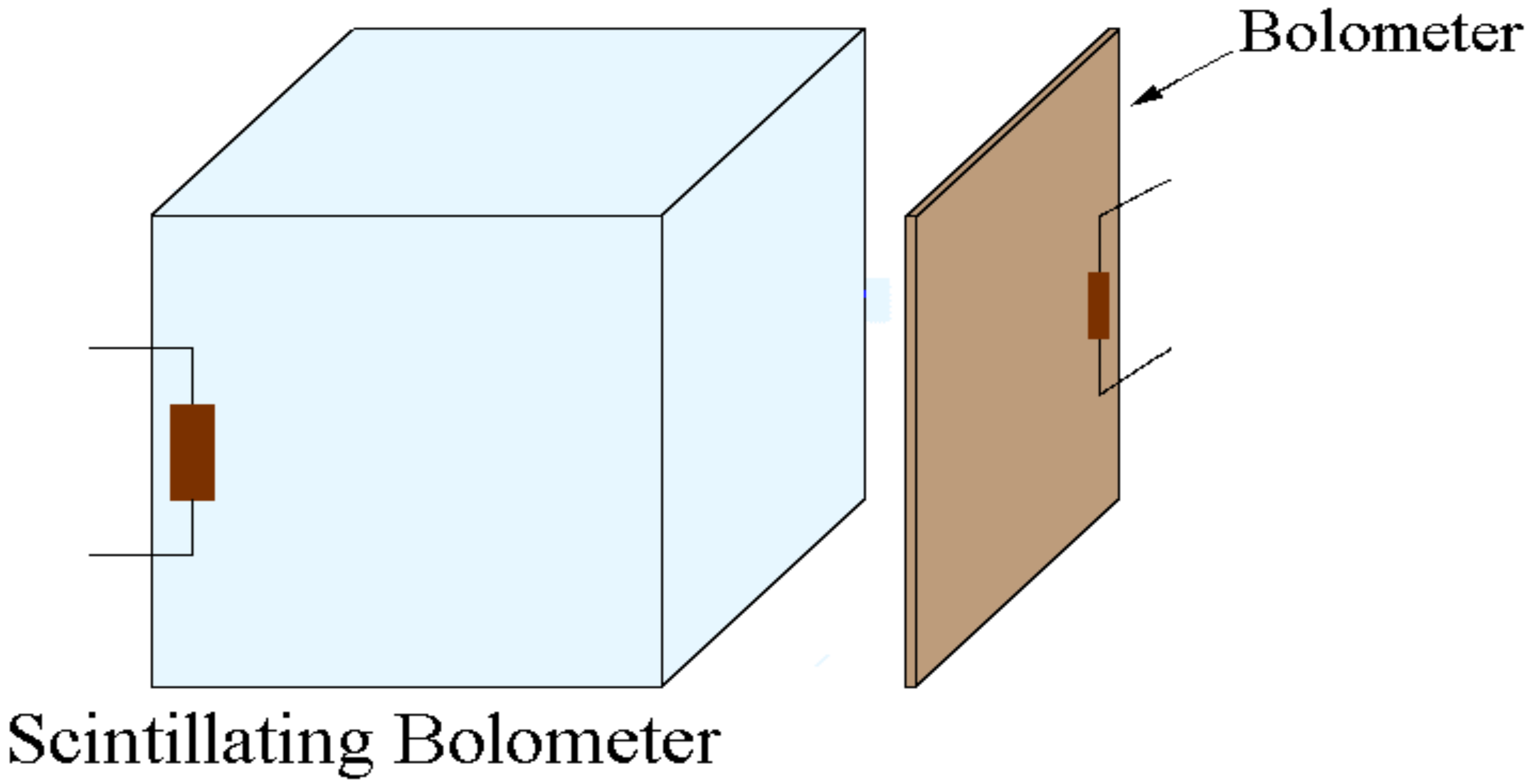

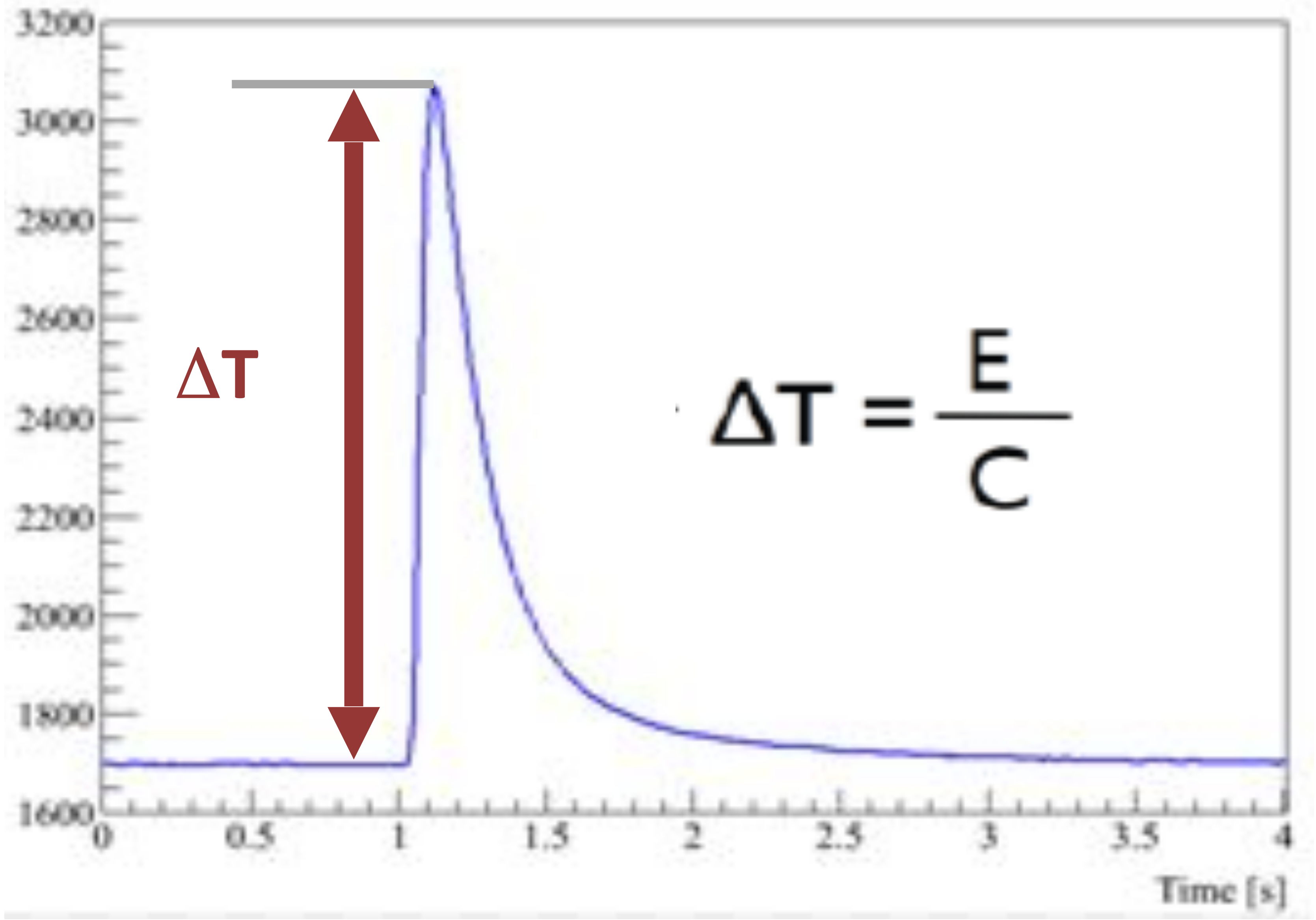

Scintillating Bolometers

- Simultaneous double readout of heat (H) and scintillation light (L)
- Fraction of the deposited energy is converted into a scintillation (up to 25%)
- effective discrimination of e/γ from α events/DM by the difference in L/H ratio

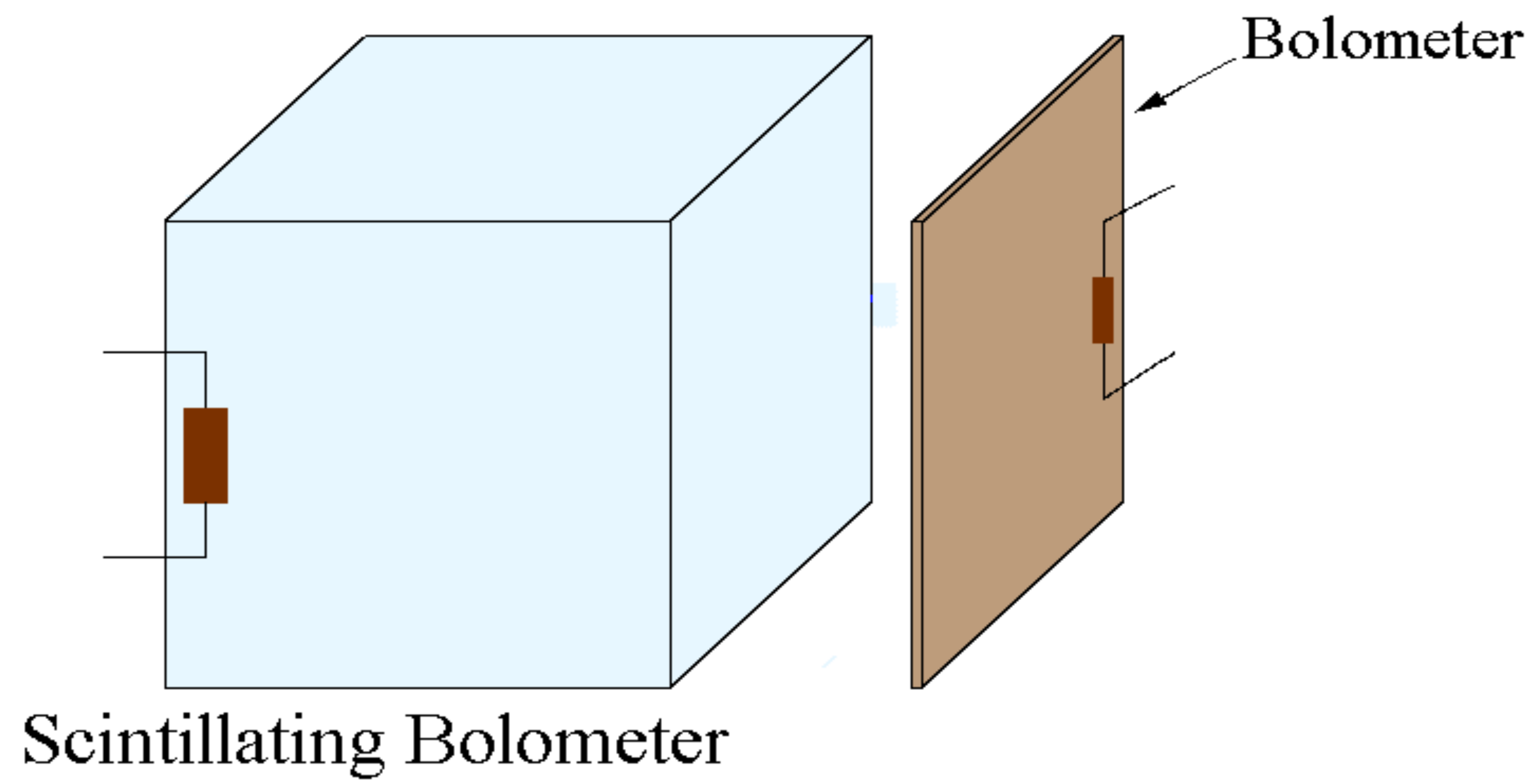

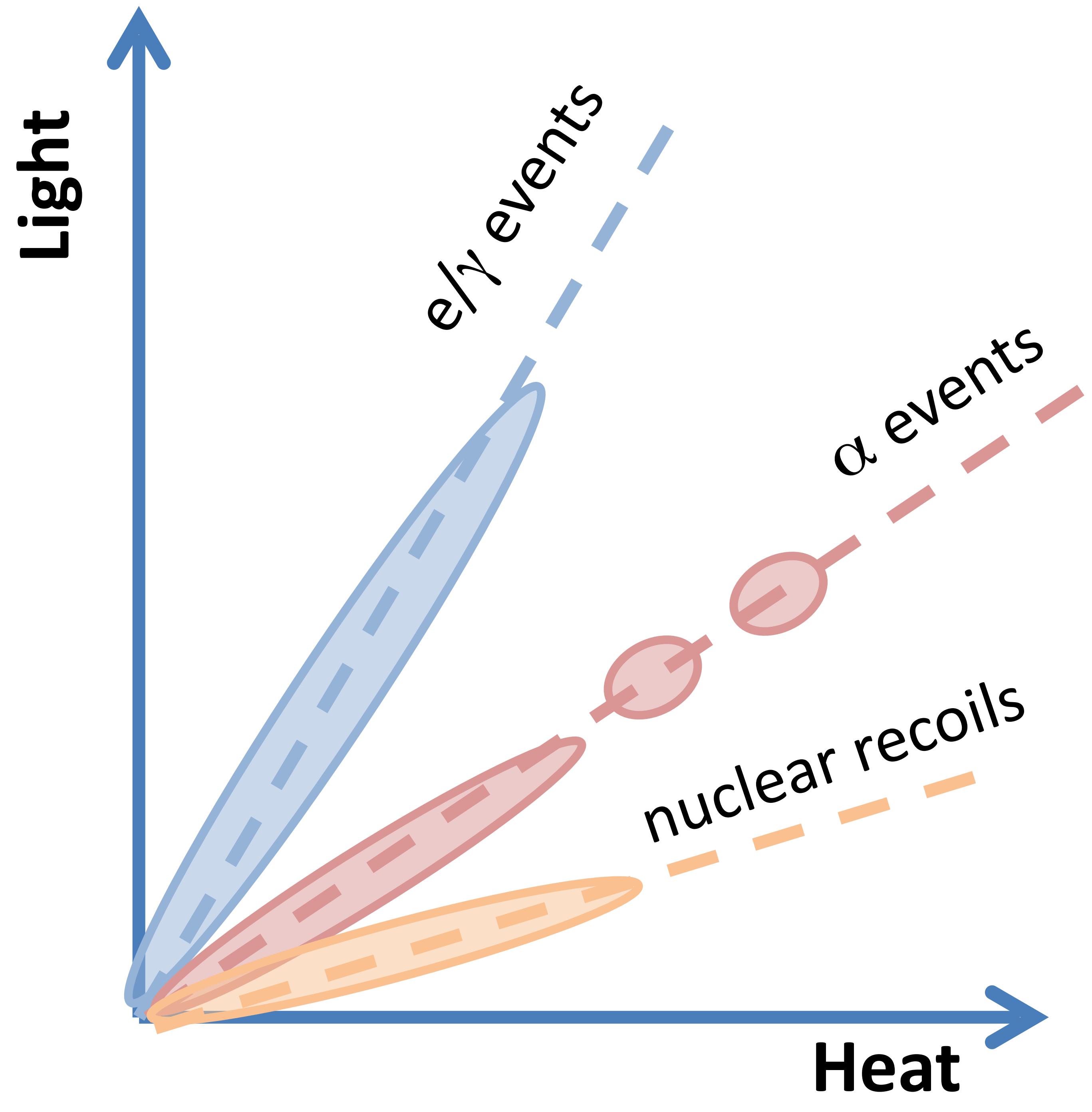

$CaWO_4$ Scintillating Bolometer

Detector module with $CaWO_4$
300 g
∅40×40 mm³

- Simultaneous double readout of heat (H) and scintillation light (L)
- Fraction of the deposited energy is converted into a scintillation (up to 25%)
- Effective discrimination of e/γ from α events/DM by the difference in L/H ratio

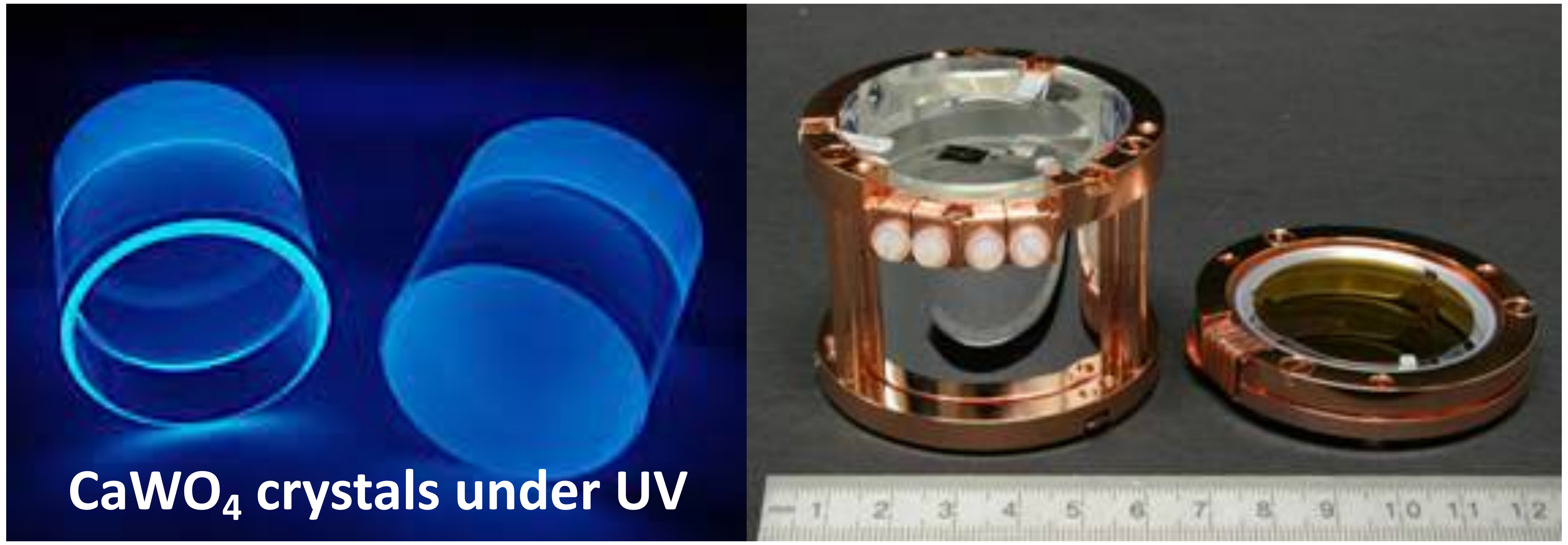

Credit: CRESST Collaboration

90.1 kg·days

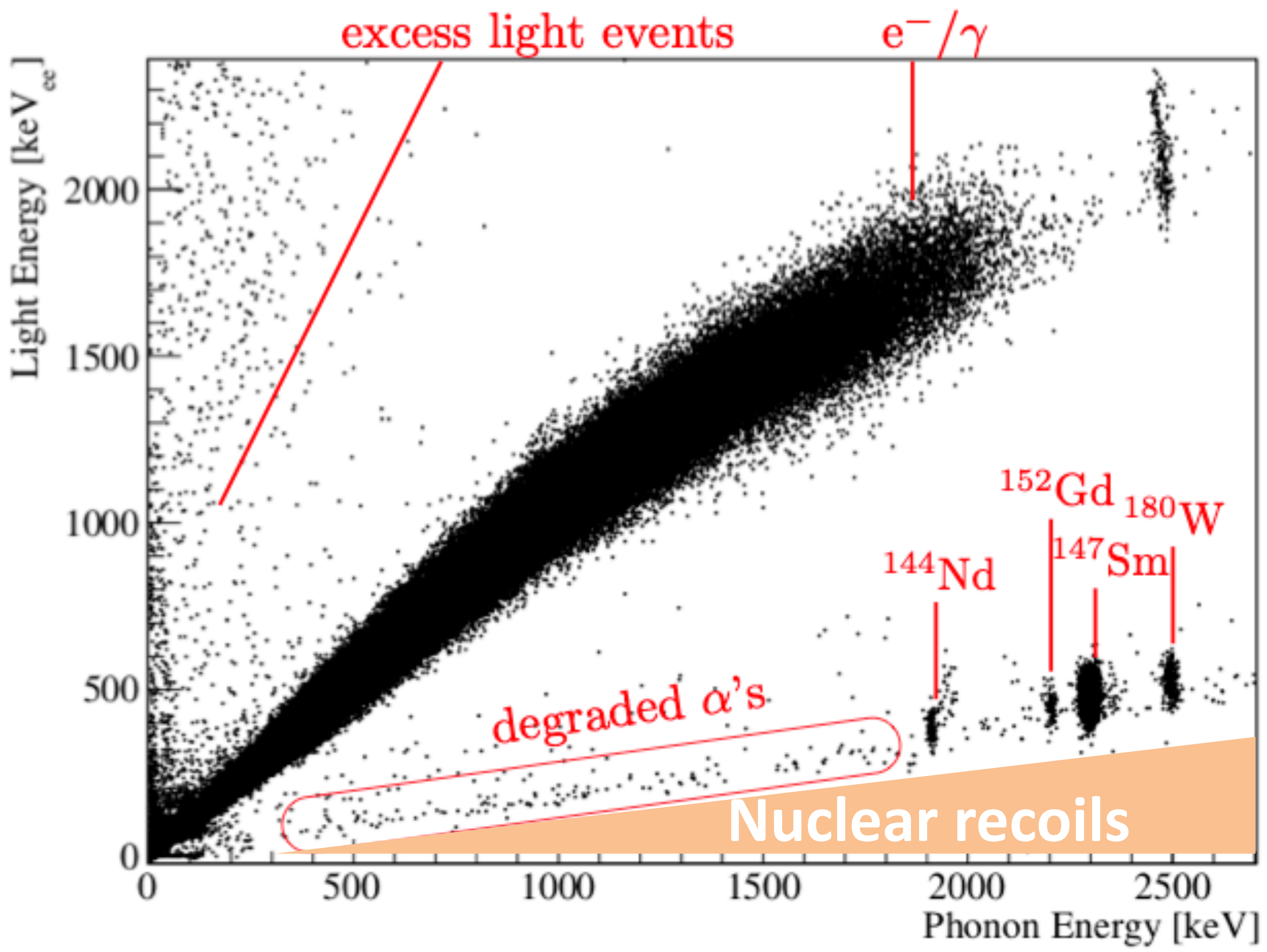

Munster *et al.*, arXiv:1403.5114

Nuclear Recoil with Scintillating Bolometer

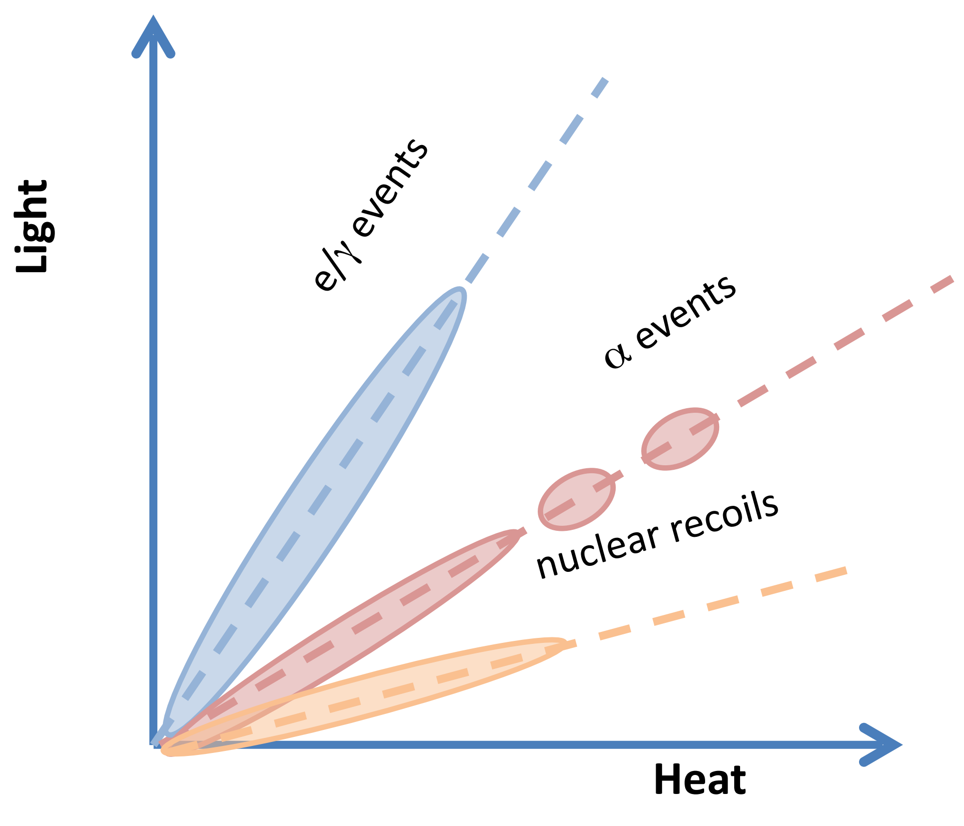

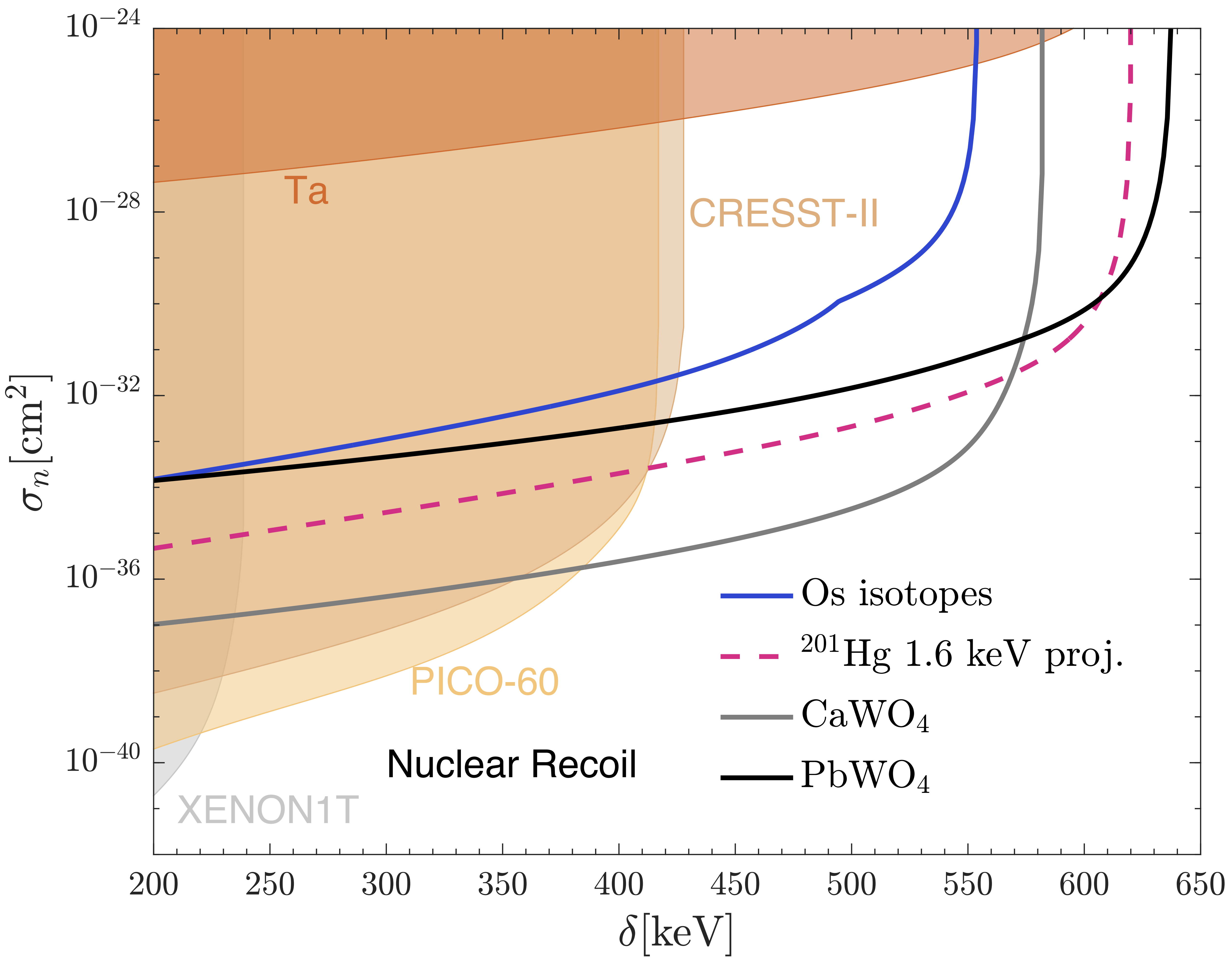

$M_\chi = 1\ \mathrm{TeV}$

NS, Nagorny, Vincent, PRD/2104.09517

Skylab and Ohyia

	Skylab	**Ohya**
Area A	$1.17\ m^2$	$2442\ m^2$
Duration t	0.70 yr	2.1 yr
Zenith cutoff angle	$\theta_D = 60°$	$\theta_D = 18.4°$
Detector material	0.25 mm thick Lexan $\times$ 32 sheets	1.59 mm thick CR-39 $\times$ 4 sheets
Detector density	1.2 g cm^{-3} Lexan	1.3 g cm^{-3} CR-39
Detector length at θ_D	1.6 cm	0.66 cm
Overburden density	2.7 g cm^{-3} Aluminum	2.7 g cm^{-3} Rock
Overburden length at θ_D	0.74 cm	39 m

Constraints on Multiple Scattering Dark Matter

$$\frac{dE}{dx}\bigg|_{th} = \frac{2E_i}{m_\chi}\left(\sum_{A\subset D}\frac{\mu_{\chi A}^2}{m_A}n_A\sigma_{\chi A}\right)\exp\left[\frac{-2}{m_\chi}\left(x_O\sum_{A\subset O}n_A\frac{\mu_{\chi A}^2}{m_A}\sigma_{\chi A}+x_D\sum_{A\subset D}n_A\frac{\mu_{\chi A}^2}{m_A}\sigma_{\chi A}\right)\right]$$

Contact interaction

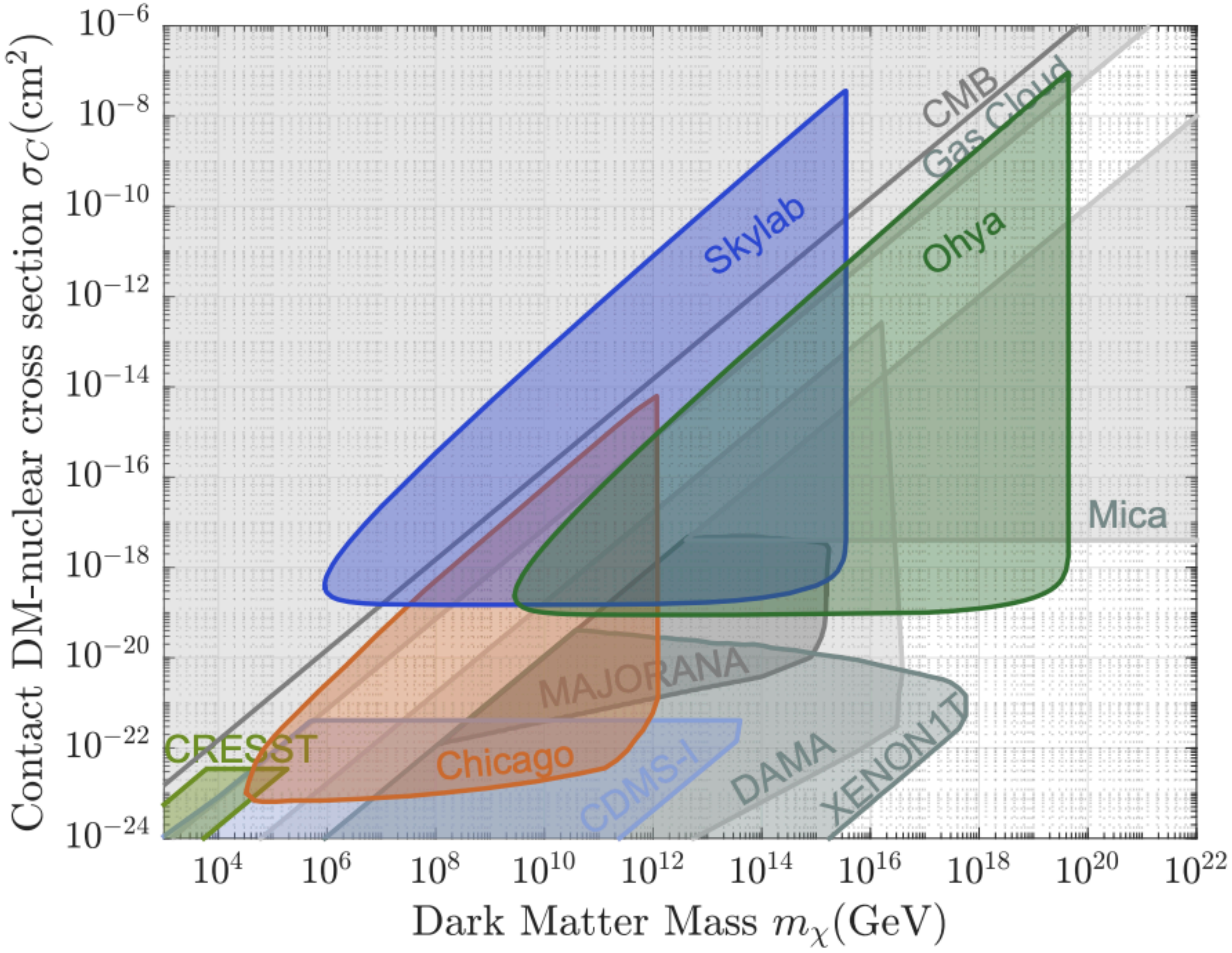

Bhoonah, Bramante, Courtman, **NS**, PRD/2012.13406

Multiple Scatter Dark Matter

DEAP collaboration, arXiv:2108.09405

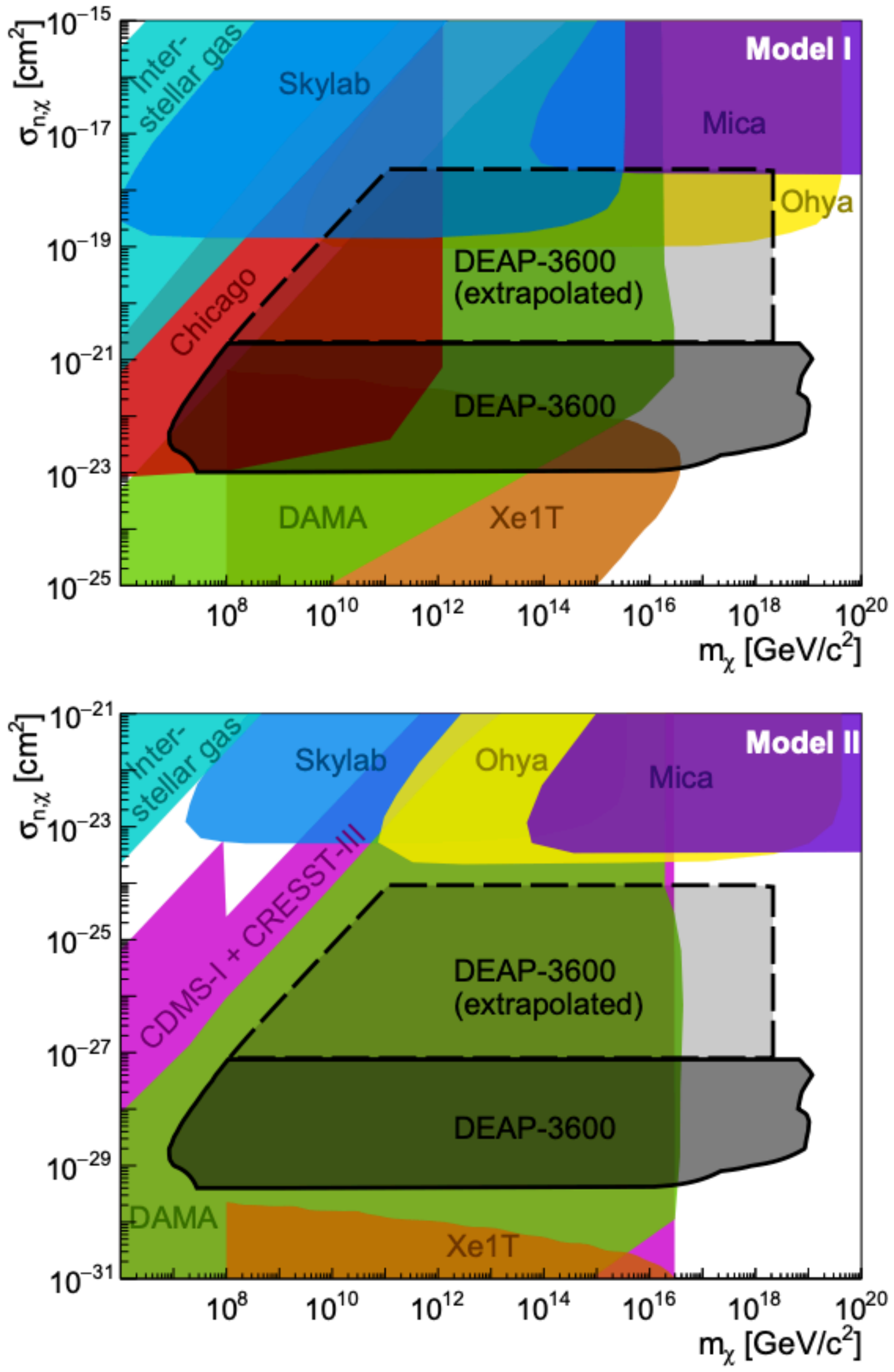

$$\frac{d\sigma_{\mathrm{T}\chi}}{dE_R} = \frac{d\sigma_{\mathrm{n}\chi}}{dE_R}|F_{\mathrm{T}}(q)|^2$$

$$\frac{d\sigma_{\mathrm{T}\chi}}{dE_R} = \frac{d\sigma_{\mathrm{n}\chi}}{dE_R}\left(\frac{\mu_{T\chi}}{\mu_{n\chi}}\right)^2 A^2|F_{\mathrm{T}}(q)|^2$$
$$\simeq \frac{d\sigma_{\mathrm{n}\chi}}{dE_R}A^4|F_{\mathrm{T}}(q)|^2,$$

Dark matter may even scatter multiple times in the detector!

Isospin-violating Dark Matter

Isospin-independent interaction

$$\sigma_j \simeq \frac{\mu_{A_j}^2}{\mu_N^2} A^2 \sigma_0$$

Isospin-violating interaction

$$\sigma_j \simeq \frac{\mu_{A_j}^2}{\mu_N^2} f_{\mathrm{IV}}^2 \sigma_0 \qquad f_{\mathrm{IV}} \equiv f_p Z_j + f_n (A_j - Z_j)$$

Reduced Detector Response

SI $\sigma_j \simeq \frac{\mu_{A_j}^2}{\mu_N^2} A^2 \sigma_0$

IVDM $\sigma_j \simeq \frac{\mu_{A_j}^2}{\mu_N^2} f_{\mathrm{IV}}^2 \sigma_0$

$$R_\sigma = \frac{\sum_j N_j \mu_{A_j}^2 f_{\mathrm{IV}}^2}{\sum_j N_j \mu_{A_j}^2 A_j^2}$$

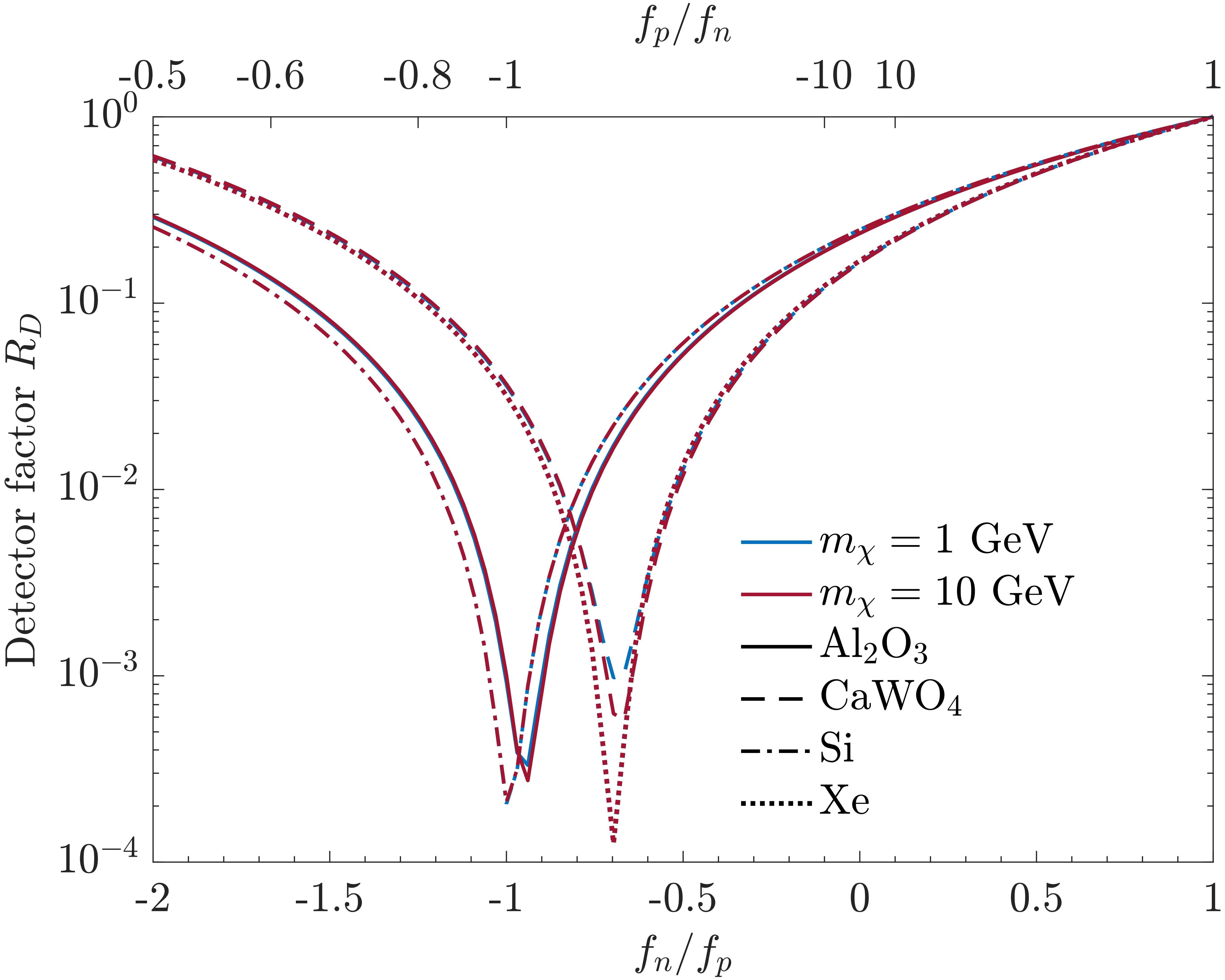

Reduced Overburden

SI $$\sigma_j \simeq \frac{\mu_{A_j}^2}{\mu_N^2} A^2 \sigma_0$$

IVDM $$\sigma_j \simeq \frac{\mu_{A_j}^2}{\mu_N^2} f_{\mathrm{IV}}^2 \sigma_0$$

$$R_{\mathrm{OF}} = \frac{\sum_j n_j \mu_{A_j}^4 f_{\mathrm{IV}}^2 / m_{A_j}}{\sum_j n_j \mu_{A_j}^4 A_j^2 / m_{A_j}}$$

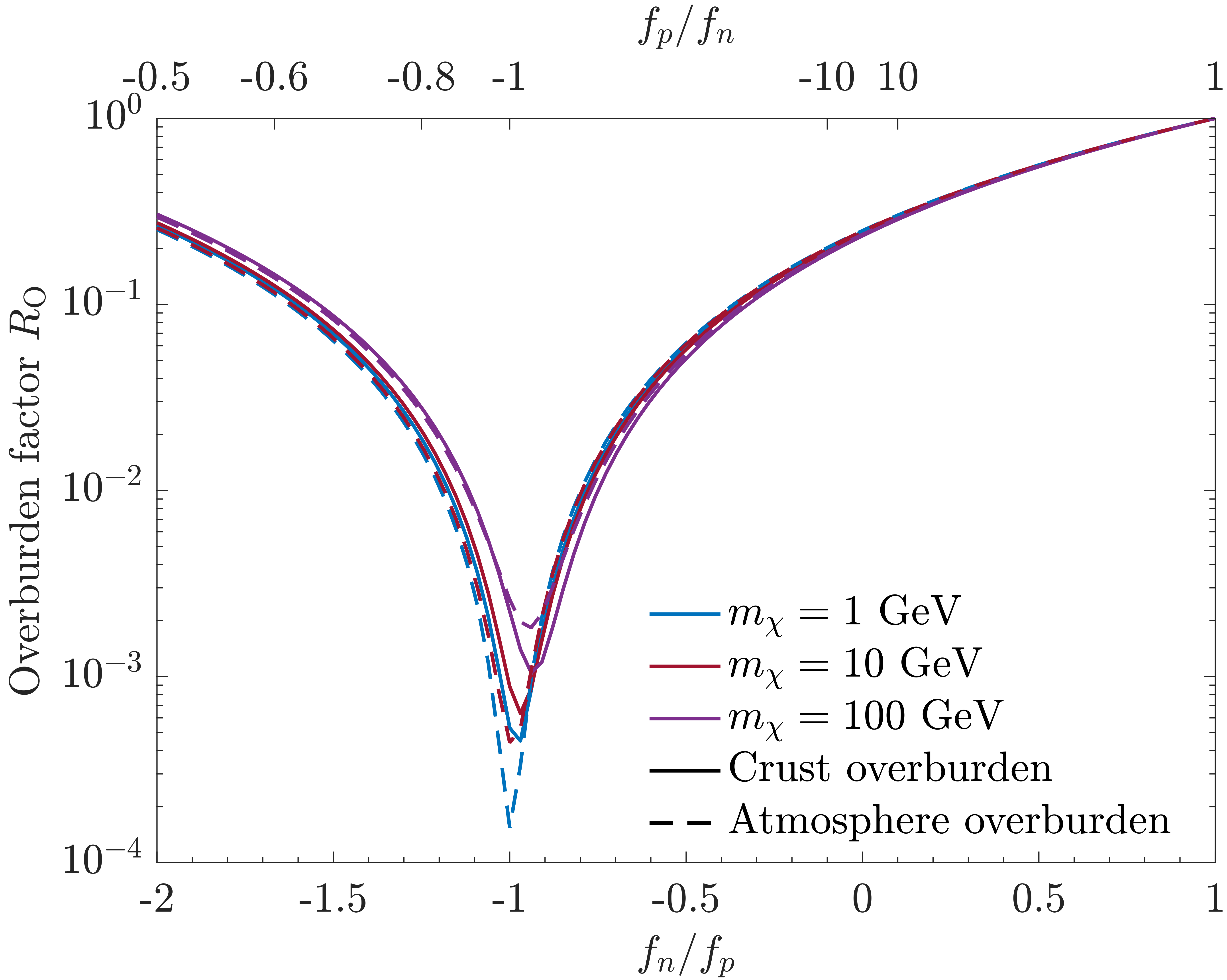

Constraints on Isospin-violating Dark Matter

Coupling to protons

Isospin conserving

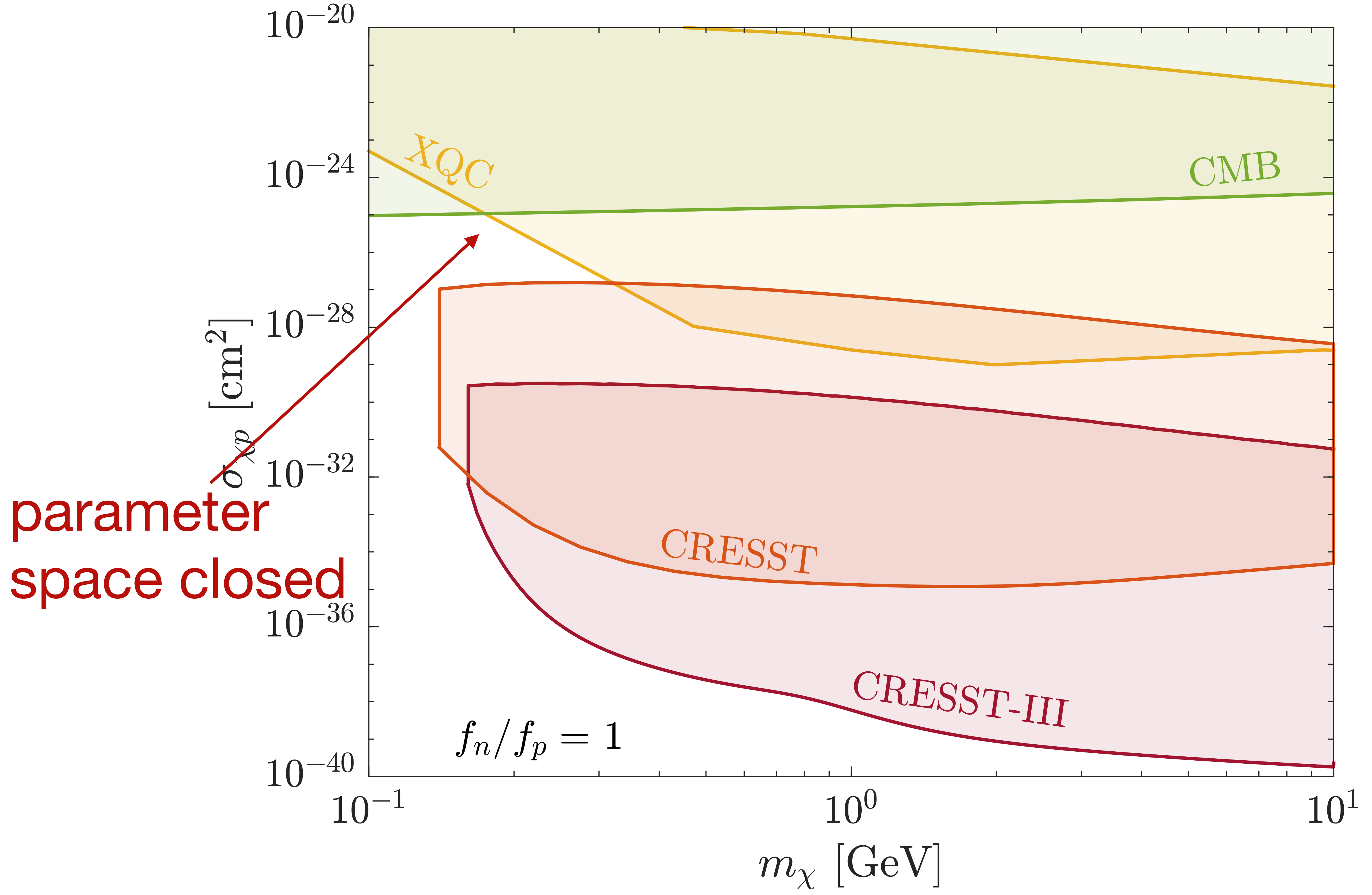

Isospin violating

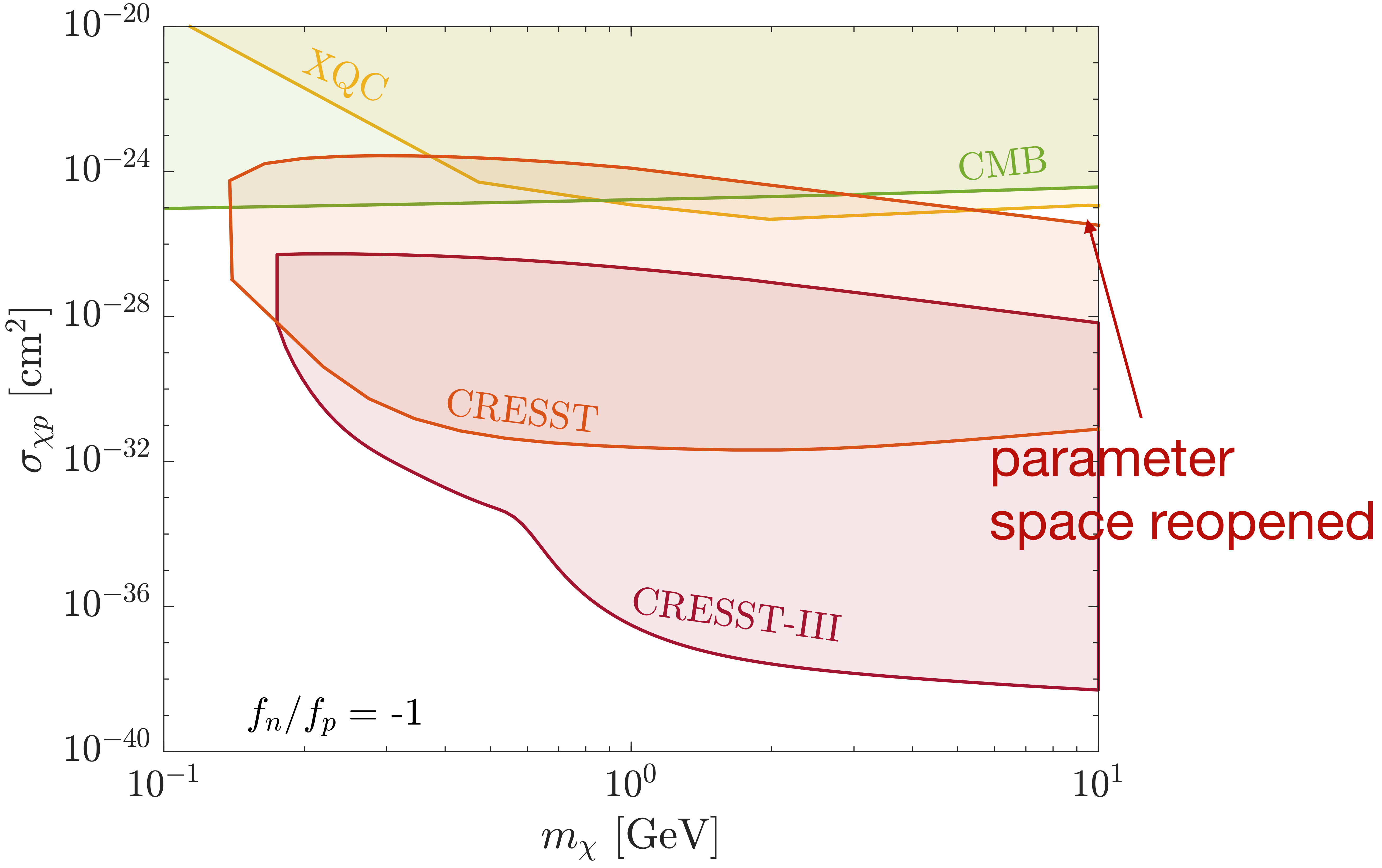

Kumar, Marfatia, **NS**, 2312.11365

Phonon Structure of Sapphire

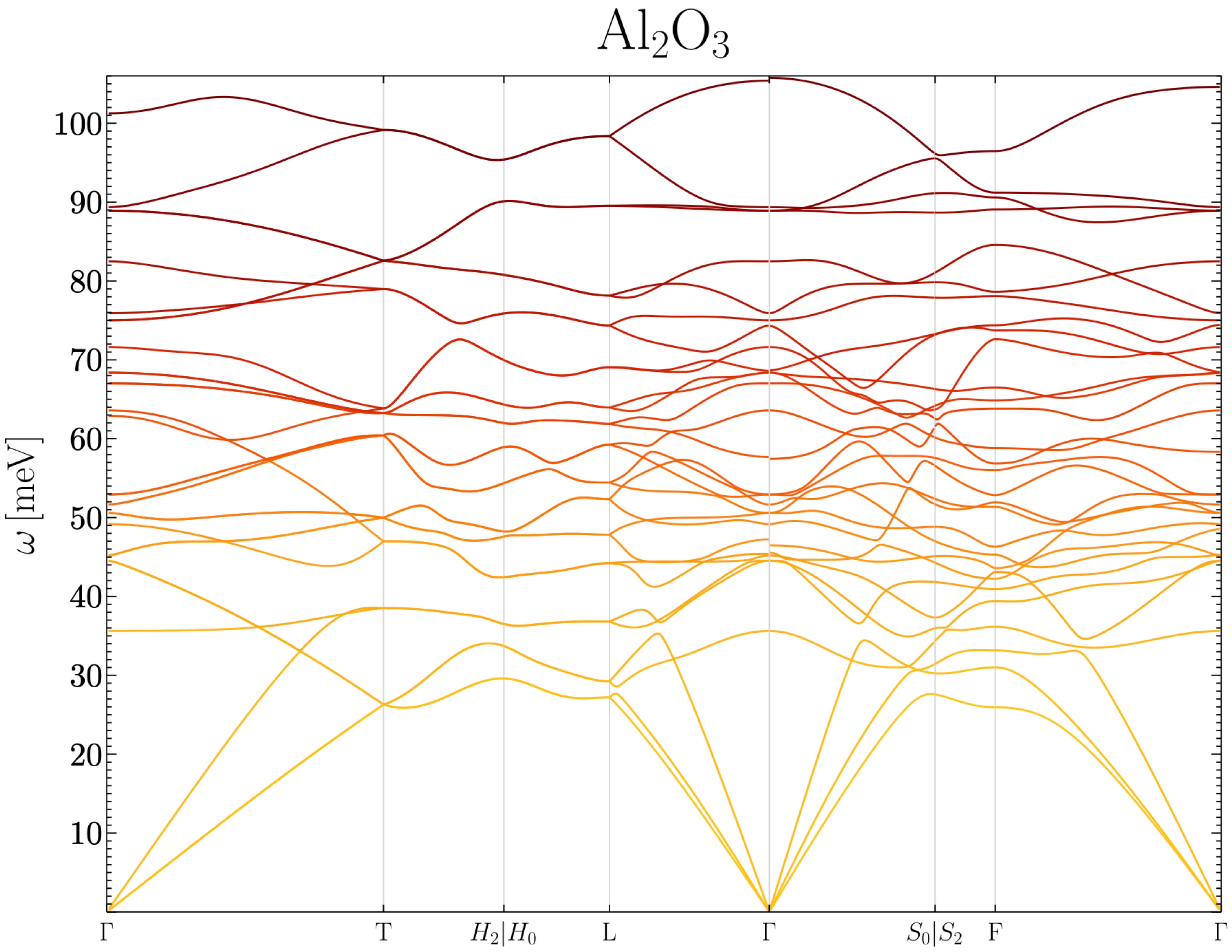

Constraints from CMB

$$\left.\frac{d^2E}{dV\,dt}\right|_{\rm inj} = \frac{f_\bullet f_{\rm e.m.}\rho_c\Omega_{\rm CDM}(1+z)^3}{M_i}\frac{dM}{dt}$$

Fraction of BH energy injection as $e^{\pm}$ and γ

$$\left.\frac{d^2E}{dV\,dt}\right|_{{\rm dep},c}(z) = h_c(z)\left.\frac{d^2E}{dV\,dt}\right|_{\rm inj}(z)$$

The injected energy is then deposited at different redshift z, in the form of ionization, excitation of the Lyman-α transition and heating of the intergalactic medium

Constraints from CMB

- BH evaporation during and after recombination leads to high energy electrons and photons, which rescatter CMB photons, suppressing the angular power spectrum on small scales

- Polarized Thomson scattering enhances EE power spectrum at lower multiples

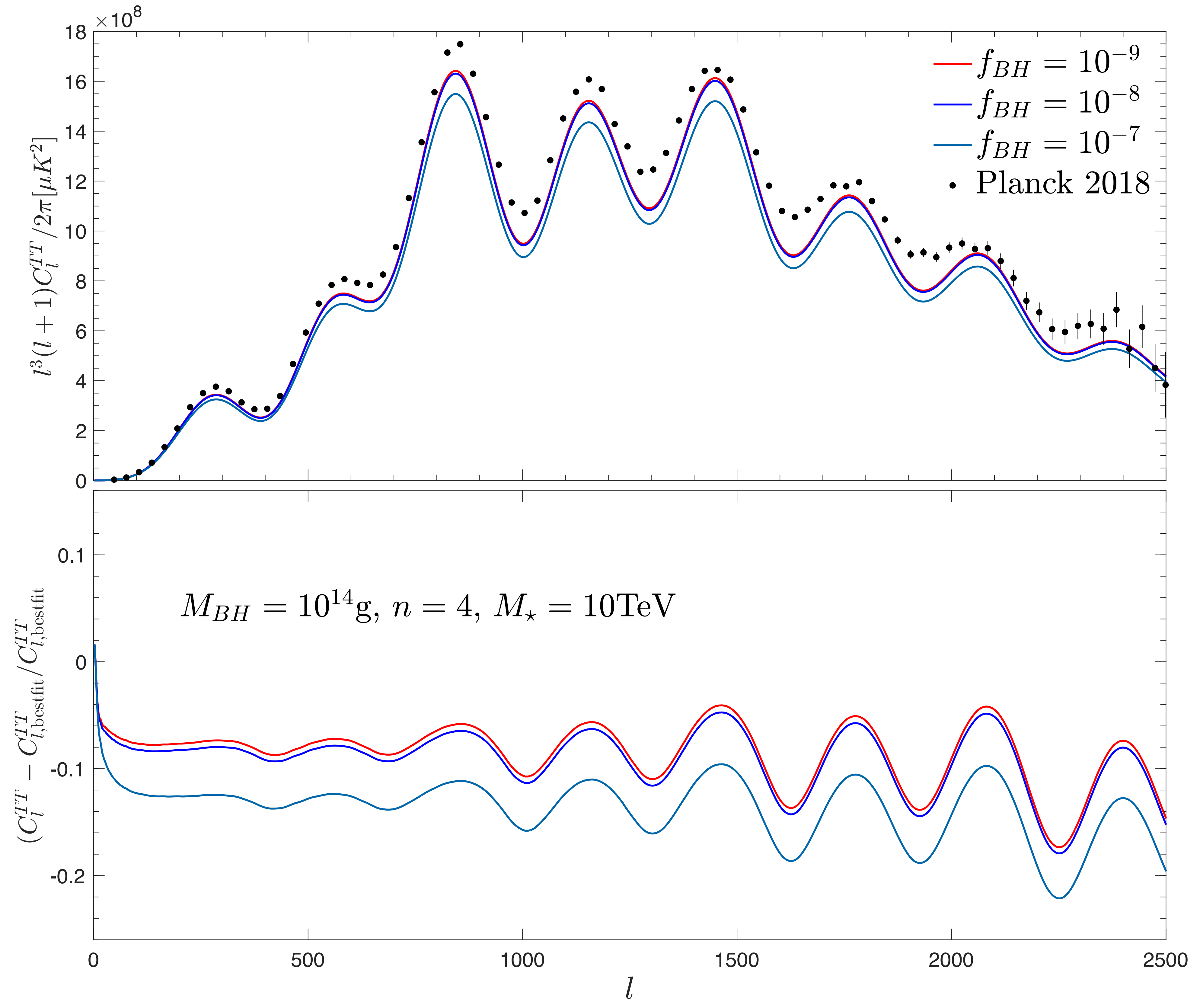

Planck 2018 high-l TT,TE, EE+low-l TT, EE+Planck lensing

Friedlander, Mack, **NS**, Schon, Vincent, PRD/2201.11761

Axion Conversion in Neutron Star

- Magnetized neutron star atmosphere—magnetosphere

$$n_{\rm GJ}(\mathbf{r}_{\rm NS}) = \frac{2\boldsymbol{\Omega}\cdot\mathbf{B}_{\rm NS}}{e}\frac{1}{1-\Omega^2 r^2 \sin^2\theta_{\rm NS}}$$

- Conversion probability

$$p = \frac{g_{a\gamma\gamma}^2 B^2}{2k|\omega_p'|}\frac{\pi m_a^5}{(k^2+m_a^2\sin^2\theta)^2}\sin^2\theta$$

Hook et al 1804.03145

Millar et al 2107.07399

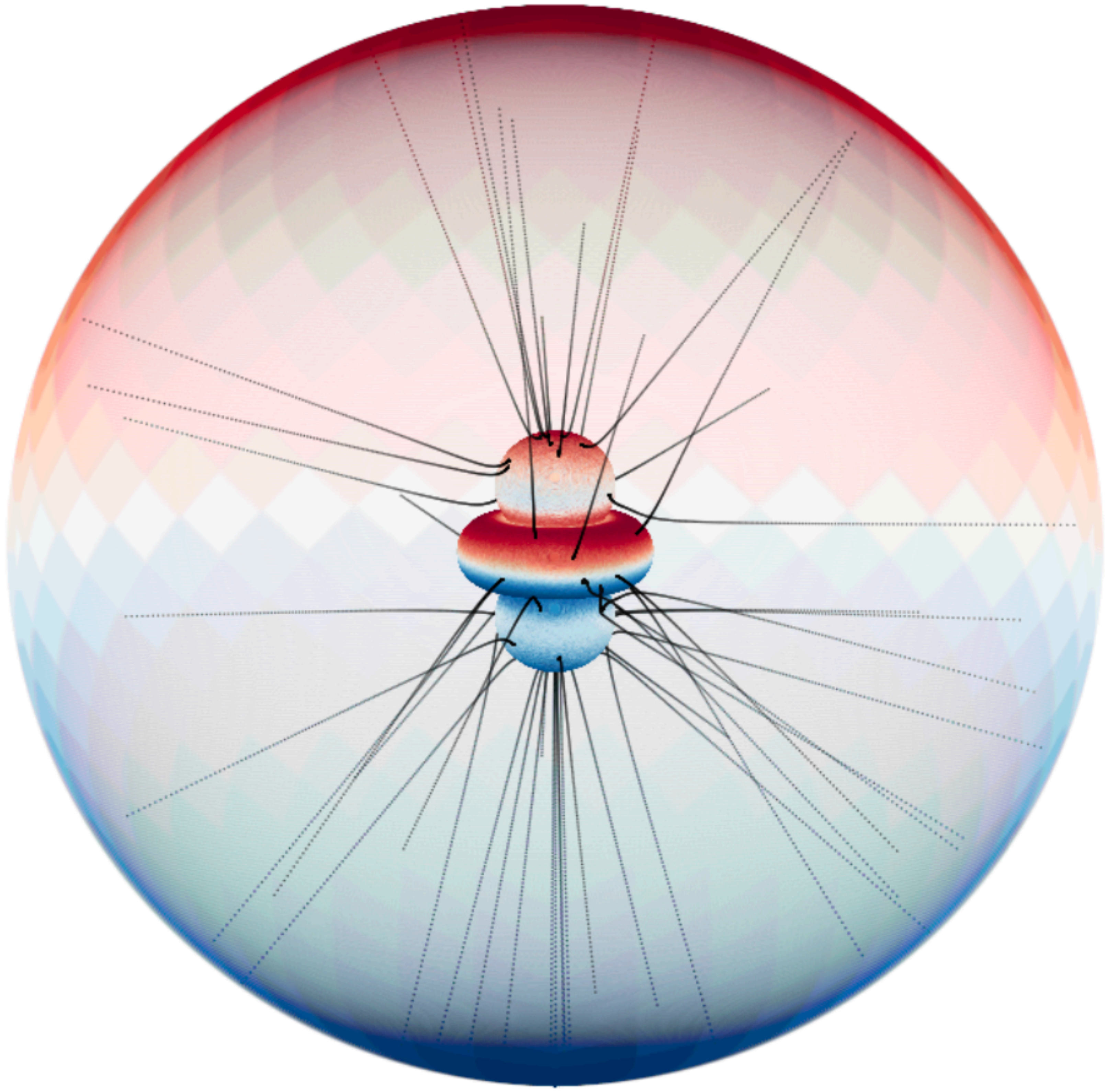

Witte et al 2104.07670

Signals from the Galactic Centre

$$S_{\rm sig} = \frac{1}{\mathcal{B} d^2} \frac{dP}{d\Omega} > S_{\rm min}$$

Signals from a single star $\delta f / f \sim v^2 \sim 10^{-6}$

Signals from stellar population $\delta f / f \sim v \sim 10^{-3}$

$$\omega_{\rm obs} = \omega \sqrt{\frac{1 - v_{\rm l.o.s}}{1 + v_{\rm l.o.s}}}$$

Doppler shift can be important!

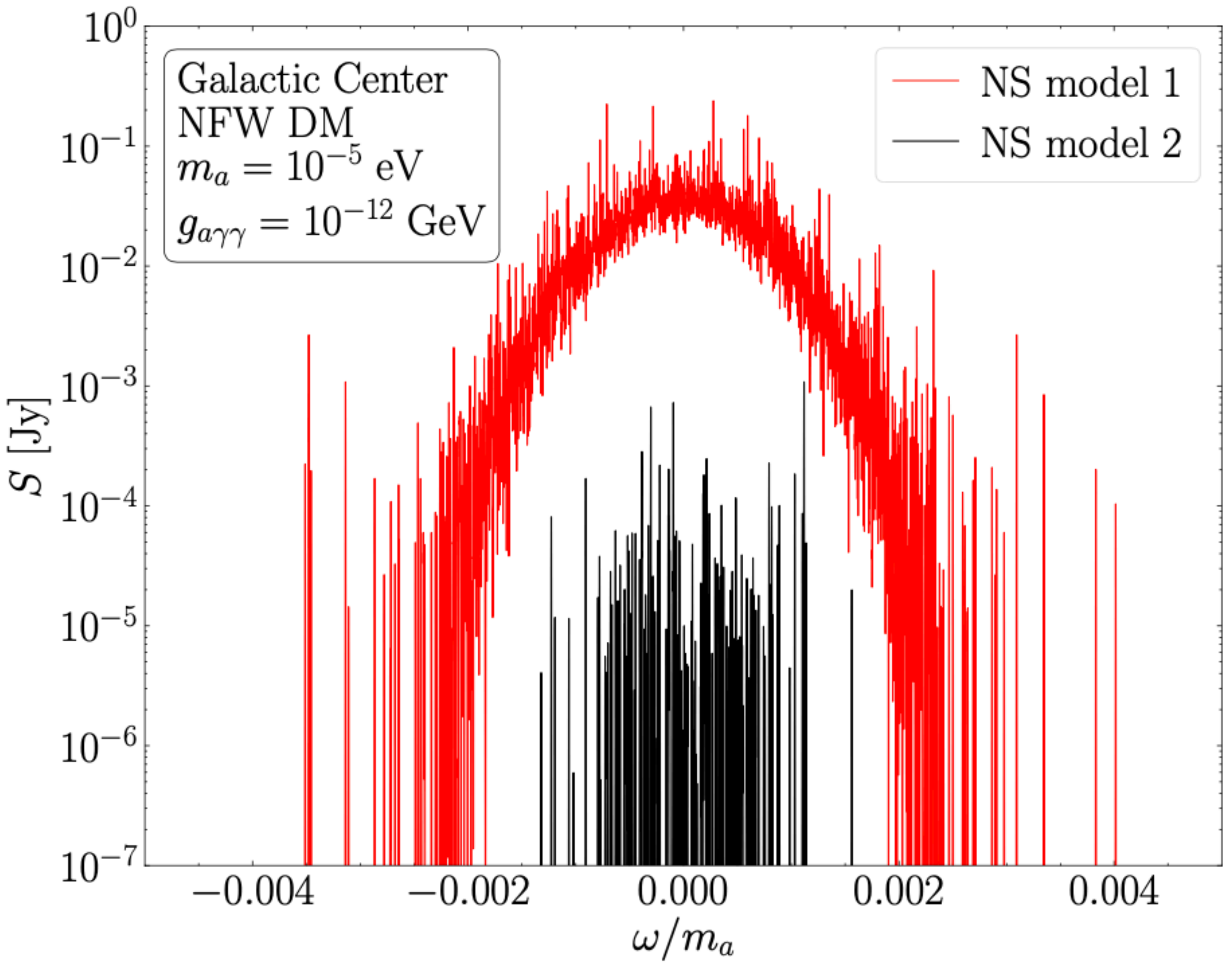

Safdi et al 1811.01020

Greybody spectra

4D BHs

$$-\frac{dM_{\bullet\to i}}{dt} = \frac{g_i}{2\pi^2}\int \frac{E\sigma_i(r_h E)}{\exp(E/T_H)\mp 1}p^2 dp$$

Scalar

Fermion

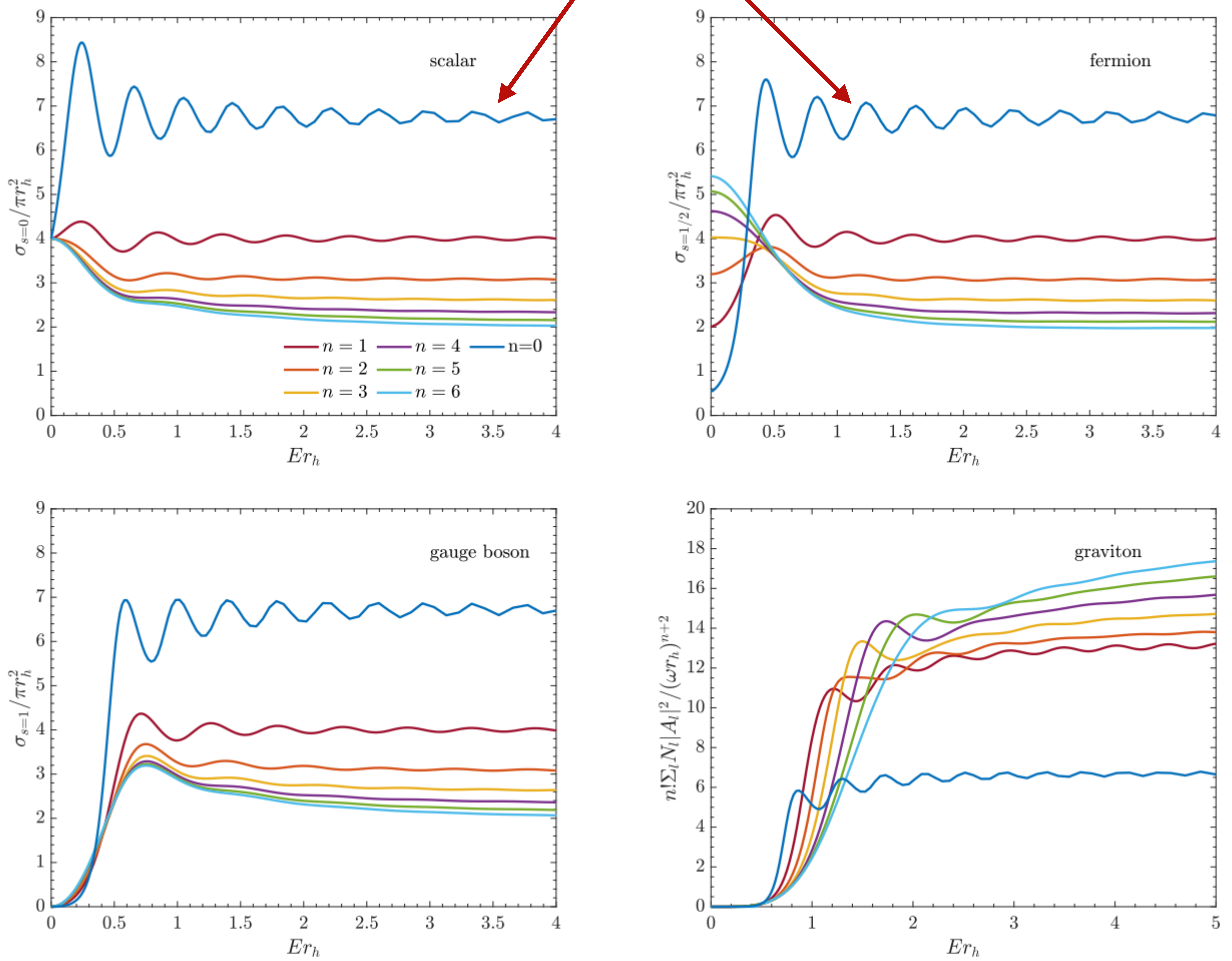

Vector

Graviton

Energy

Monte Carlo vs Single Scatter

$$C_{\oplus}^{\rm weak} = \sum_j \frac{\rho_\chi}{m_\chi} \int_0^{R_\oplus} 4\pi r^2 \int_0^\infty du_\chi f(u_\chi) \frac{w(r)}{u_\chi} \int_0^{v_e(r)} R_j^-(w \to v) |F_j(q)|^2 dv \,.$$

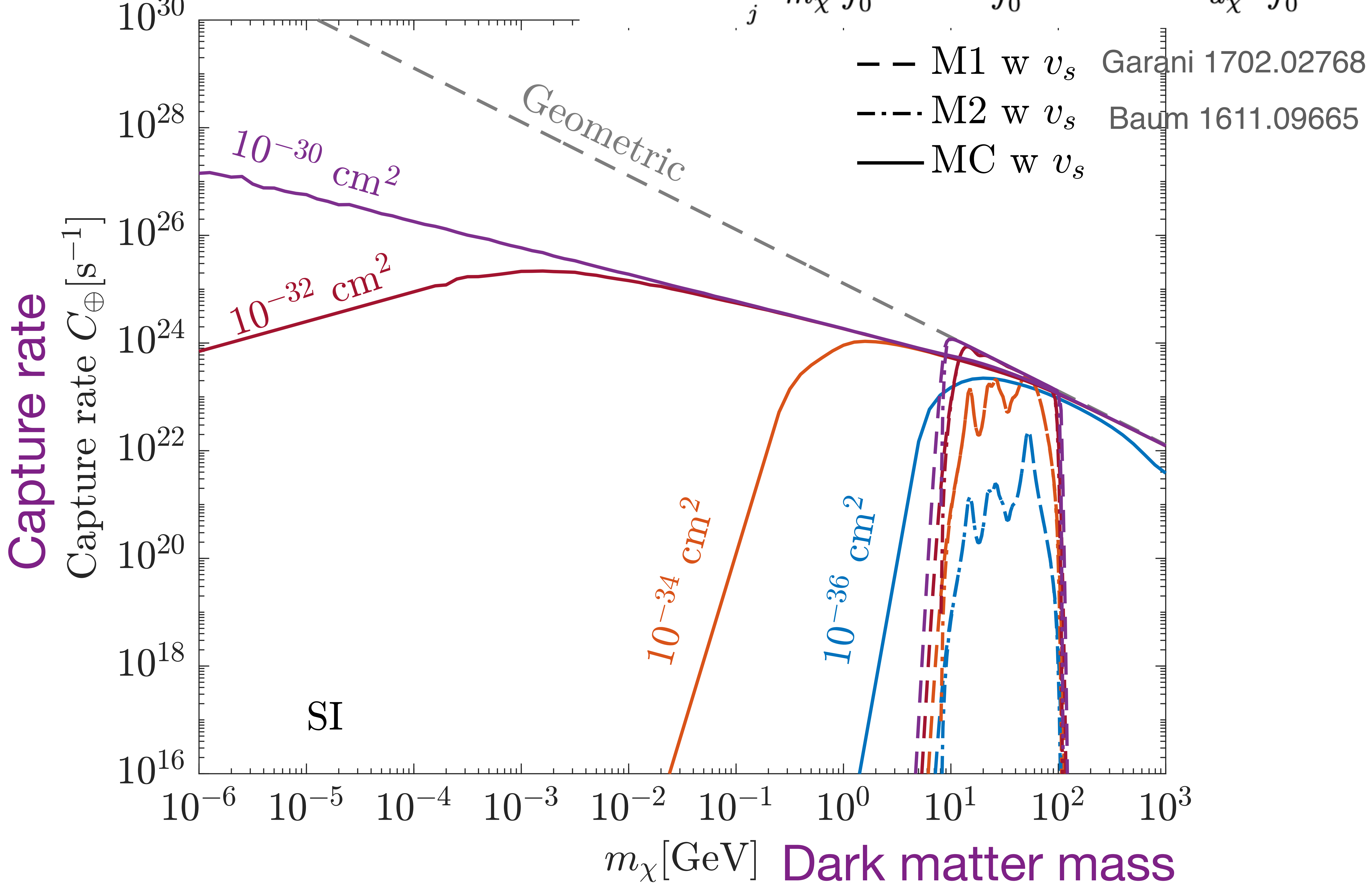

Monte Carlo vs Multi Scatter

$$C_N = f_{\rm cap}\pi R^2 p_N(\tau)\frac{\sqrt{6}\rho_\chi}{3\sqrt{\pi}m_\chi v_\chi}\left[(2v_\chi^2+3v_{\rm esc}^2)-(2v_\chi^2+3v_N^2)\exp\left(-\frac{3(v_N^2-v_{\rm esc}^2)}{2v_\chi^2}\right)\right]$$

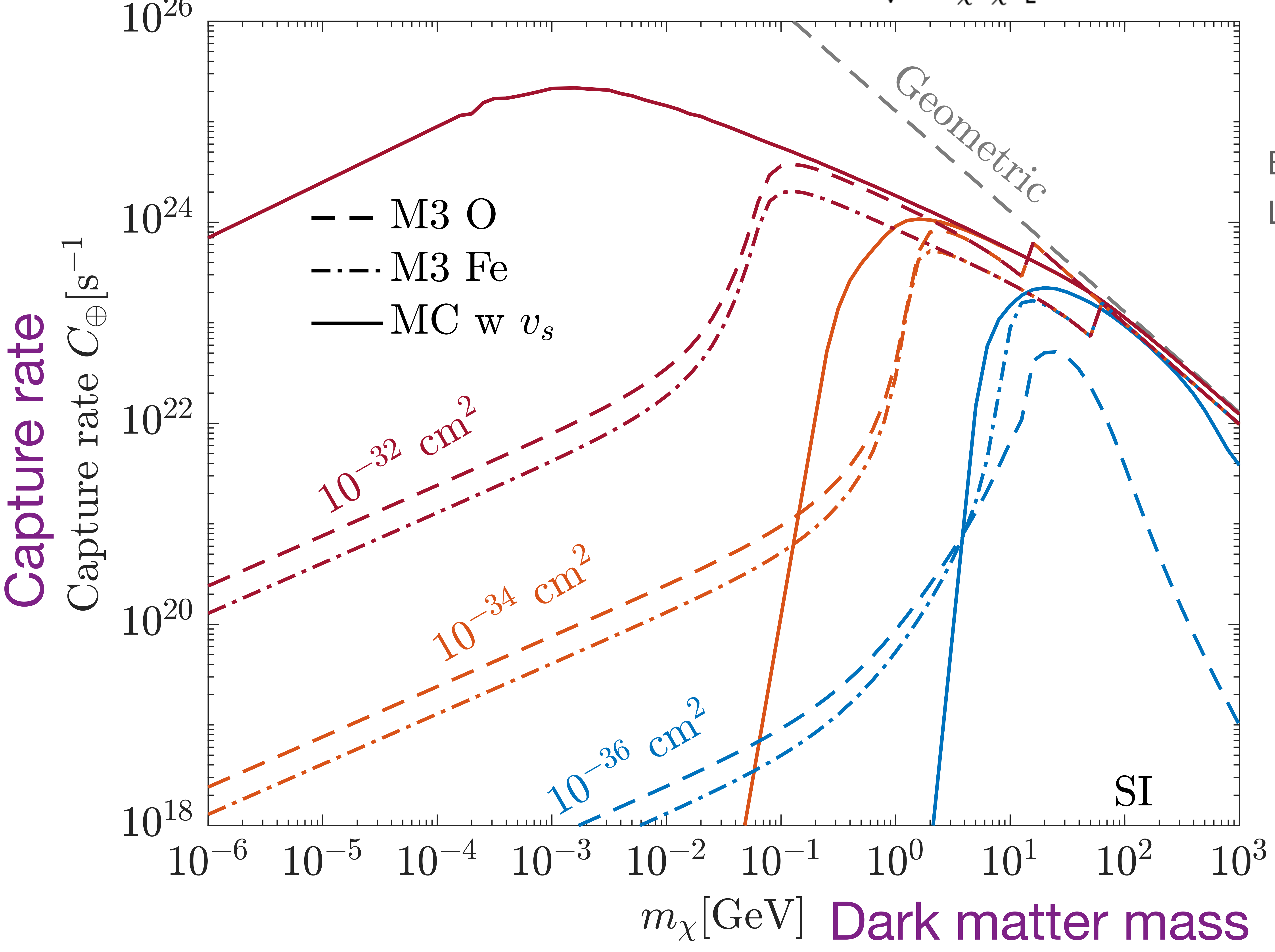

Bramante 1703.04043

Leane 2209.09834

Dark Matter Distribution

$$\frac{n_\chi(r)}{n_\chi(0)} = \left(\frac{T_\oplus(r)}{T_\oplus(0)}\right)^{3/2} \exp\left(-\int_0^r \left[\alpha(r')\frac{dT_\oplus(r')}{dr'} + m_\chi \frac{d\phi(r')}{dr'}\right] T_\oplus^{-1} dr'\right)$$

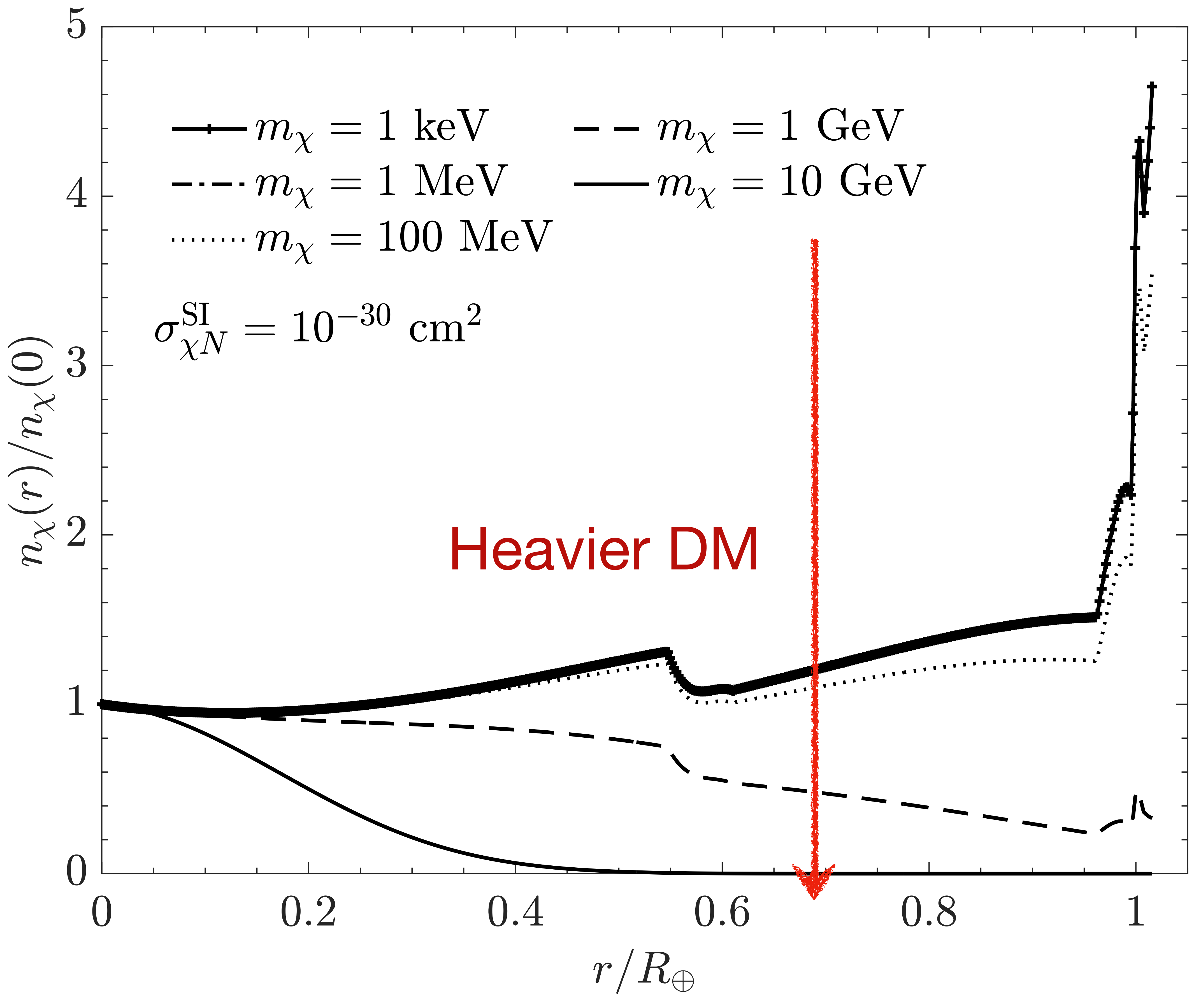

When $\sigma_{\chi N}^{SI} \gtrsim 10^{-36}$ cm^2, dark matter thermalizes with local environment due to frequent scattering

Garani 1702.02768

Heavier dark matter sinks down, lighter dark matter float

Isotropic Gamma Ray Background

direct evaporation

positron annihilation

$$\frac{d^2N_\gamma}{dEdt}(E,M) = \frac{d^2N_{\gamma,\mathrm{evap}}}{dEdt}(E,M) + \frac{d^2N_{\gamma,\mathrm{pos}}}{dEdt}(E,M) + \frac{d^2N_{\gamma,\mathrm{ics}}}{dEdt}(E,M)$$

Inverse Compton scattering

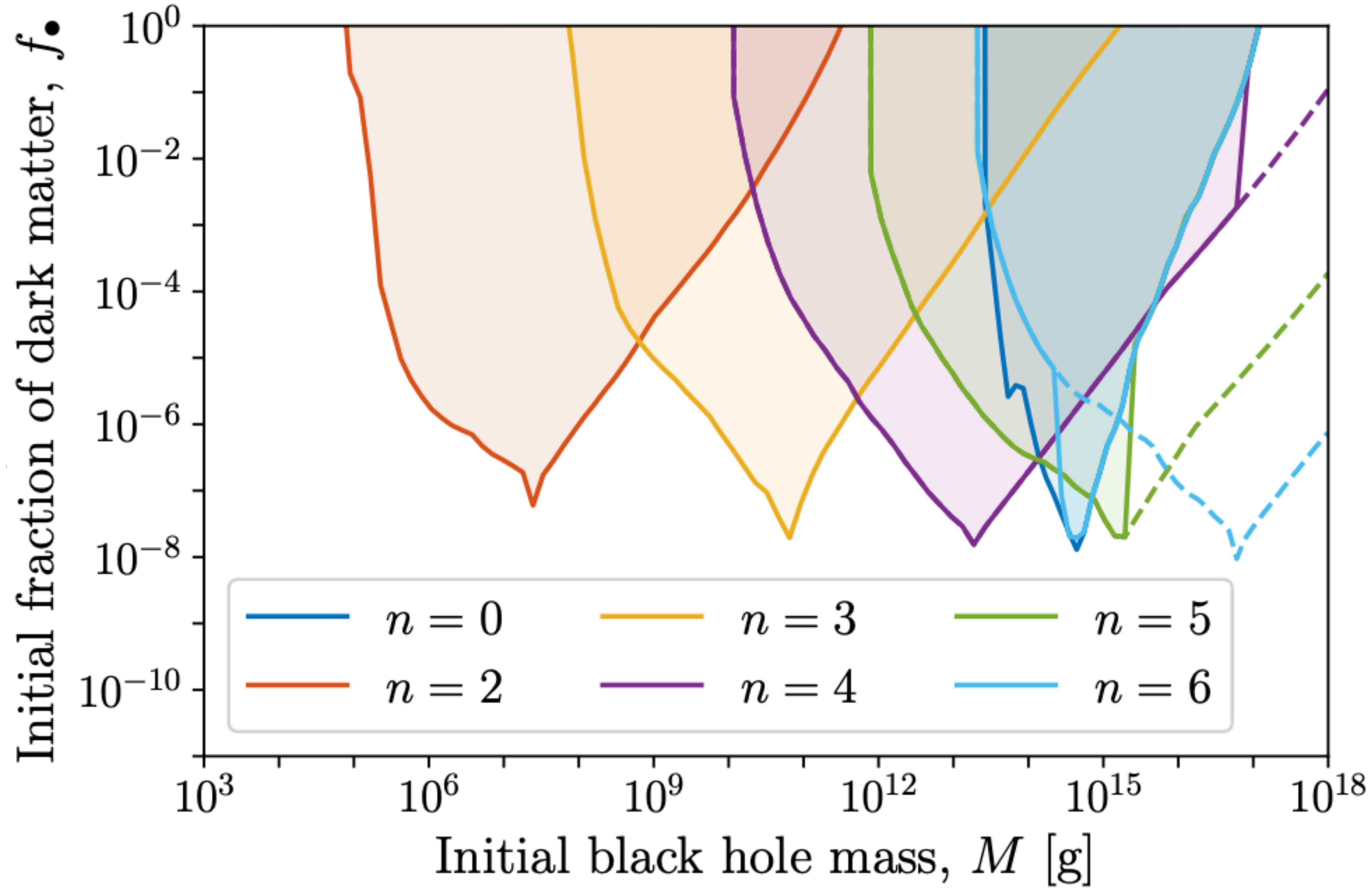

Friedlander, Mack, **NS**, Schon, Vincent, PRD/2201.11761

Dark Photon

Extra $U(1)$? $SU(3)_c \times SU(2)_L \times U(1)_Y \times U(1)'$

Pospelov' 2008
Ackerman, Buckley, Carrol, Kamionkowsk' 2008
Arkani-Hame, Finkbeine, Slatyer, Weiner' 2008

$$\mathscr{L} = -\frac{1}{4}(F_{\mu\nu}F^{\mu\nu} - 2\kappa F_{\mu\nu}F'^{\mu\nu} + F'_{\mu\nu}F'^{\mu\nu}) + \frac{m_{A'}^2}{2}A'_\mu A'^\mu - J^\mu A_\mu$$

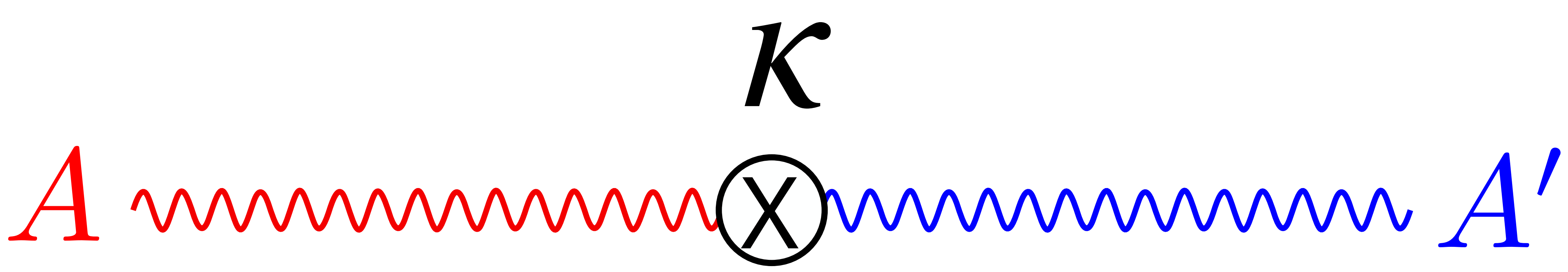

$\omega^2 \sim k^2 + \omega_p^2$

$\omega^2 = k^2 + m_{A'}^2$

Resonant Dark Photon Conversion

- Resonant conversion from dark photon to photon in the magnetosphere of a neutron star when $m_{A'} \sim \omega_p$

No magnetic field need!

- Redefine $A_\mu \to A_\mu + \kappa A'_\mu$ to remove the mixing,

$$\mathscr{L} = -\frac{1}{4}(F_{\mu\nu}F^{\mu\nu} + F'_{\mu\nu}F'^{\mu\nu}) + \frac{1}{2}m_{A'}^2 A'_\mu A'^\mu - (A_\mu + \kappa A'_\mu)J^\mu$$

- Equation of motion

$$(\omega^2 + \nabla^2)\boldsymbol{A} - \nabla(\nabla\cdot\boldsymbol{A}) + \omega^2(\boldsymbol{\chi}^p + \boldsymbol{\chi}^{\text{vac}})\cdot(\boldsymbol{A} + \kappa\boldsymbol{A}') = 0$$
$$(\omega^2 + \nabla^2)\boldsymbol{A}' - m_{A'}^2\boldsymbol{A}' + \kappa\omega^2(\boldsymbol{\chi}^p + \boldsymbol{\chi}^{\text{vac}})\cdot\boldsymbol{A} = 0$$

$$\boldsymbol{\epsilon} = 1 + \boldsymbol{\chi}^p = R_\theta^{yz}\cdot\begin{pmatrix}\varepsilon & ig & 0\\ -ig & \varepsilon & 0\\ 0 & 0 & \eta\end{pmatrix}\cdot R_{-\theta}^{yz}$$

Resonant Dark Photon Conversion

$$(\omega^2 + \partial_z^2)A_x - \partial_x\partial_z A_z + \omega^2 a\bar{A}_x = 0\,,$$
$$(\omega^2 + \partial_z^2)A_y - \partial_y\partial_z A_z + \omega^2[(\eta'\sin^2\theta + a + q\sin\theta^2)\bar{A}_y - (\eta' + q)\cos\theta\sin\theta\bar{A}_z] = 0\,,$$
$$\omega^2 A_z - \partial_x\partial_z A_x - \partial_y\partial_z A_y + \omega^2[-(\eta' + q)\cos\theta\sin\theta\bar{A}_y + (\eta'\cos^2\theta + a + q\cos^2\theta)\bar{A}_z] = 0\,.$$

- Conversion probability

$$p \simeq \frac{|\tilde{A}_y|^2 + |\tilde{A}_z|^2}{|\tilde{A}'_x|^2 + |\tilde{A}'_y|^2 + |\tilde{A}'_z|^2} \simeq \frac{\pi\kappa^2\omega_p^3(m_{A'}^2\cos\theta - \omega_p^2\sin^3\theta)^2}{6km_{A'}^4\omega'_p\sin^2\theta}$$

- The converted photon has both transverse and longitudinal polarizations, and evolves in the direction that is perpendicular to the magnetic field

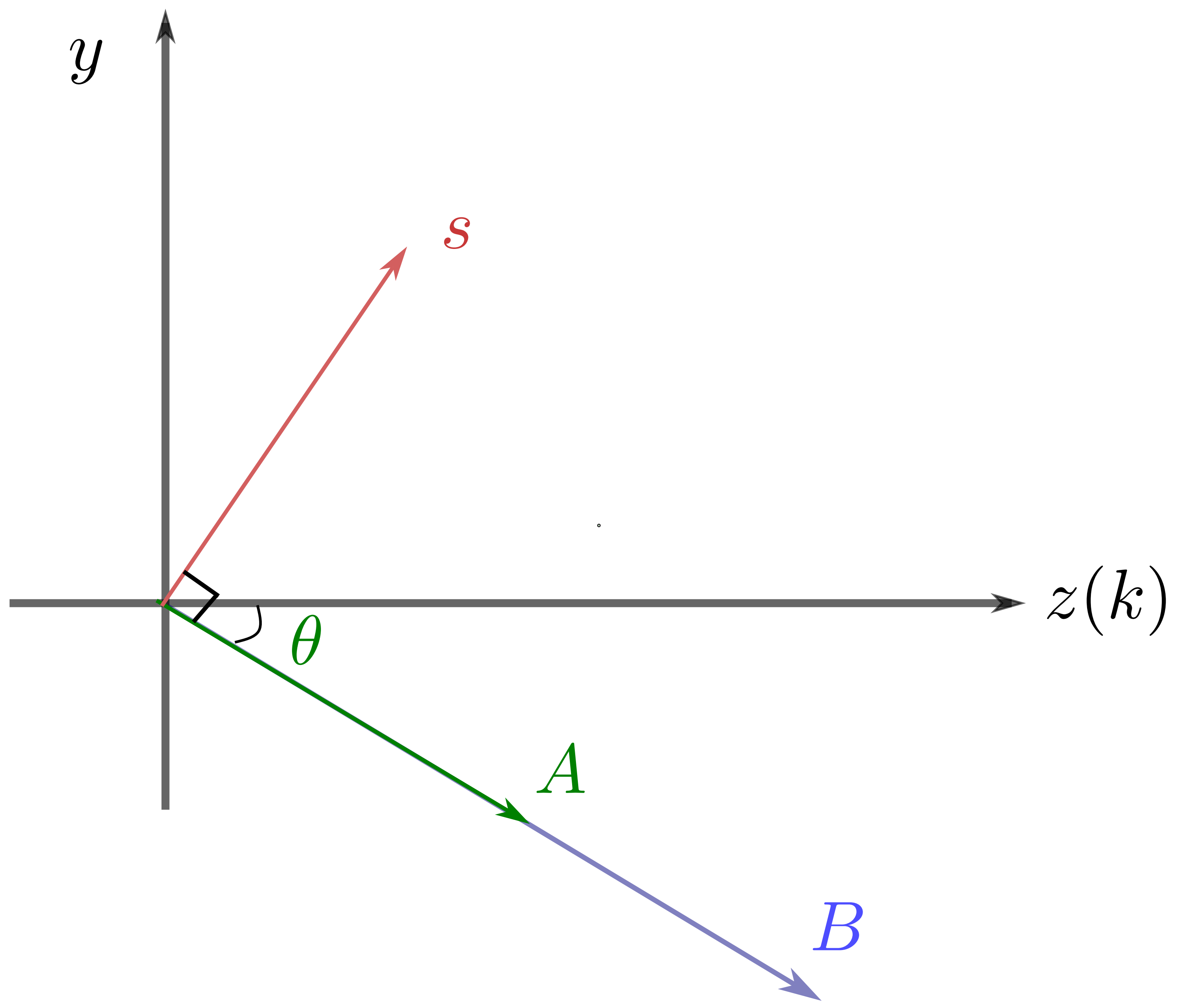

Compact Stars in the Galactic Centre

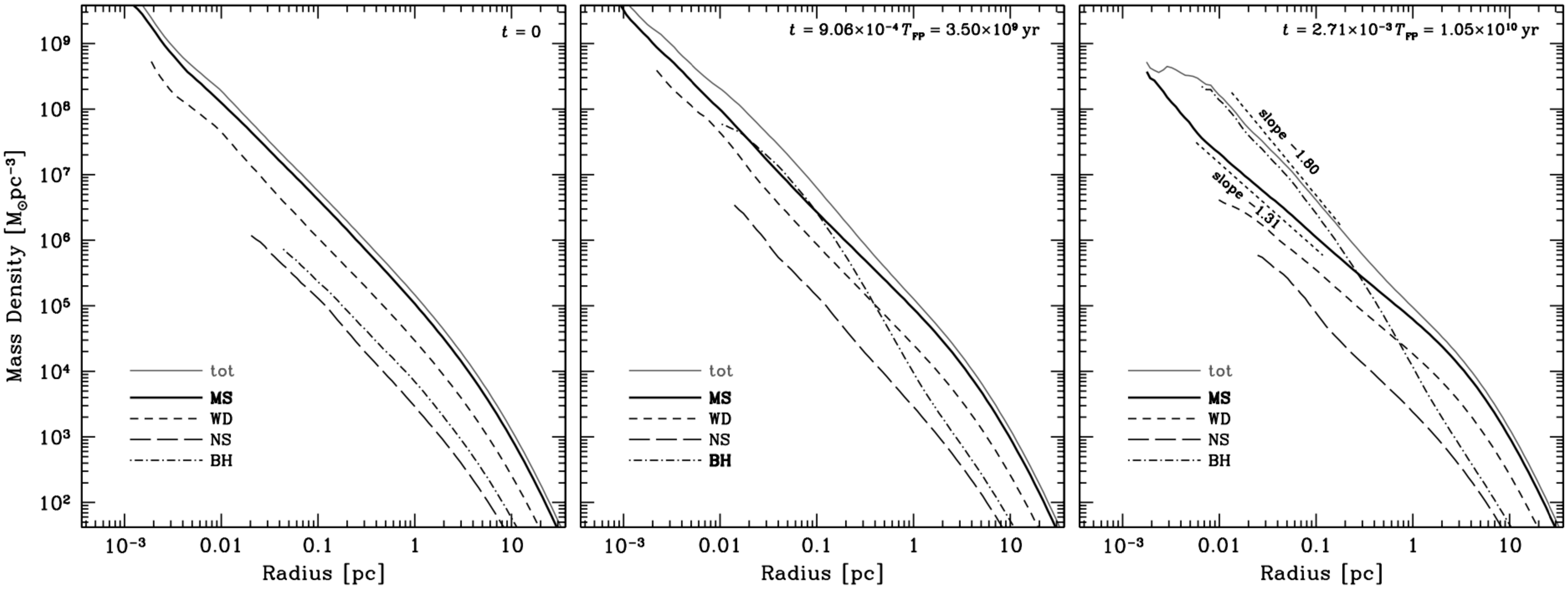

Freitag et al 2006

Radio Telescopes

Minimum detectable signal flux density

$$S_{\rm min} = \frac{\rm SEFD}{\eta\sqrt{n_{\rm pol}\mathscr{B}t_{\rm obs}}}$$

$$\text{SEFD} = 2k_B\frac{T_{\rm sys}}{A_{\rm eff}} = 2.75\ \text{Jy}\frac{1000\ \text{m}^2/\text{K}}{A_{\rm eff}/T_{\rm sys}}$$

$$S_{\rm sig} = \frac{1}{\mathscr{B}d^2}\frac{dP}{d\Omega} > S_{\rm min}$$

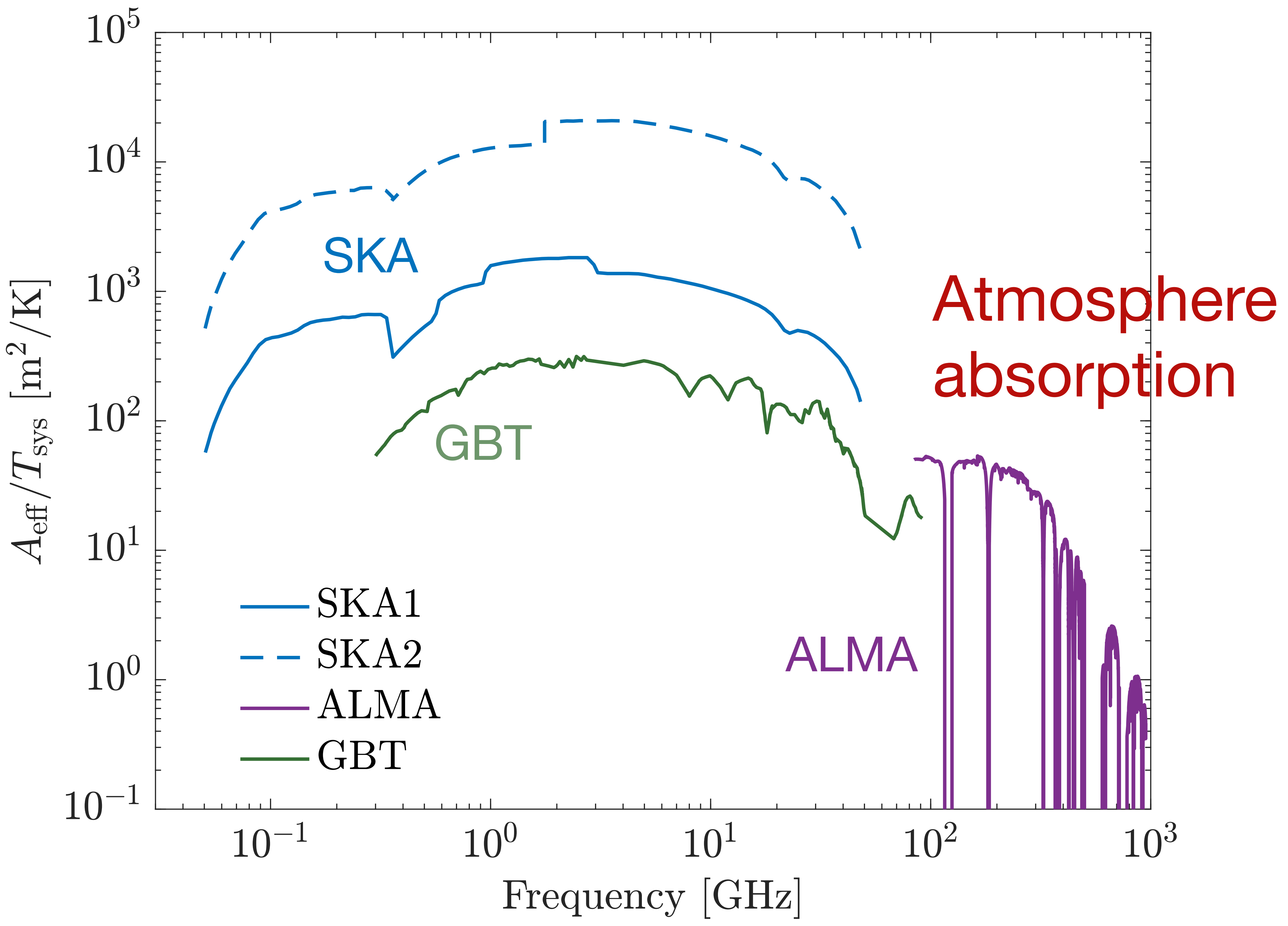

Sensitivities for Galactic Center Signals

Kinetic Mixing

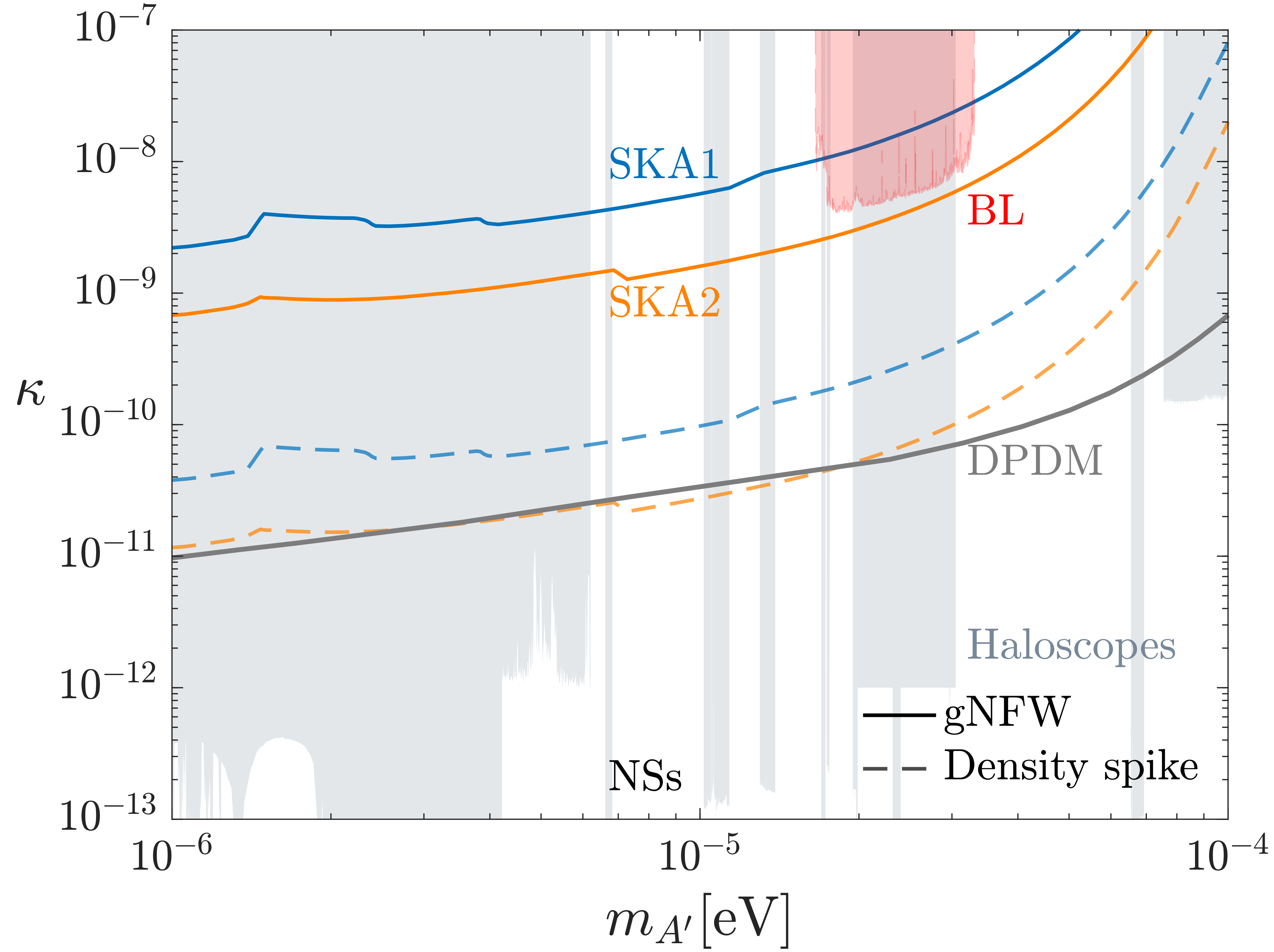

Collection of neutron stars

Dark Photon Mass

Edward Hardy, **NS**, 2212.09756

Criteria for Strong Conversion

- Strong magnetic field is NOT required
- Dense plasma ⇒ Larger dark photon mass
- High temperature ⇒ Less Inverse Bremsstrahlung absorption

$$\Gamma_{\rm IB} = \frac{8\pi\alpha^3 n_e n_{\rm ion}}{3\omega^3 m_e^2}\sqrt{\frac{2\pi m_e}{T}}\ln\left(\frac{2T^2}{\omega_p^2}\right)\left(1 - e^{-\omega/T}\right)$$

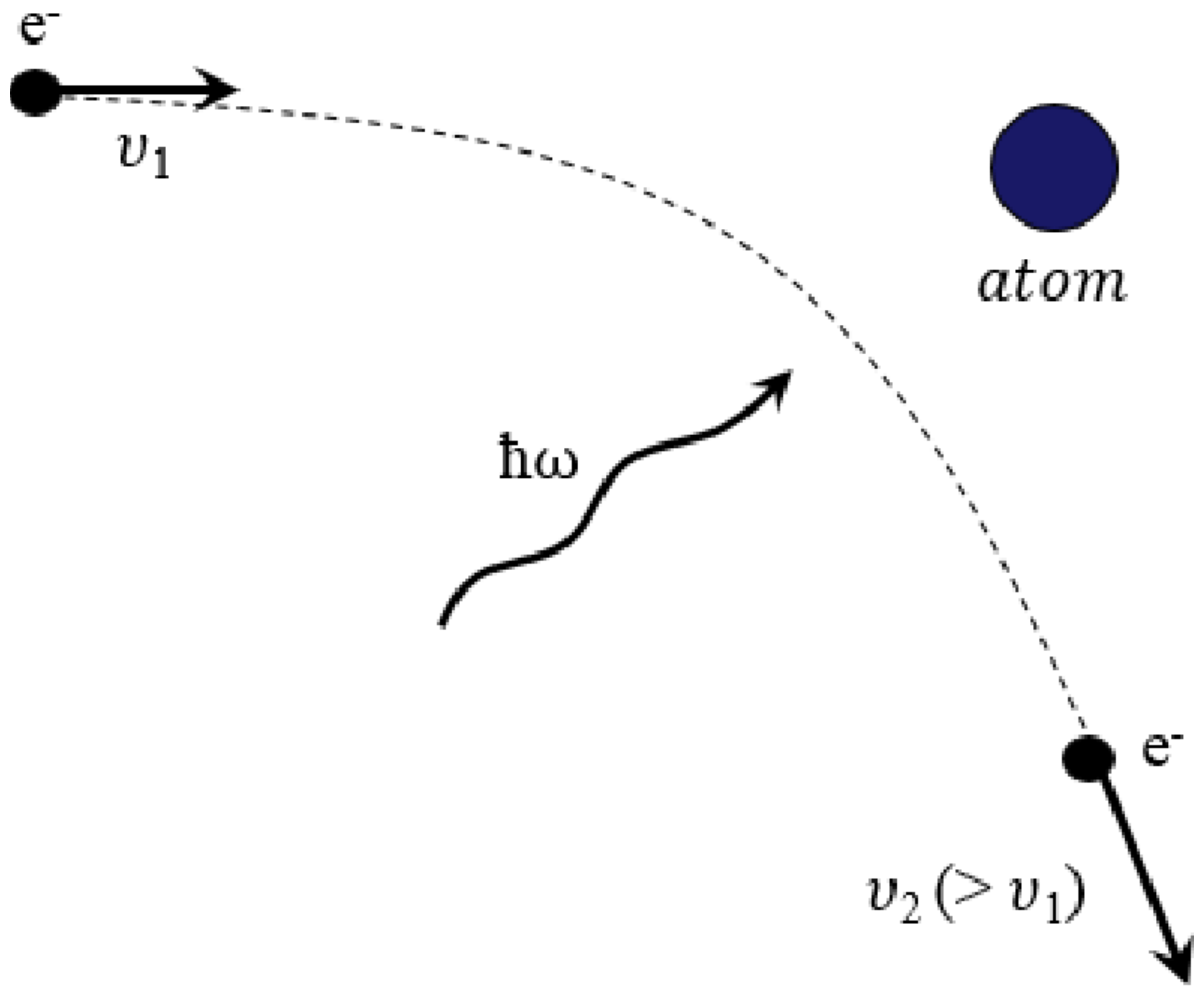

White Dwarf Atmosphere

Isotropic plasma ⇒ photon longitudinal polarization does not propagate, only transverse modes convert

$$\left[-i\frac{d}{dr}+\frac{1}{2k}\begin{pmatrix} m_{A'}^2-\omega_p^2 & -\kappa\omega_p^2 \\ -\kappa\omega_p^2 & 0 \end{pmatrix}\right]\begin{pmatrix}\tilde{A} \\ \tilde{A}'\end{pmatrix}=0\,.$$

White Dwarf Atmosphere

- Pressure gradient balances gravity $l_a \simeq \frac{kT_a r_0^2}{GM_{\rm WD}\mu m_p} = 0.06\ \mathrm{km}\left(\frac{T_a}{10^4\ \mathrm{K}}\right)\left(\frac{M_{\rm WD}}{M_\odot}\right)\left(\frac{r_0}{0.01\ R_\odot}\right)^2$
- Exponential density profile $n_e(r) = n_0 e^{-\frac{r-r_0}{l_a}}$
- Conversion probability $p = \frac{2\pi}{3}\frac{\kappa^2 m_{A'}^2}{k} l_a$
- Radio emission power $\frac{d\mathcal{P}}{d\Omega} \simeq 2p r_c^2 \rho_{A'}(r_c) v_c$

$$T_a \sim 10^4 - 10^5\ \mathrm{K},\ n_0 \sim 10^{17}\ \mathrm{cm}^{-3}$$

Sensitivities from White Dwarf Atmosphere

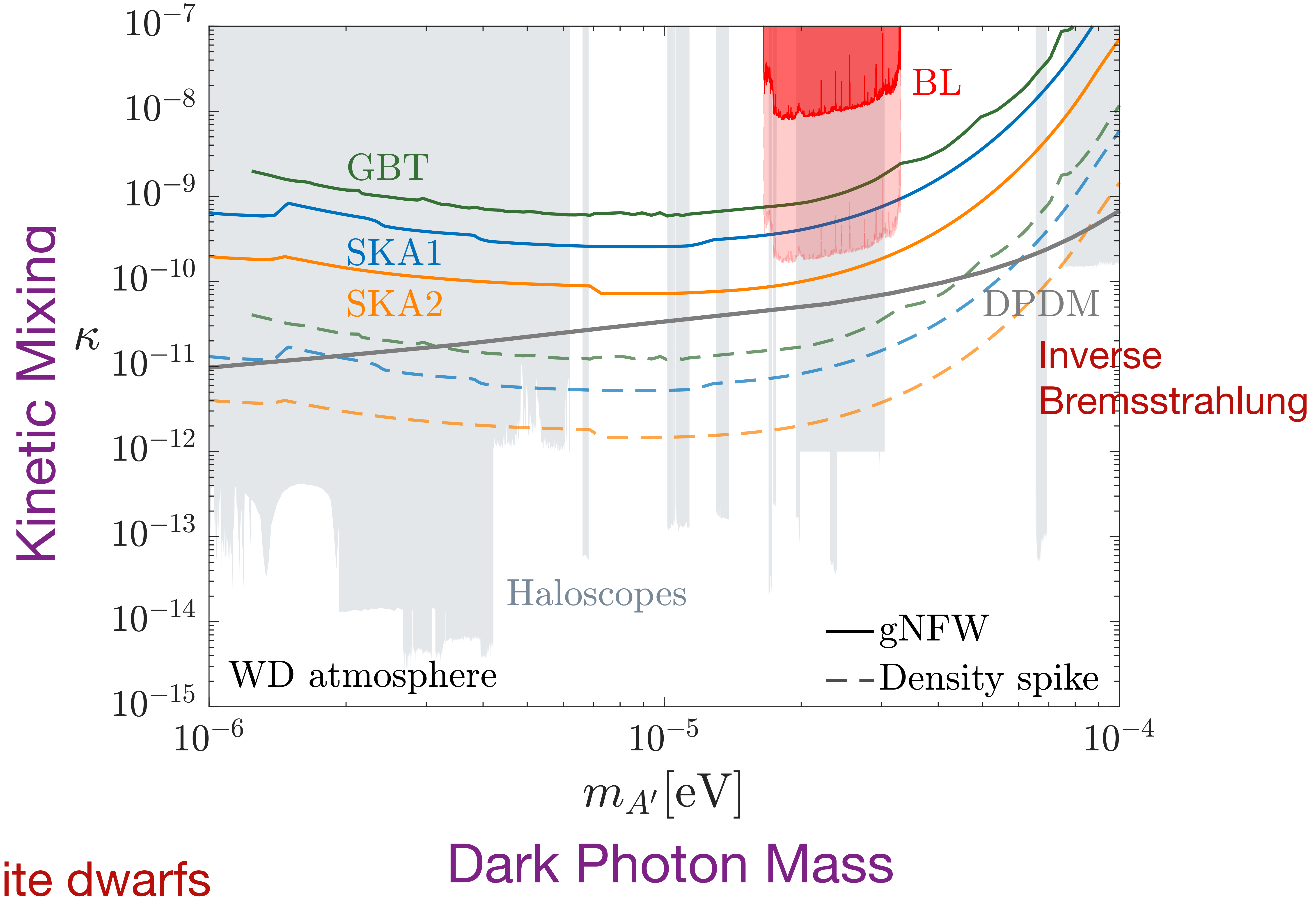

Collection of white dwarfs

Edward Hardy, **NS**, 2212.09756

White Dwarf Corona?

- Higher temperature $10^6 - 10^7$ Kelvins $\Rightarrow$ less absorption
- Exponential density profile $n_e(r) = n_0 e^{-\frac{r-r_0}{l_a}}$
- No observational evidence for hot corona in isolated white dwarfs

$$T_a \sim 10^6 - 10^7 \text{ K}, n_0 \sim ?$$

Sensitivities from White Dwarf Corona

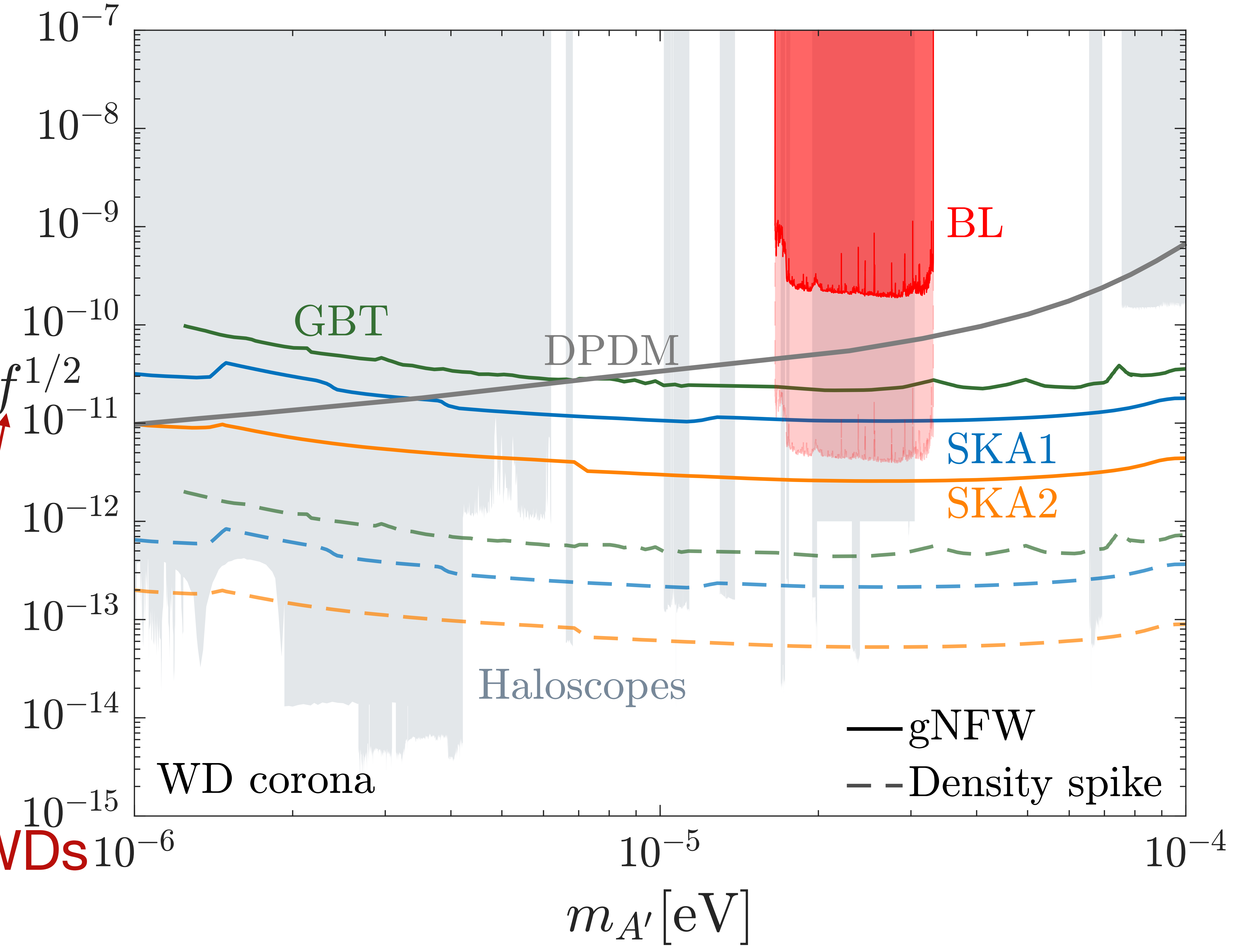

Kinetic Mixing

Fraction of WDs with corona

Collection of white dwarfs

Dark Photon Mass

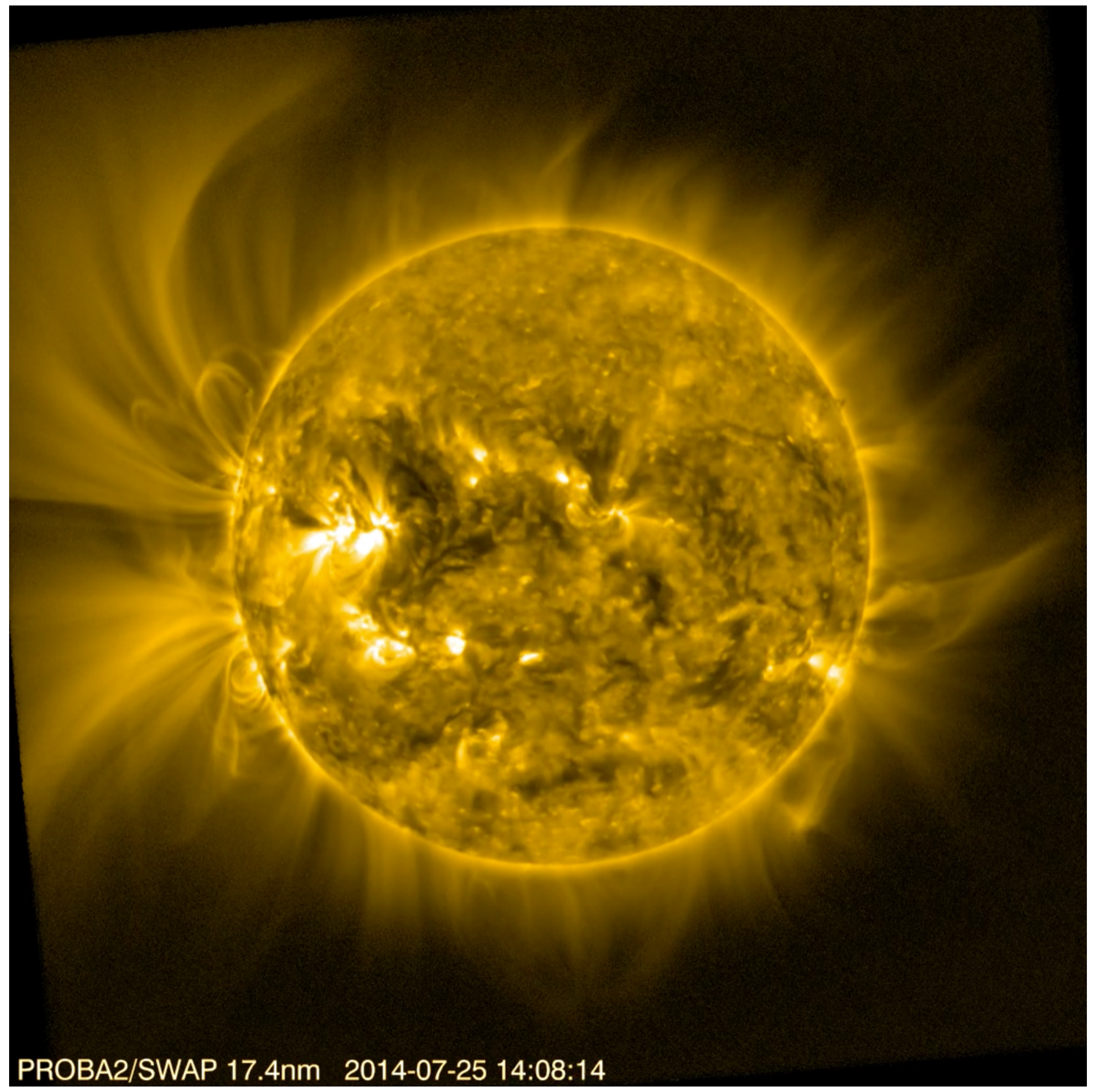

Credit: ESA

Edward Hardy, **NS**, 2212.09756

Accreting White Dwarf

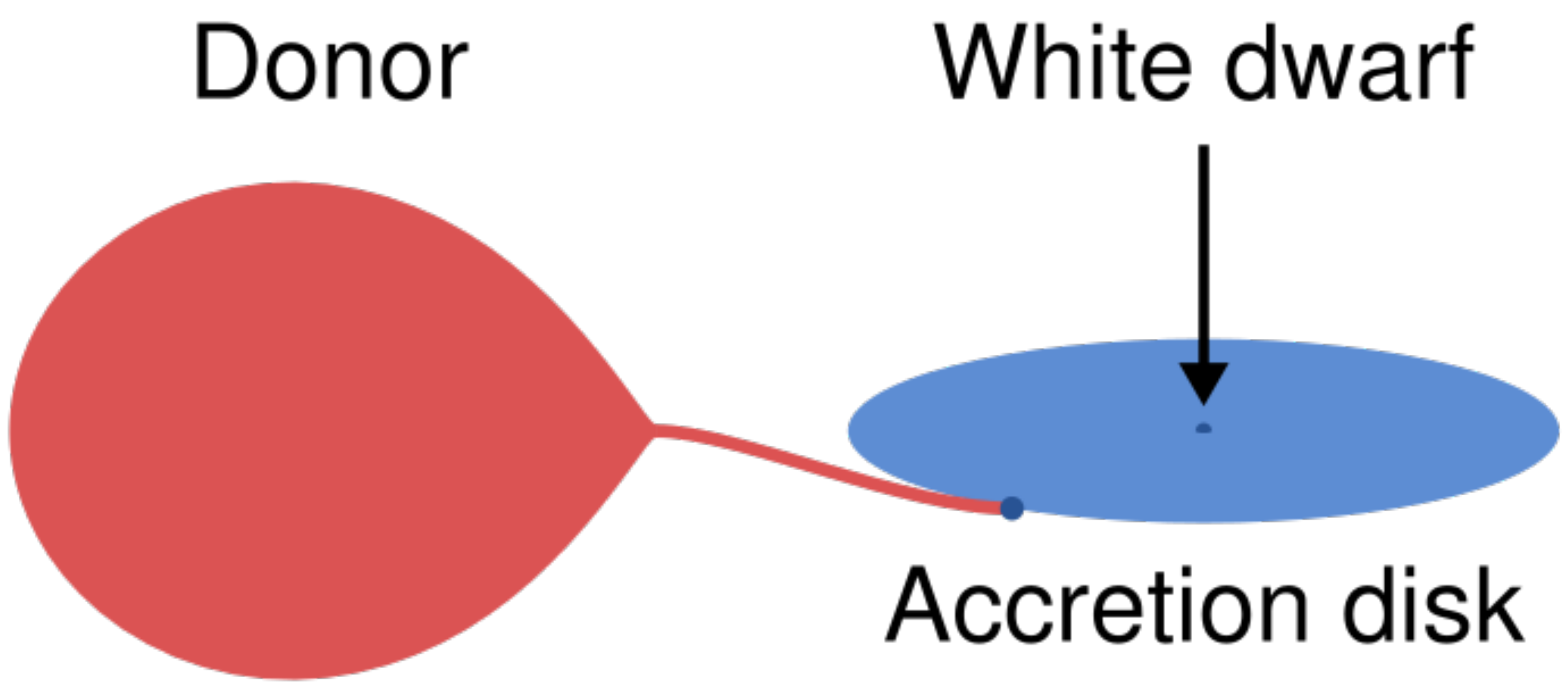

Non-magnetic cataclysmic variable

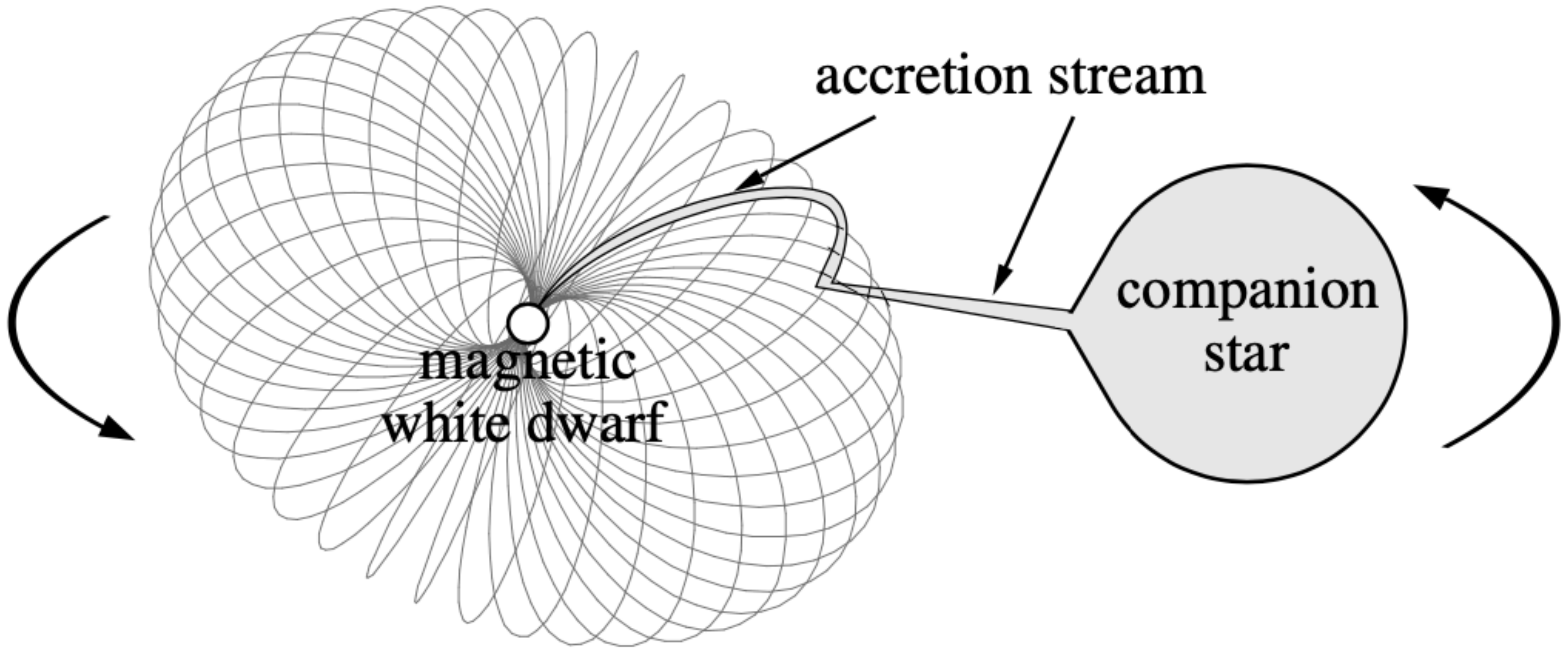

Magnetic cataclysmic variable

Non-magnetic Cataclysmic Variables

- The inner part of the disk decelerates and forms a hot boundary layer near the white dwarf surface
- High accretion rate ⇒ Black body emission from the optically-thick boundary layer
- Low accretion rate ⇒ Bremsstrahlung emission from the optically-thin boundary layer

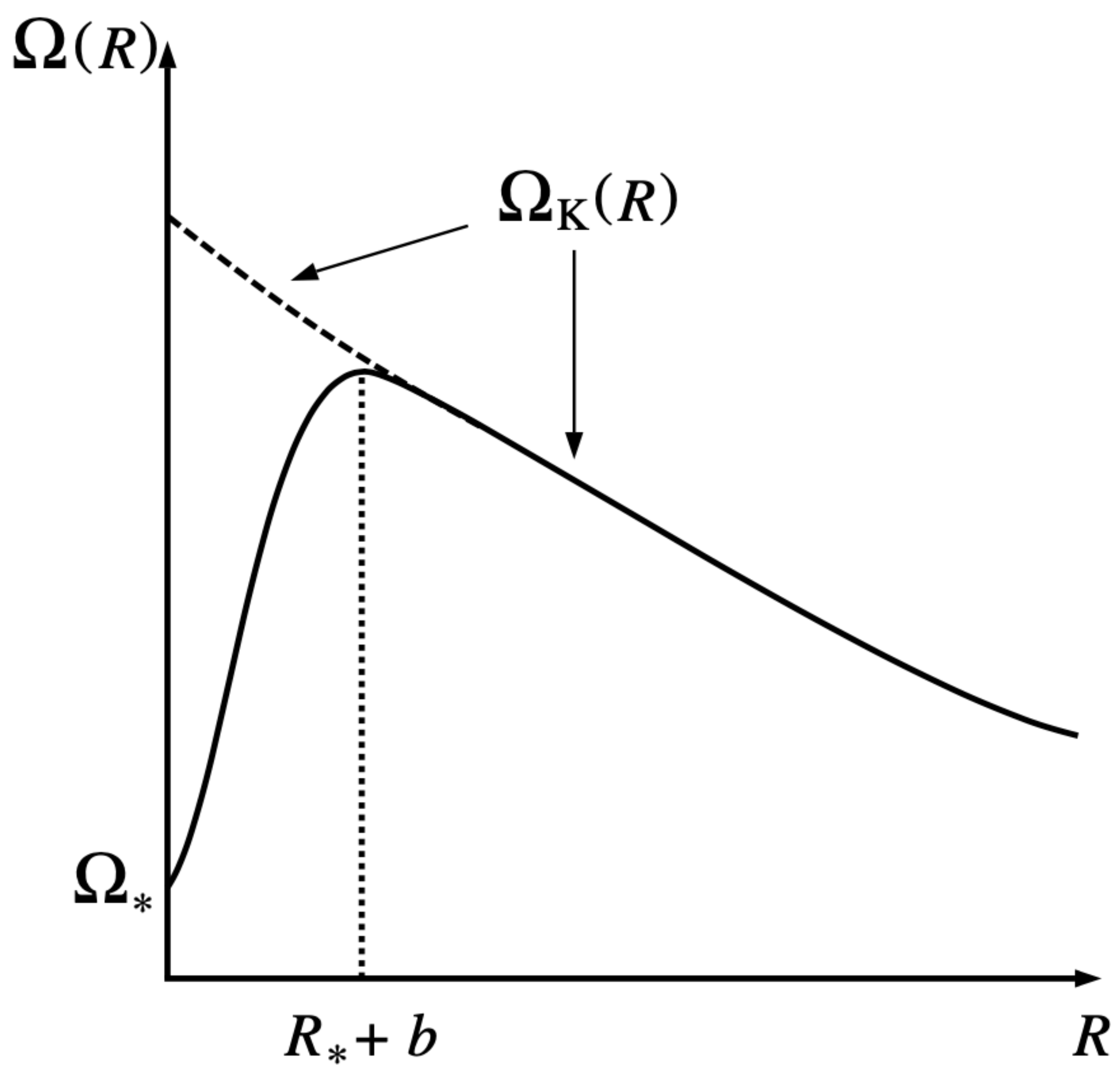

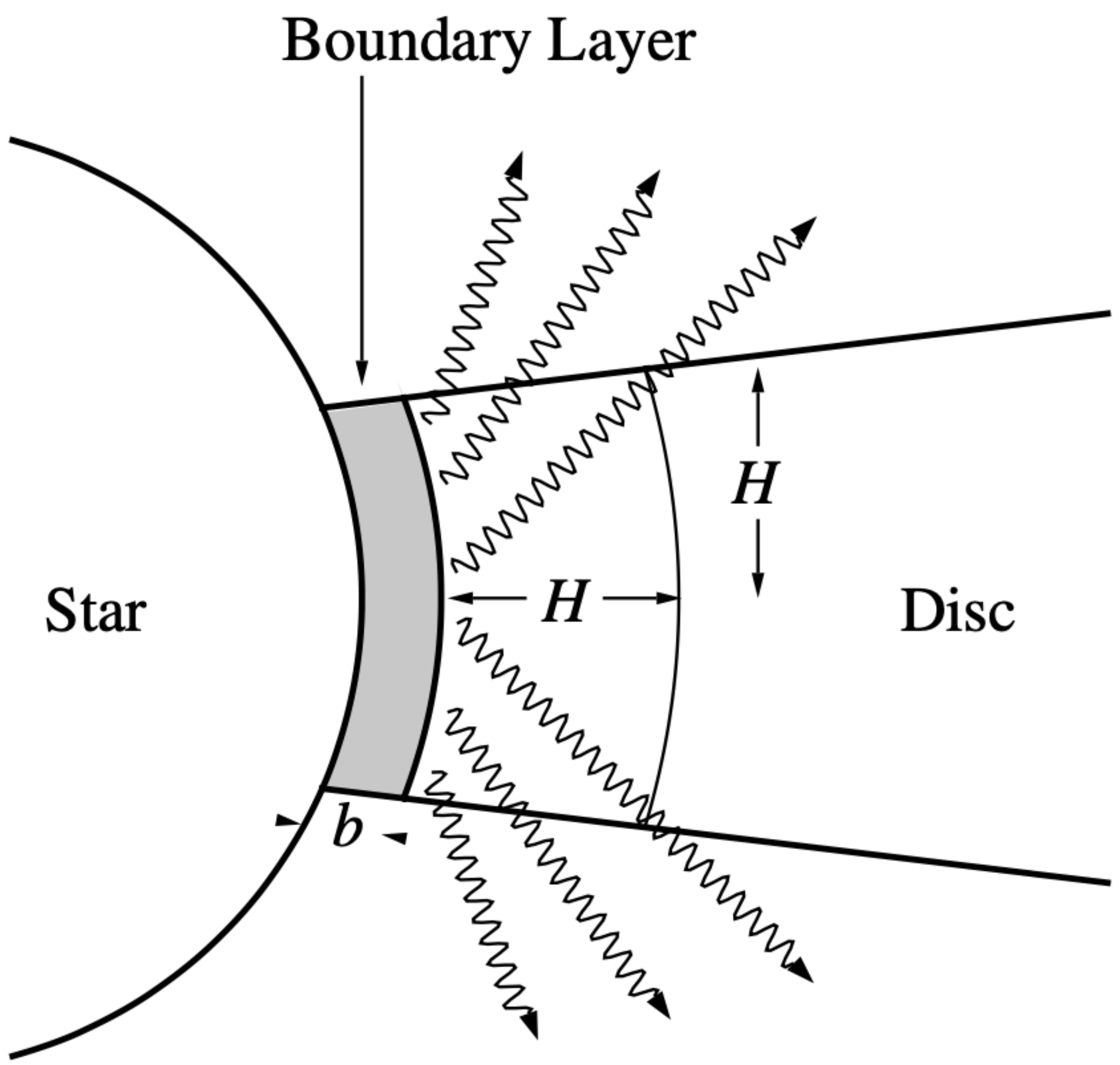

Optically Thin Boundary Layer

- Temperature $T \simeq \frac{3}{16} \frac{GM\mu m_p}{kR} \sim 10^8 \text{ K}$
- Thickness $b \simeq 600 \text{ km} \left(\frac{T_s}{10^8 \text{ K}}\right)\left(\frac{M_{\text{WD}}}{M_\odot}\right)\left(\frac{r_0}{0.01\ R_\odot}\right)^2$
- Height $H = 2 \times 10^3 \text{ km } \alpha_d^{-1/10} \dot{M}_{16}^{3/20} \left(\frac{r_0 + b}{10^5 \text{ km}}\right)^{9/8} f_r^{3/5}$
- Density profile

$$n_e = n_d \exp\left(1 - \frac{r - r_0}{b} - \frac{h^2}{H^2}\right)$$

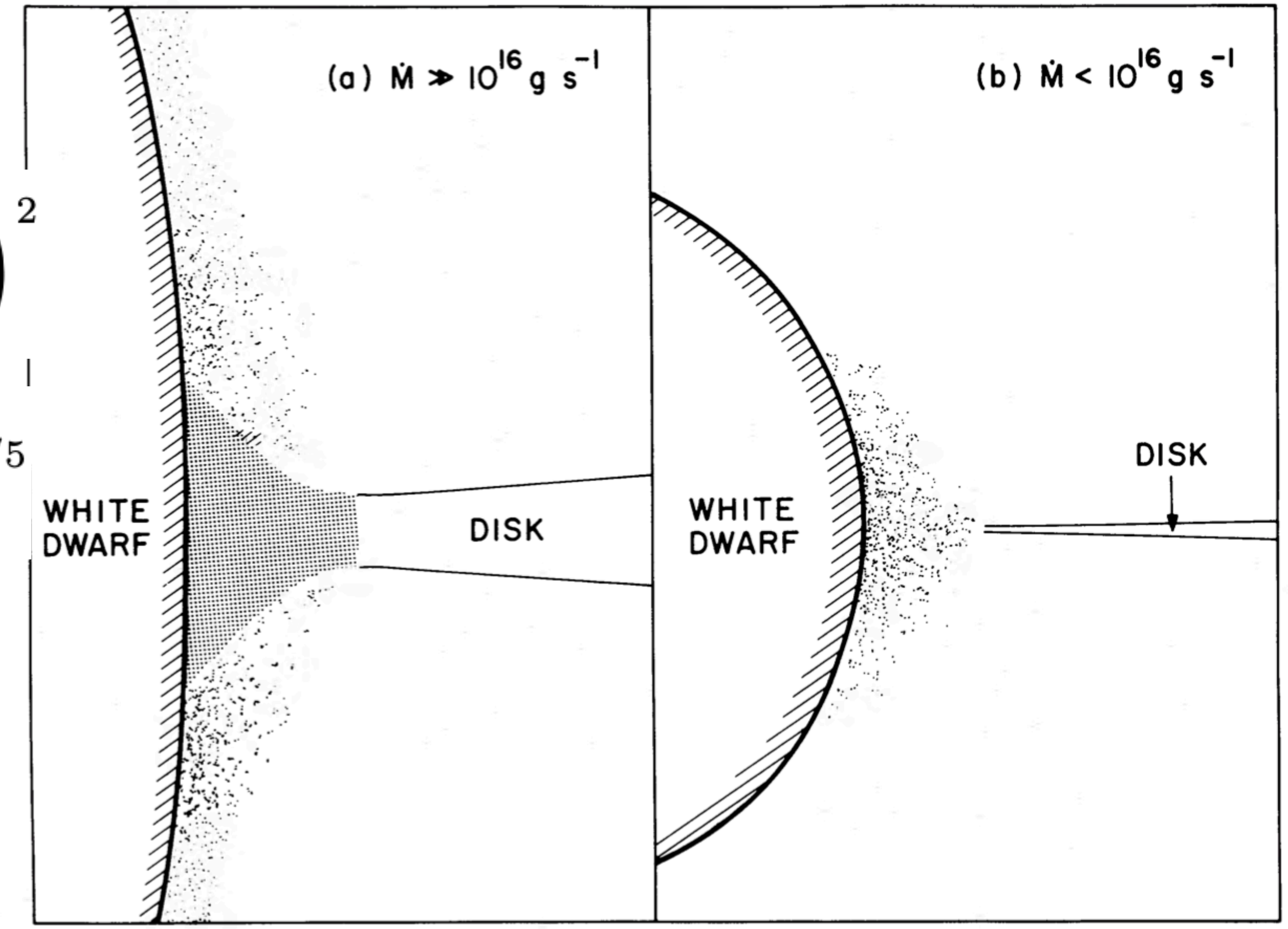

Patterson et al 1985

X-ray Map in the Galactic Center

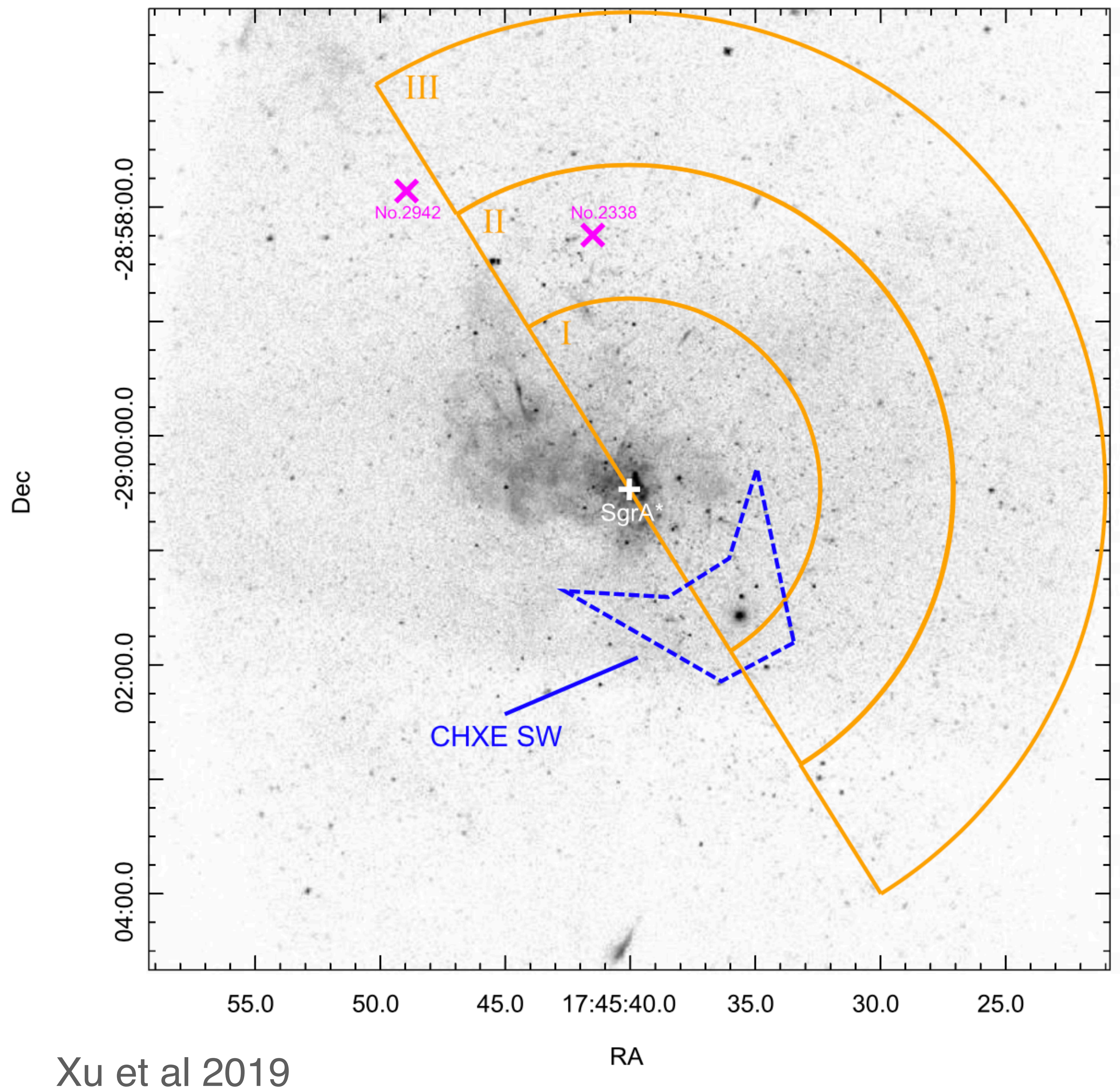

Xu et al 2019

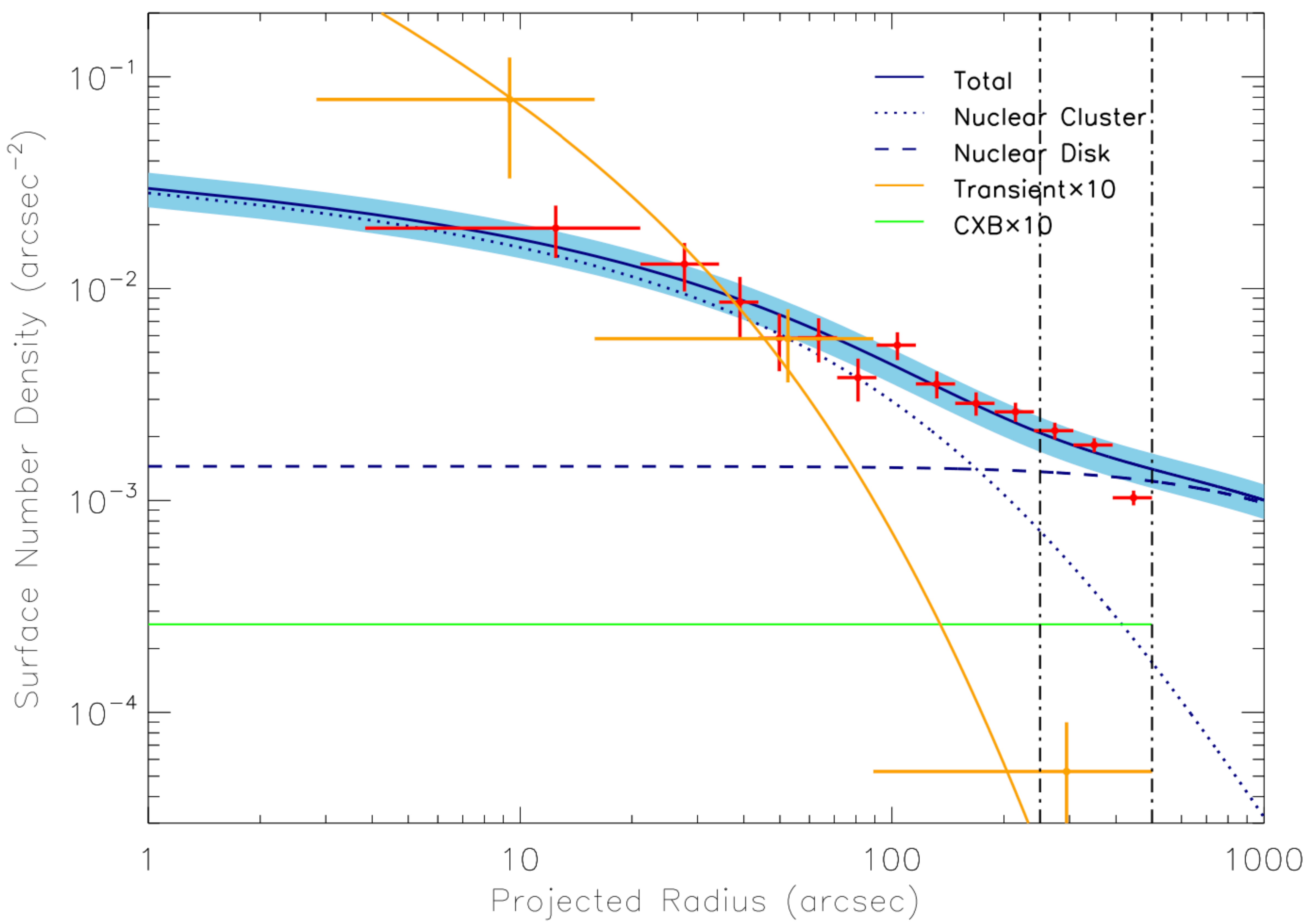

Zhu et al 1802.05073

Sensitivities from Non-magnetic Cataclysmic Variable

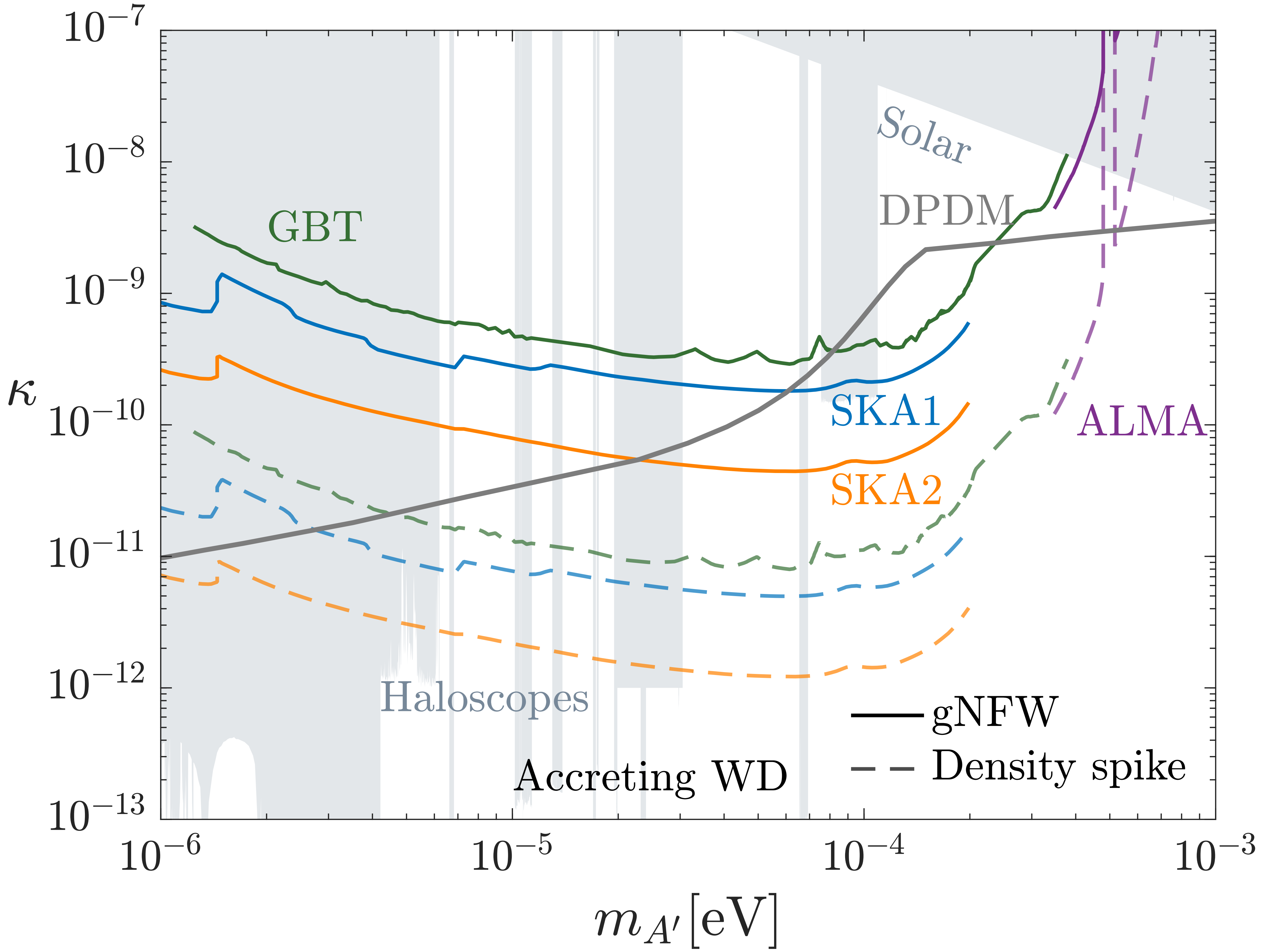

Kinetic Mixing

Dark Photon Mass

Single accreting white dwarf

Edward Hardy, **NS**, 2212.09756